

Spring 5-31-1981

Separation via multi-column pH parametric pumping

Wei Tai Yang
New Jersey Institute of Technology

Follow this and additional works at: <https://digitalcommons.njit.edu/dissertations>



Part of the [Chemical Engineering Commons](#)

Recommended Citation

Yang, Wei Tai, "Separation via multi-column pH parametric pumping" (1981). *Dissertations*. 1265.
<https://digitalcommons.njit.edu/dissertations/1265>

This Dissertation is brought to you for free and open access by the Electronic Theses and Dissertations at Digital Commons @ NJIT. It has been accepted for inclusion in Dissertations by an authorized administrator of Digital Commons @ NJIT. For more information, please contact digitalcommons@njit.edu.

Copyright Warning & Restrictions

The copyright law of the United States (Title 17, United States Code) governs the making of photocopies or other reproductions of copyrighted material.

Under certain conditions specified in the law, libraries and archives are authorized to furnish a photocopy or other reproduction. One of these specified conditions is that the photocopy or reproduction is not to be “used for any purpose other than private study, scholarship, or research.” If a user makes a request for, or later uses, a photocopy or reproduction for purposes in excess of “fair use” that user may be liable for copyright infringement,

This institution reserves the right to refuse to accept a copying order if, in its judgment, fulfillment of the order would involve violation of copyright law.

Please Note: The author retains the copyright while the New Jersey Institute of Technology reserves the right to distribute this thesis or dissertation

Printing note: If you do not wish to print this page, then select “Pages from: first page # to: last page #” on the print dialog screen

The Van Houten library has removed some of the personal information and all signatures from the approval page and biographical sketches of theses and dissertations in order to protect the identity of NJIT graduates and faculty.

INFORMATION TO USERS

This was produced from a copy of a document sent to us for microfilming. While the most advanced technological means to photograph and reproduce this document have been used, the quality is heavily dependent upon the quality of the material submitted.

The following explanation of techniques is provided to help you understand markings or notations which may appear on this reproduction.

1. The sign or "target" for pages apparently lacking from the document photographed is "Missing Page(s)". If it was possible to obtain the missing page(s) or section, they are spliced into the film along with adjacent pages. This may have necessitated cutting through an image and duplicating adjacent pages to assure you of complete continuity.
2. When an image on the film is obliterated with a round black mark it is an indication that the film inspector noticed either blurred copy because of movement during exposure, or duplicate copy. Unless we meant to delete copyrighted materials that should not have been filmed, you will find a good image of the page in the adjacent frame. If copyrighted materials were deleted you will find a target note listing the pages in the adjacent frame.
3. When a map, drawing or chart, etc., is part of the material being photographed the photographer has followed a definite method in "sectioning" the material. It is customary to begin filming at the upper left hand corner of a large sheet and to continue from left to right in equal sections with small overlaps. If necessary, sectioning is continued again—beginning below the first row and continuing on until complete.
4. For any illustrations that cannot be reproduced satisfactorily by xerography, photographic prints can be purchased at additional cost and tipped into your xerographic copy. Requests can be made to our Dissertations Customer Services Department.
5. Some pages in any document may have indistinct print. In all cases we have filmed the best available copy.

University
Microfilms
International

300 N. ZEEB RD., ANN ARBOR, MI 48106

8121973

YANG, WEI TAI

SEPARATION VIA MULTI-COLUMN PH PARAMETRIC PUMPING

New Jersey Institute of Technology

D.ENG.SC.

1981

University
Microfilms
International 300 N. Zeeb Road, Ann Arbor, MI 48106

PLEASE NOTE:

In all cases this material has been filmed in the best possible way from the available copy. Problems encountered with this document have been identified here with a check mark .

1. Glossy photographs or pages _____
2. Colored illustrations, paper or print _____
3. Photographs with dark background _____
4. Illustrations are poor copy _____
5. Pages with black marks, not original copy _____
6. Print shows through as there is text on both sides of page _____
7. Indistinct, broken or small print on several pages _____
8. Print exceeds margin requirements _____
9. Tightly bound copy with print lost in spine _____
10. Computer printout pages with indistinct print
11. Page(s) _____ lacking when material received, and not available from school or author.
12. Page(s) _____ seem to be missing in numbering only as text follows.
13. Two pages numbered _____. Text follows.
14. Curling and wrinkled pages _____
15. Other _____

SEPARATION VIA MULTI-COLUMN pH PARAMETRIC PUMPING

by

Wei Tai Yang

This dissertation is to be used only with due regard to the rights of the author. Bibliographical references may be noted, but passages must not be copied without permission of the Institute and without credit being given in subsequent written or published word.

A Dissertation submitted to the Faculty of the Graduate School
of the New Jersey Institute of Technology in partial fulfillment
of the requirements for the degree of
Doctor of Engineering Science
1981

APPROVAL SHEET

Title of Thesis: SEPARATION VIA MULTI-COLUMN pH PARAMETRIC PUMPING

Name of Candidate: Wei Tai Yang

Doctor of Engineering Science, 1981

Thesis and Abstract Approved:

Hung Tsung Chen _____ Date _____
Professor & Assistant Chairman
Chemical Engineering

Date _____

Date _____

Date _____

Date _____

ABSTRACT

Title of Thesis: SEPARATION VIA MULTI-COLUMN pH PARAMETRIC PUMPING

Wei Tai Yang, Doctor of Engineering Science, 1981

Thesis directed by: Professor H. T. Chen

This thesis presents the study of multi-column pH parametric pumping, a separation technique which applies the principle of parametric pumping and uses pH as control variable. Studies emphasize the mass transfer and the capability of separation by multi-column pH parametric pumping. Many operation modes of multi-column pH parapump are developed for varied objectives of separation. A Two-pH Levels Parapump is capable of enriching the product stream with solute components; a Three-pH Levels Parapump is capable of splitting components into two product streams. The separation capability of multi-column parapump is greatly superior to that of single-column parapump. As compared to cycling zone operation, parametric pumping gives a higher separation factor.

Hemoglobin and albumin are chosen for the experimental model system to demonstrate the separation capability of multi-column pH parametric pumping, and to verify the predictability of the models. Presented are the theoretical basis, mathematical models and methods, results of experimental studies and computer exploration, and the correlation of data with models.

VITA

Name: Wei Tai Yang

Degree and date to be conferred: D. Eng. Sc., 1981

Secondary education: Mioli High School, June 1966

Collegiate institutions attended	Degree	Date of Degree
Taipei Institute of Technology	Diploma(E.T. B.S.)	June 1, 1971
Polytechnic Institute of New York	M.S. Ch.E.	June 1, 1977
New Jersey Institute of Technology	D. Eng. Sc.	May 28, 1981

Major: Chemical Engineering

Publications: "Separation of Proteins Via Multi-Column pH Parametric Pumping," AIChE Journal, 26, 839, (1980)
"Separation of Proteins Via pH Parametric Pumping," Sep. Sci. & Tech., 15(6) 1377 (1980)
"Semi-Continuous pH Parametric Pumping: Process Characteristics and Protein Separation," Sep. Sci. & Tech., 16(1), (1981)

Positions held: Research Engineer, Union Carbide Corp

Present	Silicon Division, Sisterville, West Virginia
10/73-8/75	Chemical Engineer, Taiwan Cement Corp., Taipei, Taiwan
8/73-9/73	Chemical Engineer, China LPG Co., Taipei, Taiwan,
9/71-7/73	Second Lieutenant, China Air Force, Taiwan

ACKNOWLEDGEMENT

This thesis is dedicated to the memory of professor Hung Tsung Chen, my advisor and friend. Without his great enthusiasm, encouragement, and advice, this work would not have been possible. Grateful thanks are extended to the doctoral committee. To my coworkers, Jimmy Wu, Vicent Jajalla, David Ma, and Robert Parisi, I express my appreciation for their help with experimental aspects of this work. To the parapumpers, J. F. Chao, James Huang, Hellen Hollein, Charles Kerobo, Ura Panchunroen, and Ziki Ahmed, I appreciate their valuable discussions.

The National Science Foundation has generously provided financial support for this research through Grant CPE-7704129 and CEP-7910540. With this financial support, my work has contributed three publications in the AICHE Journal and in the Separation Science & Technology.

Most of all, I thank my family for their understanding and encouragement, without which this work would not have been possible.

TABLE OF CONTENTS

	Page
List of Figures	iii
List of Tables	vii
Chapter 1 : Introduction	1
1.1 : Principle of Separation	
1.2 : Principle of Parametric Pumping	
1.3 : Parametric Pumping and Cycling Zone Literature Review	
1.4 : Intoduction of Contents	
Chapter 2 : Protein System and pH Parametric Pumping	11
2.1 : Adsorption Equilibrium	
2.2 : Important Properties of Proteins in pH Parametric Pumping	
Chapter 3 : Theory and Mathematical Models in Parametric Pumping	17
3.1 : Equilibrium in General	
3.2 : Local Equilibrium Theory	
3.3 : Nonequilibrium Theory	
3.4 : Model Equations	
3.5 : Boundary Conditions of Elementary Parametric Pumping with Circulation	
3.6 : Analytical Solution for Simplified Model	
3.7 : Diffusion Effect of Protein	
Chapter 4 : Numerical Methode	29
4.1 : Multi-Cells in Series Model	
4.2 : Application of Local Equilibrium Theory	
4.3 : Single Cell Model	
Chapter 5 : Separation of Parapump in Single Cell Model	37
5.1 : Analytical Solution for Linear Equilibrium Iso-pH	
5.2 : Short Cut Steady State Solution for Single Cell Model	
5.3 : Graphical Method in Single Cell Model	
Chapter 6 : Experimental Study	49
6.1 : System	
6.2 : Apparatus	
6.3 : Analytical Apparatus	
6.4 : Modes of Operation	

Chapter 7	: Separation of Binary System with Single Cell Model	55
7.1	: One Column Batch Parapump	
7.2	: 2-column batch parapump	
7.3	: Experimental Results	
Chapter 8	: Separation of Multi-Component System with Single Cell Model	69
8.1	: 2-Column Batch Parapump	
8.2	: M-Column Batch Parapump	
8.3	: Open Parametric Pumping	
8.4	: Separation of Multiple Solutes System Via Open Parapump	
Chapter 9	: Multi-Cell Model and Semi-Continuous One-Column Parapump	111
9.1	: Process Description of Semi-Continuous Parapumpmp	
9.2	: Determination of Equilibrium and Mass Transfer Rate Constant	
9.3	: Validity of Model and Result of Theoretical Exploration	
Chapter 10	: Comparison of Separation by Cycling Zone and Parametric Pumping	134
10.1	: Cycling Zone and Parametric Pumping	
10.2	: Model Equations	
10.3	: Analytical solution of pH Breakthrough Curve	
10.4	: Separation of Cycling Zone for Single Solute System	
10.5	: Separation of Parametric Pumping for Single Solute System	
10.6	: Comparison of Parametric Pumping and Cycling Zone	
10.7	: 3 pH Level Cycling Zone	
10.8	: Comparison of 2 Column PP and Cycling Zone in 2 Solutes System	
Chapter 11	: Conclusions	173
Nomenclature		175
Appendix-A	: Fortran Program YUP	177
Appendix-B	: Fortran Program Z2C	194
Bibliography		203

List of Figures

Figure		Page
1.1	Schematic Device of pH Parametric Pumping	5
2.1	Schematic Diagram for the Effect of pH on Proteins	13
3.1	An Example of Batch Parapump Operation	23
3.2	Method of Characteristic for 1st order P.D.E.	27
4.1	Schematic of Multi-Cell Model	31
5.1	Description of An Elementary Batch Pump at Operation Cycle (n-1) and n	39
5.2	Schematic Diagram for (a) two-Column batch Parapump (b) One-Column Open Parapump	44
5.3	Graphical Method in Single Cell Model	48
6.1	Experimental Apparatus of Two-Column Parapump	51
6.2	The Effect of pH on Hemoglobin Adsorbance at wave length = 403 mu	53
7.1	Graphical Solution for a One-Column Parapump	57
7.2	Description of A Two-Column Parapump Operation	61
7.3	Graphical Solution for a Two-Column Parapump	63
7.4	Separation Factor vs. n for One and Two-Column Parapumps	65
7.5	Experimental Results for One-Column Parapump	66
7.6	Comparison of Experimental Results Between One- and Two-Column Parapumps	67
8.1	Graphical Solution for Two-Column Parapump - Mode 1	71
8.2	Schematic of Two-Column Parapump Operation - Mode 2	73
8.3	Graphical Solution for Two-Column Parapump - Mode 2	75

8.4	Schematic of Two-Column Parapump Operation - Mode 3	77
8.5	Graphical Solution for Two-Column Parapump - Mode 3	79
8.6	Schematic of Two-Column Parapump Operation - Mode 4	81
8.7	Graphical Solution for Two-Column Parapump - Mode 4	82
8.8	Experimental Results - Mode 1	83
8.9	Experimental Results - Mode 2	85
8,10	Experimental Results - Mode 3	86
8.11	Experimental Results - Mode 4	87
8.12	Schematic of Two-Column Parapump - Mode 3A	88
8.13	Graphical Solution for Multi-Column Parapump - Mode 5	91
8.14	Graphical Solution for Multi-Column Parapump - Mode 6	92
8.15	Graphical Solution for Multi-Column Parapump - Mode 7	94
8.16	Steady State Separation Factors vs. Number of Column Calculation Parameters, Protein A: $K_{P1}^- = 0.6$; $K_{P2}^- = K_{P3}^- = 1.5$; $K_{P1}^+ = 1.2$; $K_{P2}^+ = K_{P3}^+ = 0.5$. Protein B: $K_{P1}^- = K_{P2}^- = 0.6$; $K_{P3}^- = 1.5$; $K_{P1}^+ = K_{P2}^+ = 1.5$; $K_{P3}^+ = 0.5$	95
8.17	Schematic of Two-Column Open Parapump	97
8.18	Effect of Feed Location on Separation for Two-Column Open Parapump	98
8.19	Effect of Feed Location on Separation for 4-Column Open Parapump	99
8.20	Effect of Product Taken on Separation for 2-Column Open Parapump	101
8.21	Calculated Separation Factor in K1 and K2 Domain	104
8.22	Calculated Separation Factor for Fixed K1	106
8.23	Separation of Multiple Components System - Case 1	108

8.24	Separation of Multiple Components System - Case 2	110
9.1	Column Diagram for Semi-Continuous Parapump	112
9.2	Effect of λ on Separation	116
9.3	Effect of Circulation on Separation	117
9.4	Experimental and Calculated Concentration Transient	119
9.5	Experimental and Calculated Separation Factors	121
9.6	Effect of Flow Rate on the Height of Bed	123
9.7	Comparison of Calculated Transients with Experimental Data for Runs 4 and 8	125
9.8	Comparison of Calculated Transients with Experimental Data for Runs 6 and 7	126
9.9	Effect of Feed Size on Separation	129
9.10	Effect of the Feed Size on the Bottom Concentration	130
9.11	Effect of Column Height on Separation	132
9.12	Effect of Dead Volume on Separation	133
10.1	Schematic Diagram of (a) Multi-Cell Column (b) Cycling Zone Device, (c) Parapump Device	136
10.2	Calculated pH Breakthrough Curve	139
10.3	Calculated pH Breakthrough Curve for N=1000	140
10.4	Experimental pH Breakthrough Curve	142
10.5	pH and Concentration Wave for Albumin in R ⁺ Column: P2=5.7; P3=4.0; (3 cycle)	144
10.6	pH and Concentration Wave for Hemoglobin in R ⁻ Column P1=8.5; P2=5.7	145
10.7	pH and Concentration Wave for Albumin in R ⁻ Column P1=8.5; P2=5.7	147

10.8	pH and Concentration Wave for Albumin in R^+ Column P2=5.7; P3=4.0 (Enlargement of Fig. 10.5)	148
10.9	PH and Concentration Wave for Hemoglobin in R^+ Column P2=5.2; P3=4.0	149
10.10	Optimal Displacement of One-Column Parapump	151
10.11	Separation Factor vs. Feed Size for One-Column Parapump	152
10.12	Production Rate vs. Feed Size for One-Column Parapump and Cycling Zone	153
10.13	Compare Parapump and Cycling Zone in Separation and Production Rate	155
10.14	Continuous Operation of Parapump and Cycling Zone	156
10.15	Comparison of Continuous Parapump and Cycling Zone for B ranges from 0.0 to 1.0	157
10.16	Comparison of Continuous Parapump and Cycling Zone for B=0.7	158
10.17	Schematic Device of 3-pH Cycling Zone	160
10.18	pH and Concentration Wave in 3-pH Cycling Zone	161
10.19	pH and Concentration Wave in 3-pH Cycling Zone (enlargement)	162
10.20	Effect of pH on Relative Equilibrium Constant (KB/KA)	164
10.21	System of 3-pH Parapump	165
10.22	Effect of B on SFss	167
10.23	Effect of Displacement on SFss for 3-pH Parapump	168
10.24	Effect of Column High on SFss for 3-pH Parapump	170
10.25	Effect of Circulation on SFss for 3-pH Parapump	171
10.26	Effect of Feed on SFss for Parapump and Cycling Zone at B=0.5	172

List of Tables

Table		Page
1.	Characteristic Analysis of Separation Processes	3
2.	Parametric Pumping : Principle & Applications	6
3.	Properties of Hemoglobin and Albumin	14
4.	Experimental and Model Parameters for Two-Column Batch Parapump and Single Cell Model	89
5.	Parameters for Multi-Components Separation: Case 1	107
6.	Parameters for Multi-Components Separation: Case 2	109
7.	Parameters for Multi-Cell Model in Semi-Continuous Parapump	127

Chapter 1: Introduction

Human beings have been interested in separation principles and techniques. Thousands of years ago, separation techniques had already been applied to purify metals. In modern technology, separation has been one of the most common operations in chemical engineering application and research.

1.1: Principle of Separation

In general, separation is a process to separate components from a mixture without involving chemical reaction. The general exception is the separation by an ionic exchanger, in which a change of chemical bond between resin-counter ion and resin-solute occurs. Separation is a reverse process of mixing, which is, in the thermodynamic sense, 'sharing and spreading of available space in a system'. In most cases, mixing occurs naturally with an increase of total entropy of the system, while separation is not naturally occurring since a decrease of total entropy of the system is associated with separation.

The separation techniques most often used in chemical engineering technology are the following: distillation, adsorption, crystallization, sedimentation, filtration, extraction, and the newly developed processes such as pressure

swing adsorption, membrane separation, et cetera. Table 1 summarizes the characteristics of the most common separation processes. The separation process is analyzed with respect to its separation basis, driving force, main parameter affecting the separation basis, and the phases involved in separation process. Separation bases are the distinct properties among the components such as volatility and density. The driving force can be any force or field such as gravity field, electric field, or pressure drop. By appropriate control of the main parameter, which affects the separation basis, it is possible to enhance separation. Take distillation for an example, a separation is based on the difference in volatility of components and is caused by phase change. Temperature affects the volatility and eventually the separation, and it is possible to apply a temperature gradient on the system to obtain the multiple equilibrium stages operation (i.e. fractionation).

It is seen that the requirements for a separation process are (1) two distinct phases, (2) available separation basis, (3) available driving force. It is also seen that the control parameters are the process variables which primarily affect the separation basis.

TABLE 1. SEPARATION PROCESS

PROCESS	SEPARATION BASIS	DRIVING FORCES	MAIN PARAMETER AFFECT S.B.	PHASES INVOLVED	
				1	2
DISTILLATION	VOLATILITY	PHASE CHANGE	TEMPERATURE	G	L
EVAPORATION	VOLATILITY	PHASE CHANGE	TEMPERATURE	G	L
ADSORPTION	ADSORBILITY	MOLECULAR FORCES	PRESSURE TEMPERATURE	F	S
FILTRATION	PERMEABILITY	PRESSURE DROP	FLOW CHARACTERISTICS	F	S (NMT)
SEDIMENTATION	DENSITY	GRAVITY		L	S (NMT)
CRYSTALLIZATION	SOLUBILITY	PHASE CHANGE	TEMPERATURE	L	S
ELECTROPHORESIS	MOBILITY	ELECTRIC FIELD	TEMPERATURE	L	L
IONIC EXCHANGER	IONIC CHARGE	ELECTRIC FIELD	PH, IONIC STRENGTH	L	S
PARAMETRIC PUMPING	ANY DISTINCT CHARACTERISTIC	ANY FORCE	THERMO. VARIABLE AFFECT S.B.	F	S

F: FLUID, G: GAS, L: LIQUID, S: SOLID

NMT: NO MASS TRANSFER BETWEEN PHASES

1.2: Principle of Parametric Pumping

The principle of parametric pumping was first introduced by the late R. H. Wilhem [30]. The separation principle is based on (1) periodic alternation of the control variable (such as pressure or temperature) to induce the interface mass transfer, and (2) coupling of interphase mass transport action with the bulk fluid flow displacement. The bottom row of Table 1 shows the separation principle of parametric pumping. As in the conventional separation processes, the above three requirements for separation have to be satisfied in order to obtain separation. The operation of parametric pumping (also called Parapump) is not restricted to any single process with any particular separation basis, neither a specific driving force nor a control variable. So parametric pumping is a separation principle rather than a separation process. For example, the principle has been applied to thermal, pressure, and pH parametric pumping, as listed on Table 2. Thus parametric pumping is a separation principle, while the thermal, pressure, and pH parametric pumping are separation processes that follow the principle of parametric pumping. Figure 1.1 shows the schematic device of pH parapump.

The differences between parametric pumping and the conventional phase exchange separation operation are grouped into two categories: (1) the relative motion reverses periodically in

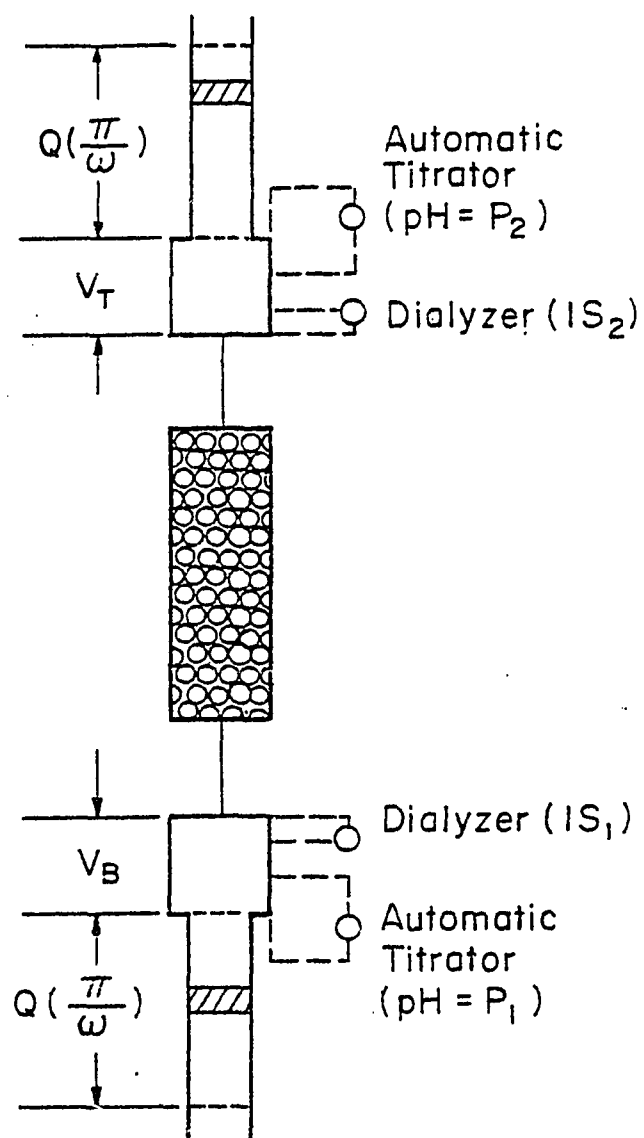


Figure 1.1 Schematic Device of pH Parametric Pumping

TABLE 2. PARAMETRIC PUMPING : PRINCIPLE & APPLICATION

A SEPARATION PRINCIPLE BASED ON

(1) PERIODIC CHANGE OF CONTROL VARIABLES.

(2) SYNCHRONOUS COUPLING OF THE ALTERNATING VELOCITY WITH
INTERPHASE FLUX.

<u>TYPE OF P.P.</u>	<u>CONTROL VARIABLE</u>	<u>SYSTEM EXAMPLE</u>
THERMAL PARAMETRIC PUMPING	TEMPERATURE	N-HEPTANE - TOLUENE
PRESSURE PARAMETRIC PUMPING	PRESSURE	NORMAL-BRANCHED HYDROCARBON
PH PARAMETRIC PUMPING	PH	HEMOGLOBIN. - ALBUMIN

parametric pumping, while the relative motion between phases is unidirectional in a conventional process. (2) The state variables (concentration, temperature, etc.) vary periodically with time in parametric pumping, while it is constant with respect to time at steady state in other continuous processes. These differences are intrinsic to the fact of coupling transport action with the periodic alternation of the control variables in parametric pumping.

Parametric pumping can be classified into two categories, based on the method of variation of process variables. (1) Direct Mode: The control variable in the entire column is changed simultaneously with the change of fluid flow direction. One example is heat introduced or removal from the wall of the entire column in thermal parametric pumping. (2) Recuperative Mode: The control variable is changed gradually from one end to the other of a column after the change of fluid flow direction. One example is to introduce hot fluid into the top of a column at the first half operation cycle, and cold fluid into the bottom of column at the next half operation cycle for thermal parametric pumping.

1.3: Parametric pumping literature review

During the last 2 decades, a number of investigations have

been done on parametric pumping. Separation of NaCl-Water system has been reported by Whilhem et al.^[29,30] and Gregory^[15]. Separation of Benzene-Hexane system has been reported by Wakao et al.^[26], Toluene-n-Heptane by Whilhem^[32] and Chen^[5, 6, 7]. Separation of Fructose-Glucose has been reported by Chen et al.^[8]. Separation of Albumin-Hemoglobin has been reported by Chen et al. ^[9, 10, 11, 12, 13].

One branch of pressure parametric pumping is better known by the name of Pressure Swing Adsorption. This process has been widely applied and commercialized in the separation of gas systems. Separation of normal-branched paraffin has been reported by Breck^[3] and Union Carbide^[18]. Hydrogen purification has been reported by Skarstrom^[24] and Weaver^[29].

Cycling Zone is another separation technique which is very similar to parametric pumping. The separation philosophy of cycling zone is almost the same as parametric pumping, except that the fluid flow is unidirectional in the former but reciprocating in the latter. As in parametric pumping, the separation of cycling zone is caused by a periodic alternation of the process control variables in a column. This alternate process was developed by Pigford. Work in this area has been reported by Baker^[1], Blum^[2], Busbice^[4], Dore^[14], Figford^[20], Gupta & Sweed^[16], Vlist^[25], Latty^[17], and Wankat^[27, 28].

1.4: Introduction of Contents

Most of earlier work in this area has been devoted to thermal-parametric pumping. On the contrary very little work has been done for pH parametric pumping. Most earlier work was done for a single column parametric pumping on a simple system. This thesis includes the single column P.P. for single component systems and multicomponent systems, and extends to multi-column parametric pumping operation. Presented also are the study of cycling zone, and the comparison of cycling zone with parametric pumping.

Several mathematical models and techniques have been employed to solve the parametric pumping equation and to study the separation and characteristics of pH parametric pumping. Methods included are a graphical method, an analytical solution, and the Stop and Go numerical method. Both equilibrium theory and nonequilibrium theory (finite mass transfer) have been applied to study parametric pumping.

Studies presented here are the theoretical basis, theoretical exploration results, and the experimental results for pH parametric pumping. A series of experiments studied on

example systems(separation of albumin-haemoglobin liquid mixture using a Sepahrose cation and anion exchanger resin adsorbent) is carried out to verify the theoretical results. These experiments demonstrate the separation by parametric pumping and cycling zone, and also confirm the models predictive ability. Portions of this thesis have appeared in papers by Chen & Yang et al. [11, 12, 13].

Chapter 2 : Protein System and pH Parametric Pumping

2.1 : Adsorption Equilibrium

Adsorption is conventionally classified into two groups, namely, Physical Adsorption, and Chemical Adsorption. The adsorption equilibrium is strongly dependent on the thermodynamic intensive variable, such as , pH, ionic strength, temperature, and pressure. Qualitatively, physical adsorption is dependent on pressure and temperature, chemical adsorption is sensitive to temperature, and ionic exchanger adsorption is mainly dependent on the charges of molecules and the concentration of the counter ions. One of the typical quantitative treatments of adsorption equilibrium has been reported by Langmuir. In Langmuir modeling, the tendency of bonding between fluid molecule with solid surface is said to be equal to the tendency of debonding of fluid molecules from the solid surface when equilibrium is established. The Langmuir equilibrium can be written as the following equations.

$$K_a \cdot C \cdot [C_{sm} - C_s] = K_d \cdot C_s \quad (2.1)$$

$$C_s = \frac{K_a \cdot C_{sm} \cdot C}{K_a \cdot C + K_d} = \frac{(K_a/K_d) \cdot C_{sm} \cdot C}{(K_a/K_d) \cdot C + 1} \quad (2.2)$$

where K_a : bounding constant
 K_d : debonding constant
 C : concentration in fluid phase
 C_s : concentration in solid phase

C_{sm} : maximum concentration for solid phase

The constants of K_a, K_d, C_{sm} are dependent on the system of interest. Equation (2.2) states that the concentration of the solid phase is nonlinearly increased with the concentration of the fluid phase, when the $(K_a/K_d) \cdot C$ is close to the order of unity. The solid phase concentration is a constant equal to $(K_a/K_d) \cdot C_{sm}$, when $(K_a/K_d) \cdot C$ is much larger than unity. The concentration in the solid phase is linear to the concentration of the fluid phase with a proportional constant $(K_a/K_d) \cdot C_{sm}$, when $(K_a/K_d) \cdot C$ is much larger than unity. Chemical adsorption is usually well described by the Langmuir equilibrium.

The model system chosen in this thesis is Hemoglobin and Albumin mixture in buffer solution, and an ionic exchanger is used as the adsorbent. Since the ionic exchanger adsorption is classified in the group of chemical adsorption, Langmuir equilibrium is applicable in this model system. The concentration of protein solute in the feed solution is very low in this thesis. Feed concentration ranges from 0.01% to 0.02% by weight for hemoglobin and albumin, the corresponding molarity is about $(1 \cdot 10^{-5})$ mole/liter. Thus the linear equilibrium relation is applicable without introducing large error in this range of concentration.

2.2 : Important Properties of Proteins in pH Parametric Pumping

The proteins are built from amino-acid. The amino group, $-NH_2$, and the carboxyl group, $-COOH$, have an ability of binding and losing hydronium ions. In low pH solution, the hydronium ions are more concentrated and are more likely to bind with amino groups and carboxyl groups; at high pH, hydronium ions are less concentrated and are more likely to dissociate from the carboxyl group and amino groups. Figure 2.1 schematically shows the effect of pH on protein structure. At a certain pH the total positive charges equal to the total negative charges in a protein molecule and the net total charge of the molecule is zero. This pH is called the Isoelectric Point. When the pH is lower than the Isoelectric Point, the predominant protein molecules have a positive net charge. When the pH is higher than the Isoelectric point, the predominant protein molecules have a negative net charge.

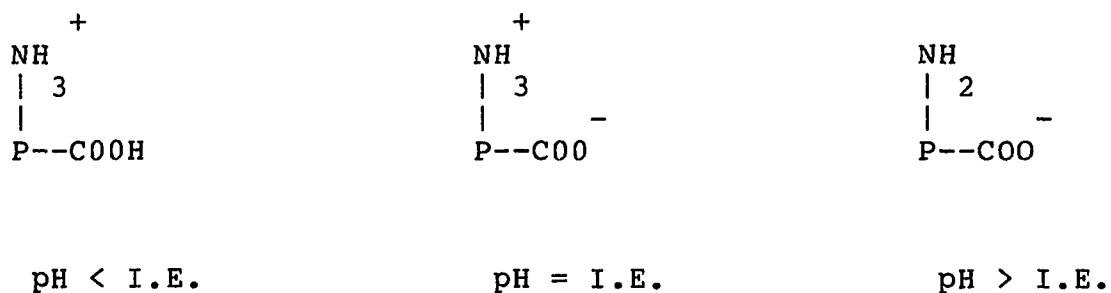


Figure 2.1

Hemoglobin and Albumin are chosen as a model system in this thesis. Some of their physical properties are available from the literature and are listed in Table 3.

Table 3

Species	Mwt	I.E.	Dm	V-403	UV-595
Hemoglobin	63,000 - 68,000	6.7	6.9×10^{-7}	1.00	0.35
Albumin	69,000 - 72,000	4.9	6.0×10^{-7}	0.00	0.35

* adsorbance read reference taken as $H_0 = 0$
 unit for wave length = μ

Mwt : molecular weight

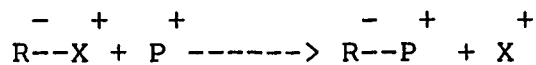
I.E.: isoelectric point

Dm : mass diffusivity = cm^2/sec

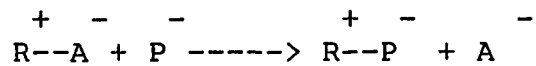
As shown in the above table, the molecular weights of hemoglobin and albumin are very close to each other, and thus separation methods based on molecular size will not be useful to separate hemoglobin and albumin. Since the difference in isoelectric point for these two component is about 2., we may take the advantage of this difference in isoelectric point as the

separation basis in parametric pumping.

Since we know that the protein molecule consists of many charged groups, such as amino groups and carboxyl groups, an ionic exchanger will work as a good adsorbent for protein molecules. For example, the cation exchanger can exchange cations with positively charged molecule as:



and the anion exchanger can exchange anions with negatively charged molecule as:



The above exchange process is actually a mass transfer of protein from liquid phase to solid phase. The protein adsorption by an ionic exchanger is reversible. The protein may be exchanged back to fluid phase by using excess counter ions, or by changing the net charges on the protein molecule, which will reduce the bonding stability. For example, if R^-P^+ stands for the protein adsorbed by cation the ion exchanger at a pH lower than its isoelectric point, when the solution changes pH to a value higher than its isoelectric point, the protein increases its negative charges and the net charges of protein will be negative. The bonding is weakened and protein has a higher tendency to be replaced by a counter ion and goes back to the

fluid phase; thus the mass transfer from solid phase to liquid phase is achieved. The above information gives the idea of protein separation by pH parametric pumping, i.e. using pH as the control variable, an ionic exchanger as the adsorbent, the difference of isoelectric points as the separation basis, and the ionic electric field as the driving force. Thus the requirements of parametric pumping operation are completed.

Hemoglobin & albumin are ready to be separated by applying the principle of parametric pumping. The result of separation by parametric pumping will be discussed in Chapter 7,8,9 and 10; separation by cycling zone is included in Chapter 10.

Chapter 3 : Theory and Mathematical Models in Parametric Pumping

3.1 : Equilibrium in General

For systems involving two phases, the mass distribution relationship between the phases is usually described by equilibrium theory. The theory says that apparently no change takes place in a system at an equilibrium state. In double film theory, it is assumed that two films exist in the boundary of two phases, and equilibrium is reached for these two films. We can write the following equations for the mass distribution at the equilibrium films.

$$X^* = f(Y^*, PZ1, PZ2, PZ3, \dots PZn) \quad (3.1)$$

Y^* : concentration in fluid phase

X^* : concentration in solid phase

Equation (3.1) expresses the equilibrium relationship between the solid phase concentration X^* and the liquid phase concentration Y^* , under the physical parameters $PZ1, PZ2, \dots PZn$, which affect the equilibrium. The theory most commonly applied in parametric pumping has been the local equilibrium theory and the non-equilibrium theory, in which the system is governed by finite mass transfer.

3.2 : Local Equilibrium Theory

In local equilibrium theory, the system is considered as having equilibrium established instantaneously and locally between phases. Interpretation of local equilibrium theory indicates that the thickness of the film is zero, the concentration of the bulk of fluid is equal to the concentration of fluid film, and the film is in equilibrium with the concentration of solid phase. Thus equation (3.2) is applied. Since the adsorption occurs on the surface of the solid, the corresponding concentration of the amount of solute being adsorbed, X , is equal to the equilibrium concentration of the solid, X^* , thus equation (3.3) is applicable.

$$Y = Y^* \quad (3.2)$$

$$X = X^* \quad (3.3)$$

Equation (3.1) can be rewritten as equation (3.4).

$$X = f(Y, PZ_1, PZ_2, \dots, PZ_n) \quad (3.4)$$

3.3 Nonequilibrium theory

Nonequilibrium theory states that the concentration of the bulk fluid is not equal to that of the liquid film, where the film is in equilibrium with the solid concentration. The system is governed by a finite rate of interphase mass transfer, no

instantaneous equilibrium is established. Theoretically, it would take infinite time for mass transfer to establish the exact equilibrium. Thus mass transfer rate is the control step. In this case, equation (3.2) is not applicable, while equation (3.3) is still applicable for the same reasons as stated in the previous section. Thus equation (3.1) can be rewritten as:

$$X = f^*(Y, PZ1, PZ2, \dots PZn) \quad (3.5)$$

We may further define a function f' inverse to function f as:

$$Y = f'^*(X, PZ1, PZ2, \dots PZn) \quad (3.6)$$

3.4 : Model Equations

In order to describe the behavior of parametric pumping, a model for parametric pumping was set up from the theoretical background and simulated by computer. The model equations include the equation of continuity, the equation for control variable balance, the interphase mass transfer equation, and the phase equilibrium relationship. The model for pH parametric pumping is described as follows:

Equation of Continuity:

$$\frac{\partial X}{\partial t} + \frac{\partial Y}{\partial t} + u \cdot \nabla Y = Dm \cdot \nabla^2 Y \quad (3.7)$$

Equation of interphase mass transfer

$$\frac{\partial X}{\partial t} = \lambda \cdot (Y - Y^*) \quad (3.8)$$

where $1/\lambda$ is the resistance

For fluid flow through porous medium with porosity = e , equation (3.7) can be written :

$$(1-e) \frac{\partial X}{\partial t} + \frac{\partial Y}{\partial t} + e \cdot u \nabla Y = e D_m \nabla^2 Y \quad (3.9)$$

For system of pH parametric pumping, the main parameter affect the phase equilibrium is the pH. The equation of (3.6) can be written :

$$Y^* = f(X, \text{pH}) \quad (3.10)$$

Model of control variable: The control state variable, pH, is a function of location (x, y, z) and time, t , and can be written :

$$\text{pH} = f(x, y, z, t, \text{constants}) \quad (3.11)$$

Equation (3.11) is a function to describe pH at any location and time, with given process constants such as initial pH and input pH, et cetera. The specific pH model studied in this thesis is described in chapter 10. Equations (3.8), (3.9), (3.10), and (3.11) are solved simultaneously to obtain the state variables of the system. The above 4 equations can be solved either

analytically or numerically for the 4 dependent variables in terms of the independent variables, $x, y, z,$ and t .

pH Model Equation:

One of the pH models studied in this thesis is an equation analogous to the equation of continuity(3.9). This pH model equation, as shown in equation (3.12), is used to correlate the control variable--pH--for the pH parametric pumping.

$$C_{pf} \cdot \frac{\partial \text{pH}}{\partial t} + C_{ps} \cdot \frac{\partial \text{pH}}{\partial t} + C_{pf} \cdot u \cdot \frac{\partial \text{pH}}{\partial z} = 0 \quad (3.12)$$

In equation (3.12), the parameter C_{pf} and C_{ps} stand for the pH capacity of fluid phase and solid phase, and are analogous to the volume of fluid phase and solid phase in the equation of continuity(3.9). It has to be pointed out that the equation of continuity is only valid for quantities such as mass and heat, which obey the conservation rule. Since pH is not a quantity obeying the conservation rule, equation(3.12) is an approximation model rather than an exact equation of continuity.

3.5 : Boundary Condition of Elementary Parametric Pumping

The initial condition and boundary condition are required with the equations (3.8) - (3.11) to complete a model of the system. As an illustration, we discuss the initial conditions and boundary conditions of a rather simple parapump for which the flow process is shown in Figure 3.1. As shown in Figure 3.1, there are 4 steps within a cycle, namely, (1) downward displacement, (2) downward circulation, (3) upward displacement, (4) upward circulation. Since the system includes 3 subsystems, column, top reservoir, and bottom reservoir, the initial conditions and boundary conditions are required for all 3 subsystems.

Initial Conditions:

$$\text{column: } pH(z,0) = P_0(z) \quad (3.13-a)$$

$$Y(z,0) = Y_0 \quad (3.13-b)$$

$$X(z,0) = X_0 \quad (3.13-c)$$

$$\text{Top Reservoir: } Y_{TR}(0) = Y_0 \quad (3.13-d)$$

$$\text{Bottom Reservoir: } Y_{BR}(0) = Y_0 \quad (3.13-e)$$

Boundary Conditions:

$$(1) \text{ Column: } (a) \quad n \cdot t_c < t < n \cdot t_c + t_1 + t_2$$

$$pH(0,t) = p_{HR}(T) \quad (3.14-a)$$

$$Y(0,t) = Y_{TR}(t) \quad (3.14-b)$$

$$pH(L,t) = \text{finite} \quad (3.14-c)$$

$$Y(L,t) = \text{finite} \quad (3.14-d)$$

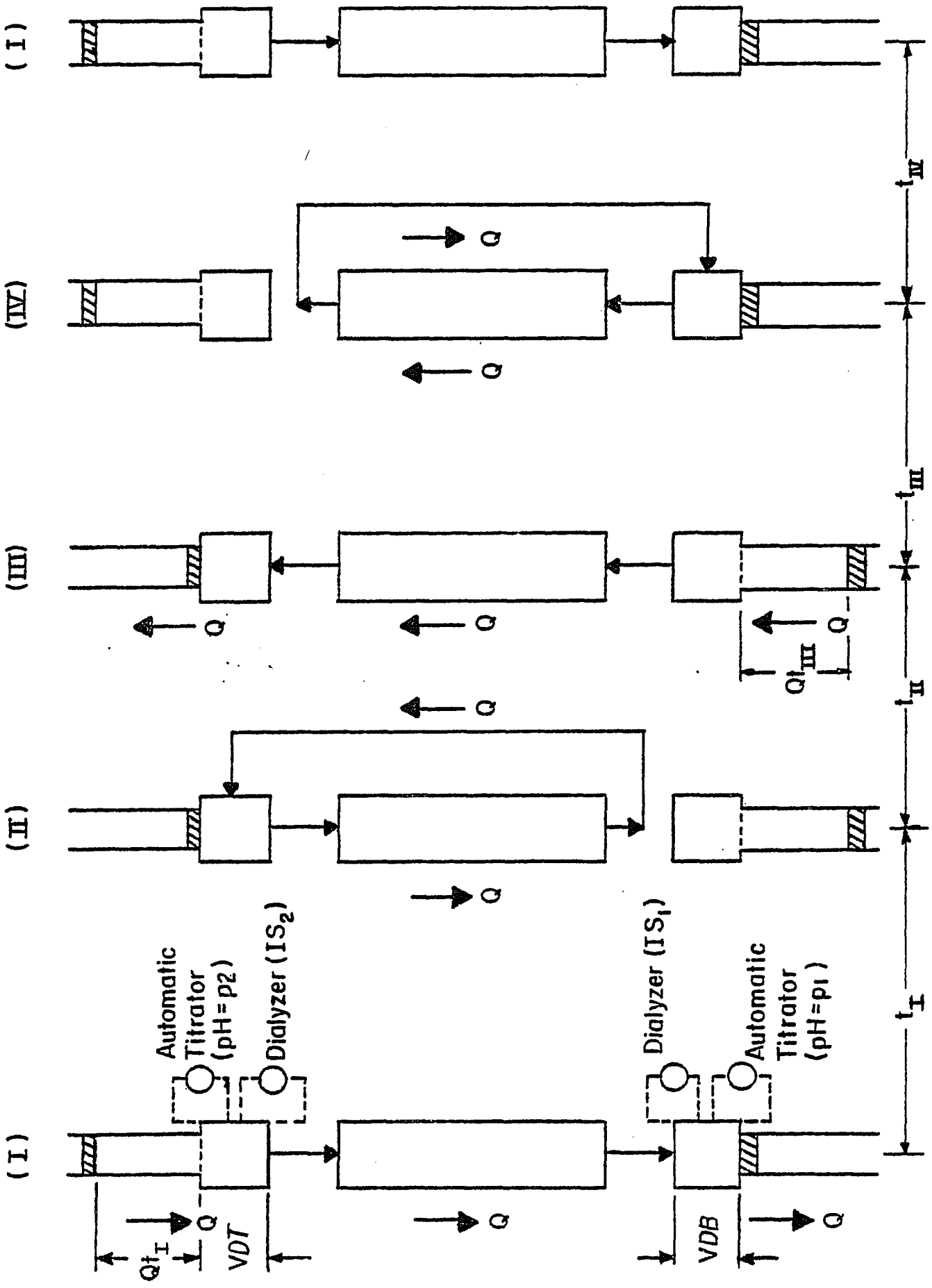


Figure 3.1 An Example of Batch Parapump Operation

$$(b) \quad n \cdot t_c + t_1 + t_2 < t < (n+1) \cdot t_c$$

$$pH(0,t) = \text{finite} \quad (3.15-a)$$

$$Y(0,t) = \text{finite} \quad (3.15-b)$$

$$pH(L,t) = pHR(B) \quad (3.15-c)$$

$$Y(L,t) = YBR(t) \quad (3.15-d)$$

$$(2) \quad \text{Top Reservoir: } pHR(T) = P_2 \quad (3.16)$$

$$(a) \quad n \cdot t_c + t_1 + t_2 < t < n \cdot t_c + t_1 + t_2 + t_3$$

$$YTR(t) = \frac{V_d \cdot YTR(n \cdot t_c + t_1 + t_2) + \int_{n \cdot t_c + t_1 + t_2}^t Q(t) \cdot Y(0,t) \cdot dt}{V_d + \int_{n \cdot t_c + t_1 + t_2}^t Q(t) \cdot dt} \quad (3.17-a)$$

$$(b) \quad n \cdot t_c + t_1 + t_2 + t_3 < t < (n+1) \cdot t_c + t_1$$

$$YTR(t) = YTR(n \cdot t_c + t_1 + t_2 + t_3) \quad (3.17-b)$$

$$(c) \quad n \cdot t_c + t_1 < t < n \cdot t_c + t_1 + t_2$$

$$\frac{YTR(t)}{t} = \frac{Q(t)}{V_d} [Y(L,t) - YTR(t)] \quad (3.17-c)$$

$$(3) \quad \text{Bottom Reservoir: } pHR(B) = P_1 \quad (3.18)$$

$$(a) \quad n \cdot t_c < t < n \cdot t_c + t_1$$

$$YBR(t) = \frac{V_d \cdot YTR(n \cdot t_c) + \int_{n \cdot t_c}^t Q(t) \cdot Y(1,t) \cdot dt}{V_d + \int_{n \cdot t_c}^t Q(t) \cdot dt} \quad (3.19-a)$$

$$(b) \quad n \cdot t_c + t_1 < t < n \cdot t_c + t_1 + t_2 + t_3$$

$$YBR(t) = YBR(n \cdot t_c + t_1) \quad (3.19-b)$$

$$(c) \quad n \cdot t_c + t_1 + t_2 + t_3 < t < (n+1) \cdot t_c$$

$$\frac{\partial YBR(t)}{\partial t} = \frac{Q(t)}{Vd} [Y(0,t) - YBR(t)] \quad (3.19-c)$$

3.6 : Analytical Solution for Simplified Model

When the local equilibrium theory is applied, equation (3.9) can be rewritten as:

$$\frac{\partial X}{\partial t} = -\frac{\partial}{\partial t} f(Y, pH) \quad (3.20)$$

If we further assume a linear equilibrium relation $f(Y, pH) = K(pH) Y$, and D_m is small enough to neglect the effect of diffusion, then the equation of continuity can be rewritten as:

$$e \cdot \frac{\partial Y}{\partial t} + e \cdot u \cdot Y + (1-e) \cdot K(pH) \frac{\partial Y}{\partial t} = 0 \quad (3.21)$$

For a cylindrical packed column, the gradient in the angular direction ($\partial Y / \partial \theta$) and the radial direction ($\partial Y / \partial r$) are small compare to the gradient in the axial direction ($\partial Y / \partial z$), and are negligible. Thus equation (3.21) can be rewritten as:

$$\left[1 + \frac{1-e}{e} \cdot K(pH) \right] \frac{\partial Y}{\partial t} = -u \cdot \frac{\partial Y}{\partial z} \quad (3.22)$$

Equation (3.22) is a first order partial differential equation, which

can be solved by the Method of Characteristic. Rewriting equation (3.22) one obtains:

$$\frac{\partial Y}{\partial t} = -a \frac{\partial Y}{\partial z} \quad (3.23)$$

$$\text{where } a = \frac{u}{1 + K(\text{pH})(1-e)/e} \quad (3.24)$$

The solution can be written as:

$$Y(z,t) = f(v(z,t)) \quad (3.25)$$

where: f is an arbitrary function, and

$v(z,t) = \text{constant}$ is a solution of Equation (3.25-A)

$$\frac{dz}{dt} = a(z,t) \quad (3.25-A)$$

When a is only dependent on t , the solution can be written as:

$$Y(z,t) = Y(z_0, t_0) \quad (3.26)$$

where: z_0 and t_0 are given, and

$$z = z_0 + \int_{t_0}^t a \, dt \quad (3.27)$$

and $t > t_0$

For the case where the pH is constant, $K(\text{pH})$ is constant in the range from ' t_0 ' to ' t ', and thus $a = \text{constant}$ in that period of time. The solution can be written as :

$$Y = f[(z-z_0) - a(t-t_0)] \quad (3.28)$$

for pH = constant when $t > t_0$

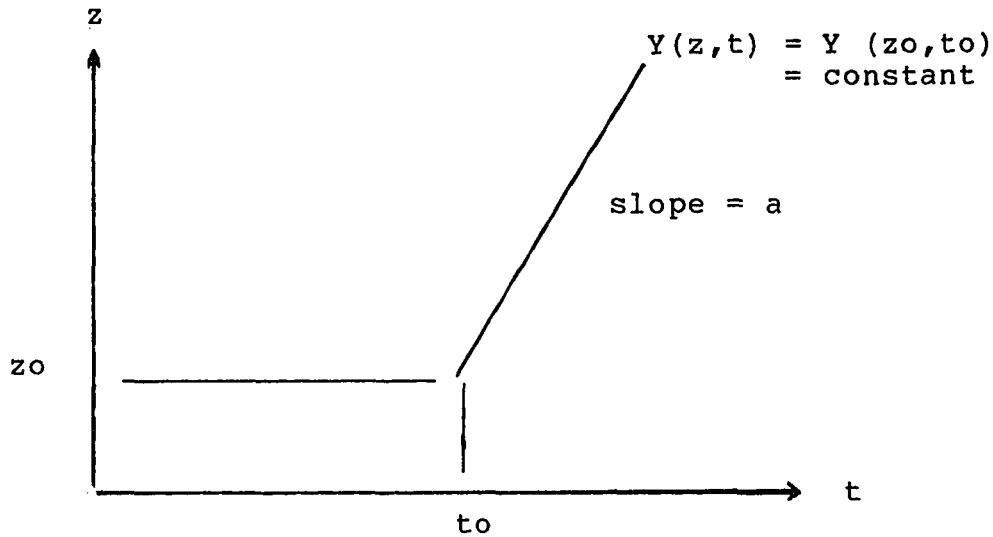


Figure 3.2

Equation (3.28) states that the constant concentration wave appears as a straight line in the (z, t) domain when $a = \text{constant}$, as shown in Figure 3.2. This constant concentration line is called the characteristic line. By the definition of 'a' in equation 3.24, the constant concentration travels in (z, t) domain with a velocity equal to the fluid velocity times a factor $1/[1 + K(1-e)/e]$. This constant velocity is often called the concentration wave velocity. Thus as long as the initial condition is known, the concentration in (z, t) domain is given by the method of characteristic. This solution is called the Method of Characteristic since the dependent variable is constant on the characteristic line. This method has been widely applied in the direct mode of parametric pumping.

When the initial conditions and one of the boundary conditions (inlet fluid) are known, the concentration profile can be calculated for a system of parametric pumping. The solution can be solved by graphical method or by digital computer.

For a more complete model, the analytical solution is difficult. For example, when λ is not infinitely large, and D_m is not small enough to neglect the diffusive effect, no analytical solution has been reported to the best of our knowledge. Most results are obtained by applying the numerical method with digital computer calculations.

3.7 : Diffusion Effect of Protein

The diffusivities of hemoglobin and albumin are shown in table 2.1 . It is seen that both proteins have a rather small diffusivity. Since $D_m = 7 \times 10^{-7}$ (cm²/sec), and the gradient is larger than the Laplacian of Y in z direction, the convection term overwhelms the diffusion term in equation (3.9) and the diffusion effect is negligible. In chapter 8, the correlated mass transfer rate constant $\lambda = 5 \times 10^{-3}$ (1/sec), is also much larger than the diffusivity, and again demonstrates that neglecting of the diffusion term in equation (3.9) is reasonable and introduces no significant error.

Chapter 4 : Numerical Method

4.1 : Multi-Cells in Series Model:

The discussion in the last section of chapter 3 allow us to neglect the axial diffusion effect. The lowest backward finite difference of the equation of continuity with $D_m=0$, can be written as follows:

$$\frac{Y(z,t) - Y(z,t-dt)}{dt} + \frac{1-e}{e} \frac{X(z,t) - X(z,t-dt)}{dt} + u \frac{Y(z,t-dt) - Y(z-dz,t-dt)}{dz} = 0 \quad (4.1)$$

When we choose dt and dz in a such way that $dz=u dt$, equation (4.1) can be rearranged and becomes:

$$Y(z,t) - Y(z-dz,t-dt) + \frac{1-e}{e} [X(z,t) - X(z,t-dt)] = 0 \quad (4.2)$$

In order to apply equation (4.2) in parametric pumping, we divide the column (height = h), into N_z cells, thus each cell has a height of dz ($dz=h/N_z$). The time domain is divided into N_t increments of time and thus $dt = dz/u$. We define i for the series number of cells, and j for the series number of time increment. For the convenience of computer calculation, we change the notation (z,t) to (i,j) for the i -th cell and j -th time increment. As shown in Figure 4.1, (i,j) stands for cell of height from $z-dz$ to z , and for time from $t-dt$ to t . Equation


(4.2) can be rewritten to the form:


$$Y(i,j) - Y(i-1,j-1) + \frac{1-e}{e} [X(i,j) - X(i,j-1)] = 0 \quad (4.3)$$

Equation (4.3) states that the change of total mass is zero for the fluid flow from the (i-1)-th cell and the solid in the i-th cell. This equation is the foundation of the STOP and GO method. The Stop and Go algorithm includes the following two steps.

- (1) Go Step: fluid is instantaneously transferred from one cell to the next cell. No interphase mass transfer occurs because the time for fluid transfer is assumed zero.
- (2) Stop : Fluid is stagnant and interphase mass transfer is occurring for a time period $dt=dz/u$.

The algorithm of STOP & GO is also shown in Figure 4.1. It is seen that a column is divided into N_z cells. Figure 4.1(a) shows the STOP step at $t=j-1$, mass transfer is occurring between the adjacent fluid phase and solid phase at each cell ($i-1$, i , $i+1$ in the figure). Figure 4.1(b) shows, at GO step, fluid is transferred up with a displacement equal to the fluid volume of a cell. Fluid originally in (i-1) cell is transferred to i-th cell. Figure 4.1(c) again shows the STOP step after the GO step, mass transfer proceeds between the adjacent solid phase and liquid phase for a time period of dt .

 Solid Phase

 Liquid Phase

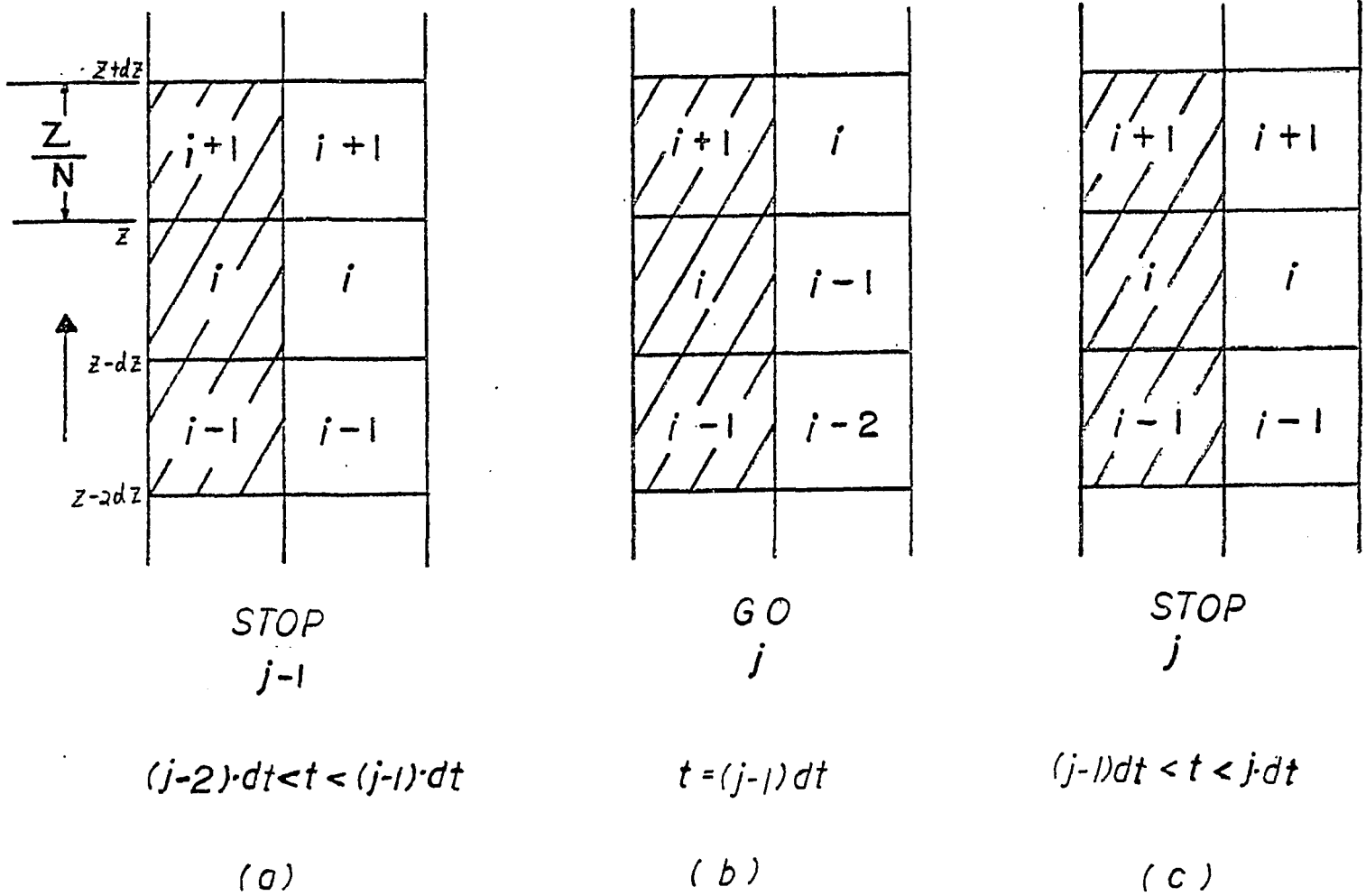


Figure 4.1 Schematic of Multi-Cell Model with Stop & Go Methode.

The interphase mass transfer equation(3.8), can be written in the same form as equation (4.3), and becomes:

$$\frac{\partial X(i,j)}{\partial t} = \lambda [Y(i,j) - Y^*(i,j)] \quad (4.4)$$

for $(j-1) dt < t < j dt$

$$Y^*(i,j) = f' [X(i,j), pH(i,j)] \quad (4.5)$$

pH Model Equations:

When we apply the above approach to the equation (3.12), one can obtain:

$$pH(i,j) = pH(i,j-1) \cdot B + pH(i-1,j-1) \cdot (1-B) \quad (4.6)$$

$$\text{where } B = C_{pf}/(C_{pf}+C_{ps})$$

Equation (4.6) is convenient to use for calculating the pH in each cell by the Stop and Go method and multi-cells model. A more general pH model, as shown in equation (4.7), is considered in multi-cells model. The new pH in thr cell after each transfer step is established according to equation (4.7), is dependent on the pH of fluid flow into the cell and the original pH of the solid phase.

$$\text{pH}(i,j) = \text{pH}(i,j-1) \cdot B + \text{pH}(i-1,j-1) \cdot C \quad (4.7)$$

$$B = B_0 [1 - g \cdot \text{ABS}(\text{pH} - \text{pHRF})] \quad (4.8)$$

The above pH wave equation is rather an empirical model, where B and C are the measures of relative buffer capacities for fluid and solid phase in cell. Note that the pH wave model has its theoretical background instead of arbitrary equation. When $C=0$, the solid phase buffer capacity is none, thus the pH in the column completely depends on the fluid pH. Since the buffer capacity is pH dependent, value B is correlated with pH by equation (4.7). $B=B_0$ at the referenced pH value pHRF. g is a constant and stands for the linear sensitivity of the buffer capacity on pH varied from pHRF. When $g=0$, buffer capacity is independent on pH value, $B=B_0=\text{constant}$. Study of pH wave equation with $B = 1-C = \text{constant}$ has been reported by Wankat.

Equations (4.3), (4.4), (4.5), and (4.7) are used to do the numerical calculation of $\text{pH}(i,j)$, $Y^*(i,j)$, $X(i,j)$, and $Y(i,j)$. The algorithm used here is first to calculate pH by equation (4.7), then substitute equations (4.3) and (4.5) into equation (4.5), and $X(i,j)$ can be solved for the time increment $(j-1) dt - j dt$. After $X(i,j)$ is solved from equation (4.4), $Y(i,j)$ can be obtained from equation (4.3) $X(i,j)$.

When equation (4.3) is substituted into equation (4.4), we

obtain:

$$\frac{\partial X(i,j)}{\partial t} = \lambda \cdot \left\{ Y(i-1,j-1) + \frac{1-e}{e} [X(i,j) - X(i,j-1)] - Y^*(i,j) \right\}$$

(4.9)

for $(j-1) \cdot dt < t < j \cdot dt$

For non-linear equilibrium relation, such as Langmuir equilibrium, equation(4.9) is a non-linear differential equation with respect to $X(i,j)$. A numerical method such as Runge Kutta method can be applied to solve equation (4.5) and(4.9) simultaneously. For linear equilibrium relation, equation (4.5) can be written as:

$$Y^*(i,j) = X(i,j)/K(\text{pH}) \quad (4.10)$$

Substitute equation (4.10) to (4.9), and one can obtain:

$$\frac{\partial X(i,j)}{\partial t} = \lambda \left\{ Y(i-1,j-1) - \frac{1-e}{e} [X(i,j) - X(i,j-1)] - X(i,j)/K(\text{pH}) \right\}$$

(4.11)

for $(j-1) \cdot dt < t < j \cdot dt$

The STOP & GO algorithm assumes that $X(i,j)$ and $Y(i,j)$ are homogeneous in the cell. The $X(i,j)$ is only dependent on time in the time period from $(j-1) \cdot dt$ to $j \cdot dt$. Thus the partial derivative can be replaced by the total derivative in equation (4.11). Thus equation (4.11) becomes a first order linear ordinary differential equation with dependent variable $X(i,j)$, independent variable t , and constants $Y(i-1,j-1)$ and $X(i,j-1)$, which is given in previous ($t=j-1$) calculation. Since the first

order linear ODE always has a solution, one can obtain a solution as shown in equation (4.12) .

$$\begin{aligned}
 X(i,j) &= \frac{Y(i-1,j-1) + R X(i-1,j-1)}{RK} \\
 &+ [X(i,j-1) - \frac{Y(i-1,j-1) + R X(i,j-1)}{RK}] \exp(-\lambda \cdot RK \, dt) \quad (4.12) \\
 \text{where } R &= (1-e)/e \\
 RK &= (1-e)/e + 1/K(\text{pH})
 \end{aligned}$$

4.2 : Application of Local Equilibrium Theory

When local equilibrium is applied, RANDA is infinitely large, and $Y=Y^*$. The equilibrium of X and Y can be written:

$$X(i,j) = f[Y(i,j), \text{pH}(i,j)] = f[Y^*(i,j), \text{pH}(i,j)] \quad (4.13)$$

and equation (4.3) becomes :

$$\begin{aligned}
 Y(i,j) &= Y(i-1,j-1) \\
 &- \frac{1-e}{e} \{f[Y(i,j), \text{pH}(i,j)] - f[Y(i,j-1), \text{pH}(i,j-1)]\} \quad (4.14)
 \end{aligned}$$

Equation (4.14) along with information of pH and equilibrium relations, $f(Y, \text{pH})$, will complete the requirements to calculate the concentration, $Y(i,j)$. To obtain the information in the column, the pH, X, and Y has to be calculated for every cell at every j-th time increment. For a column has N_z cells, and operated for the total time increments equal to N_t , then the total number of calculations is $N_z N_t$. In chapter 9, we

assume the pH wave velocity is equal to the fluid velocity, $B=1.0$ and $C=0.0$. In chapter 10, equation (4.7) is used to correlate the pH, and we assume the equilibrium constant $K(\text{pH})$ is proportional to the pH at the pH range of interest.

4.3 : Single Cell Model

When $N_z=1$, we consider the whole column as a uniformed cell. This single cell model is a lot simpler than multi-cell model. For a system consisting of two reservoirs and one column, we can denote the top reservoir as $i=1$, the column as $i=2$, and the bottom reservoir as $i=3$. Equation (4.14) can be rewritten to give equation of the single cell model, (4.17).

$$Y(2,j) = Y(1,j-1) - \frac{1-e}{e} \{f[Y(2,j),\text{pH}(2,j)] - f[Y(2,j-1),\text{pH}(2,j-1)]\} \quad (4.15)$$

Equation (4.15) gives the new equilibrium concentration of the column, $Y(2,j)$, after the fluid of top reservoir is transferred into the column. The single cell model largely simplify the mathematical calculation and still gives qualitative accuracy. It is attractive because of its simplicity and its handiness when dealing with a complicated process.

Chapter 5 : Separation of Parapump in Single Cell Model

As stated in chapter 4 , the single cell model describes the behavior of a uniform column. In the real world the column may not be completely uniform, but the single cell model is desired because of its simplicity and capability in qualitative prediction. In this chapter we will use this model to examine some simple cases of parametric pumping.

5.1 : Analytical Solution for Linear Equilibrium Iso-pH

As an illustration in this section, an analytical solution is derived from finite difference equation for an One-Column Batch Parapump. Equation (4.15) is applied to examine the behavior of the One-Column Batch Parametric Pumping, as shown in Figure 5.1 . Under the single cell model, the whole column is considered completely uniform, and the entire fluid in either reservoir is in equilibrium with the entire solid phase. We denote the total solid volume in the packed bed column as V_s , and the total fluid volume in equilibrium with the solid phase as V_R , of which includes the void volume of column and the reservoir dead volume. Since a solid volume V_s is in equilibrium with the fluid volume V_R , therefore e and $1-e$ in equation (4.15) can be replaced by V_R and V_s . It is convenient to write $\langle Y_T \rangle_j$ for $Y(1,j)$, and $\langle Y_B \rangle_j$ for $Y(3,j)$.

We further change j to n where n stand for the number of cycles in parametric punmping operation. It is seen in Figure 5.1 that $Y(2,j) = Y(3,j) = \langle YB \rangle_n$ for $j=2n$, and $Y(2,j) = Y(1,j) = \langle YT \rangle_n$ for $j=2n-1$. We can write the mass blance for the $(n-1)$ th cycle and the n -th cycle (j from $2(n-1)-1$ to $2n$) as the following equations.

$$\langle YB \rangle_{n-1} K_{p1} Vs + \langle YT \rangle_{n-1} VR = \langle YT \rangle_{n-1} (VR+Vs K_{p2}) \quad (5.1)$$

$$\langle YT \rangle_n K_{p2} Vs + \langle YB \rangle_{n-1} VR = \langle YB \rangle_n (VR+Vs K_{p1}) \quad (5.2)$$

rearrange equation (5.2), and one obtains:

$$\langle YT \rangle_n = \langle YB \rangle_{n-1} \frac{-VR}{K_{p2} Vs} + \langle YB \rangle_n \frac{(VR+Vs K_{p1})}{K_{p2} Vs} \quad (5.3)$$

For $(n-1)$ -the cycle equation (5.3) can be rewritten as:

$$\langle YT \rangle_{n-1} = \langle YB \rangle_{n-2} \frac{-VR}{K_{p2} Vs} + \langle YB \rangle_{n-1} \frac{(VR+Vs K_{p1})}{K_{p2} Vs} \quad (5.4)$$

Substitute equations (5.3) and (5.4) to (5.1), one can obtain:

$$\langle YB \rangle_n + b \langle YB \rangle_{n-1} + c \langle YB \rangle_{n-2} = 0 \quad (5.7)$$

where

$$- b = \frac{1 + p q}{p q} \quad (5.8)$$

$$- c = \frac{1}{p q} \quad (5.9)$$

and

$$p = 1 + K_{p2} Vs/VR \quad (5.10)$$

$$q = 1 + K_{p1} Vs/VR \quad (5.11)$$

Apply the finite difference operator to equation (5.10), one obtains:

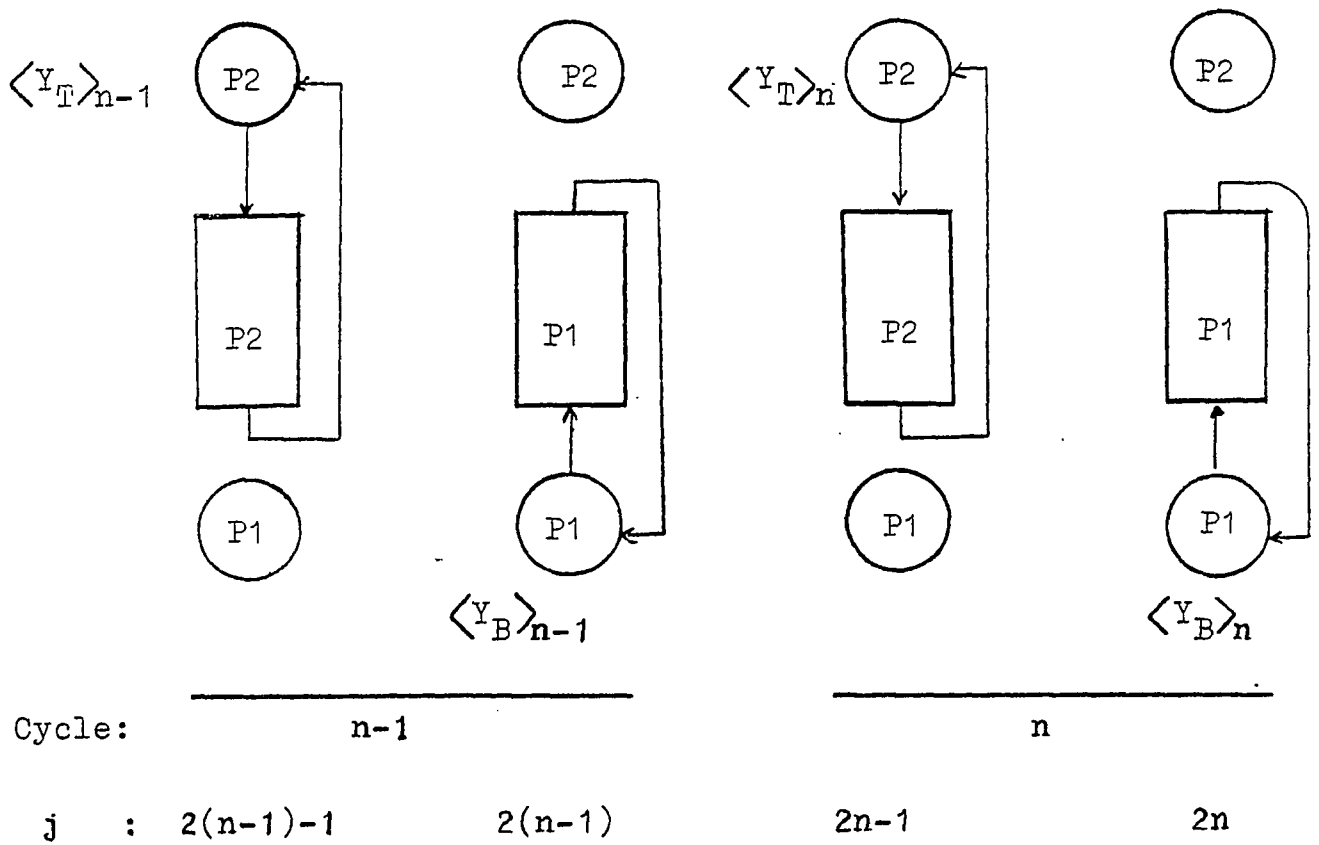


Figure 5.1 Description of An Elementary Batch Parapump
at Operation Cycle (n-1) and n.

$$(E^2 + b E + C) \langle YB \rangle_n = 0. \quad (5.14)$$

Equation (5.14) is a second order linear finite difference equation (F.D.E.) and E is the finite difference operator. Two boundary conditions are required to obtain the complete solution for a 2nd order F.D.E.

$$\text{at } n=0, \quad \langle YB \rangle_0 = Y_0 \quad (5.15)$$

at $n = 1$, $\langle YB \rangle_n$ can be calculated from $\langle YB \rangle_0$ and $\langle YT \rangle_0$

$$\langle YB \rangle_1 = Y_0 \quad (p + pq) / (p q) \quad (5.16)$$

Solve equation (5.14) with (5.15) and (5.16), one obtains the complete solution as follows:

$$\frac{\langle YB \rangle_n}{Y_0} = \frac{(p-1)(q+1)}{p q - 1} + \frac{q-p}{p q - 1} (p q)^{-n} \quad (5.17)$$

By applying the same procedure for the top reservoir, one can obtain the solution for $\langle YT \rangle_n$ as:

$$\frac{\langle YT \rangle_n}{Y_0} = \frac{(q+1)(q-1)}{p q - 1} + \frac{q(p-q)}{p q - 1} (p q)^{-n} \quad (5.18)$$

and the separation factor $\langle YB \rangle_n / \langle YT \rangle_n$, can be obtained by dividing equation (5.17) by equation (5.18), and becomes:

$$SF_n = \frac{\langle YB \rangle_n}{\langle YT \rangle_n} = \frac{(p-1)(q+1) + (q-p)(p q)^{-n}}{(q+1)(q-1) + (p q - q)(p q)^{-n}} \quad (5.19)$$

When n is very large, equation (5.19) becomes:

$$SF_{ss} = \frac{K_{p2}}{K_{p1}} \quad (5.20)$$

The final separation factor is equal to the ratio of K_{p2} to K_{p1} . When K_{p1} is equal to K_{p2} , no separation will be achieved. Separation is obtainable as long as K_{p1} is not equal to K_{p2} . Equation (5.20) also gives the following important information.

$$\langle YB \rangle_{ss} K_{p1} = \langle YT \rangle_{ss} K_{p2} = \langle XT \rangle_{ss} = \langle XB \rangle_{ss} \quad (5.20-a)$$

The above relations state that the final concentration is established when the solid phase equilibrates with both the fluid in top reservoir and in bottom reservoir.

5.2 : Short-Cut Steady State Solution for Single Cell Model

From the previous section, when the concentration of the solid phase reaches equilibrium with the concentration of both fluids in top and bottom reservoirs, no further mass transfer between phases occurs, and the concentration of solid phase reaches a final value. The steady state solution is obtainable without involving the transit concentration by applying the equilibrium criterion- $\langle XT \rangle_{ss} = \langle XB \rangle_{ss}$. The mass balance for a cycle in steady state can be written as follows:

$$V_s \langle XB \rangle_{ss} + V_{DT} \langle YT \rangle_{ss} = V_{DT} \langle YT \rangle_{ss} + V_s \langle XT \rangle_{ss} \quad (5.21-a)$$

$$V_s \langle XT \rangle_{ss} + V_{RB} \langle YB \rangle_{ss} = V_{RB} \langle YB \rangle_{ss} + V_s \langle XT \rangle_{ss} \quad (5.21-b)$$

The total mass of system in steady state is equal to the initial state mass and can be written as:

$$W_s = V_{RT} \langle YT \rangle_o + V_{RB} \langle YB \rangle_o + V_s \langle X \rangle_o \quad (5.22-a)$$

$$= V_{RT} \langle YT \rangle_{ss} + V_{RB} \langle YB \rangle_{ss} + V_s \langle X \rangle_{ss} \quad (5.22-b)$$

The steady state criterion is:

$$\langle XB \rangle_{ss} = \langle XT \rangle_{ss} = X_{ss} \quad (5.23)$$

The equilibrium relations of Y and X are:

$$\langle YB \rangle_{ss} = f'(\langle XB \rangle_{ss}) = f'(X_{ss}, P1) \quad (5.24-a)$$

$$\langle YT \rangle_{ss} = f'(\langle XT \rangle_{ss}) = f'(X_{ss}, P2) \quad (5.24-b)$$

The 5 independent equations 5.23 to 5.26 can be solved for 5 unknowns, $\langle YT \rangle_{ss}$, $\langle YB \rangle_{ss}$, $\langle X \rangle_{ss}$, $\langle XB \rangle_{ss}$, and $\langle XT \rangle_{ss}$.

We then apply the following linear equilibrium relations.

$$\langle Y \rangle = f'(\langle X \rangle, pH) = \langle X \rangle / K(pH) \quad (5.25)$$

$$\langle Y_T \rangle_{ss} = X_{ss}/K_{P2} \quad (5.26)$$

$$\langle Y_B \rangle_{ss} = X_{ss}/K_{P1} \quad (5.27)$$

We can obtain X_{ss} by substituting (5.26) and (5.27) into (5.23).

$$X_{ss} = \frac{W_s}{\frac{VRT}{K_{P2}} + \frac{VRB}{K_{P1}} + V_s} \quad (5.28-a)$$

$$\langle Y_T \rangle_{ss} = \frac{W_s/K_{P2}}{\frac{VRT}{K_{P2}} + \frac{VRB}{K_{P1}} + V_s} \quad (5.28-b)$$

$$\langle Y_B \rangle_{ss} = \frac{W_s/K_{P1}}{\frac{VRT}{K_{P2}} + \frac{VRB}{K_{P1}} + V_s} \quad (5.28-c)$$

and the steady state separation factor is:

$$SF_{ss} = \frac{\langle Y_B \rangle_{ss}}{\langle Y_T \rangle_{ss}} = \frac{f'(X_{ss}, P1)}{f'(X_{ss}, P2)} = \frac{K_{P2}}{K_{P1}} \quad (5.29)$$

Here the results agree with those in the previous section. It is seen this method gives a quick result of final separation based on the single cell model. The same procedure can be applied to a two-column batch parametric pumping as shown in Figure 5.2(a). The results are as follows: results.

$$\langle Y_T \rangle_{ss} = (W_s/D) K_{P2}^+ K_{P1}^- / K_{P2}^- \quad (5.30)$$

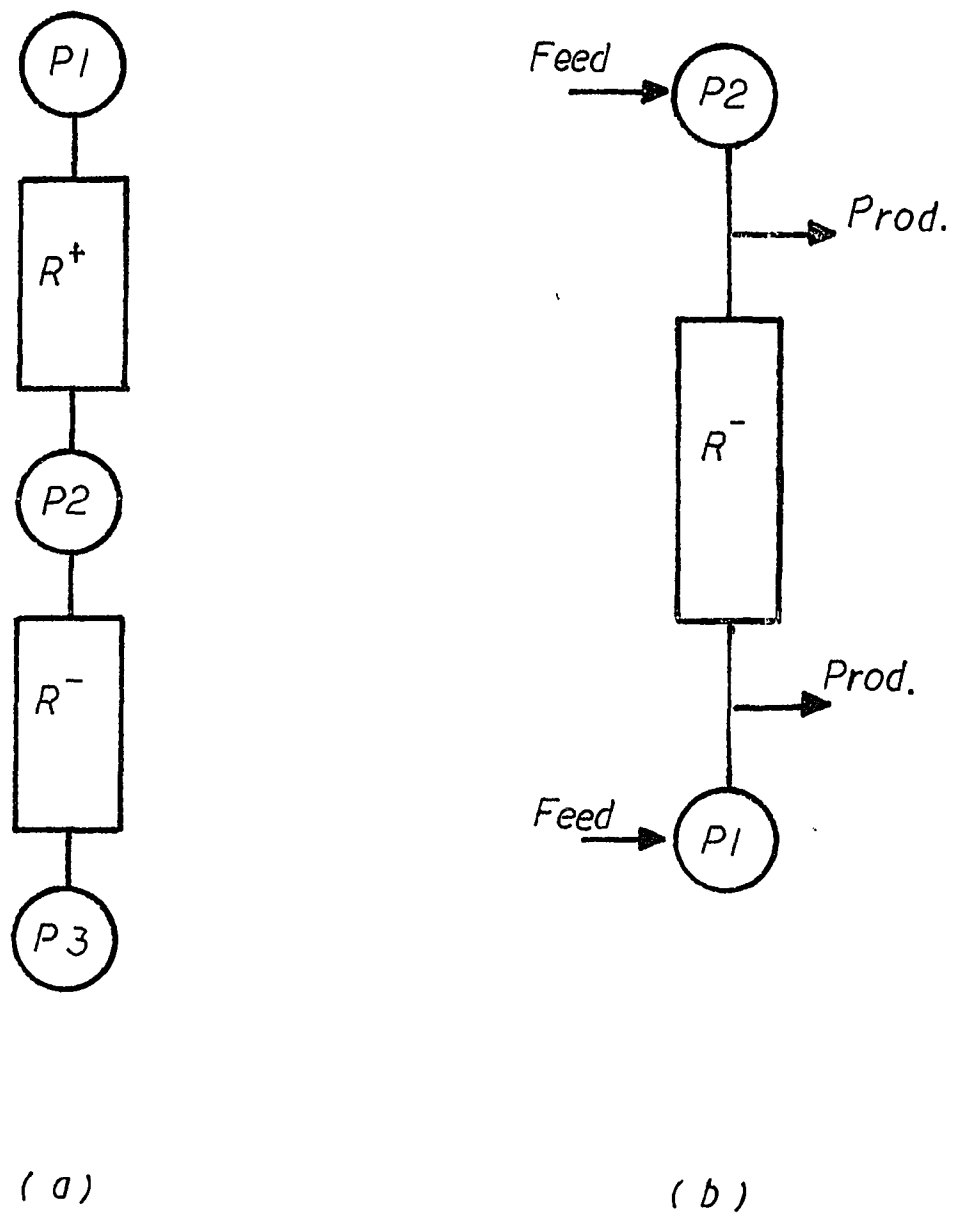


Figure 5.2 Schematic Diagram for (a) Two-Column Parapump
(b) One-Column Open Parapump

$$\langle Y_M \rangle_{ss} = (W_s/D) \cdot K_{P1}^+ \cdot K_{P1}^- / K_{P2}^- \quad (5.31)$$

$$\langle Y_B \rangle_{ss} = (W_s/D) K_{P1}^+ \quad (5.32)$$

$$SF_{ss} = \frac{\langle Y_B \rangle_{ss}}{\langle Y_T \rangle_{ss}} = \left(\frac{K_{P1}^+}{K_{P2}^+} \right) \left(\frac{K_{P2}^-}{K_{P1}^-} \right) \quad (5.33)$$

$$\text{wher } W_s = (V_R + V_s K_{P1}^-) \cdot Y_o + (V_R + V_s K_{P2}^+) \cdot Y_o + V_R \cdot Y_o$$

$$D = K_{P1}^+ \cdot (V_R + V_s K_{P1}^-) + V_R \cdot K_{P2}^+ \cdot K_{P1}^- / K_{P2}^- + K_{P1}^+ \cdot (V_R + V_s K_{P2}^+) \cdot K_{P1}^- / K_{P2}^-$$

and V_R : fluid volume in each reservoir
 V_s : solid volume in each column

Since the two column parametric pumping consists two kind of ionic exchanger, the equilibrium constant K is function of the pH and the type of ionic exchanger. The above result assumes that $X = f(Y, \text{pH}, \text{Exchanger}) = K(\text{pH}, \text{Exchanger}) Y$. We have also denoted $K(p_1, \text{Cation Exchanger})$ as K_{P1}^- , $K(p_2, \text{Anion Exchanger})$ as K_{P2}^+ , and so on. For multi-column batch parametric pumping with two pH level- p_1 and p_2 , it is easy to derive the steady state separation factor as shown in equation (5.36), in which the 1, 2, 3, ... stand for the series number of columns.

$$SF_{ss} = \left(\frac{K_{P1}^-}{K_{P2}^+} \right)_1 \left(\frac{K_{P2}^+}{K_{P1}^-} \right)_2 \left(\frac{K_{P1}^-}{K_{P2}^+} \right)_3 \left(\frac{K_{P2}^+}{K_{P1}^-} \right)_4 \dots \quad (5.36)$$

The steady state solution is obtainable for a one column open parapump as shown in Figure 6.2(b). The open parapump has feed introduced into the resevoir and product withdrawing from

the system. When we apply the above procedures, one can obtain the following results.

$$\langle YB \rangle_{ss} = \frac{Y_o(1+2 K_{P2} Vs/F)}{1 + (K_{P1}+K_{P2}) Vs/F} \quad (5.37)$$

$$\langle YT \rangle_{ss} = \frac{Y_o(1+2 K_{P1} Vs/F)}{1 + (K_{P1}+K_{P2}) Vs/F} \quad (5.38)$$

$$SF_{ss} = \frac{1+2 \cdot K_{P2} \cdot Vs/F}{1+2 \cdot K_{P1} \cdot Vs/F} \quad (5.39)$$

Where F : the feed per half cycle = product per half cycle

The steady state solution for more complicated system in single cell model is possible. This thesis only includes the above results as illustrations. as examples.

5.3 : Graphic Method in Single Cell Model

Equation (4.15) can be rewritten as:

$$\frac{f[Y(i,j)] - f[Y(i,j-1)]}{Y(i,j) - Y(i,j-1)} = \frac{X(i,j) - X(i,j-1)}{Y(i,j) - Y(i,j-1)} = \frac{-e}{1-e} \quad (5.40)$$

Equation 5.40 states that the mass conservation gives a straight line on the (Y,X) domain with a slope = $-e/(1-e)$. As shown in Figure 5.3, from a given point of $[Y(i-1,j-1),$

$X(i,j-1)$], the point $[Y(i,j), X(i,j)]$ will lie on the straight line of slope = $-e/(1-e)$ which passes through the point $[Y(i-1,j-1), X(i,j-1)]$. When further constraint is applied to the system, such as the equilibrium constraint $X=f(Y)$, then the point $[Y(i,j), X(i,j)]$ must also lie on the equilibrium curve $X = f(Y)$. Thus the point $[Y(i,j), X(i,j)]$ must be the intersection point of equilibrium curve and the mass conservation line as shown in Figure 5.3 . The above graphical method is applied further to batch parapumps, and is described in more detail in chapter 7. In this chapter, we has seen that 3 methods are applicable with the single cell model to obtain a quick prediction of separation by parametric pumping.

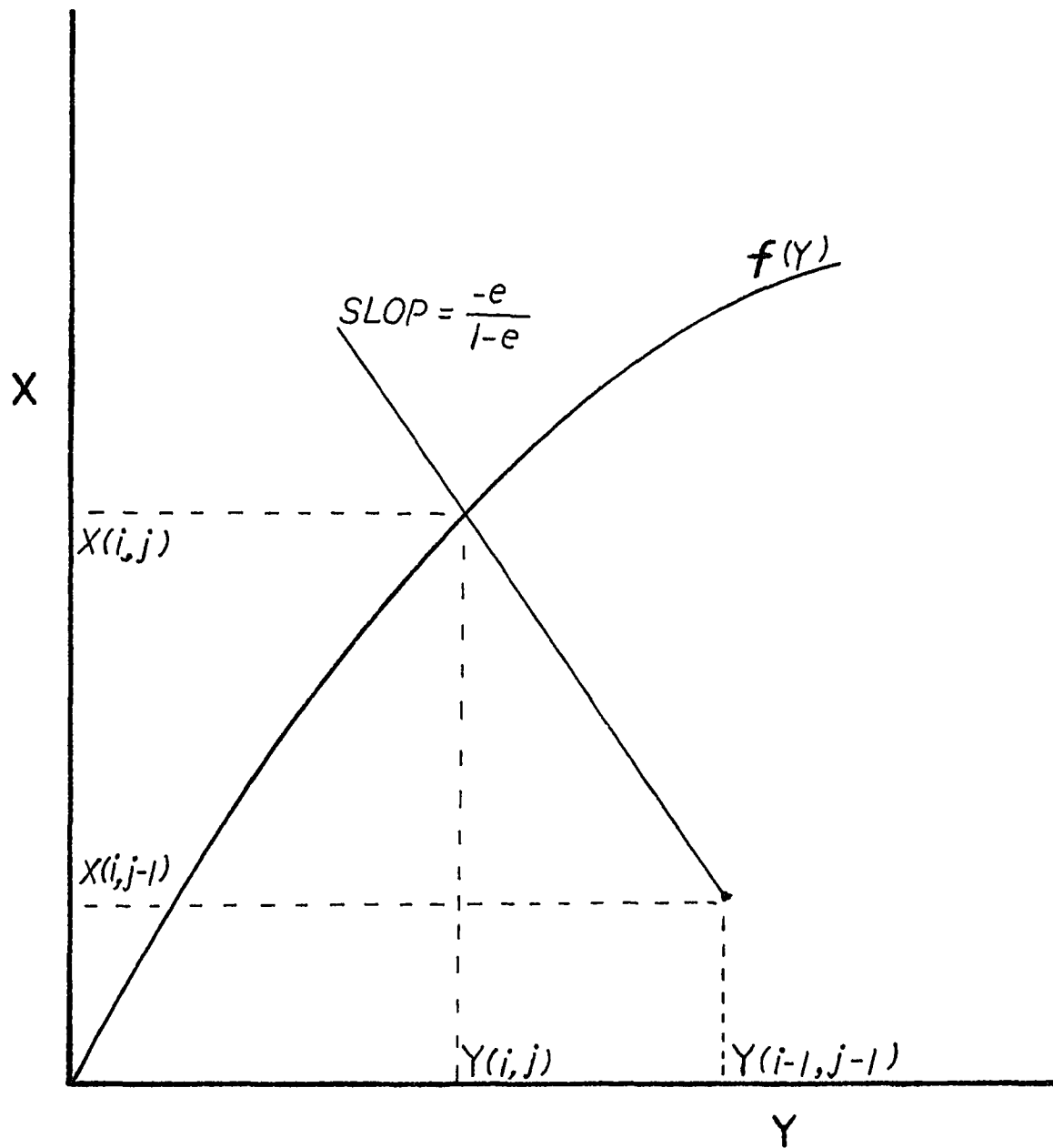


Figure 5.3 Graphical Method in Single Cell Model

Chapter 6 : Experimental Study

The theoretical study in the previous chapter gives a theoretical demonstration and prediction of separation capability by parametric pumping. The experimental studies are carried out to test the behavior, and to demonstrate the separation by parametric pumping. Nevertheless, experimental results are required to determine the parameters for a given system, and to verify the validity of the theoretical model.

6.1 : System

In this thesis, the system chosen for experimental study is hemoglobin - albumin - buffer solution - solid adsorbent. The adsorbents used are CM-Sepharose cation exchanger and Deae-Sepharose anion exchanger (manufactured by Phamacia Fine Chemical Co.). The ionic exchangers are cross linking styrene base resin, and the particle size is ranging from 40 to 160 μ (micron), and porosity is about 0.75 at normal operation condition. The properties of hemoglobin and albumin have been described in more detail in Chapter 2.

6.2 : Apparatus

A typical experimental apparatus for two-column parapump is schematically shown in Figure 6.1 . The apparatus consists of two chromatographic columns(manufactured by Phamarcia Fine Chemicals Co.) and 3 reservoirs connected by the 2 columns. The temperature of the columns and reservoirs are controlled to 5 - 10 degree centigrade by circulating a heat transfer medium in the thermostat jackets. The inside diameter of the column is 16 mm. One column is packed with Deae-Sepharose anion exchanger and the other with CM-Sepharose cation exchanger(manufactured by Phamarcia Fine Chemicals). The fluid flow within the columns is reciprocating and pumped by two P-3 peristaltic reversible pumps. The pumps are wired to a timer controller to control the flow direction and flow displacement. The pH level in the reservoirs is maintained constant by titrating with hydrochloric acid and sodium hydroxide solutions. Magnetic stirrers are used to ensure complete mixing with the titration in the reservoir. Three hollow fiber dialyzers(manufactured by Spectrum) were used to keep the ionic strength constant for the solution in the reservoirs. The dialyzer consists of membrane bundles which allow the small molecules such as buffer ions and water molecules to flow through the membrane while the large molecules, such as protein, can not permeate through the membrane. In operation, the protein solution flows inside the hollow fiber bundles and the buffer solution flows outside of the bundles. For

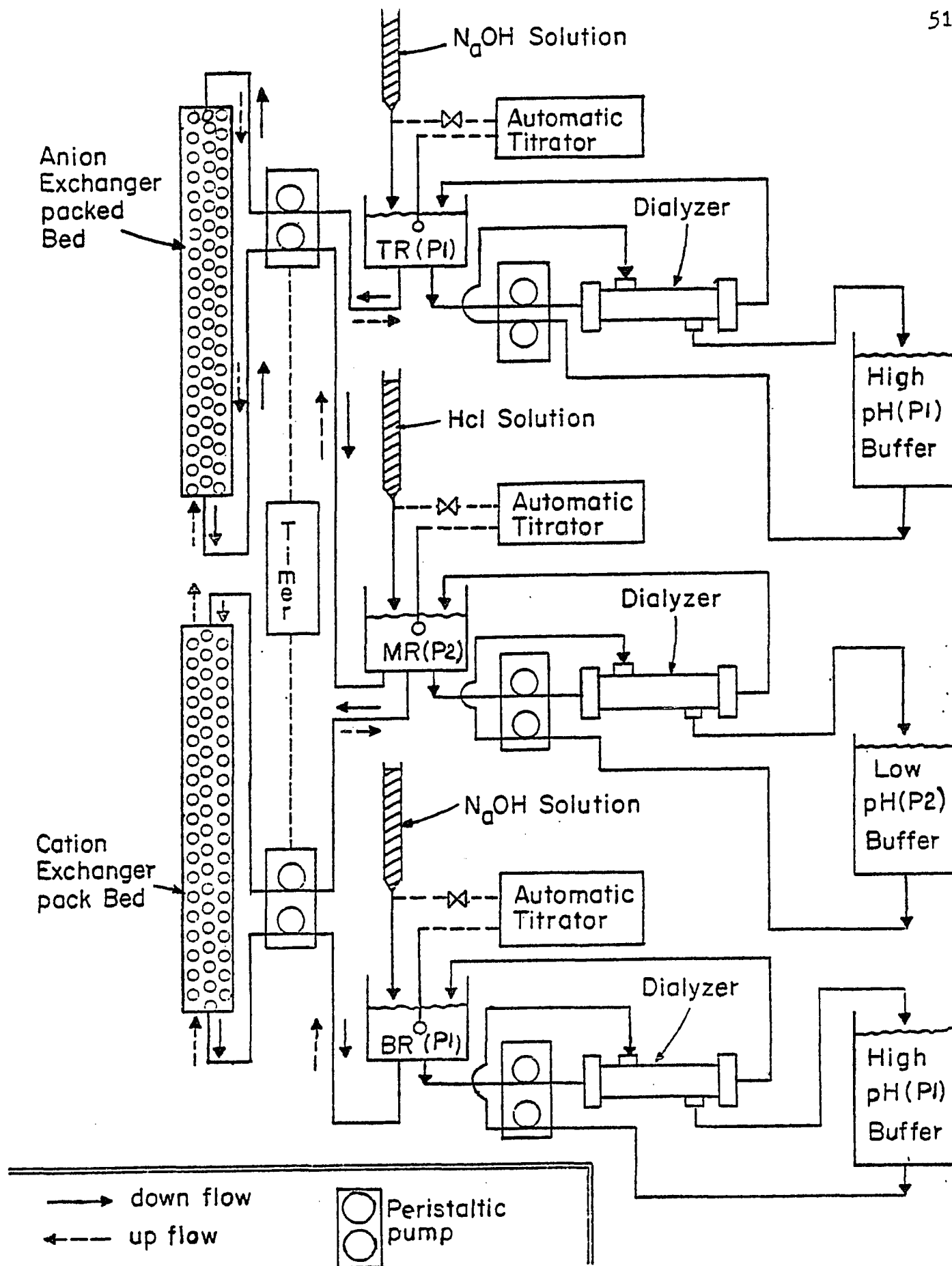


Figure 6.1 Experimental Apparatus of Two-Column Parapump

multi-column parapump, the apparatus includes more columns and reservoirs. The fundamental functions and operations of the apparatus for multi-column parapumps is same as that in two columns parapumps.

6.3 : Analytical Apparatus

The experimental results of parapump is examined in terms of the concentration of the product stream for open parapump and the concentration of the solution in the reservoirs for batch parapump. A spectrophotometer (Bausch & Lomb-710) is used to measure the concentration of proteins. To identify the concentration of individual species from a mixture of two components, at least two independent measurement are required. The method applied in this thesis is first to determine the hemoglobin concentration directly from the absorbance at wavelength=403 μ (millimicron), and then to determine the total proteins by the Bio-Rad Protein assay at wavelength=595 μ . The concentration of albumin is obtained by subtract the hemoglobin from the total proteins.

The absorbance of hemoglobin at 403 μ is strongly dependent on the pH level of the solution. Figure 6.2 shows the relative absorbance of hemoglobin for pH range of 4.0 to 8.5, with a standard absorbance equal to unity at pH=6.0 . Figure 6.2 is

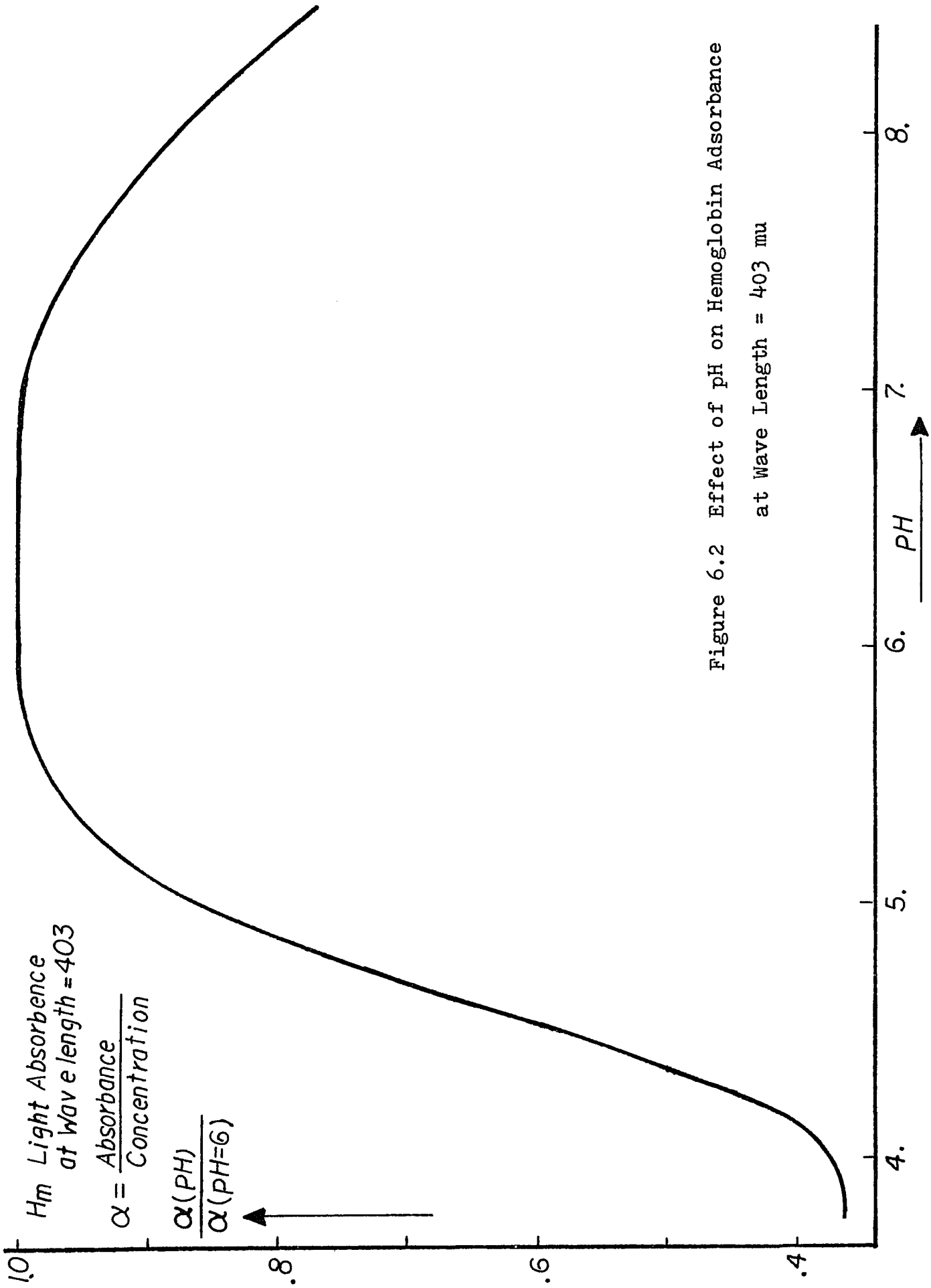


Figure 6.2 Effect of pH on Hemoglobin Adsorbance
 at Wave Length = 403 mμ

used to calculate the hemoglobin concentration for pH variance.

6.4 : Modes of Operation

Many modes of operation have been experimentally studied in this thesis. For a system of single solute, such as Albumin-Buffer Solution-Adsorbent and Hemoglobin-Buffer Solution-Adsorbent, experiments have been run by one-column and two-column parapump. System of two solutes, hemoglobin and albumin in buffer solution, has been experimentally studied in one-column and two-column parapumps. Among the two-column parapumps, there are many different operation modes. The experimental results for batch parapump is discussed in chapter 7 and 8, the semi-continuous one-column parapump in chapter 9, and the cycling zone in chapter 10. Included in chapter 7, 8, 9, and 10 are also the theoretical correlation and results by computer exploration. Experimental data for columns more than or equal to 3 is not included in this thesis.

Chapter 7 : Separation of Binary System with Single Cell Model

Studies of a binary system (1 solute in buffer solution) is presented in this chapter. Included are the graphical method, the theoretical prediction by single cell mode and the experimental results.

7.1 : One Column Batch Parapump

The one-column parapump consists of a column packed with an ion exchanger (cation or anion) and two reservoirs attached to each end. The parapump has dead volumes VDT and VDB for the top and bottom reservoirs, respectively. Initially, the mixture to be separated fills the column voids, the top reservoir, and the bottom dead volume. The top reservoir is maintained at a low pH level(P2) by an automatic titrator while a second titrator is used to keep the bottom reservoir at a high pH level(P1). The buffer ionic strengths of the solutions in both top and bottom reservoirs are kept at IS2 and IS1, respectively, by means of two hollow fiber dialyzer. The flow procedure(see Figure 3.1) has four distinct steps in each cycle:

- (I) The low pH(P2) fluid from the top reservoir enters the top of the column, while the solution emerging from the other end enters the bottom reservoir. The displacement Qt_I is set to be equal to the void volume of the column VE; that is, $Qt_I=VE$.

- (II) Circulation between the top reservoir and the column: This will ensure a complete shift of the pH and ionic strength in the column to P2 and IS2, respectively. Also, at the end of the step, the concentrations in both top reservoir and column are identical.
- (III) The high pH(P1) fluid from the bottom reservoir enters the bottom of the column, and the solution emerging from the other end enters the top reservoir, with the displacement $Qt_{III} = VE$, and
- (IV) Circulation between the column and the bottom reservoir: This will allow the pH and ionic strength to shift back to P1 and IS1, respectively, and at the end of the step the concentration in the column will be the same as that in the bottom reservoir.

Note that the flow rate within the column is always equal to reservoir displacement rate Q . The duration of circulation t_{II} or t_{IV} , which can be determined experimentally, depends on VE and VDB (or VDT), pH, and the ionic strength in both the column and reservoir. Figure 7.1 is a graphical solution for one-column system. The assumptions made here are:

- (1) The solute will be distributed between the solid and fluid phases according to the function,

$$X = f(Y, \text{pH}) \quad (7.1)$$

- (2) The duration of circulation t_{II} or t_{IV} , is long enough so that at the end of the step II or IV a phase equilibrium is established.

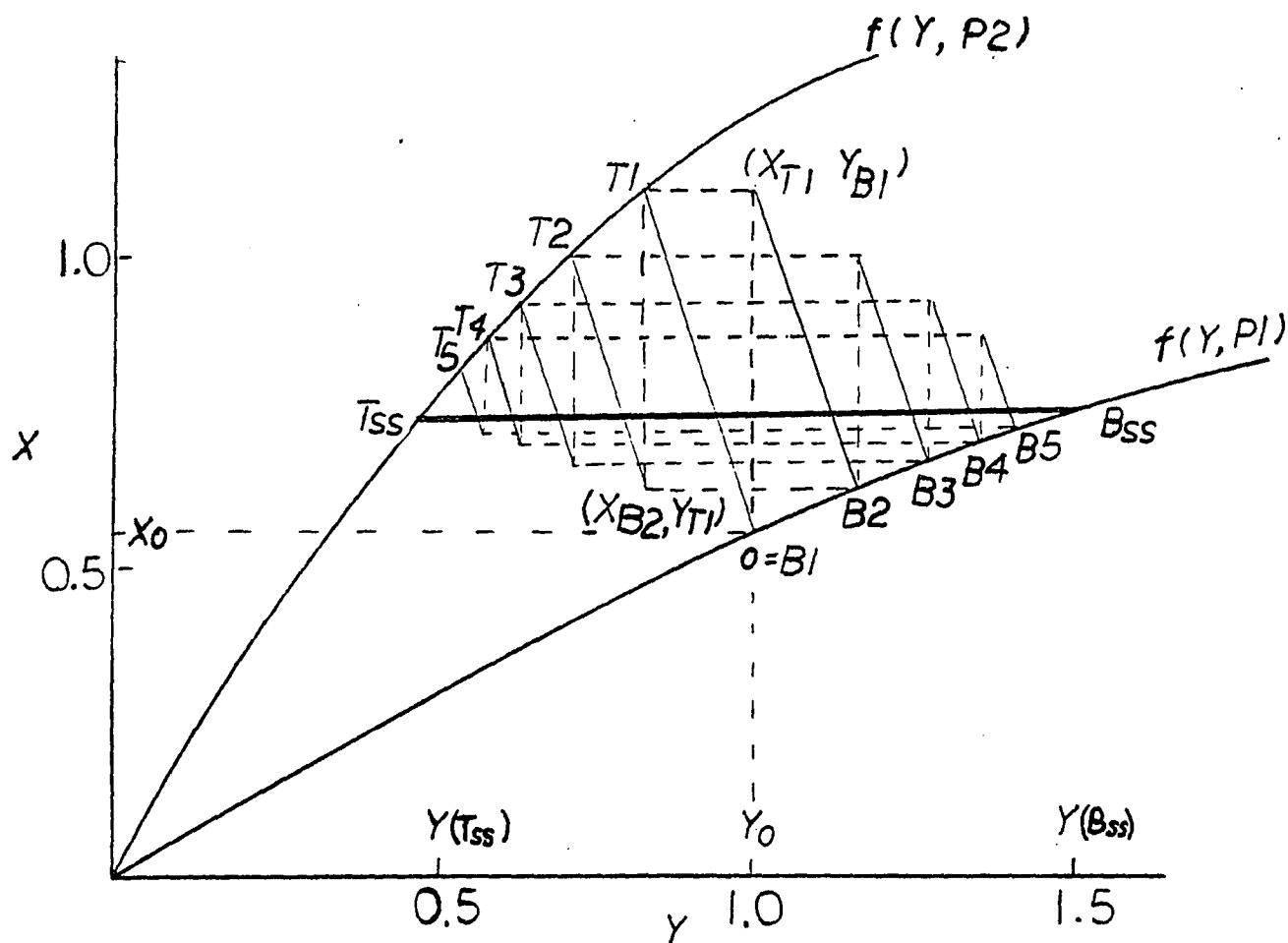
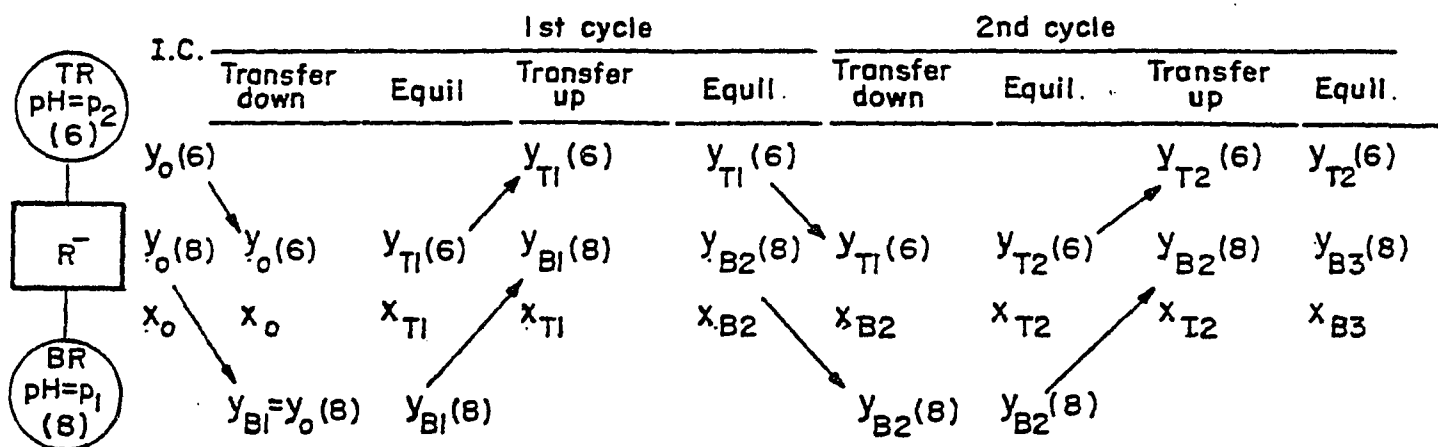


Figure 7.1 Graphical Solution for a One-Column Parapump

Figure 7.1 shows that a parapump consists of a column packed with cation exchanger and two reservoirs attached to each end. The pH values of the top and bottom reservoirs are maintained at given levels $P_2(=6.)$ and $P_1(=8.)$, respectively. The operation begins with the column filled with a mixture of concentration Y_0 , everywhere at equilibrium with the solid. The initial pH in the column is high (P_1). Also, there is fluid of the same initial concentration in the top and bottom reservoir. The dead volume of the two reservoirs are equal ($V_{DT}=V_{DB}$). Let X and Y be the concentrations of A in the solid phase and fluid phase, respectively. Using Equation 7.1, we draw two equilibrium curves $f(Y, P_1)$, $f(Y, P_2)$ on a X - Y diagram. The initial concentration in the column ($Y_0; X_0$) is represented by the point O . One cycle of the operation includes four steps, and the effect of the operation for the first cycle is as follows:

(1) Transfer down: The fluid in the TR (top reservoir) is transferred to the column, and the fluid in the column is transferred to the BR (bottom reservoir). Therefore, the bottom reservoir concentration for the first cycle is Y_0 .

(2) Circulation and equilibration at P_2 : The column pH is changed from P_1 to P_2 . The two phases are then allowed to equilibrate at P_2 . This leads to a new composition in the column, $[Y(T_1); X(B_1)]$, represented by the point T_1 . The point is located at the intersection of equilibrium curve $f(Y; P_2)$ and of the operation line passing through $(Y_0; X_0)$. The slope of the

operation is ST, and is obtained by the mass balance constraint, i.e.,

$$ST Y(T(n-1)) + X(Bn) = ST Y(Tn) + X(Tn) \quad (7.2)$$

where $n = 1, 2, 3, \dots$

$$ST = - \frac{VDT + VE}{Vs} \quad (7.3)$$

(3) Transfer Up: The solution in the column is brought to the TR and the solution in the BR is returned to the column. The composition in the column is now $(Y(B1); Y(T1))$.

(4) Circulation and equilibration at P1: The column pH is shifted back to P1. A phase equilibrium is reestablished. The new equilibrium point $(Y(B2); X(B2))$, represented by the point B2, is located at the intersection of the equilibrium curve $f(Y, P1)$ and of the operation line passing through $(Y(B1); X(T1))$ and having a slope of SB, and is obtained from the following mass balance,

$$SB Y(B(n-1)) + X(T(n-1)) = SB Y(Bn) + X(Bn) \quad (7.4)$$

where $n = 1, 2, 3, \dots$

$$SB = - \frac{VDB + VE}{Vs} \quad (7.5)$$

This completes the first cycle. The second cycle will start from a transfer of the fraction $Y(T1)$ from the TR to the column and the fraction $Y(B2)$ to the BR. We then follow the steps described above (see Figure 7.1). If the procedures are repeated

in each of the succeeding cycles, one can see that as n becomes large, the top and bottom reservoir concentrations will approach steady values, i.e., $Y(T_{ss})$ and $Y(B_{ss})$, respectively. At steady state, the solid phase has a constant composition which is in equilibrium with both $Y(T_{ss})$ and $Y(B_{ss})$, i.e.,

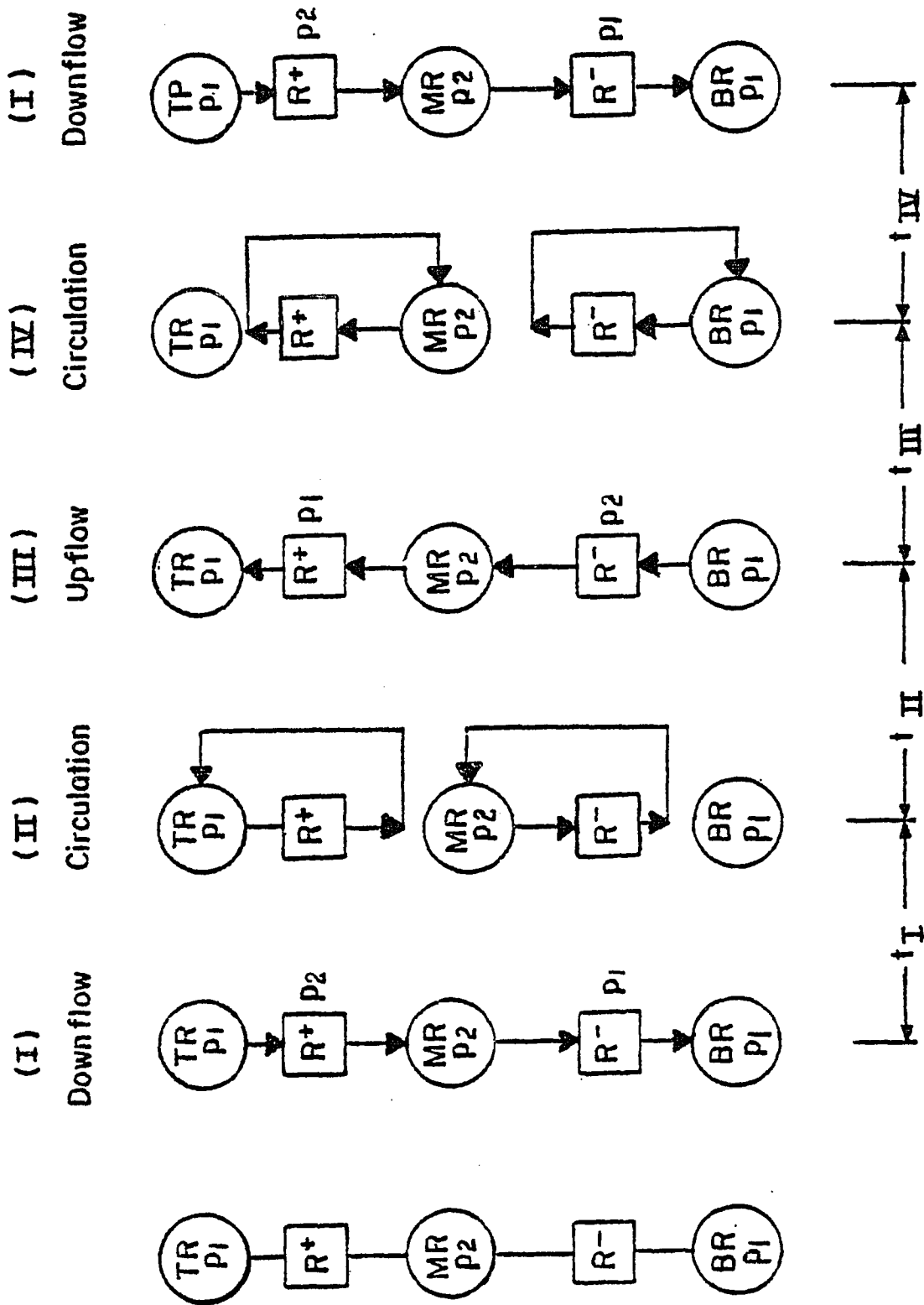
$$X_{ss} = f[Y(B_{ss});P_1] = f[Y(T_{ss});P_2] \quad (7.6)$$

and therefore, the line $\overline{T_{ss} B_{ss}}$ must be parallel to the horizontal axis.

7.2 : 2-column batch parapump

The 2-column parapump consists of two columns and three reservoirs as shown in Figure 7.2. One of the columns is packed with a cation exchanger (R^-) and the other with an anion exchanger (R^+). The pH level for the top and bottom reservoirs is maintained at $P_1(=8.)$ and that for the middle reservoir is kept at $P_2(=6.)$. Initially, the top reservoir and both columns are filled with a mixture of the concentration Y_0 . The R^- and R^+ columns are respectively in equilibrium at $P_1(=9.)$ and $P_2(=6.)$. As shown in Figure 7.2, one cycle of operation is described as follows:

- (I) Pump the fluid from the top reservoir (TR) through the R^+ column, the middle reservoir (MR) and the R^- column to the bottom reservoir (BR), for time t_I .
- (II) Circulation the fluid between the TR and the R^+



Mode I : $IB < p_2 < IA < p_1$

Figure 7.2 Description of A Two-Column Parumpump Operation

column, and between the MR and the R^- column, for time t_{II} .

(III) Pump the fluid from the bottom reservoir through the R^- column, MR and R^+ column to the top reservoir, for time t_{III} , and

(IV) Circulate the fluid between the MR and the R^+ column, and between BR and the R^- column.

The procedure is repeated for each of succeeding cycles. The graphical representation is shown in Figure 7.3. In this figure, the linear equilibrium relationship is assumed and $f(Y, pH, EX) = K(pH, EX) Y$. Since the parapump consists 2 types of exchanger (EX) and 2 pH levels, there are four equilibrium lines with slope respectively, K_{P1}^+ , K_{P2}^+ , K_{P1}^- , and K_{P2}^- . K_{P1}^- and K_{P2}^- are the equilibrium constants for solute A in the R^- column, while K_{P1}^+ and K_{P2}^+ are for A in the R^+ column. For the purpose of illustration, we further assume that $K_{P2}^- = K_{P1}^+$ and $K_{P1}^- = K_{P2}^+$. However, other conditions are conceivable. The graphical construction is similar to that described for the one column system. From Figure 7.3 $Y(Tss)$, $Y(Mss)$ and $Y(Bss)$ are respectively the steady state concentrations for the top, middle, and bottom reservoirs. Connecting the points Tss, Mss', Mss'', and Bss, a two step staircase is formed. Note that at steady state, the concentration in the middle reservoir is such that it is in equilibrium with both cation and anion exchangers at P2, i.e.,

$$X^+ = K_{P1}^+ Y(Tss) = K_{P2}^+ Y(Mss) \quad (7.7)$$

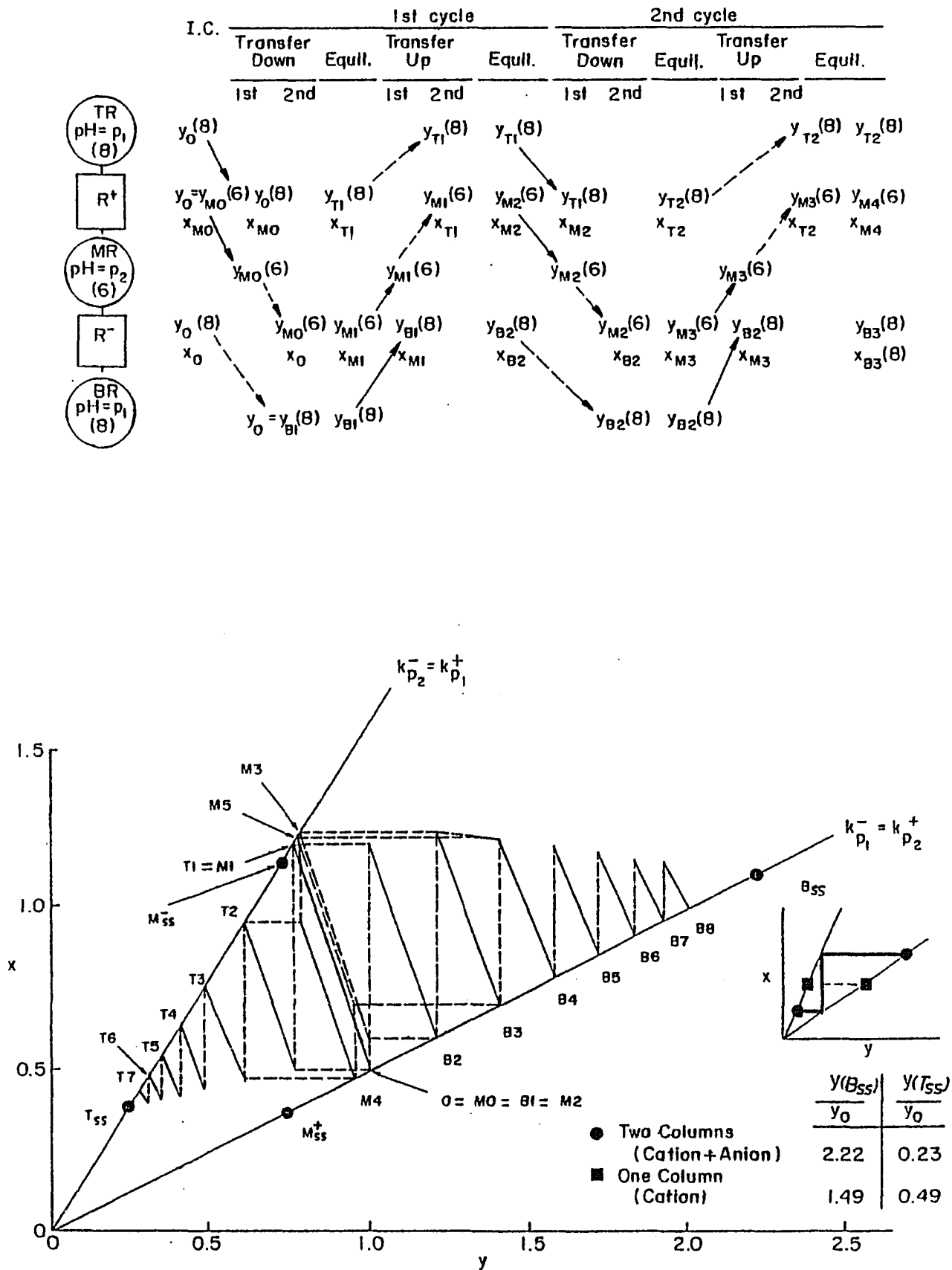


Figure 7.3 Graphical Solution for Two-Column Batch Parapump

$$X^- = K_{P1}^- Y(Bss) = K_{P2}^- Y(Mss) \quad (7.8)$$

$$\text{and, } Y(M^-ss) = X^- / K_{P2}^- = X^+ / K_{P2}^+ = Y(M^+ss) \quad (7.9)$$

In the R^+ column, the solute A migrates from the high pH end (pH=8.) toward the low pH end (pH=6.), whereas in the R^- column, it moves in the opposite direction. Therefore, we accumulate the solute A at the high pH end of the R^- column, i.e., the bottom reservoir. If we replot Figures 7.1 and 7.3 to show the separation factor ($\langle YB \rangle_n / \langle YT \rangle_n$) vs. n (Figure 7.4), one can see that the two-column system is much preferable.

7.3 : Experimental Results

The experimental apparatus was described in chapter 5. The systems selected to be examined experimentally were Hemoglobin-buffer and albumin-buffer. The results are shown in Figures 7.5 and 7.6. For all runs, the displacement was set approximately equal to the void volume (VE), and the flow rate was 0.017cc/sec (1cc/min).

Figure 7.5 illustrates the separation factor ($\langle YB \rangle_n / \langle YT \rangle_n$) vs. n for a one column parametric pump. Initially, the feed solution containing a solute (hemoglobin or albumin) was present in the reservoirs. The column and the bottom reservoir dead volume were filled with feed solution of pH=8. The buffer solutions were made from monobasic and dibasic sodium phosphate. The top and bottom reservoirs were

$$SF = \frac{Y(B_n)}{Y(T_n)}$$

$$p_2 < IA < p_1; \quad \frac{V_R}{V_S} = 3$$

$$k_{p_2}^- = k_{p_1}^+ = 1.58$$

$$k_{p_1}^- = k_{p_2}^+ = 0.5$$

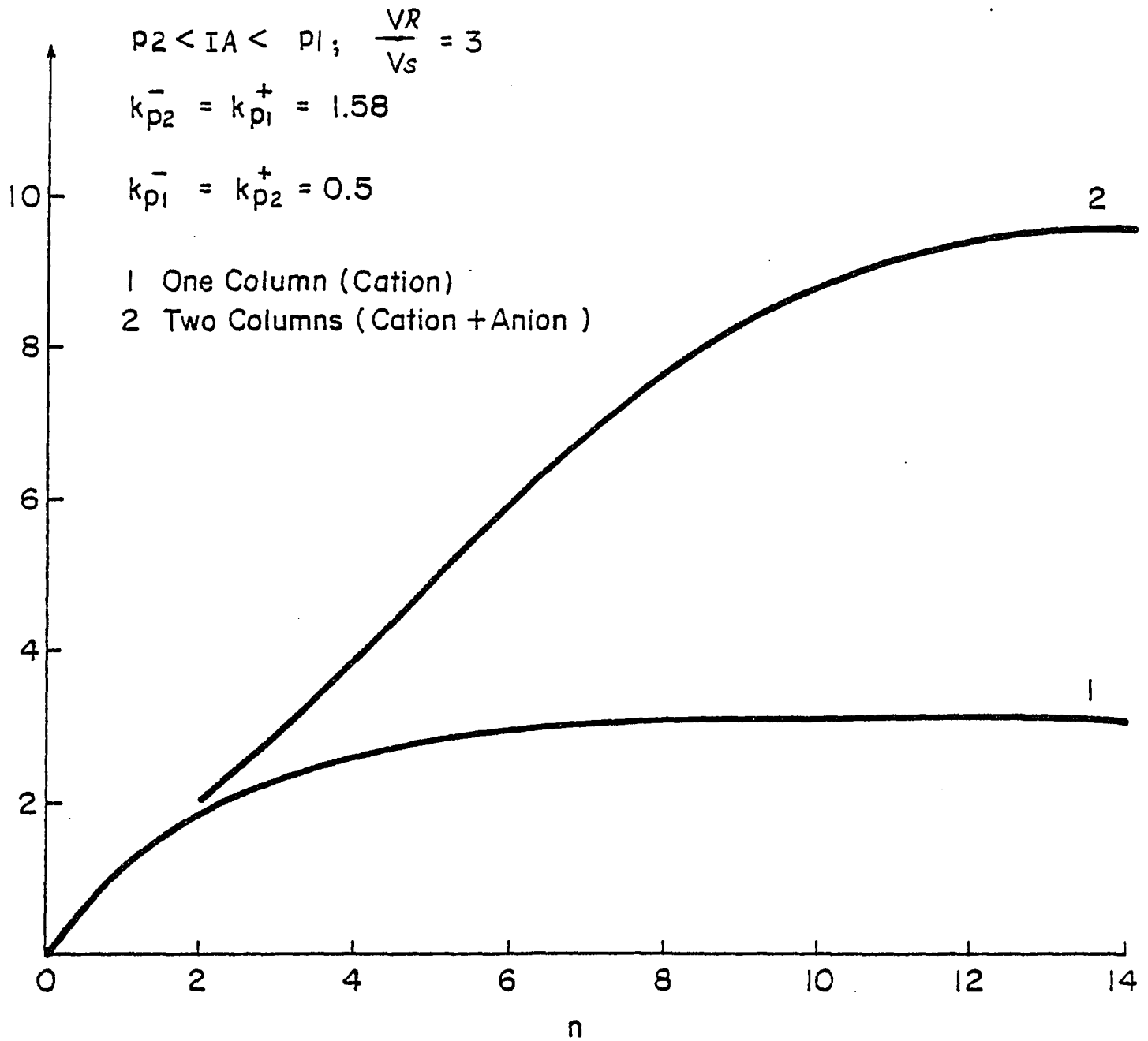


Figure 7.4 Separation Factor vs. n for One- and Two- Column Parapump

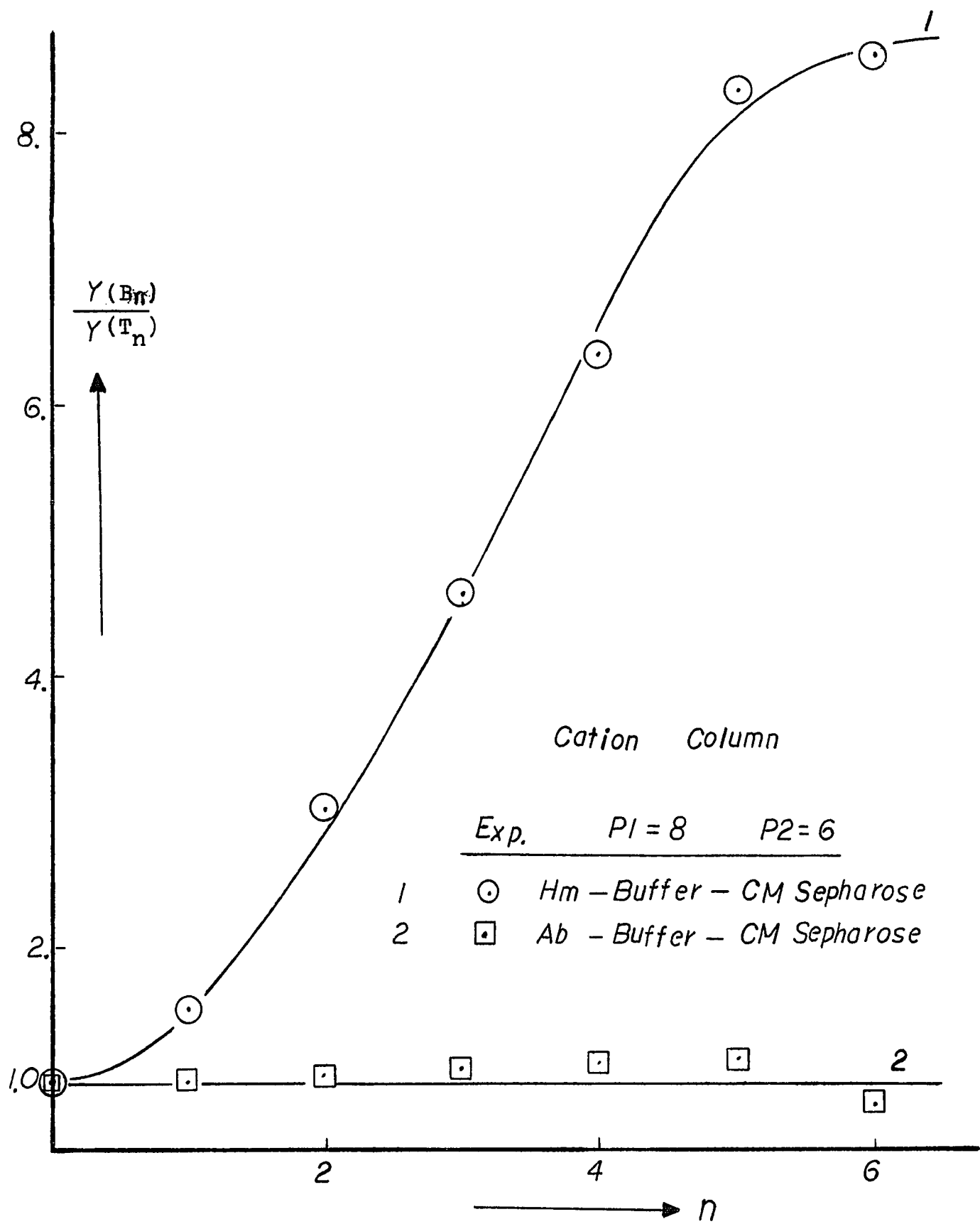


Figure 7.5 Experimental Results for One-Column Parapump.

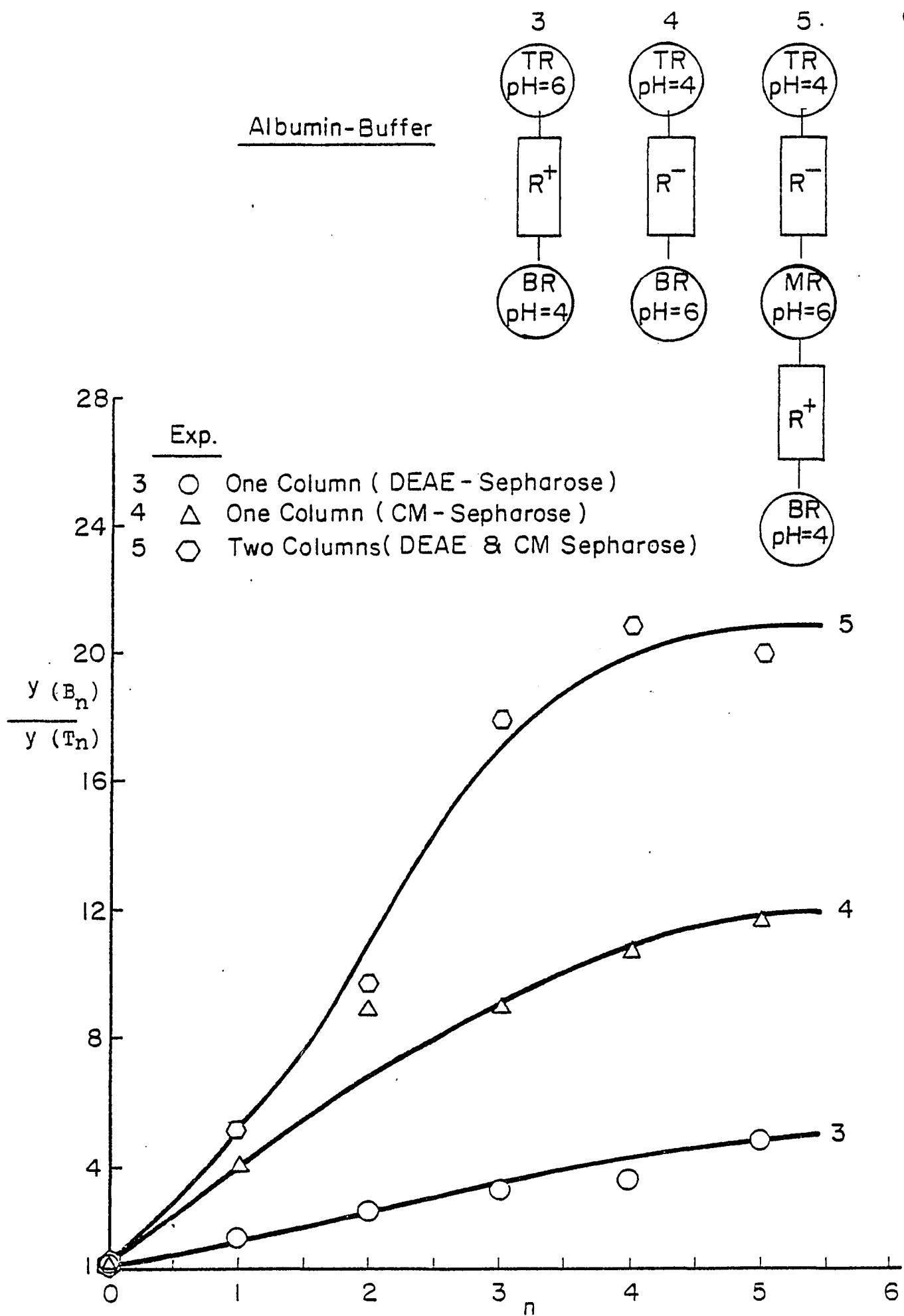


Figure 7.6 Comparison of Experimental Results for One- and Two-Column Systems

respectively maintained at pH=6(P2) and pH=8(P1) so that the isoelectric point of hemoglobin would lie between the two pH levels. As a result of a change in the column pH, hemoglobin experiences a change in the net charge, and migrates toward the high pH end (the bottom reservoir). Thus, the separation factor(SF) for hemoglobin increases with n and approaches a limiting value. For the case of albumin, the isoelectric point of albumin is below P2, and the net charge is always negative during upflow and downflow. As a result, the adsorption of albumin in the pH levels(P1 and P2) is negligible, thus albumin concentration is unaffected by this parapump operation, and remains the original concentration.

Figure 7.6 shows the comparison of one- and two-column parapumps. For all cases(runs 3, 4, and 5) the solute(albumin) was present in the columns and reservoirs in concentration Y_0 initially. Two pH levels(4. and 6.) were chosen to bracket the isoelectric point of albumin. The buffers used for this part of experiments were mixtures of acetic acid, sodium acetate and sodium choride. As the theory predicts, Albumin is concentrated at the low pH end of the R^+ column(Run 3) and the high pH end of the R^- column (Run 4). Also, the two column parapump has much higher separation capability than the one-column units. The experimental results have demonstrated the separation capability of two column parapump, and qualitatively agree with the prediction by the single cell model.

Chapter 8 : Separation of Multi-Component System
With Single Cell Model

In this chapter, many modes of parapump operation are studied. The single cell model and the linear equilibrium relationship are applied to examine the behavior of parapump and to guide the experimental studies. Studies of separation in ternary system (2 solutes in buffer solution) by 2-column batch parapump are presented in Section 8.1 and by multi-column batch parapump in Section 8.2. Studies of open parapump (operation with feed introduced to and products withdrawn from system) is presented in Section 8.3, and the separation of multiple solutes are presented in Section 8.4. Included in this chapter are also the theoretical prediction by single cell model with graphical presentation, experimental results, and the correlation of experimental data with the single cell model. For a ternary system which consists of protein A, B, and buffer solution, we are concerned with the separation of two proteins. The proteins, A and B, have the isoelectric points I_A and I_B , respectively, and $P_3 < I_B < P_2 < I_A < P_1$, where P_1 , P_2 , and P_3 are the pH levels in the reservoirs. Thus, both A and B will bear negative charges at P_1 , and positive charges at P_3 , while A will carry a positive charge and B will carry a negative charge at P_2 . Therefore, A will be taken up by a suitable cationic exchanger at

P2 or P3 and released at P1, whereas B will be taken up at P3 and released at P2 or P1. A reversed effect will occur if an anion exchanger is selected.

8.1 : 2-Column Batch Parapump

In this section, the effort is emphasized on splitting 2 proteins in buffer solution. Four modes of 2-column parapumps were studied. Figures 7.2, 8.2, 8.4, and 8.6, show the operations of Mode 1, 2, 3, and 4, respectively. The steady state concentrations in the reservoirs are graphically shown in Figures 8.1, 8.3, 8.5, and 8.7. For the purpose of simplification, it is assumed that for protein A, $K_{P2}^- = K_{P3}^+$ and $K_{P2}^+ = K_{P3}^+$, and for protein B, $K_{P1}^+ = K_{P2}^+$ and $K_{P1}^- = K_{P2}^-$. However, other conditions are conceivable. The four modes of pump operations are described as follows:

Mode 1:

The 2-column parapump described in Section 7.2 is the first mode considered. Since the operations is the same as that stated in Section 7.2, here we only discuss the result of separation for two proteins in buffer solution. The graphical construction for the concentration profile is made in the same way as previously described. From the previous section, a two

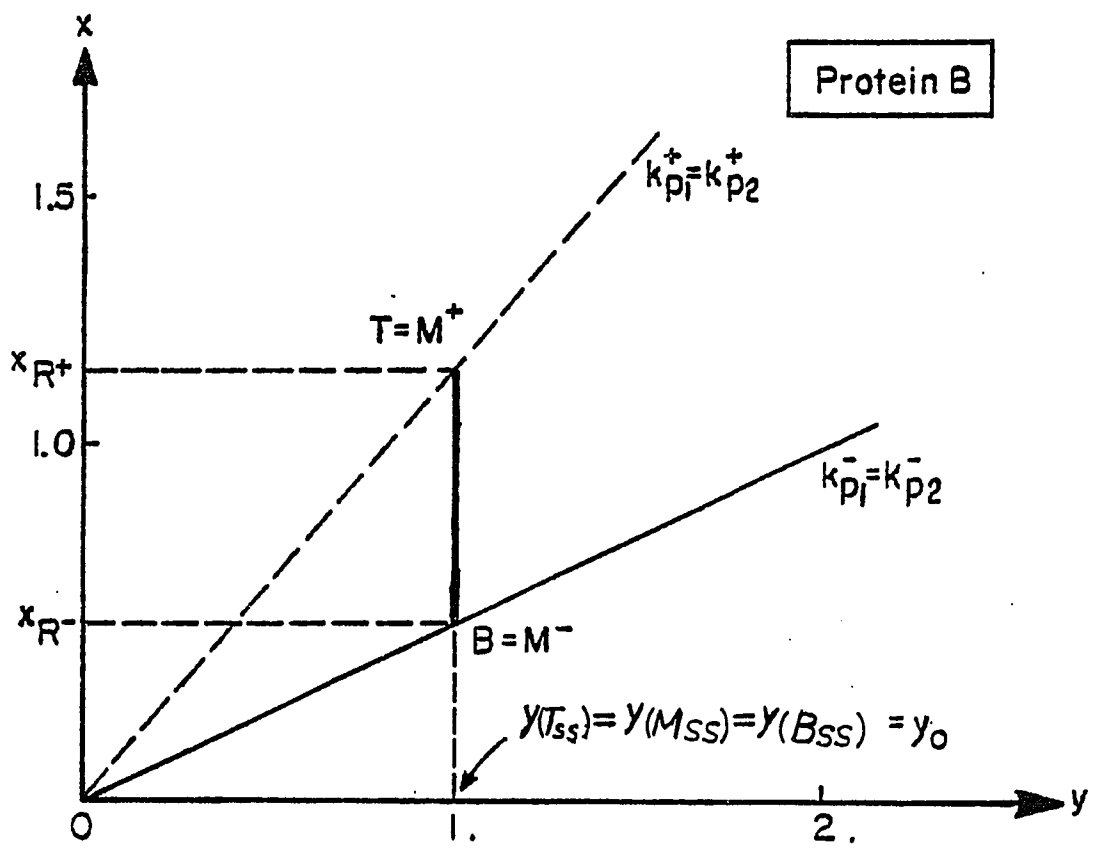
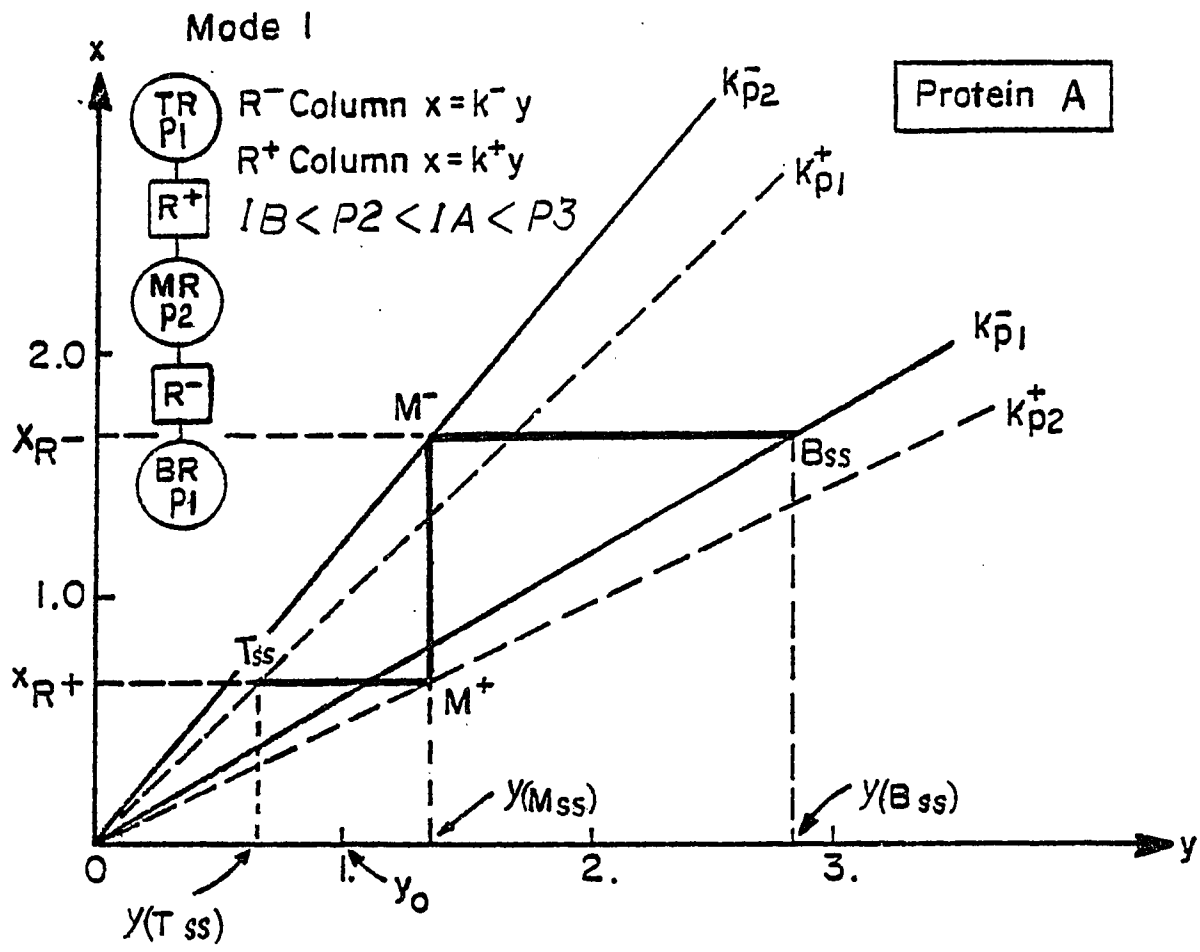


Figure 8.1 Graphical Solution for Two-Column Parapump-Mode 1.

step staircase is formed for protein A (upper diagram of Figure 8.1).

In the R^+ column, the protein A migrates from the high pH end(P1) toward the low pH end(P2), whereas in the R^- column, protein A migrates from the low pH end (P2) to the high pH end (P1), i.e., the bottom reservoir. From the lower diagram of Figure 8.1, no separation occurs for protein B, i.e., $[Y(B_{ss})/Y(T_{ss})] = 1$. It should be pointed out that, though B carries the same charge at P1 and P2, there may be a difference in the K values at these pH levels (depending on the ionic strength), and some amount of separation may occur on B. Mode 1 works well for enriching protein A, and is attractive when the objective is to obtain a product in which one component is concentrated.

Mode 2:

The parapump contains five reservoirs, two top, one middle, and two bottom reservoirs, respectively with pH = P1, P3, P2, P1, and P3. As shown in Figure 8.2, the flow system has eight distinct steps in cycle:

- (I) Pump the fluid from the TR(P1) through the R^+ column, MR and R^- column to the BR(P1), for time t_I .
- (II) Circulate the fluid between the TR(P1) and R^+ column, and between the MR and the R^- column.
- (III) Pump the fluid from the BR(P3) through the R^- column, MR, and the R^+ column to the TR(P1) for time t_{III} .

Mode 2: $P3 < IB < P2 < IA < P1$

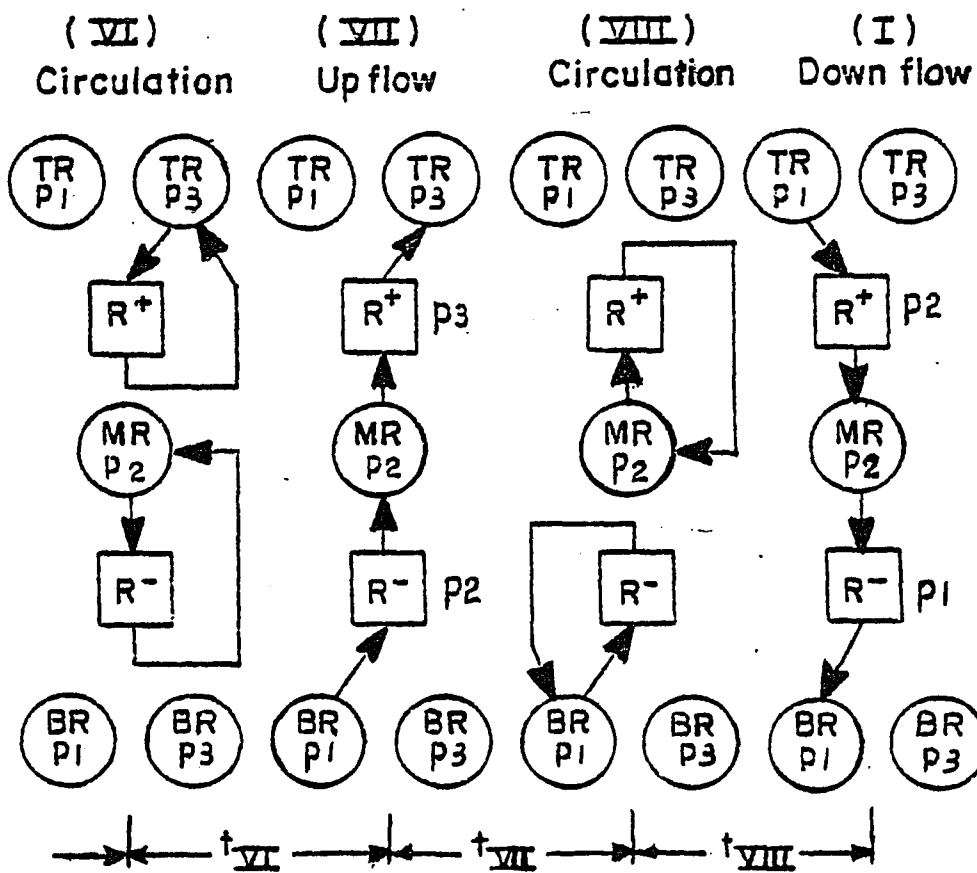
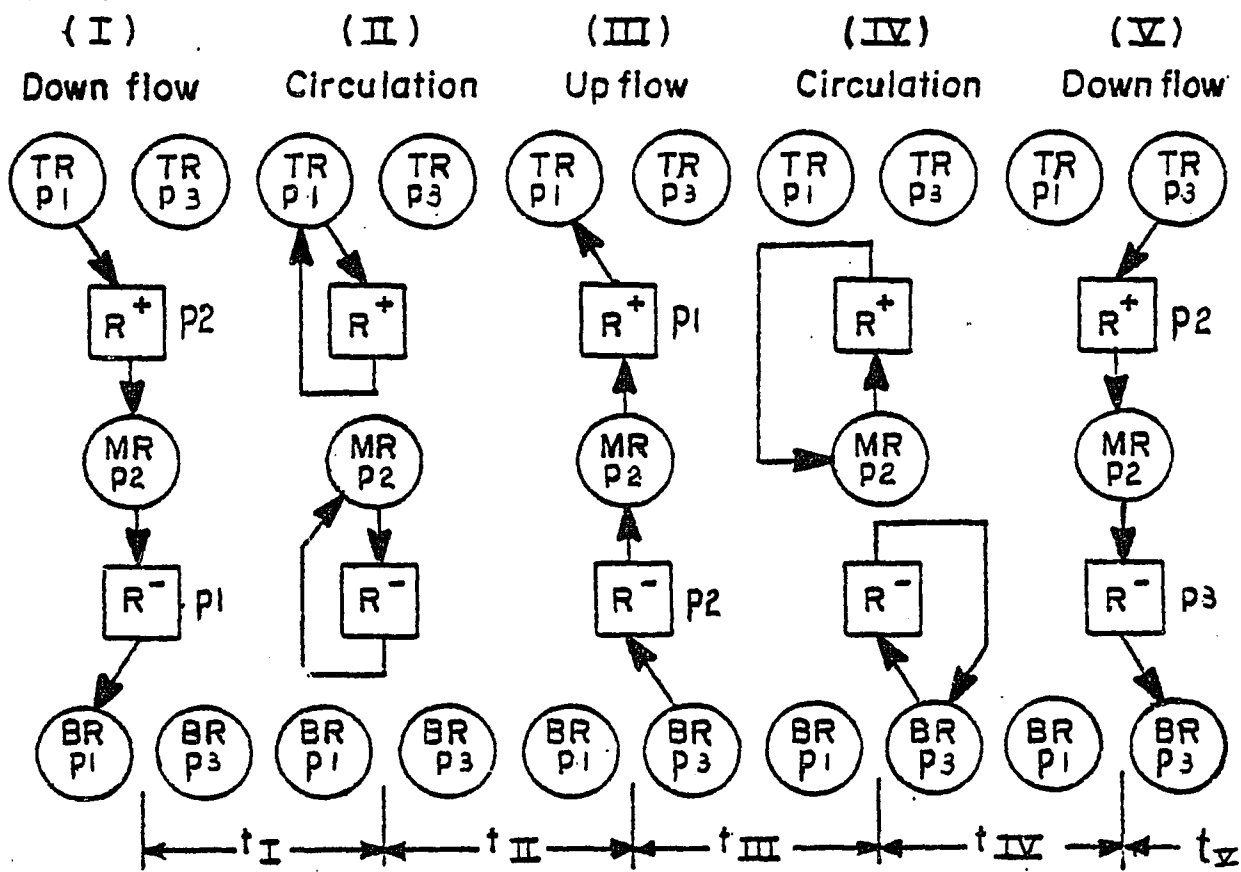


Figure 8.2 Schematic of Two-Column Parapump Operation-Mode 2

- (IV) Circulate the fluid between the BR(P3) and the R^- column, and between the MR and the R^+ column, for time t_{IV} .
- (V) Pump the fluid from the TR(P3) through the R^+ column, MR and R^- column to the BR(P3), for time t_V .
- (VI) Circulate the fluid between the TR(P3) and the R^+ column, and between the MR and R^- column for time t_{VI} .
- (VII) Pump the fluid from the BR(P1) through the R^- column, MR, and R^+ column to the TR(P3), for time t_{VII} .
- (VIII) Circulate the fluid between the BR(P1) and the R^- column, and between the MR and the R^+ column for time t_{VIII} .

The steady state concentrations in the reservoirs are graphically presented in Figure 8.3. At steady state ($n \rightarrow$ large number),

$$X^+ = K_{P1}^+ [Y(Tss)]_{P1} = K_{P3}^+ [Y(Tss)]_{P3} = K_{P2}^+ Y(Mss) \quad (8.1)$$

and

$$X^- = K_{P1}^- [Y(Bss)]_{P1} = K_{P3}^- [Y(Bss)]_{P3} = K_{P2}^- Y(Mss) \quad (8.2)$$

Connecting the points T_{P1} , T_{P3} , M_{P2}^+ , M_{P2}^- , B_{P3} , and B_{P1} , a two step staircase is formed for both proteins, A and B. However, the concentration of A in the bottom reservoir BR(P1) is much higher than that in TR(P1), while the concentration of B in the top reservoir TR(P3) is much greater

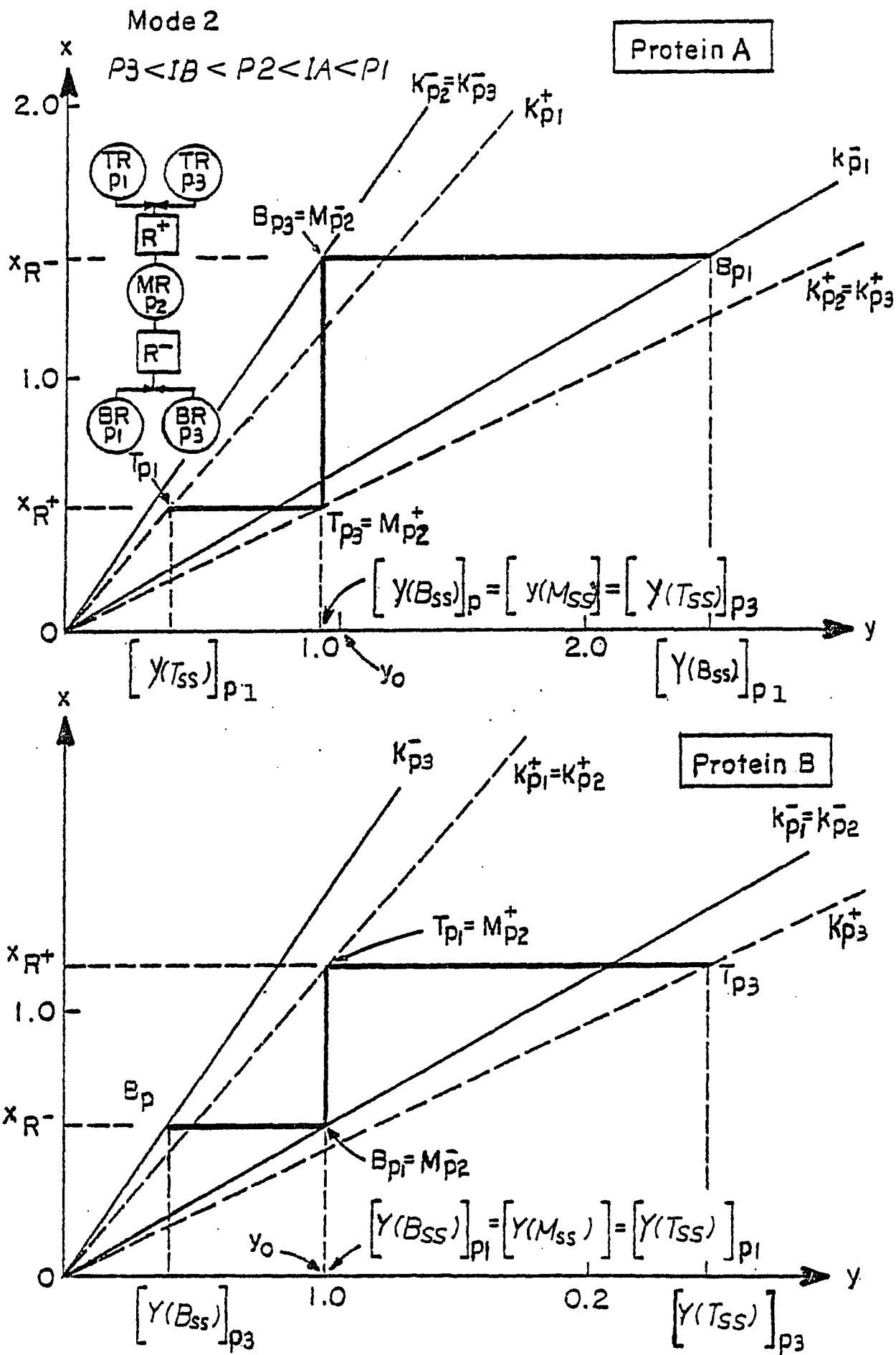


Figure 8.3 Graphical Solution for Two-Column Parapump-Mode 2

than that in BR(P3). This separation phenomenon can be explained as follows: The pH levels, P1, P2, and P3 bracket the isoelectric points of A and B, i.e., $P2 < I_A < P1$ and $P3 < I_B < P2$. Thus in the R^- column, A and B respectively migrate toward the BR(P1) and the MR(P2), whereas in the R^+ column, A and B respectively, move toward the MR(P2) and TR(P3). In other words, A and B migrate in opposite directions and concentrate respectively in BR(P1) and TR(P3).

Mode 3:

This parapump has four reservoirs; one top, two middle, and one bottom reservoirs, respectively with pH= P2, P1, P3, and P2. Flow sequences(Figure 8.4) for one cycle are:

- (I) Pump the fluid from TR through the R^+ column to the MR(P1), and at the same time, pump the fluid from the MR(P3) through the R^- column to the BR, for t_I .
- (II) Circulate the fluid between the TR and the R^+ column, and between the MR(P3) and the R^- column for time t_{II} .
- (III) Pump the fluid from the BR and R^- column, and between the MR(P3) and R^+ column to TR, for time t_{III} .
- (IV) Circulate the fluid between the BR through the R^- column, and between the MR(P3) and R^+ column for time t_{IV} .
- (V) Pump the fluid from the TR through the R^+ column to

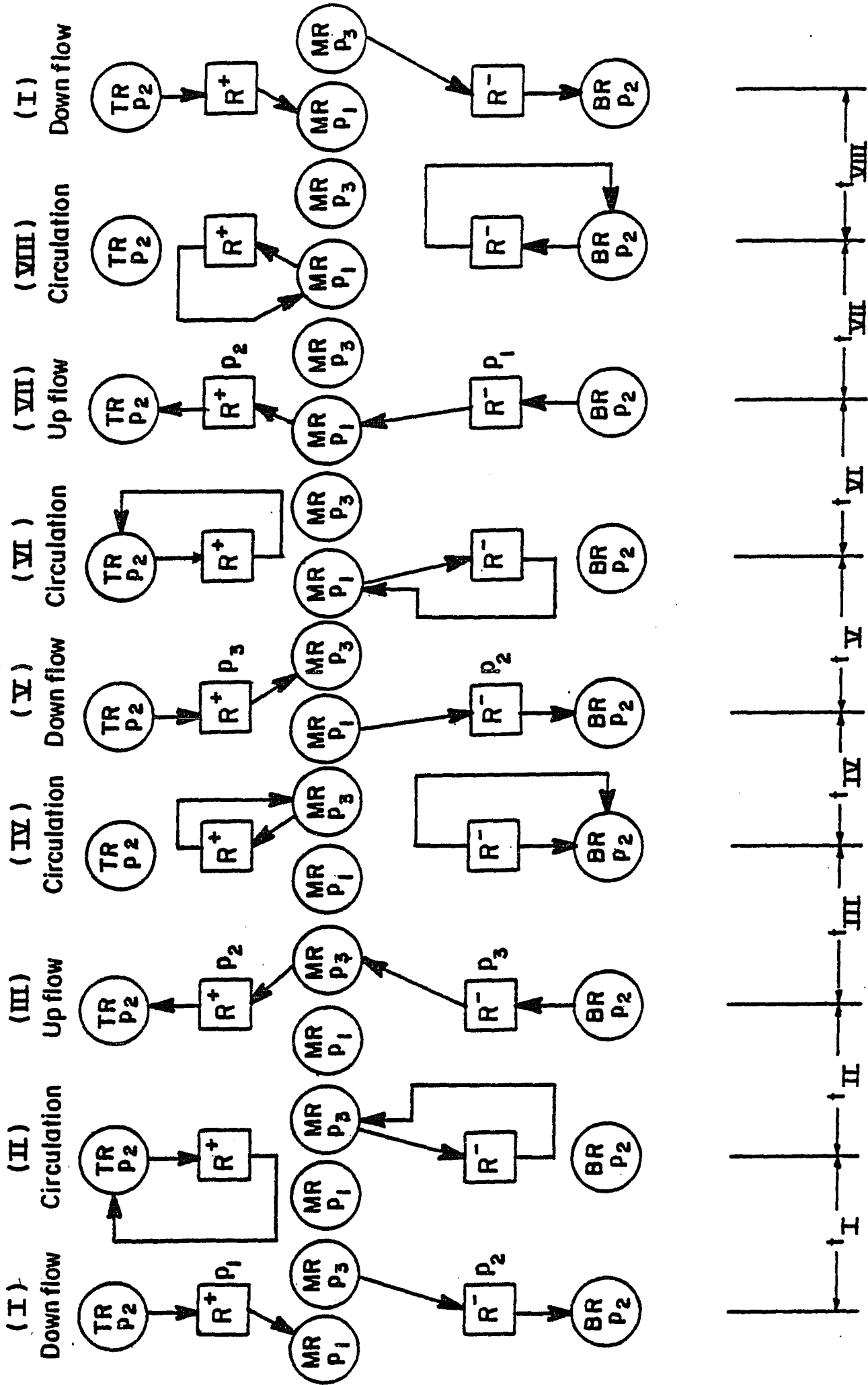


Figure 8.4 Mode 3 : $p_3 < IB < p_2 < IA < p_1$

the MR(P3), and at the same time pump the fluid from the MR(P1) through the R^- column to BR, for time t_V .

(VI) Circulate the fluid between the TR and the R^+ column, and between the MR(P1) and the R^- column, for time t_{VI} .

(VII) Pump the fluid from the BR through the R^- column, MR(P1), and R^+ column to TR for time t_{VII} .

(VIII) Circulate the fluid between the BR and the R^- column, and between the MR(P1) and the R^+ column for time t_{VIII} .

Figure 8.5 shows the steady state concentrations in the reservoirs. At steady state, the average concentration of the middle reservoirs (MR(P1) and MR(P3)) is such that:

$$X^+ = K_{P2}^+ Y(Tss) = 0.5 [K_{P1}^+ Y(MR^+)_{P1} + K_{P3}^+ Y(MR^+)_{P3}] \quad (8.3)$$

$$X^- = K_{P2}^- Y(Tss) = 0.5 [K_{P1}^- Y(MR^-)_{P1} + K_{P3}^- Y(MR^-)_{P3}] \quad (8.4)$$

$Y(M^-_{ss})$ and $Y(M^+_{ss})$ in Figure 8.5 is defined as:

$$Y(M^+_{ss}) = 0.5 [Y(MR^+)_{P1} + Y(MR^+)_{P3}] = Y(M^-_{ss}) = 0.5 [Y(MR^-)_{P1} + Y(MR^-)_{P3}] \quad (8.5)$$

where $Y(MR^+)_{P1}$ and $Y(MR^+)_{P3}$ are the steady state solute concentrations from the R^+ column to MR(P1) and MR(P3) respectively, respectively, whereas $Y(MR^-)_{P1}$ and $Y(MR^-)_{P3}$ are those from the R^- column to MR(P1) and MR(P3) respectively.

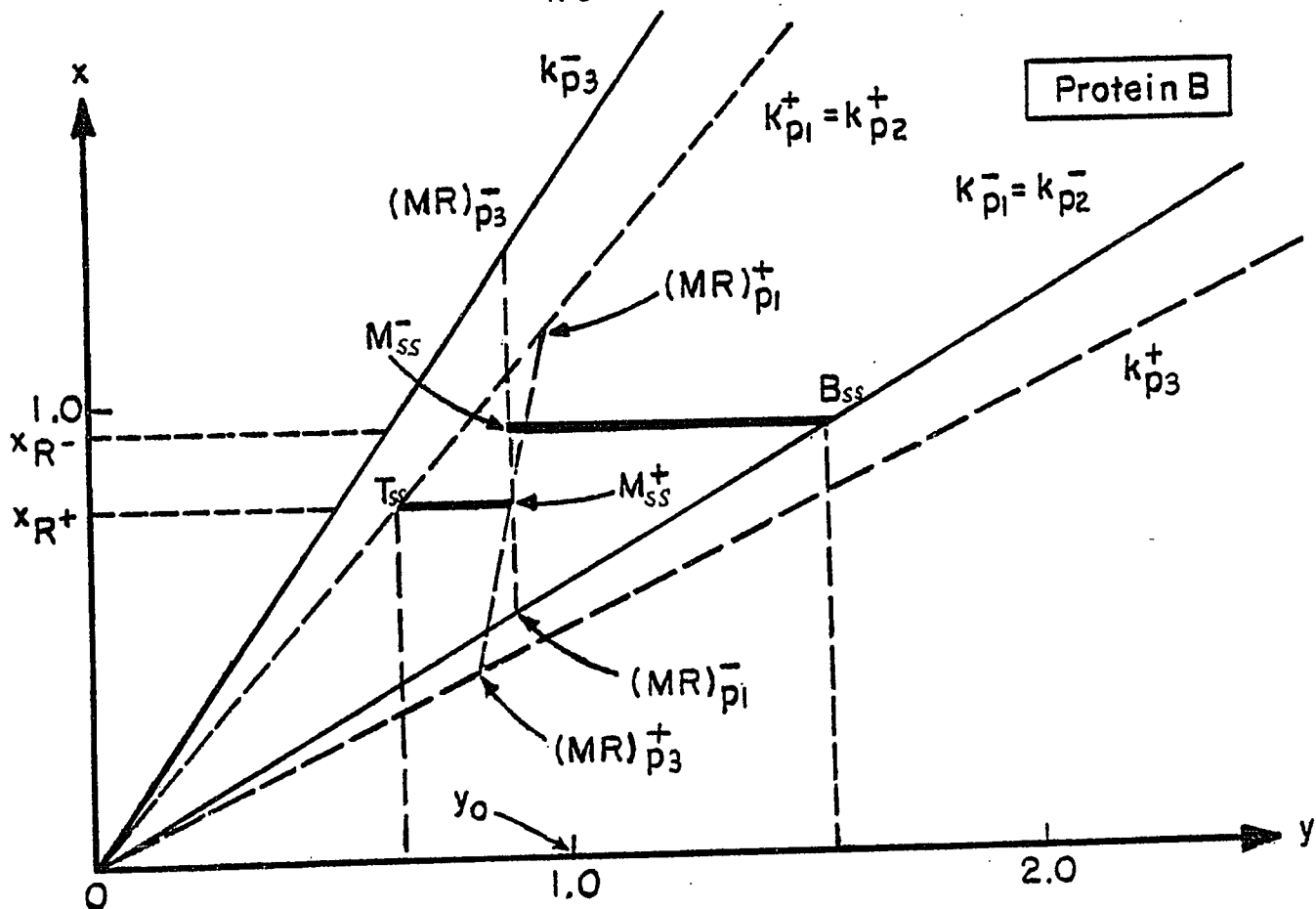
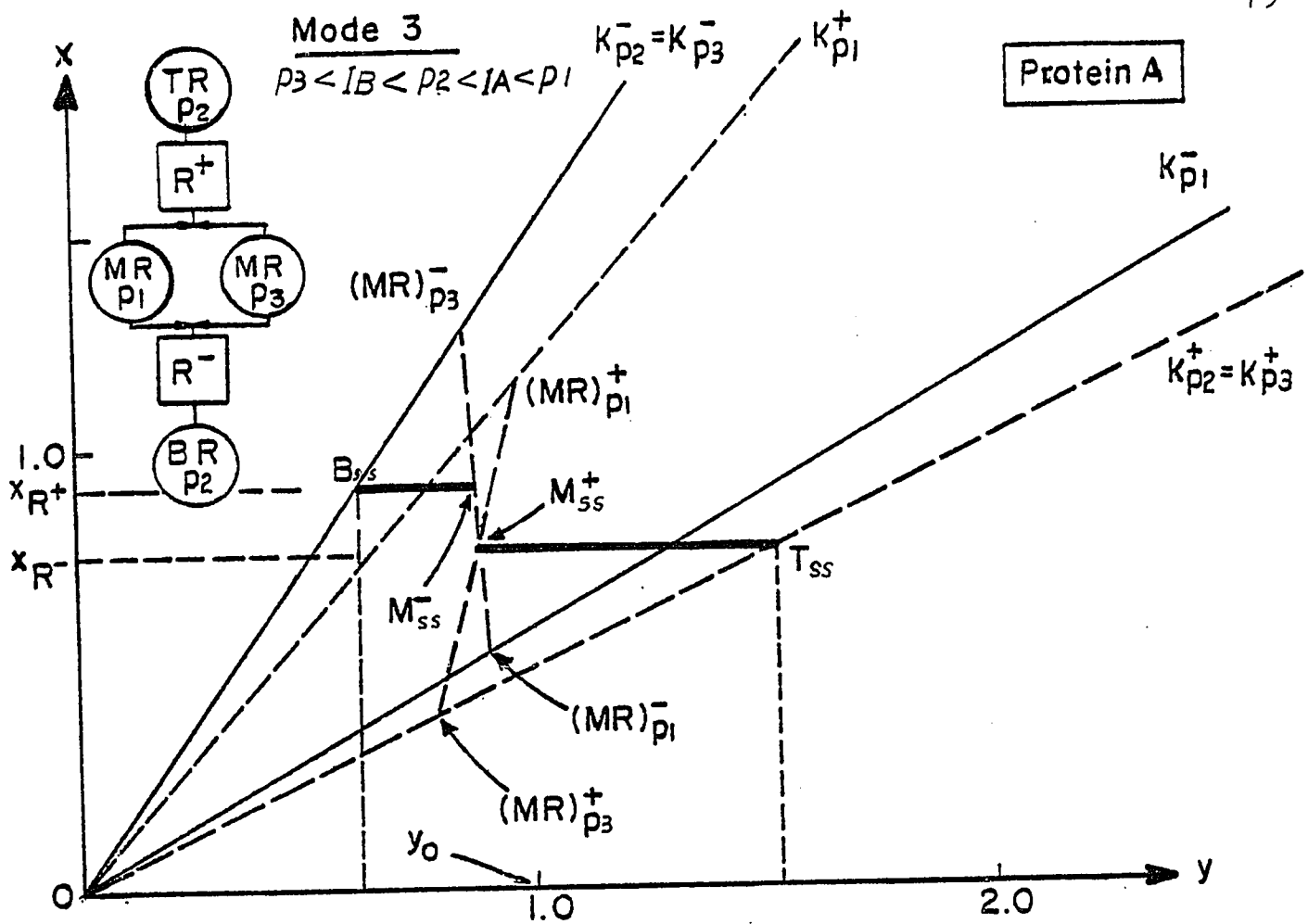


Figure 8.5 Mode 3, Graphical Solution

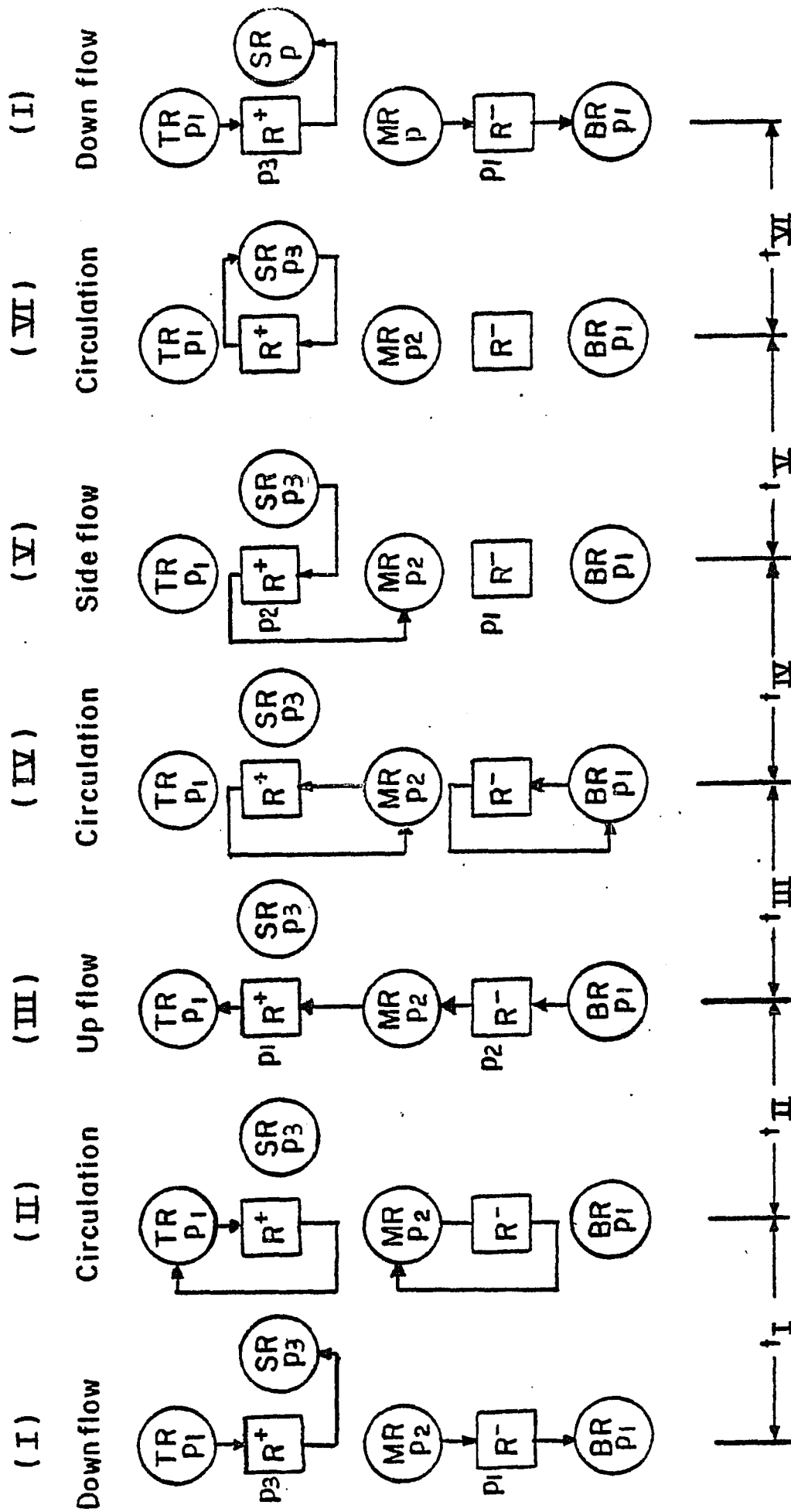
The results shown in Figure 8.5 are very similar to those from Mode 2. A and B move in opposite directions, but for this case, protein A migrates upward to the top reservoir (pH=P2), while B moves downward to the bottom reservoir (pH=P2).

Mode 4 :

This mode includes four reservoirs, TR, MR, SR (Side Reservoir), and BR, respectively with pH = P1, P2, P3, and P1. One cycle of operation is described as follows:

- (I) Pump the fluid from TR through the R^+ column to SR, and at the same time pump the fluid from the MR through the R^- column to the BR, for time t_I .
- (II) Circulate the fluid between the TR and R^+ column, and between the MR and the R^- column, for time t_{II} .
- (III) Pump the fluid from the BR through the R^- column, MR, and R^+ column to the TR, for time t_{III} .
- (IV) Circulate between the BR and R^- column, and between the MR and R^+ column, for time t_{IV} .
- (V) Pump the fluid from the SR through the R^+ column to the MR, for time t_V .
- (VI) Circulate between the SR and R^+ column for t_{VI} .

The steady state concentrations are shown in Figure 8.7. Proteins A and B are enriched in the BR and SR, respectively. Note that by this mode, protein B has no separation in the R^- column, and thus only one step staircase is formed.



Mode 4 : $P3 < IB < P2 < IA < P1$

Figure 8.6 Schematic of TwO-Column Parapump Operation-Mode 4

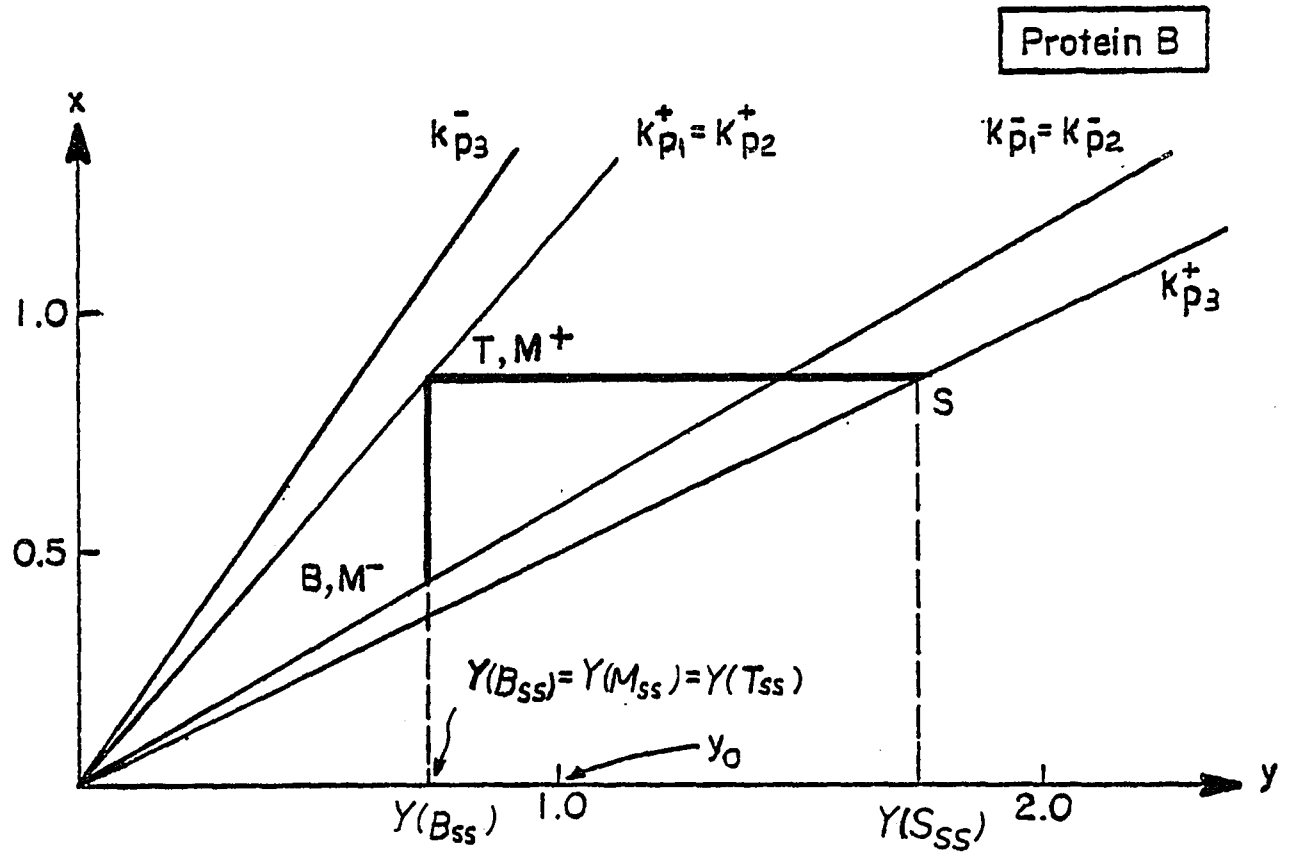
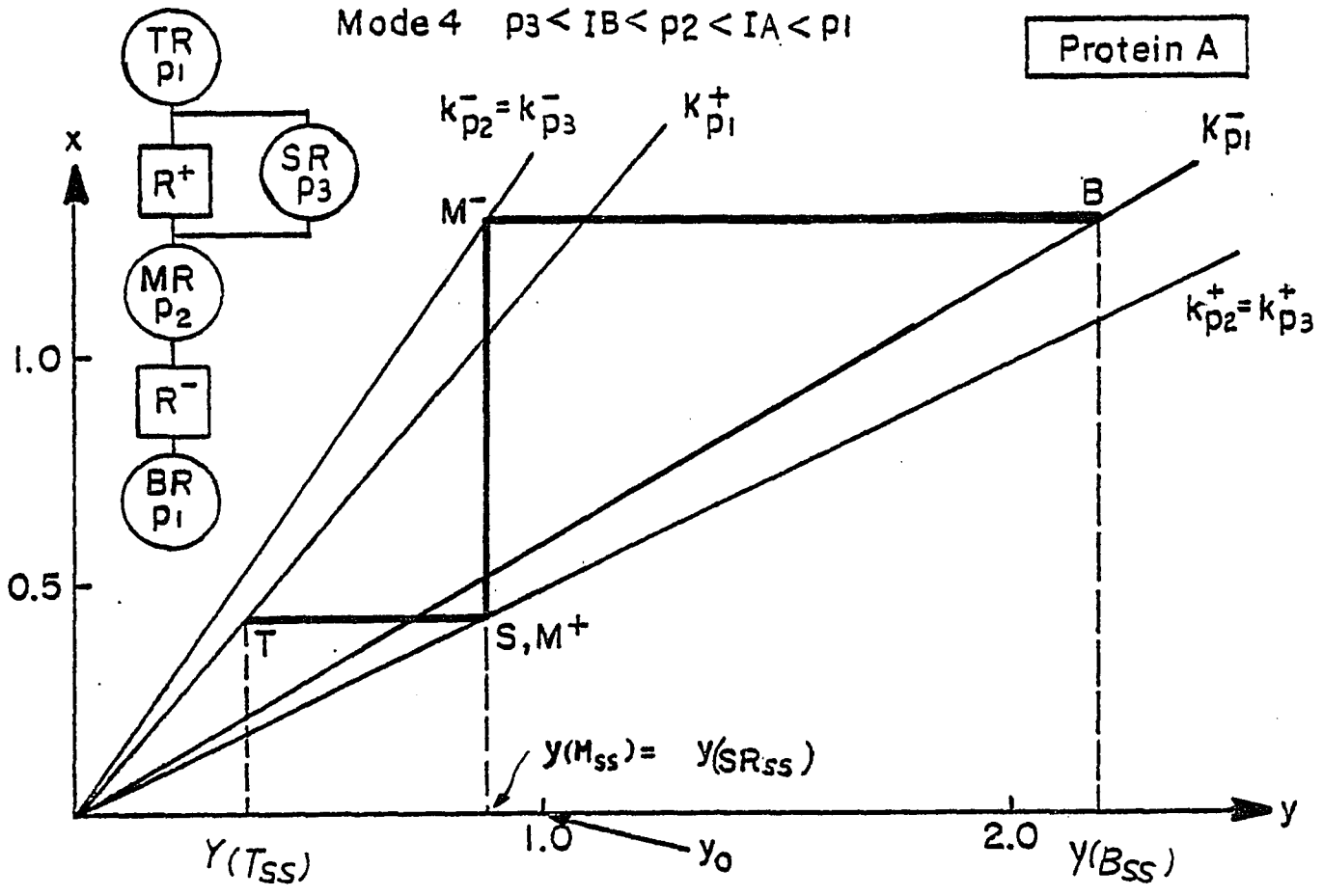


Figure 8.16 Graphical Solution for Two-Column Parapump-Mode 4.

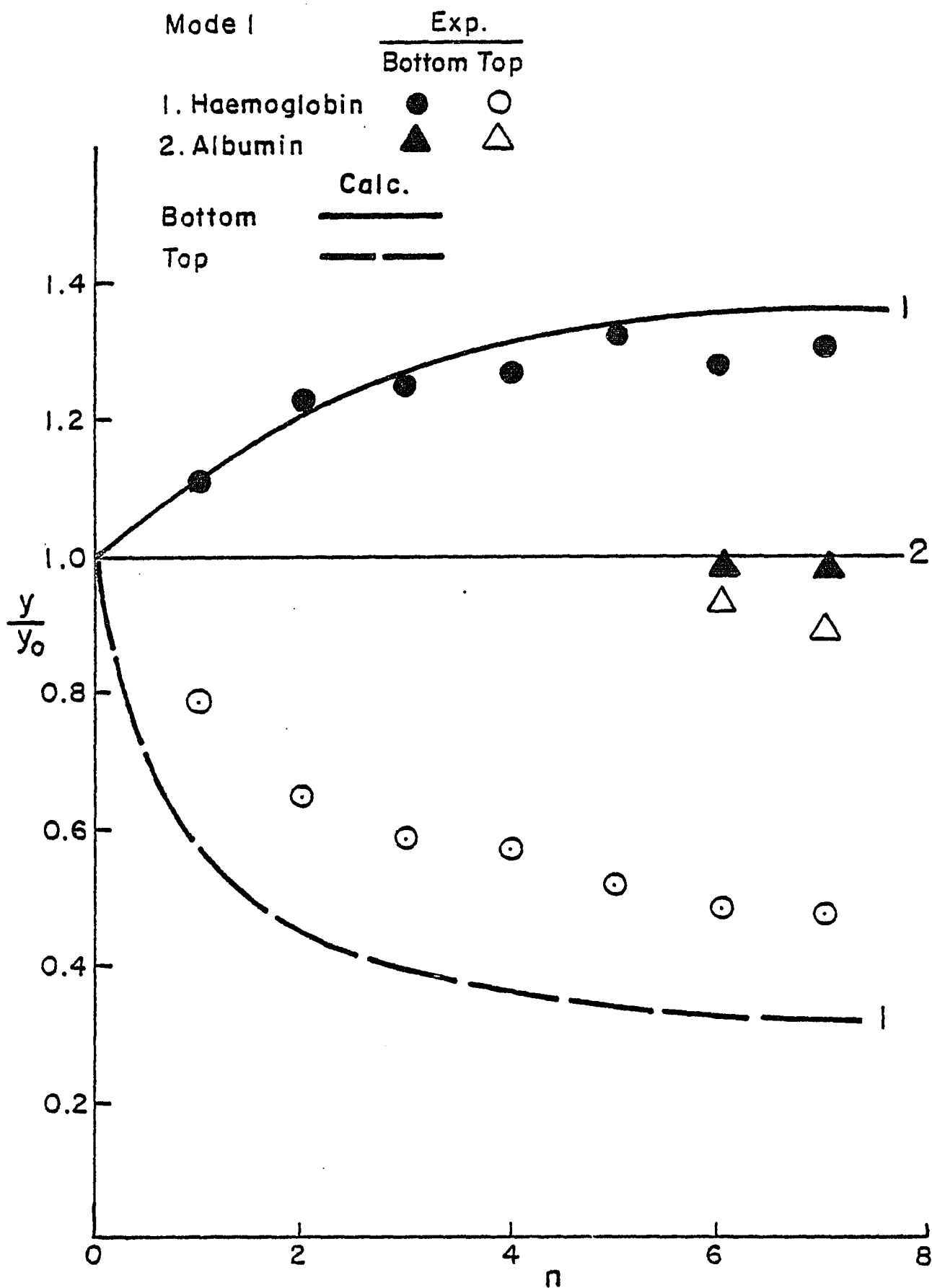


Figure 8.8 Experimental Results-Mode 1

Experimental Results of a Two Protein System:

The experimental results are presented in Figures 8.8 to 8.11, for Mode 1, 2, 3, and 4, respectively. Note the experimental results in Figure 8.11 are obtained from the modified Mode 3 (i.e., Mode 3-A; see Figure 8.12). Table 4 summarizes the experimental and model parameters. These plots show the top and bottom reservoir concentration (also the side reservoir concentrations for Mode 4) versus number of cycles. Curves computed from the theory described above are also given. The calculated results agree reasonably well with the observed values.

Figure 8.8 and 8.11 show that by the use of modes 1 or 4, the hemoglobin concentration in the bottom reservoir builds up from cycle to cycle, and approaches a steady value as n becomes large. However, albumin migrates toward the side reservoir when Mode 4 is used, whereas no separation occurs when Mode 1 is applied. The concentration profiles for Mode 2 are presented in Figure 8.9. As the model predicts both the hemoglobin and albumin migrate in the opposite direction, and concentrate in the bottom (P1) and top (P3) reservoirs respectively. Figure 8.10 shows the concentration profile of the proteins for Mode 3-A operation. It is seen that hemoglobin moves toward the top reservoir and albumin moves toward the bottom reservoir. As a result, hemoglobin is concentrated and albumin is depleted in the top reservoir; albumin is concentrated and hemoglobin is depleted in the bottom reservoir.

Mode 2
 1. Haemoglobin
 2. Albumin

Exp.			
Bottom		Top	
P ₁	P ₃	P ₁	P ₃
●		○	
	■		□

Calc.

Bottom
 Top

—————
 - - - - -

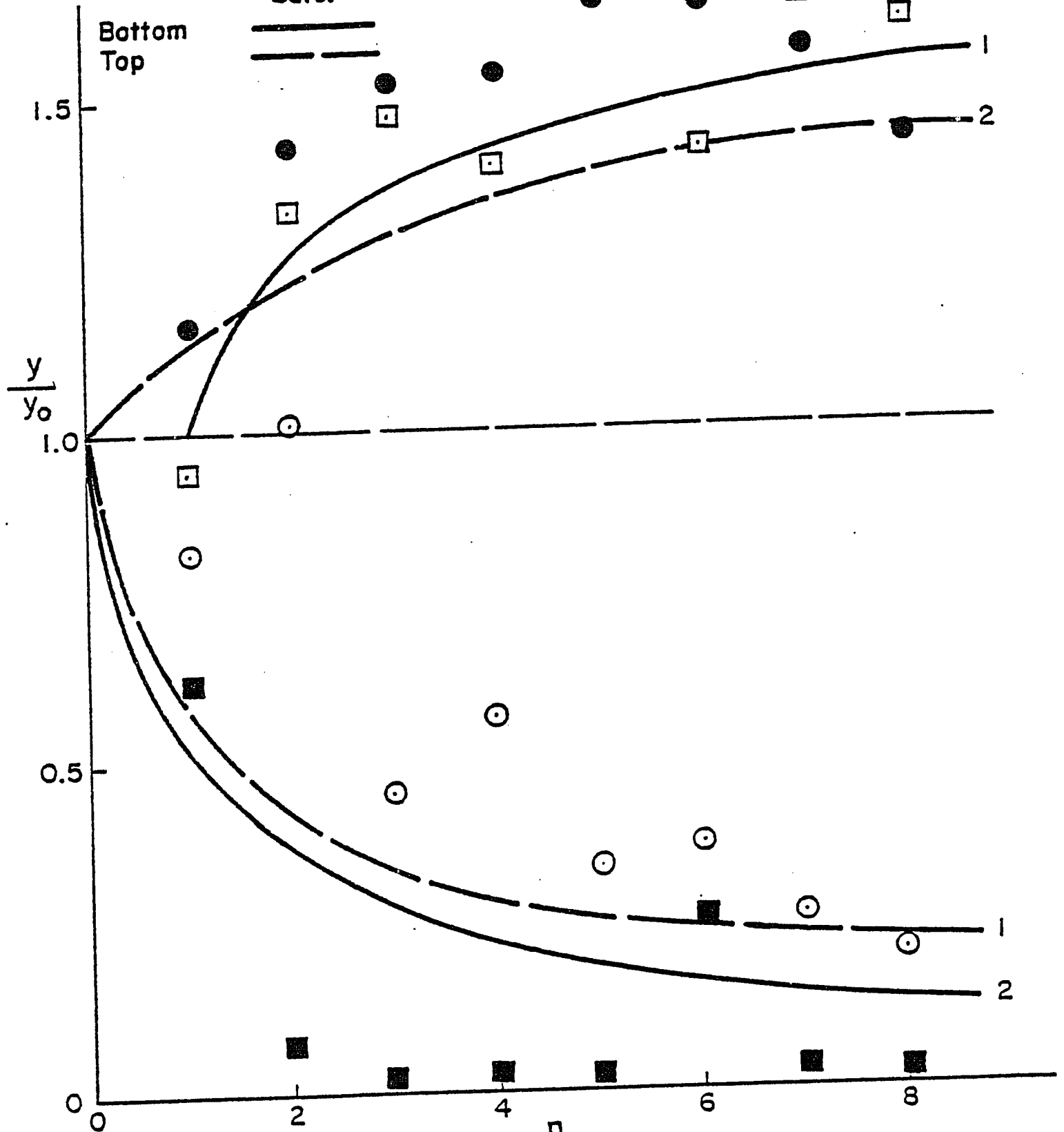


Figure 8.9 Experimental Results - Mode 2

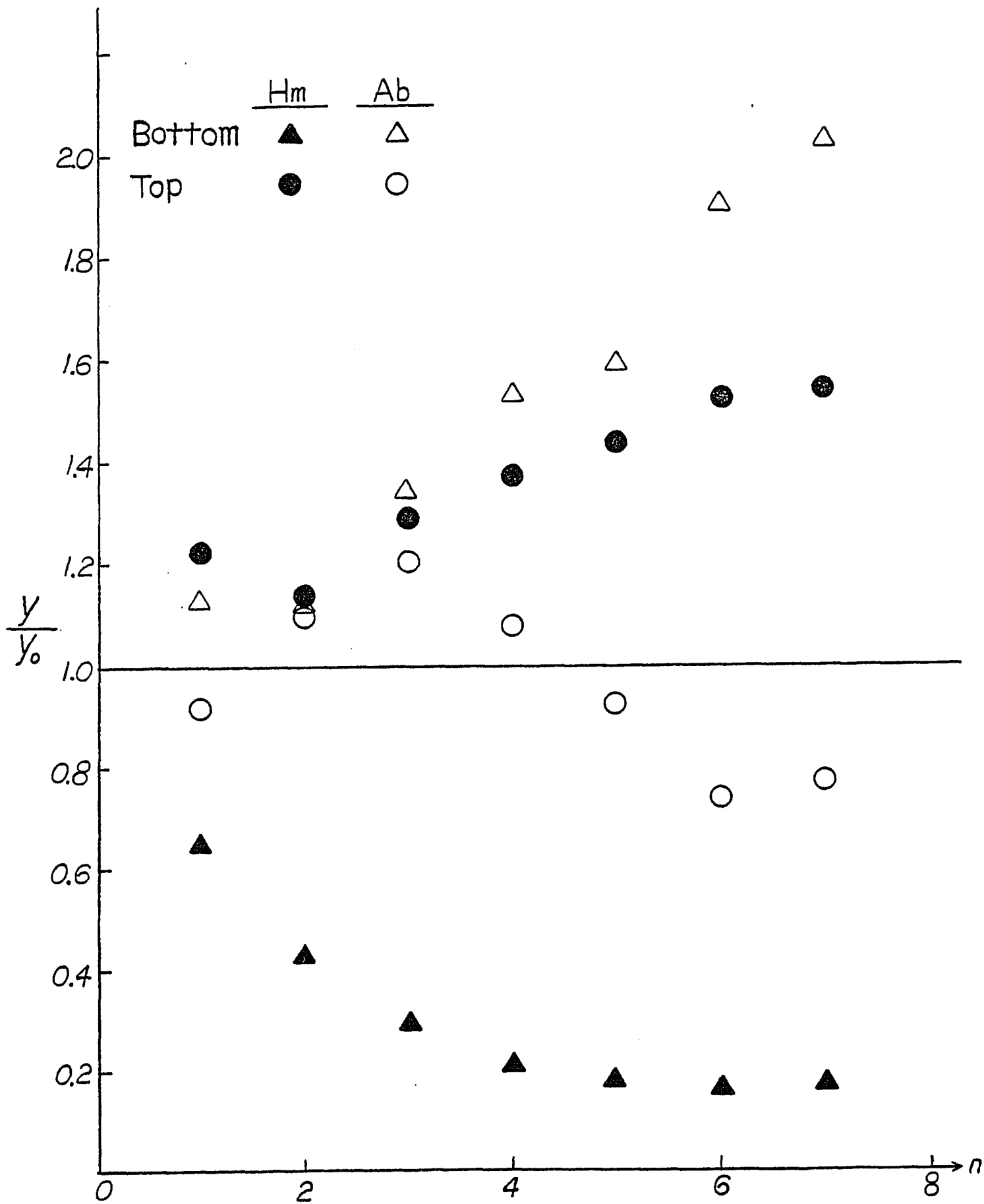


Figure 8.10 Experimental Results-Mode 3

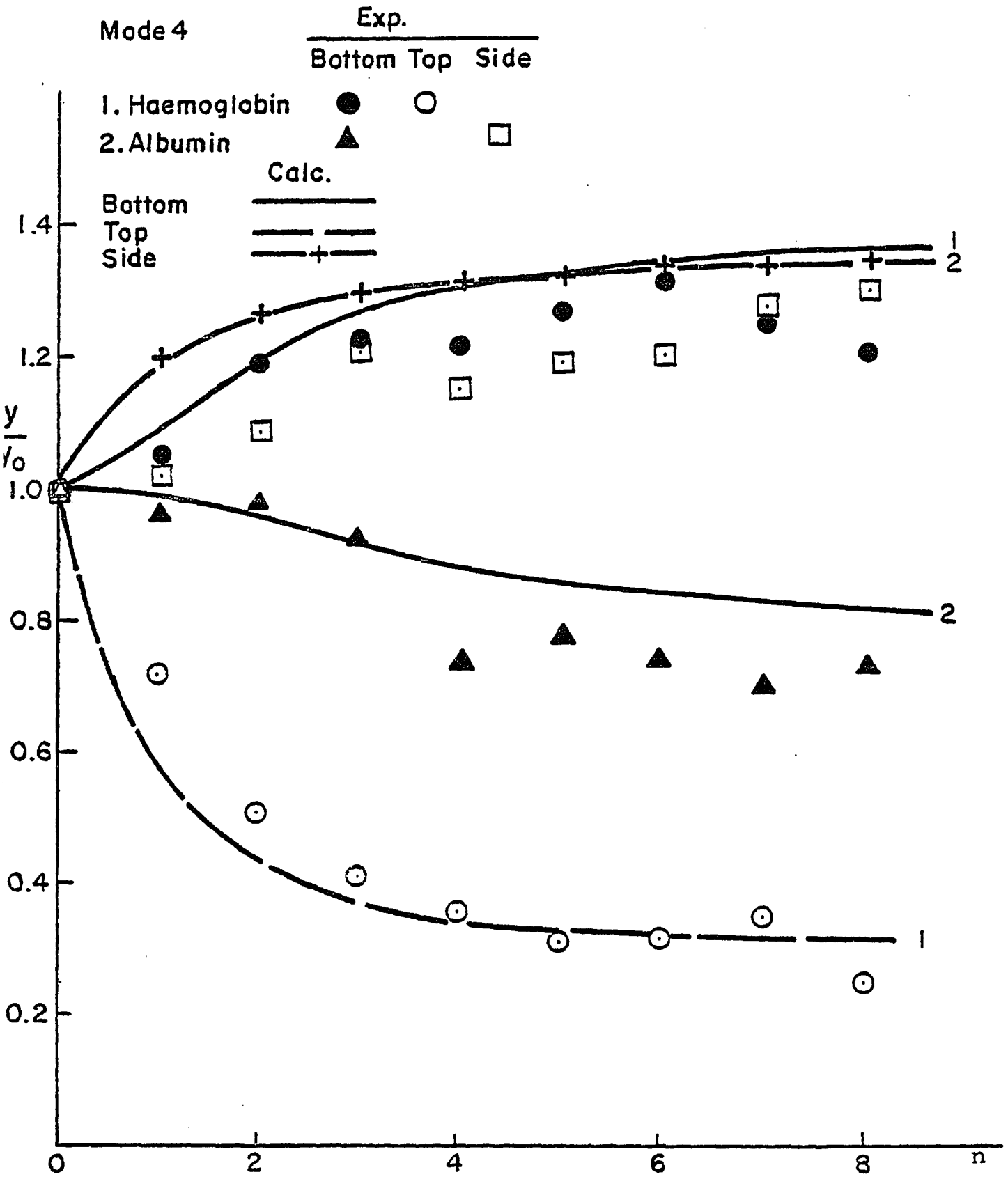
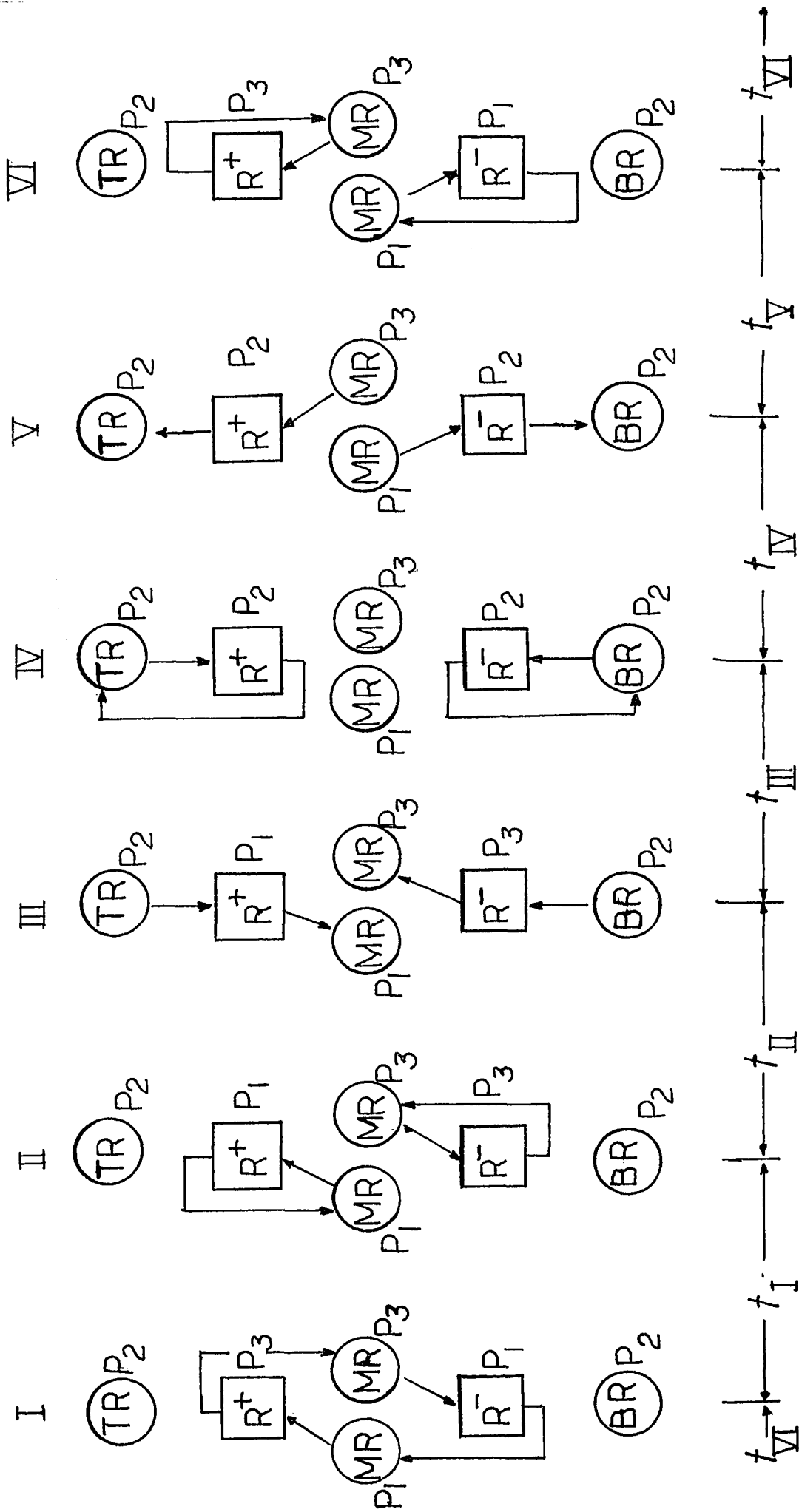


Figure 8.11 Experimental Results- Mode 4



Mode 3A: $P_1 > I_A > P_2 > I_B > P_3$

Figure 8.12 Schematic of Two-Column Parapump-Mode 3A.

TABLE 4. EXPERIMENTAL AND MODEL PARAMETERS

$Q = 1.67 \times 10^{-8}$; Feed: Haemoglobin = 0.02 wt %
 m³/s Albumin = 0.02 wt %
 $P_1 = 8.5$; $P_2 = 6.2$

$$IS_1 = \begin{bmatrix} \text{Tris.-NaOH} & 0.15\text{M} \\ \text{-Maleate} & \\ \text{NaCl} & 0.05\text{M} \end{bmatrix}; IS_2 = \begin{bmatrix} \text{Tris.-NaOH} & 0.15\text{M} \\ \text{-Maleate} & \\ \text{NaCl} & 0.05\text{M} \end{bmatrix}$$

Haemoglobin: $k_{\nu_1}^- = 1.4$; $k_{\nu_2}^- = 2.0$

$k_{\nu_1}^+ = 3.0$; $k_{\nu_2}^+ = 1.0$

Albumin: $k_{\nu_1}^- = 1.5$; $k_{\nu_2}^- = 1.5$

$k_{\nu_1}^+ = 2.5$; $k_{\nu_2}^+ = 2.5$

	Mode 1	Mode 2	Mode 4
$(V+V_T^*)/\bar{V}$	1.5	1.88	1.5
P_3	4.2	3.8	4
$IS_3 \begin{bmatrix} \text{Acetic Acid- Na-Acetate} \\ \text{NaCl} \end{bmatrix}$	—	0.15M	0.2M
	—	0.05M	0.2M
$m^3 \times 10^6$	$Qt_1 = Qt_{III} = 15$ $Qt_{II} = Qt_{IV} = 30$	$Qt_1 = Qt_{III} = Qt_V =$ $Qt_{VII} = 15$ $Qt_{II} = Qt_{IV} = Qt_{VI} =$ $Qt_{VIII} = 30$	$Qt_1 = Qt_{III} = Qt_V = 15$ $Qt_{II} = Qt_{IV} = Qt_{VI} = 30$
	Mode 1	Mode 2	Mode 4
Haemoglobin			
$k_{\nu_3}^-$	—	4.0	—
$k_{\nu_3}^+$	—	0.3	1.0
Albumin			
$k_{\nu_3}^-$	—	4.5	—
$k_{\nu_3}^+$	—	2.0	1.5

* $V_T = V_B = V_{MS} = V_{SB}$

The equilibrium constants K used for computations (Table 4) were determined experimentally. Note that K is a function of ionic strength and pH. In subsequent chapters, we will discuss the procedure for determining the K value.

8.2: M-Column Batch Parapump

The two column system described above can be extended to multi-column systems (Figures 8.13 to 8.15). The systems consist of a series of M columns. The columns with odd numbers are packed with anion exchanger, and the remaining columns are with cation exchangers. The graphical construction for concentration profile can be made in the same way as described for the one- and two-column parapump systems.

Mode 5:

This system is the extension of mode 1. The pH in both top and bottom reservoirs are maintained at P_1 . The pH values for the middle reservoirs, $MR_1, MR_2, \dots, MR_{M-1}$ are respectively $P_2, P_1, P_2, \dots, P_2$. For protein A, an M -Step staircase is formed and a very high separation factor ($Y(B_{ss})/Y(T_{ss})$) can be obtained when M becomes large. Thus, this parapump system operating with pH levels of P_1 and P_2 ($P_2 < I_A < P_1$), is capable of removing protein A from the top reservoir and concentrating it in the bottom reservoir. However, protein B remains unaffected.

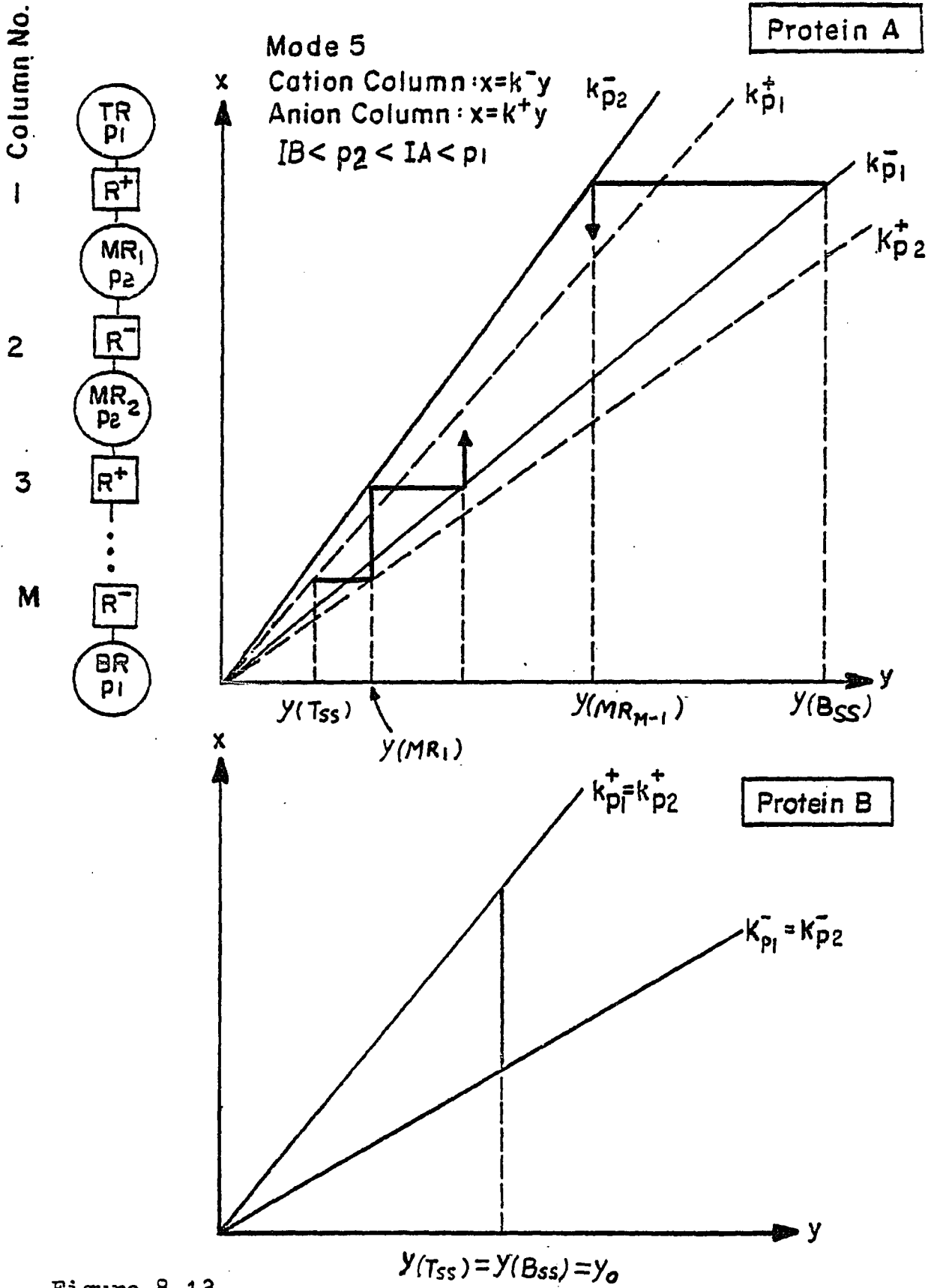


Figure 8.13
 Graphical Solution for Multi-Column Parapump-Mode 5.

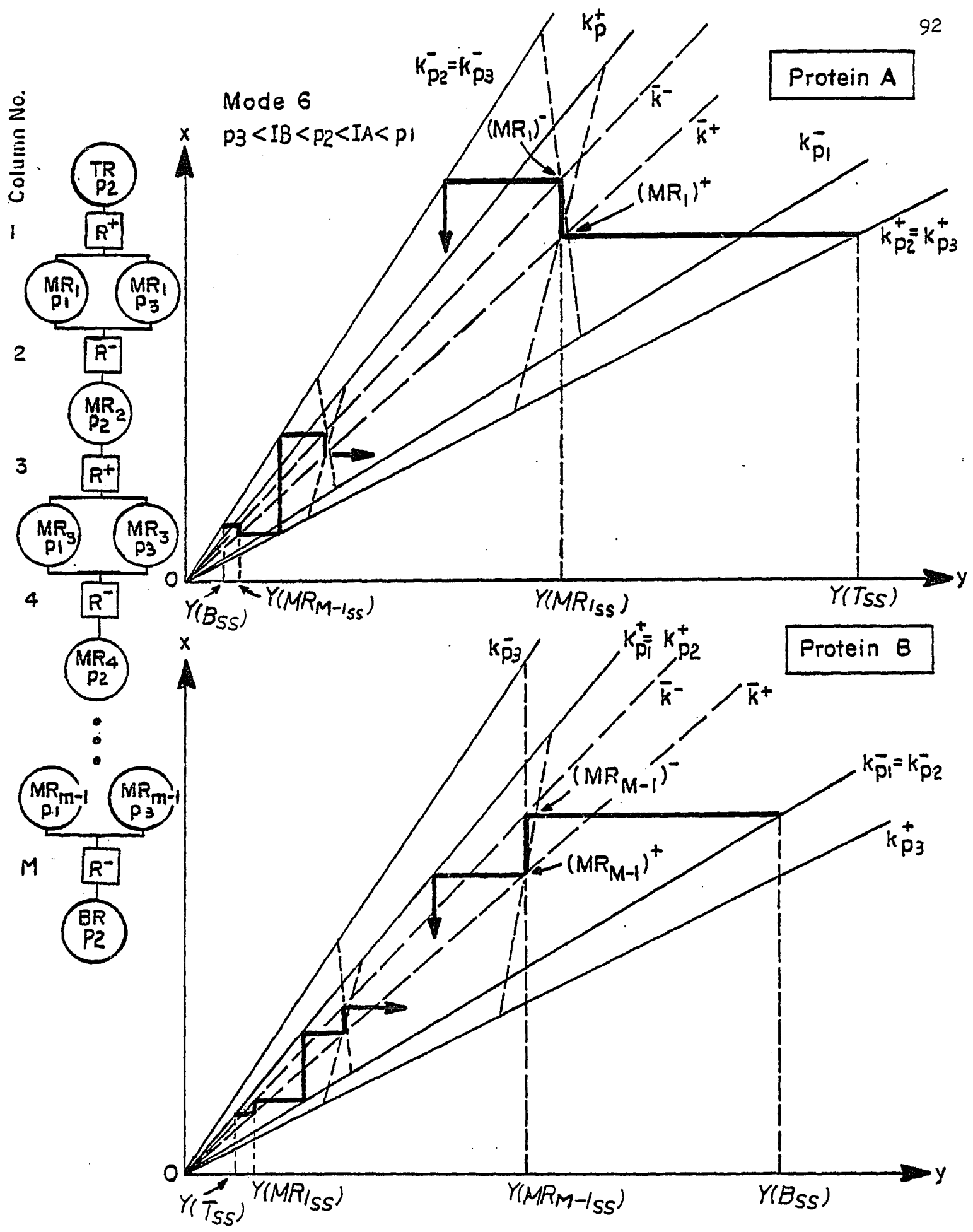


Figure 8.14 Graphical Solution for Multi-Column Parapump-Mode 6

Mode 6:

As one can see from Figure 8.14, this mode is a combination of modes 2 and 3. As a result, this mode gives an M-Step staircase for both protein A and B on X-Y diagram. Furthermore, protein A migrates upward and concentrates in the top reservoir, while protein B moves downward. Thus, A and B split from each other. As M becomes larger, SF ($Y(Tss)/Y(Bss)$) approaches infinity for protein A, while SF approaches zero for protein B.

Mode 7:

As shown in Figure 8.15, the system is a generalization of Mode 4. There are top and bottom reservoirs, and (M-1) middle reservoir and (M/2) side reservoirs. The side reservoirs, and are maintained at pH=P3, and the remaining remaining reservoirs have the same pH values as those for Mode 5. As shown in Figure 8.15, for protein A, an M-step staircase is formed and the separation factor increases as M increases. It is also shown, that A is concentrated in the bottom reservoir and Protein B moves toward the side reservoir. Since the reservoirs are so arranged that only one staircase is obtained for protein B.

Figure 8.16 shows the dependence of the steady state separation factor (SF) of M. For all three modes (Modes 5, 6, and 7), SF for protein A increases as the M increases. For protein B, SF decreases as M increases for a paramup operating with Mode 6, and remains constant for Mode 8. However, no separation will take place for B when Mode 5 is used.

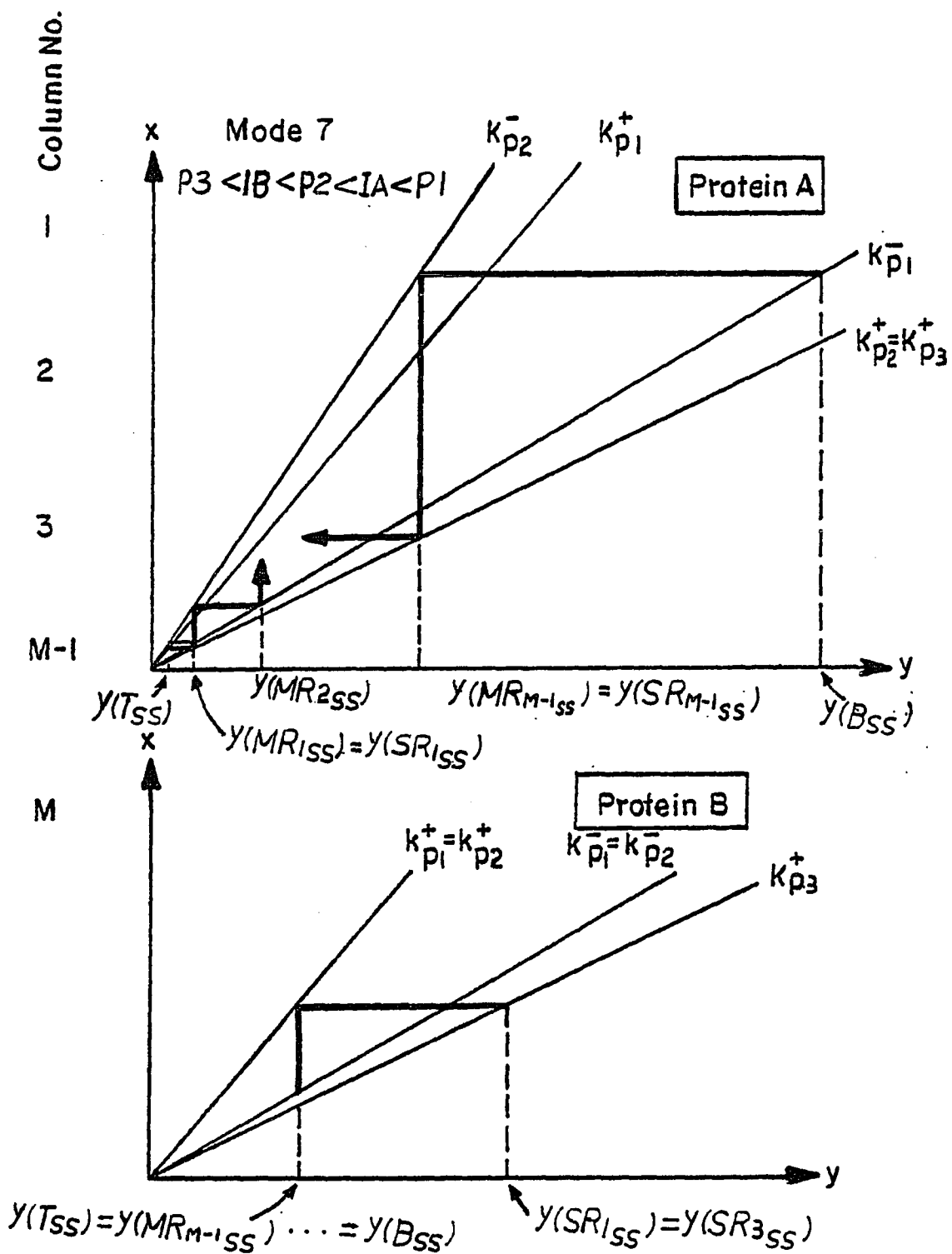
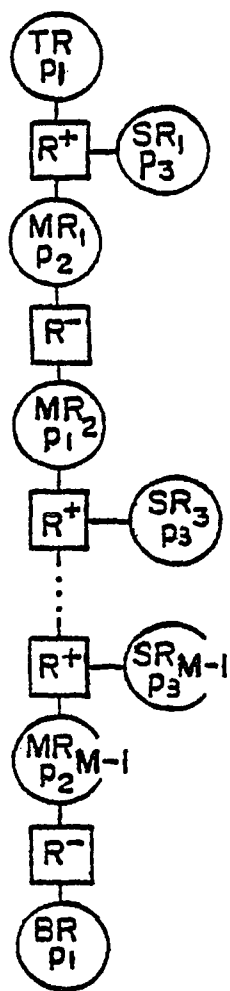


Figure 8.15 Graphical Solution for Multi-Column Paracolumn-Mode 7

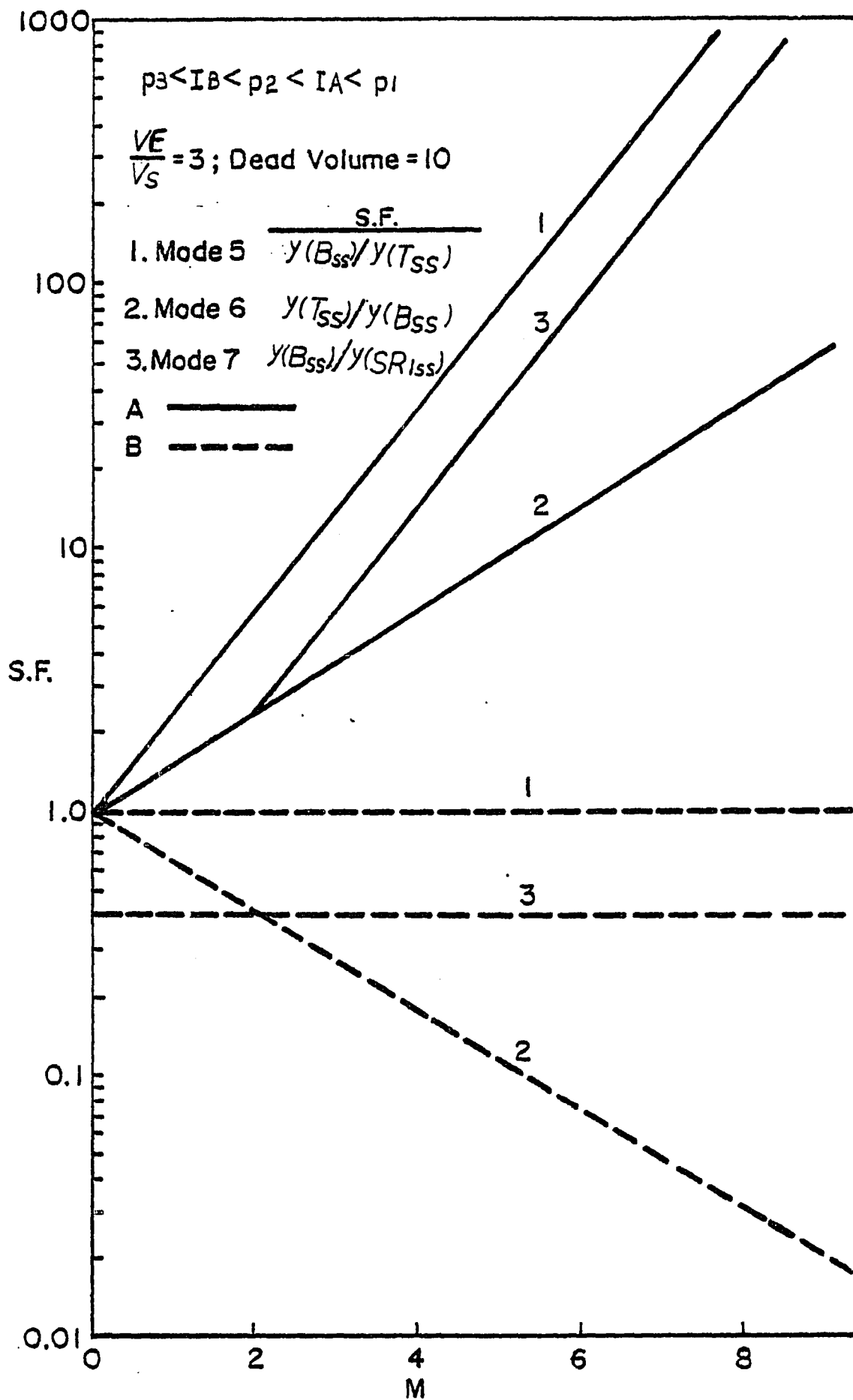


Figure 8.16 Steady State SF_{SS} VS. Number of Column

8.3: Open Parametric Pumping

In this section, we shall discuss the open parapump with the single cell model. The open parapump includes feed stream introduced to, and product stream withdrawn from, the parapump. Figure 8.17 shows the operation procedure in a cycle for 2-column open parapump. It is seen that the operation is similar to that of Mode 3 of batch parapump. An additional step is added to withdraw the products and to introduce feed into the reservoir. The displacement is adjusted unevenly corresponding to the feed location, so that the reservoir volume is unchanged after an operation cycle. For example, we may feed the top reservoir 12 cc per cycle, and displace 18cc down from the top reservoir to the bottom reservoir in the first step, and then 12 cc for the other displacement steps as shown in Figure 8.18. Thus the gained 6 cc in the bottom reservoir is withdrawn as product, and the volume of the bottom reservoir is unchanged at the end of the cycle. For the top reservoir, the loss of 6 cc in displacement and 6 cc in product is balanced with 12cc feed to this reservoir. The effect of feed location on separation is studied on two-column and four-column open parapumps with the parameters: feed=12cc/cycle, resevoirs volume=30cc, and the height of each packed bed = 8 cm. The results are shown in Figures 8.18 and 8.19. The values of K for each component at each ionic exchanger and pH level is also listed in Figure 8.18. One can see from Figure 8.18 that the best feed location is the middle

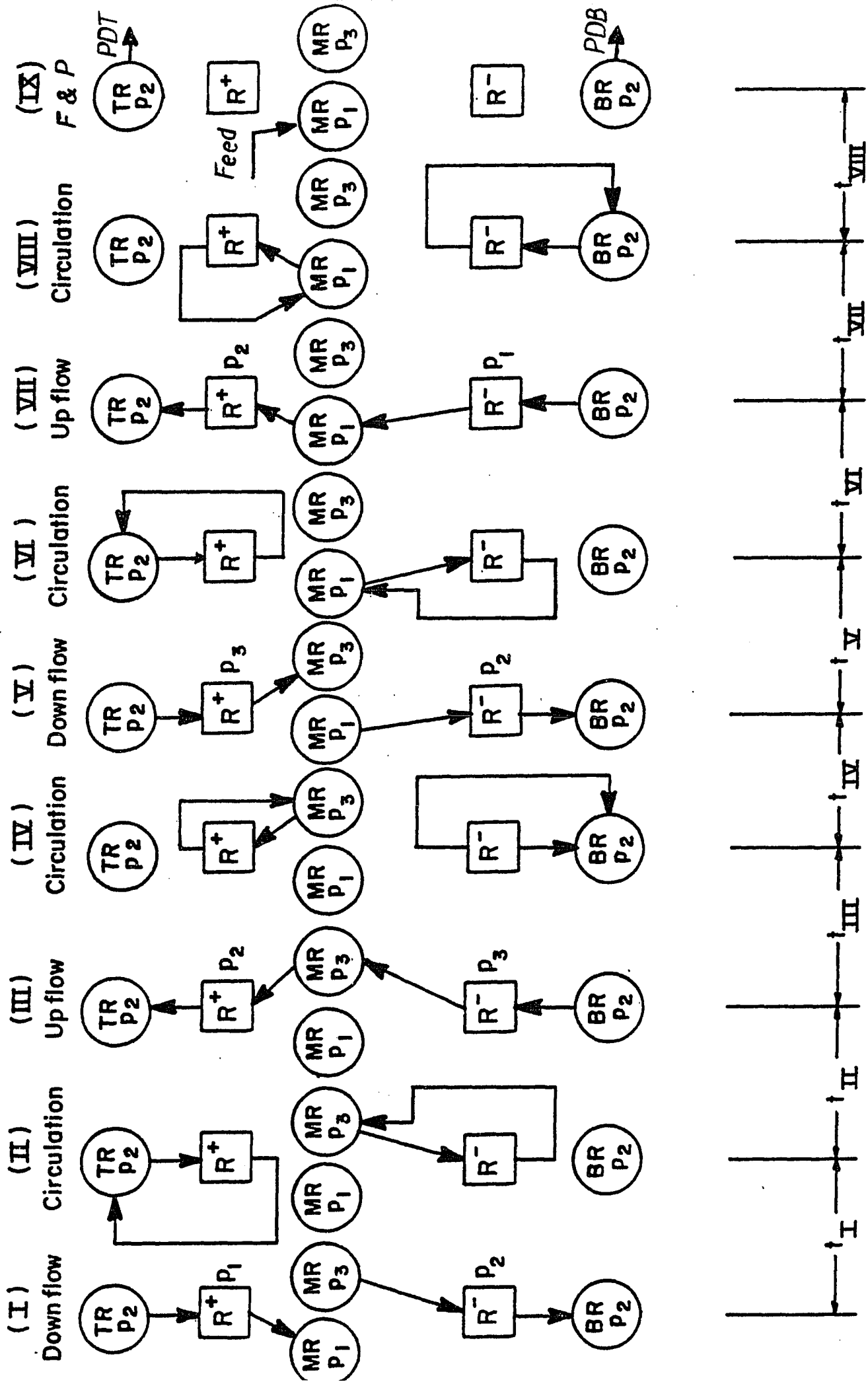


Figure 8.17 Schematic of Two-Column Open Parapump

Curve	1	2	3	4
Feed Location	P ₁	P ₃	P ₂ TOP	P ₂ BOT

Comp.	K _{P1} ⁺	K _{P2} ⁺	K _{P3} ⁺	K _{P1} ⁻	K _{P2} ⁻	K _{P3} ⁻
A	1.2	0.4	0.4	0.6	1.5	1.5
B	2.0	2.0	0.5	0.6	0.6	1.8

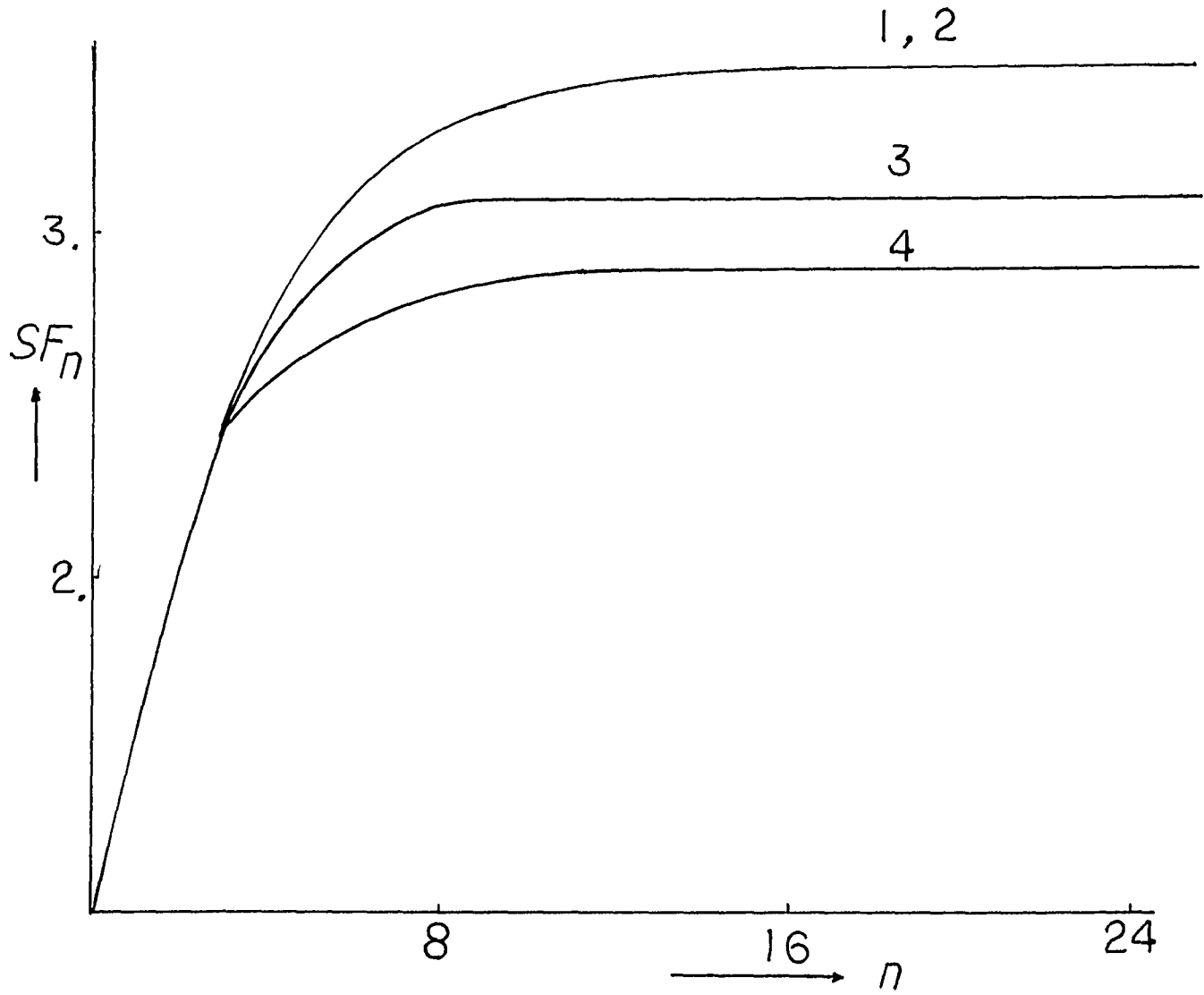
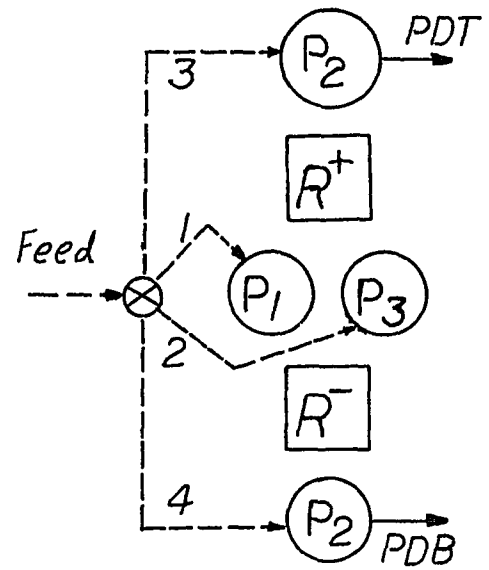


Figure 8.18 Effect of Feed Location on Separation for 2-Column Parapump.

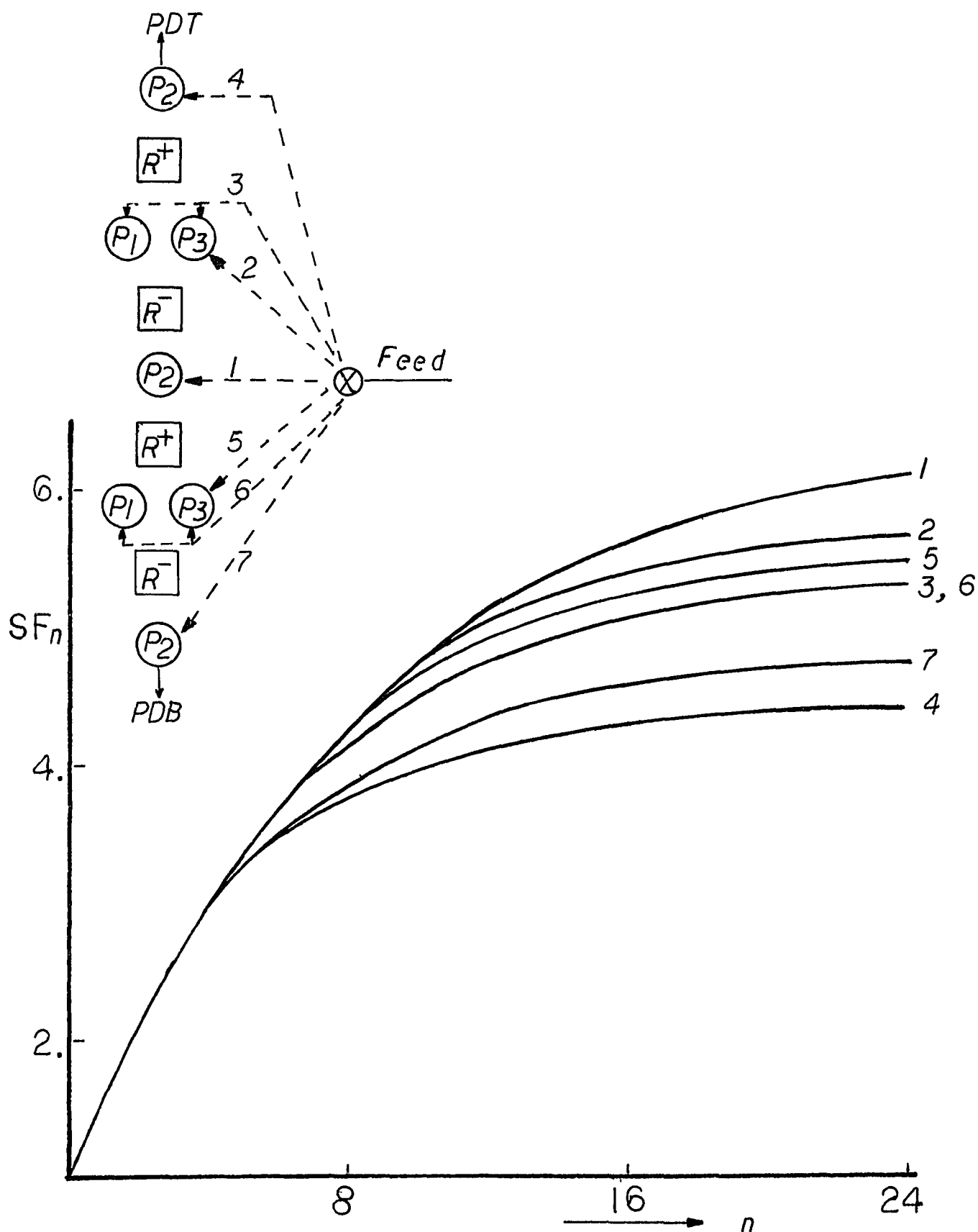


Figure 8.19 Effect of Feed Location on Separation for 4-Column Open Parapump

reservoir (curve 1 and 2). Separation is poor for the feed introduced into the top and bottom reservoir (curve 3 and 4). The study of feed location on 4-column open parapump is shown in Figure 8.19. It is also seen that the best separation is obtained when feed is introduced into the central reservoir (curve 1 in Figure 8.19). The computation parameters used in Figure 8.19 are the same values as those in Figure 8.18. These results are explained as follows. When feed is introduced into the middle reservoir, the fluid has an even chance to be separated by the two columns; when feed is introduced into the top or bottom reservoir, feed solution mixes with product and causes poor separation. This phenomenon is similar to that in distillation in which feed is usually not introduced to the condenser or to the reboiler. Figure 8.20 shows the separation of 2-column open parapump with uneven product stream. Feed the middle reservoir (pH=Pl) with 12 cc per cycle, and products are withdrawn from the top and bottom reservoir in 5 patterns as shown in Figure 8.20. It is seen that the best separation is obtained when the volumes for top and bottom products are equal (curve 3). It is also seen that when one product stream is zero, the separation is very poor, and no separation at steady state (Curves 1,5). The separation factor for uneven product stream is defined in equation (8.6) .

$$SF = \begin{bmatrix} YA \\ -- \\ YB \end{bmatrix} \begin{bmatrix} YB \\ -- \\ YA \end{bmatrix} \frac{PDT \ PDB}{(F/2) \ (F/2)} \quad (8.6)$$

where PDT : volume of top product per cycle
PDB : volume of bottom product per cycle

Curve	cc PDT	cc PDB	Total Recovery
1	12.	0.	.515
2	9.	3.	.629
3	6.	6.	.651
4	3.	9.	.618
5	0.	12.	.507

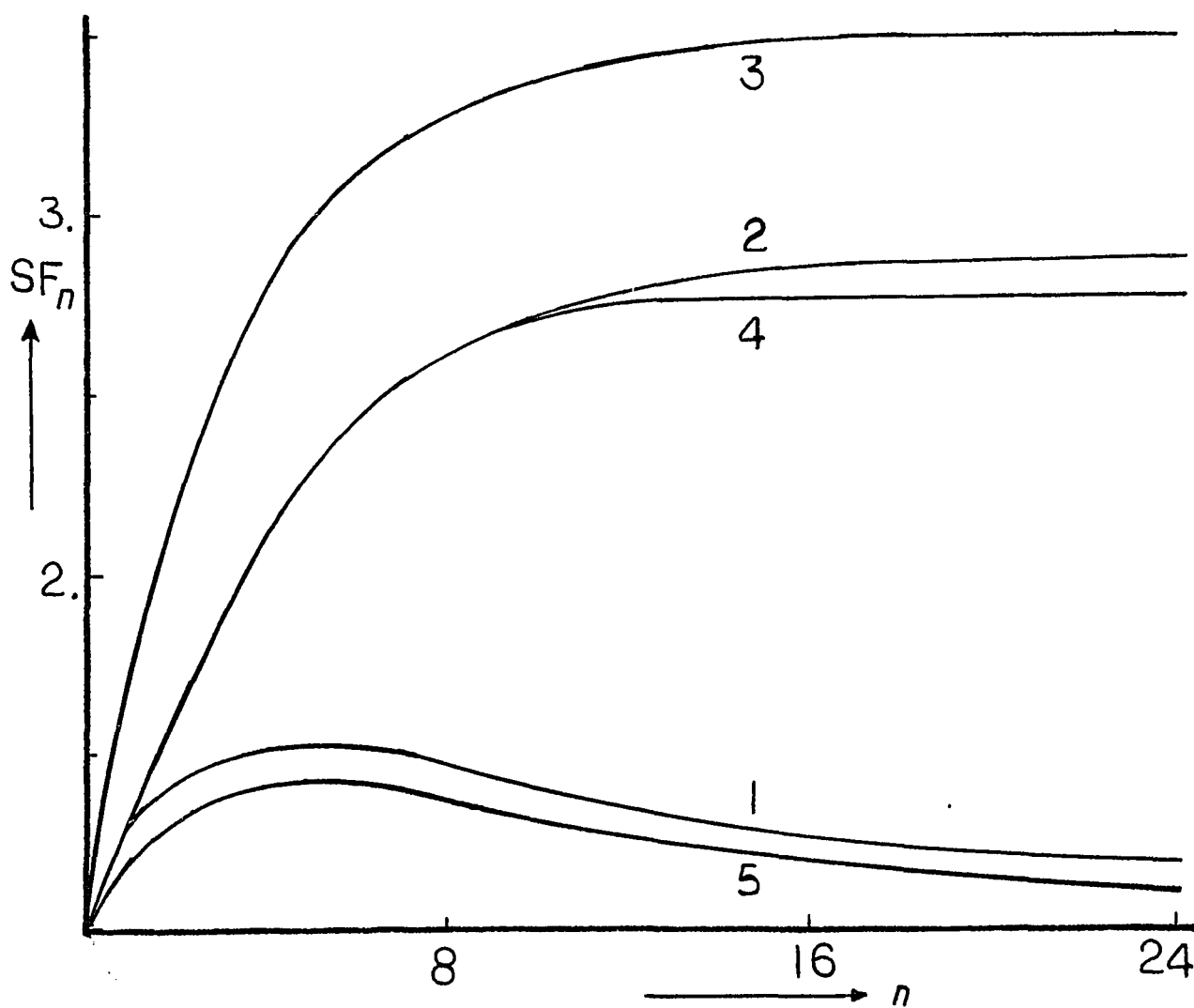
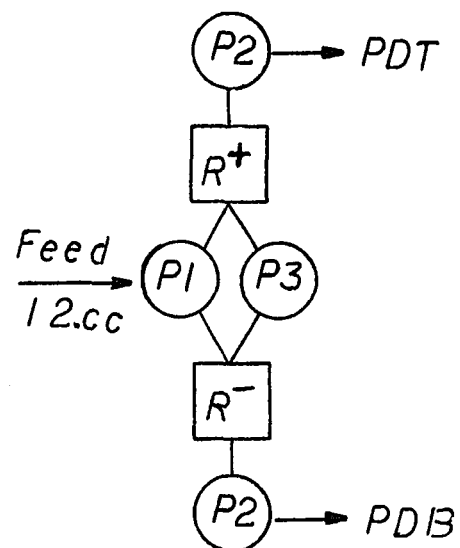


Figure 8.20 Effect of Product Taken on Separation for 2-Column Open Parapump.

$$F = PDT + PDB : \text{volume of feed per cycle}$$

It is seen in equation 8.17, that the 3rd term of the right hand side is maximum when $PDT=PDB=(F/2)$. It has to be pointed out that equation 8.17 is not applicable when one of the product streams is equal to zero. The total recovery, as defined in equation (8.7), is listed on the 4th column of the insert table.

$$Rc\% = \frac{PDT \ Y_A \ \text{Top} + PDB \ Y_B \ \text{Bot}}{F \ (Y_A+Y_B) \ \text{feed}} \quad (8.7)$$

The maximum recovery is obtained when the sizes of top and bottom products are equal for the values of K listed in the figure. It is understood that, for particular interest the uneven product stream may be desired. For example, when we are only interested in the top product stream, optimization will be emphasized on the top product stream.

The Effect of Equilibrium Constant :

It is understood that the separation of parapump is caused by the shift of equilibrium distribution as the control variable changes. The effect of the value K on separation is studied on the 4-column open parapump. Feed solution is introduced into the center reservoir and products are withdrawn from the top and bottom reservoirs. The amount of feed is equal to half of the void volume of a column, VE , .ie., $(F/2)=PDT=PDB=(VE/4)$. The

parapump is operated with 3 pH levels, P1, P2, and P3, and $P1 > IA > P2 > IB > P3$. For illustration, the K values are grouped into two values, K1 and K2, for all components in the 3 pH levels and two ionic exchangers. K1 stand for the adsorption favor equilibrium constant, and K2 for the adsorption unfavor equilibrium constant. We denote K1 for proteins at pH higher than I.E. in the anion column and for proteins at pH lower than I.E. in the cation column; K2 for proteins at pH lower than I.E. in the anion column and for proteins at pH higher than I.E. in the cation column.

$$K1=K(P1,An,A)=K(P2,An,B)=K(P2,An,B)=K(P2,C,A)=K(P3,C,A)=K(P3,C,B)$$

$$K2=K(P3,An,A)=K(P2,An,A)=K(P3,An,B)=K(P1,C,A)=K(P1,C,B)=K(P2,C,B)$$

where: An = Anion Exchanger ; C = Cation Exchanger

Figure 8.21 plots the calculated steady state separation factor on the K1 and K2 domain. The curves in the figure stand for constant separation factor. For given K1 and K2, one can use this figure to estimate the separation results by interpolating these constant separation curves. Note that Figure 8.21 is symmetric to the diagonal line ($SF_{ss}=1.$). Above the diagonal line, where SF_{ss} is higher than 1., is the region of normal operation. Below the diagonal line, SF_{ss} is less than unity, and the parapump is operated in the region of reverse separation. For

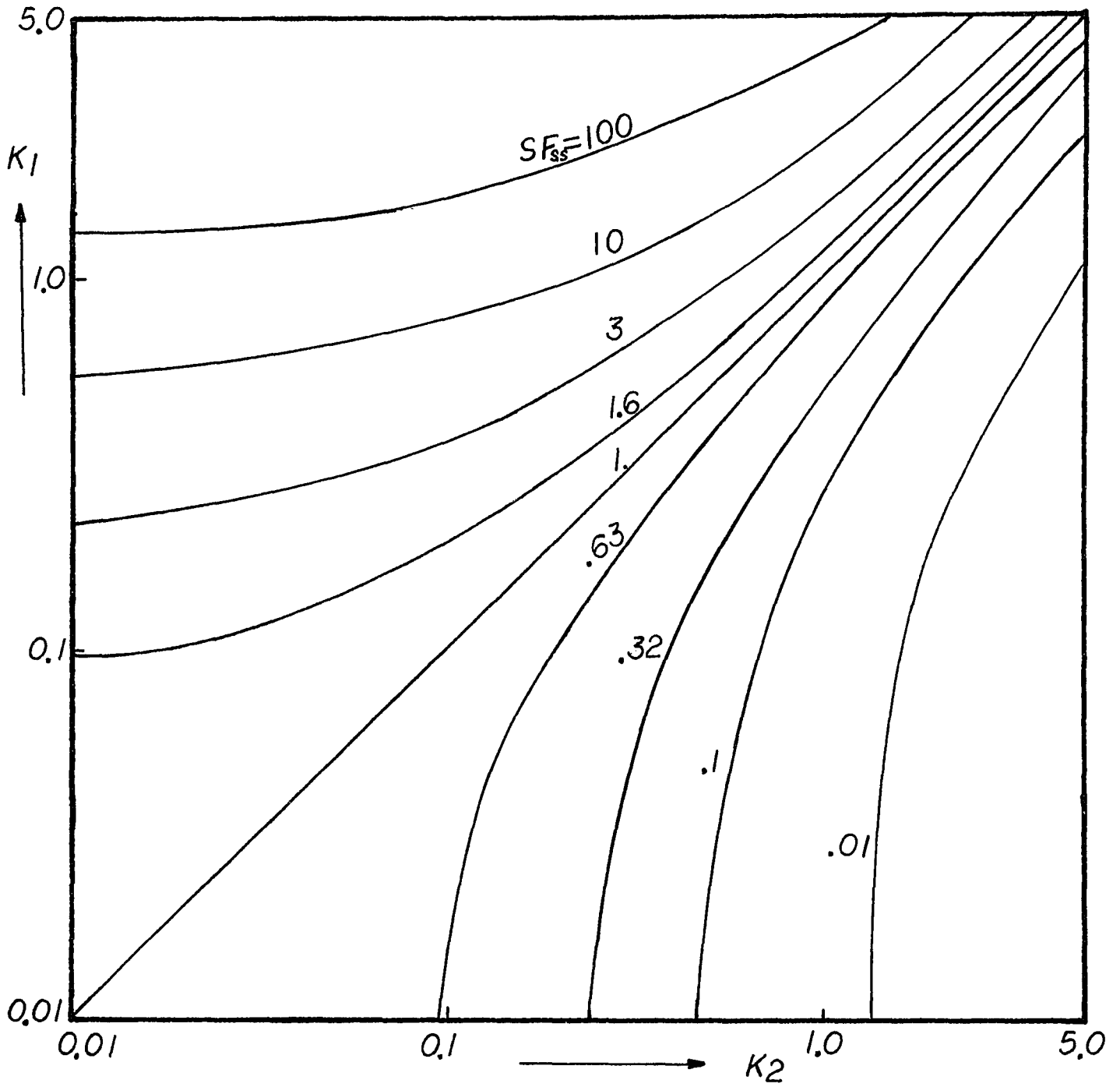


Figure 8.21 Calculated Separation Factor in K_1 and K_2 Domain

convenience, Figure 8.22(a;b) plots the separation factor versus (K_1/K_2) with fixed parameter K_1 . Figure 8.22(a) is plotted for the normal separation and Figure 8.22(b) is for reverse separation region. The two Figures are mirror images to each other.

8.4 : Separation of Multiple-Solute System Via Open Parapump

A system of multiple components mixture is studied on 6-column open parapump. It is assumed that there is no interference between the components. The feed consists of 6 components, namely, A, B, C, D, E, and F, and the corresponding isoelectric points are I_A , I_B , I_C , I_D , I_E , and I_F . The arrangement of the three pH levels will affect the separation significantly. Two cases of pH arrangement have been studied.

Case 1: Choose three pH levels P_1 , P_2 , and P_3 , such that,

$$P_1 > I_A > I_B > I_C > P_2 > I_D > I_E > I_F > P_3$$

For the purpose of illustration, we grouped the equilibrium constants of each component into 2 values as shown in Tables 5 and 6. For each component a higher K value is assigned to $pH > I.E.$ in anion column and to $pH < I.E.$ in cation column; a smaller value of K is assigned to $pH < I.E.$ in anion column and to $pH > I.E.$ in anion column.

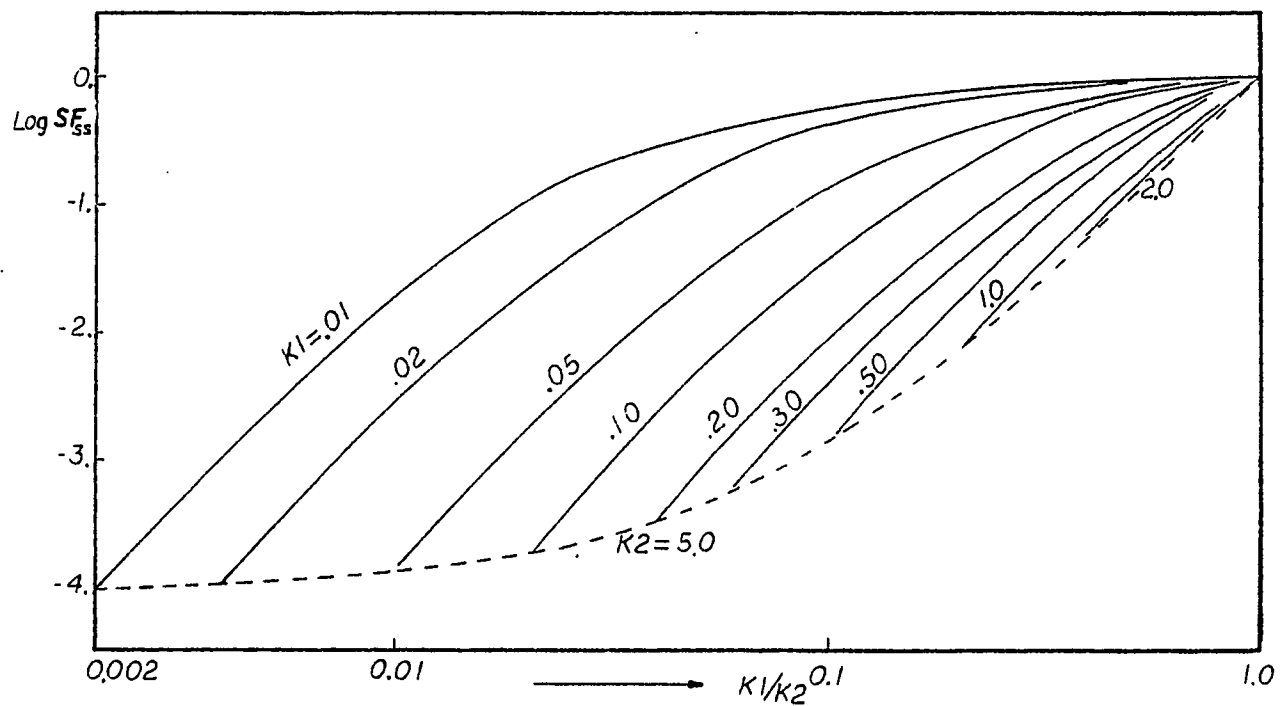
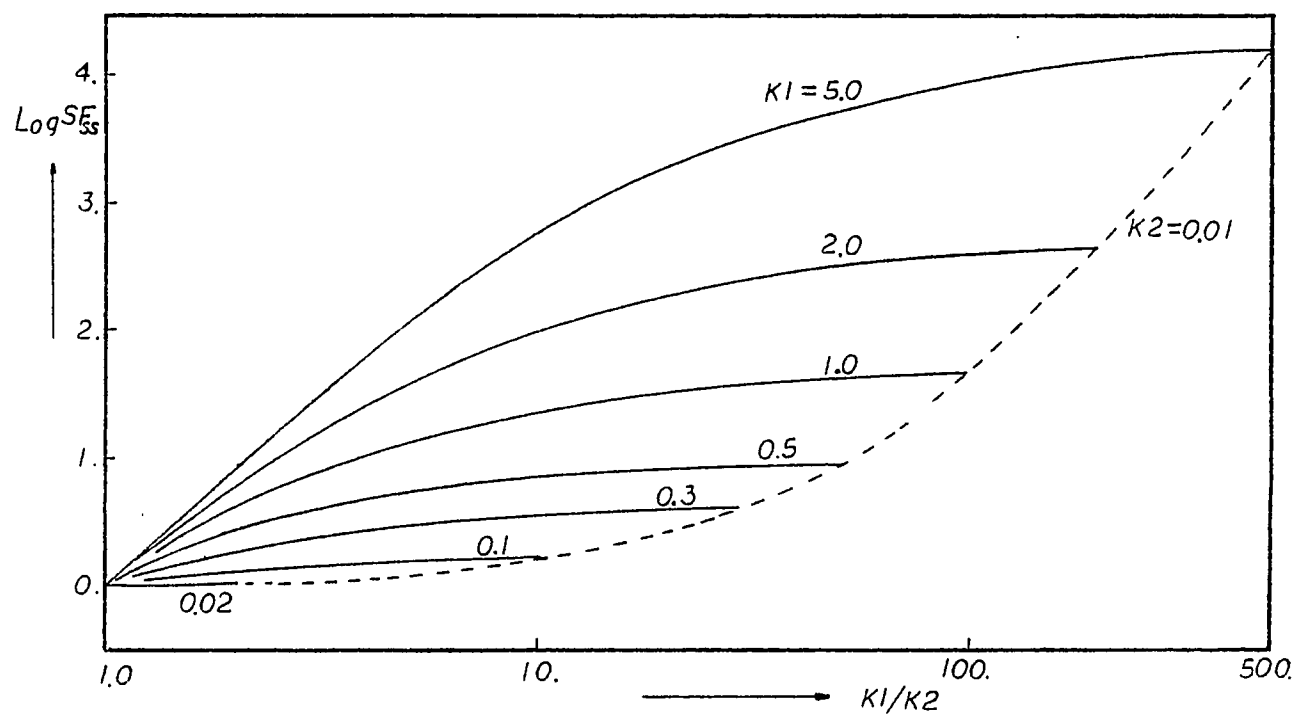


Figure 8.22 Calculated Separation Factor with Fixed $K1$

Table 5: Case 1

Comp.	anion exchanger			cation exchanger		
	P1	P2	P3	P1	P2	P3
A	1.6	0.5	0.5	0.5	1.6	1.6
B	1.5	0.5	0.5	0.5	1.5	1.5
C	1.4	0.5	0.5	0.5	1.4	1.4
D	1.3	1.3	0.5	0.5	0.5	1.3
E	1.2	1.2	0.5	0.5	0.5	1.2
F	1.1	1.1	0.5	0.5	0.5	1.1

Figure 8.23 shows the calculated $\langle Y_i \rangle_{PDT} / \langle Y_i \rangle_{PDB}$ versus the number of cycle operation. The computation is based on an equal molarity feed $F=6\text{cc/cycle}$, the two product streams $PDT=PDB=F/2$, height of each column = 8cm, and reservoir volume = 20cc. It is seen in Figure 8.23, that components A, B and C are more concentrated in the top product stream, and components D, E, and F are more concentrated in the bottom product stream.

Case 2: Choose three pH levels P1, P2, and P3, such that,

$$I_A > P_1 > I_B > I_C > P_2 > I_D > I_E > P_3 > I_F$$

The equilibrium constants used for calculation are listed in Table 6.

Case 1

$$P_1 > I_A > I_B > I_C > P_2 > I_D > I_E > I_F > P_3$$

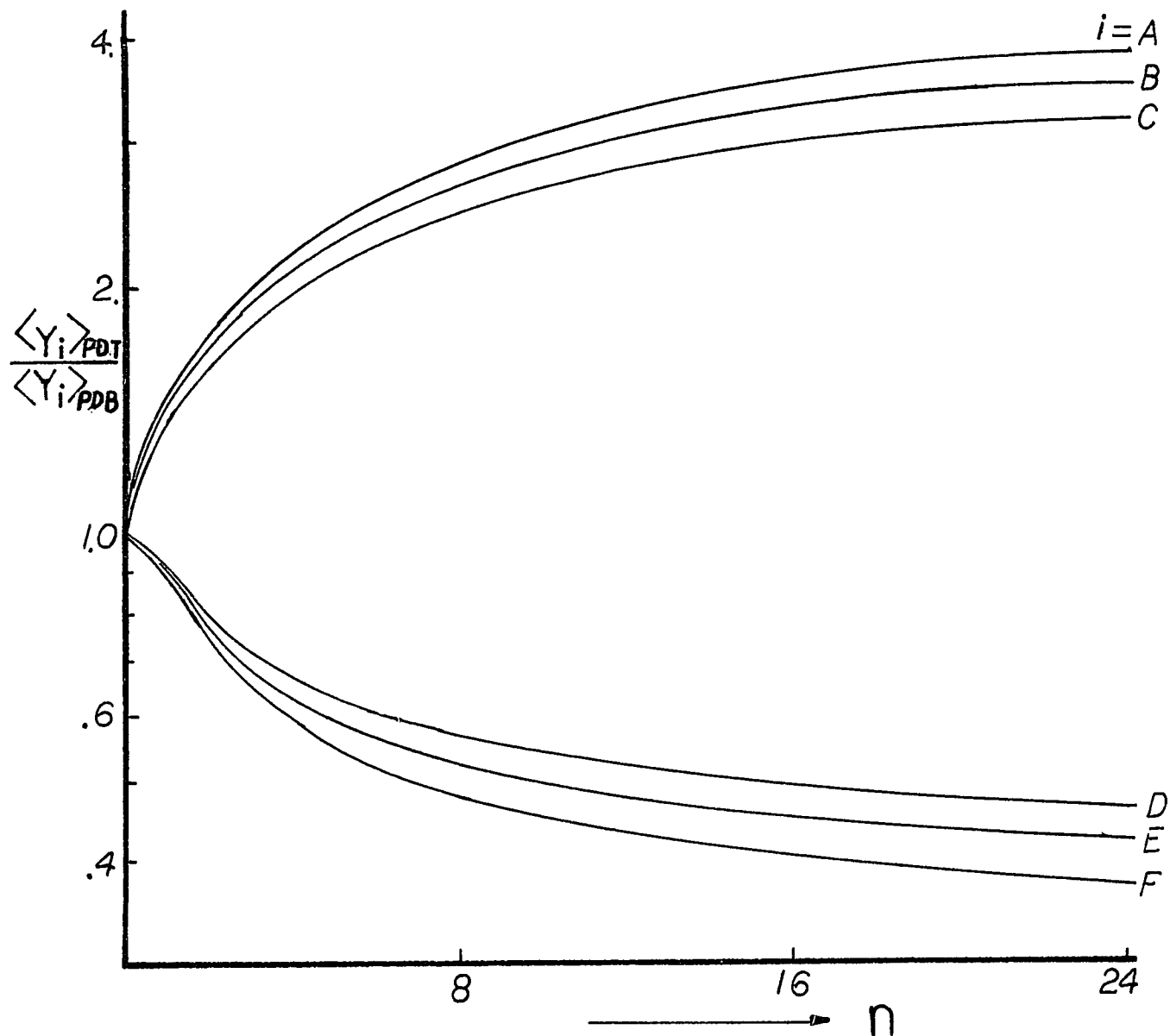


Figure 8.23 Separation of Multiple Components System-Case 1

Table 6 : Case 2

Comp.	anion exchanger			cation exchanger		
	P1	P2	P3	P1	P2	P3
A	0.5	0.5	0.5	1.6	1.6	1.6
B	1.5	0.5	0.5	0.5	1.5	1.5
C	1.4	0.5	0.5	0.5	1.4	1.4
D	1.3	1.3	0.5	0.5	0.5	1.3
E	1.2	1.2	0.5	0.5	0.5	1.2
F	1.1	1.1	1.1	0.5	0.5	0.5

The results for case 2 are shown in Figure 8.24. As one can see, components B and C are concentrated in the top product stream; component D and E are concentrated in the bottom product stream; component A and F are equally distributed in the top and bottom product streams. No separation is predicted for components A and F because the 3 pH levels are all higher than the isoelectric point of component F and lower than that of component A.

Case 2

$$I_A > P_1 > I_B > I_C > P_2 > I_D > I_E > P_3 > I_F$$

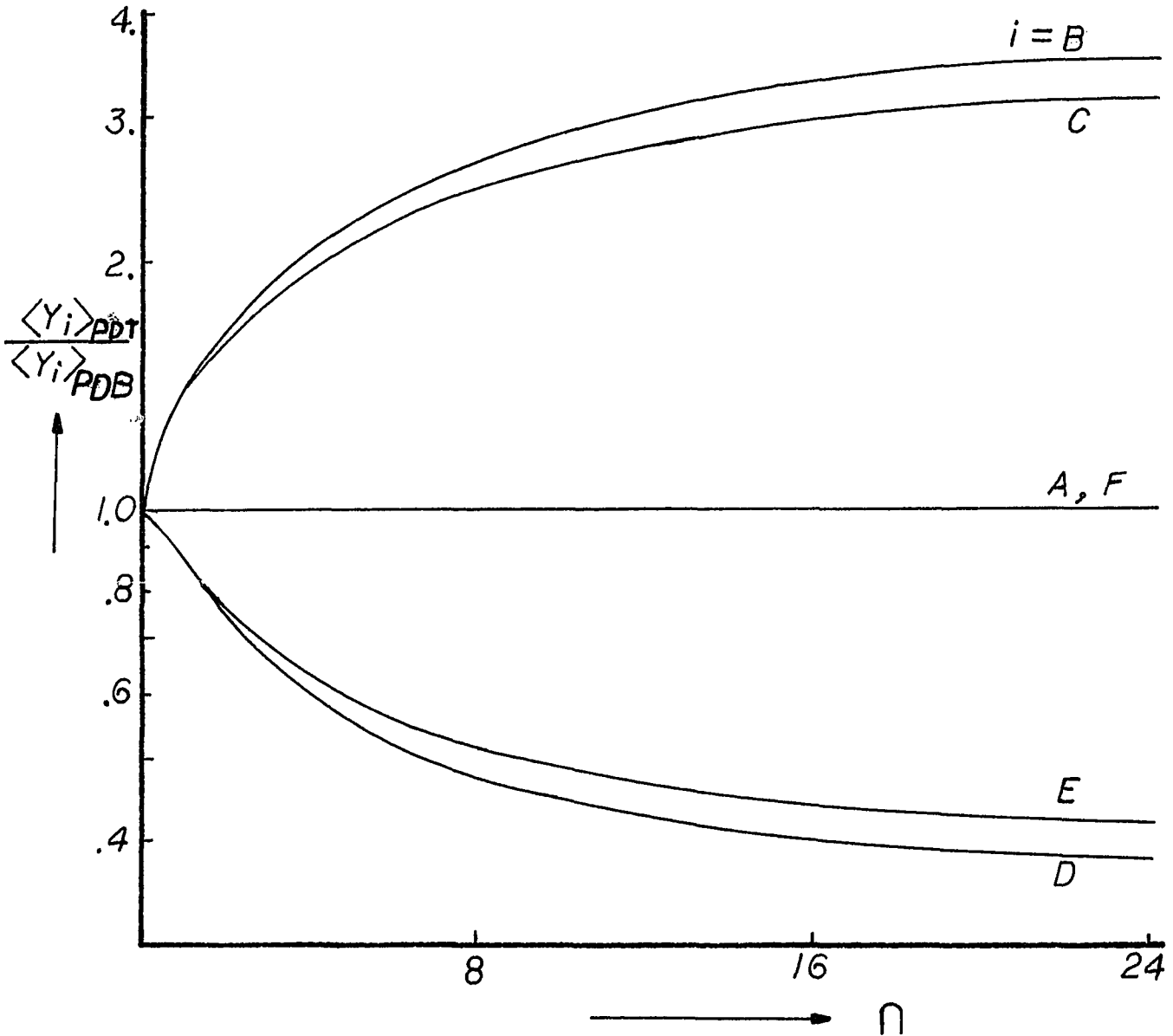


Figure 8.24 Separation of Multiple Components System-Case 2

Chapter 9 : Multi-Cell Model and Semi-Continuous One-Column Parapump

The multi-cell in series model, as described in Chapter 4, is used to examine a semi-continuous one column parapump. In this chapter, equations (4.3), (4.5), linear equilibrium relationship, and equation (4.7) with $B=1$ are applied simultaneously to solve the pH, X, and Y. Since $B=1$ in equation 4.7, the change of pH is assumed sharply and as quickly as the bulk fluid flow velocity. The emphasis of this chapter is to examine the dynamic characteristics of the column of the Parapump. Included are the distribution profile of state variables, kinetic parameters, equilibrium parameters in the one-column open parapump.

9.1: Process Description of One-Column Semi-Continuous Parapump

Figure 9.1 shows the operation of a semi-continuous one-column parapump. The one-column parapump studied here has been described in previous chapters. It has already been shown that protein A can be separated from a mixture provided that its isoelectric point, I_A , lies between the two pH levels, i.e., $P_2 < I_A < P_1$. The flow system of the semi-continuous parapump has eight distinct stages in each cycle(Figure 9.1):

(I) Pump the low pH(P_2) fluid from the top reservoir to the

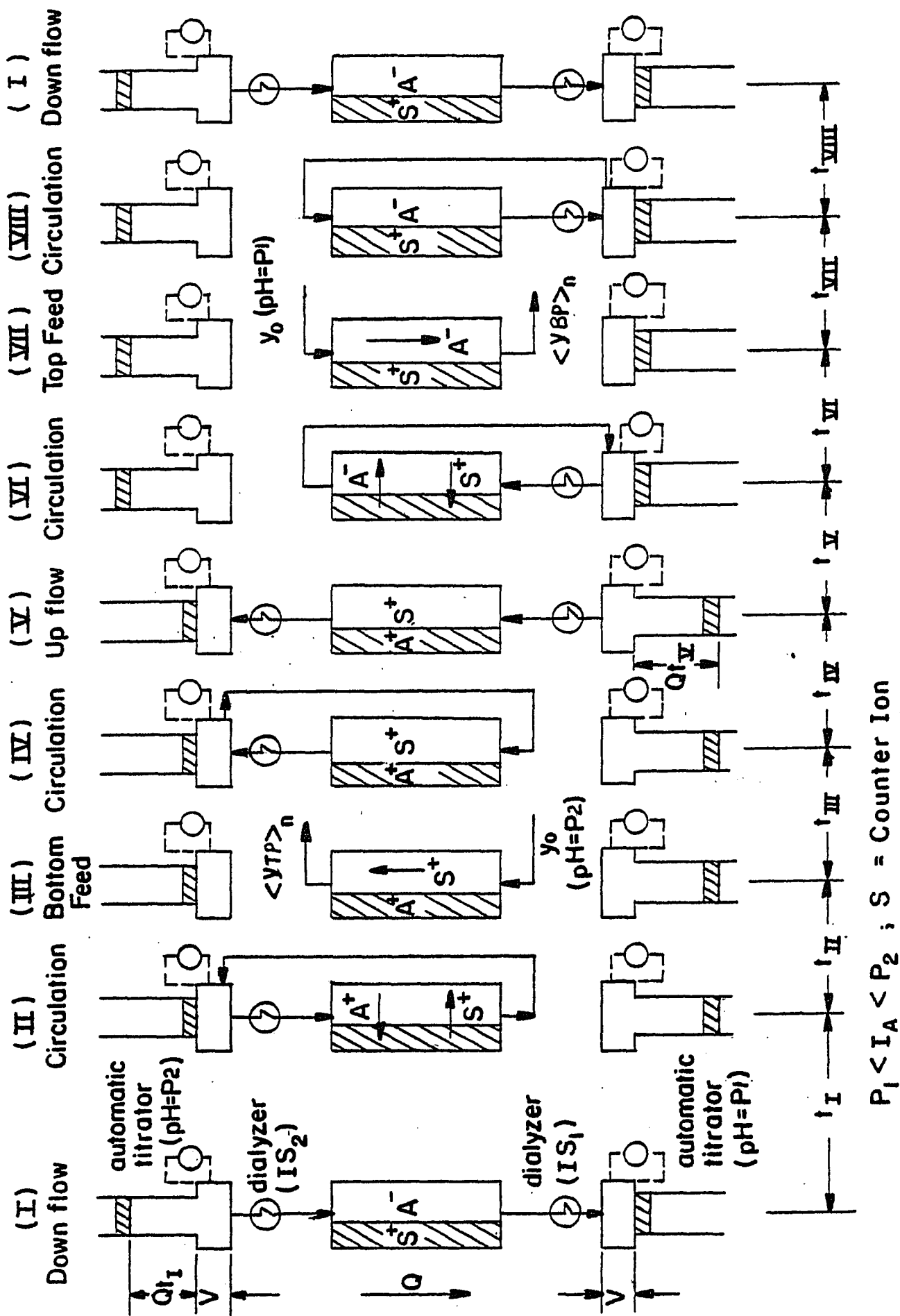


Figure 9.1 Column Diagram for Semi-Continuous Parapump

- top of the column for time t_I , while the solution emerging from the other end enters the bottom reservoir.
- (II) Circulate the fluid between the top reservoir and the column for time t_{II} . During this step the pH in the column is ensured to change from P1 to P2. As a result, the counter ions(S+) are exchanged for the positively charged protein(A+) originated from the top reservoir.
- (III) Feed at the bottom of the column with the mixture of pH=P2 for time t_{III} , and simultaneously a top product free of A is removed from the column at the same rate. In addition, the solute is initially presents in the bottom feed is exchanged for S+.
- (IV) Circulate the fluid between the top reservoir and the column for time t_{IV} . This will allow the concentration in the column and the top reservoir to become uniform.
- (V) Pump the fluid with pH=P1 from the bottom reservoir to the bottom of the column for time t_V , and at the same time the solution free of protein A flows out of the column to the top reservoir.
- (VI) Circulate the fluid between the bottom reservoir and the column for time t_{VI} . This will insure that the pH in the column is shifted back to P1, and desorption of A occurs. S+ shifts back to the bed and the ion

exchanger is then regenerated.

(VII) Feed at the top with the mixture of pH = P1 for time t_{VII} , while a product rich in A is withdrawn from the bottom of the column.

(VIII) Circulate the fluid between the column and the bottom reservoir. This will result a uniform concentration between the column and the bottom reservoir. One cycle is thus completed.

By repeating the process described above in the succeeding cycles, one may see that in the limit of a large number of cycles, the system is capable of removing A from the feed streams and transferring it to the bottom product stream. Note that the flow rate, Q , within the column is always identical to the reservoir displacement rate. The volumes of the bottom and top feed (Qt_{III} and Qt_{VII}) are respectively equal to those of the top and bottom products. Also, the upward and downward flow have the same displacement, i.e. $Qt_I = Qt_V$.

9.2 : Determination of Equilibrium and Mass Transfer

To implement the computation of concentration profiles, we must have the equilibrium constants, K_1 and K_2 , and the rate constant, λ . These parameters can be determined experimentally via the following modes of parapump operation:

Mode 8: No circulation ($t_c = t_{II} = t_{IV} = t_{VI} = t_{VIII} = 0$)

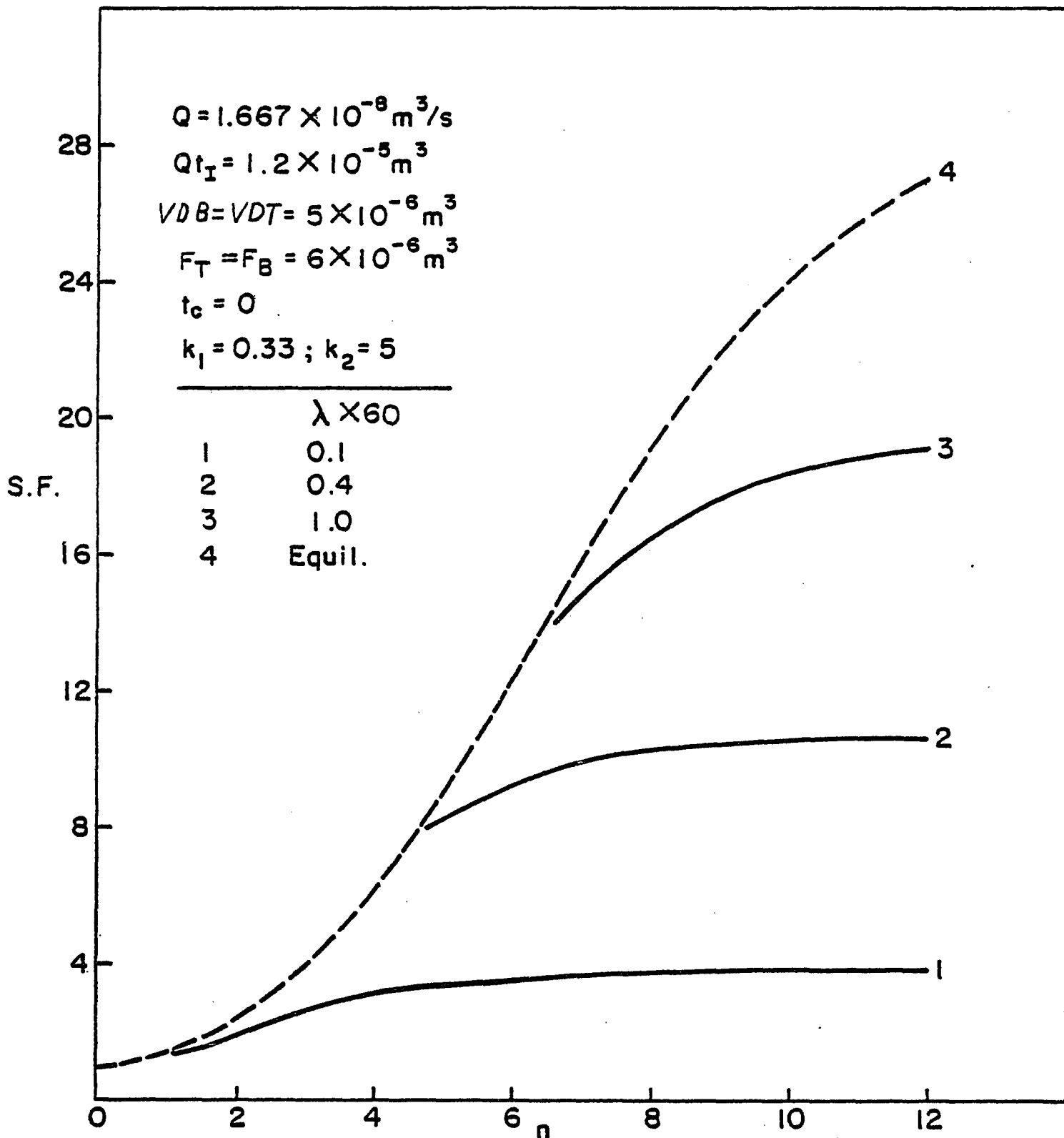
Figure 9.2 shows the calculated separation factor ($\langle YBP \rangle_n / \langle YTP \rangle_n$) vs. number of cycles for several values of λ . As expected, this parameter does significantly affect the separation. For small λ , little mass transfer occurs between phases and hence little separation takes place. As λ increases, the amount of interphase mass transfer increases toward a limit imposed by equilibrium.

Mode 9: With circulation and assume that:

$$t_{II} = t_{IV} = t_{VI} = t_{VIII} = t_c$$

where t_c = time duration of circulation.

Figure 9.3 shows the calculated separation factors vs. n for $\lambda = 1.667 \times 10^{-3}$ and 6.667×10^{-3} . As t_c increases SF will increase or decrease, depending on the value of λ , and approach a limit-equilibrium condition. When the value of λ is small (e.g. 1.667×10^{-3}), SF increases with t_c . However, for a larger value of λ (e.g. 6.667×10^{-3}), an opposite effect will result. Also as t_c increases, the mixing between the column and reservoir becomes significant; and at the end of each circulation step (i.e., steps II, IV, VI or VIII in Figure 9.1), the adsorption column should have a uniform concentration in either fluid or solid phase.

Figure 9.2 Effect of λ on Separation

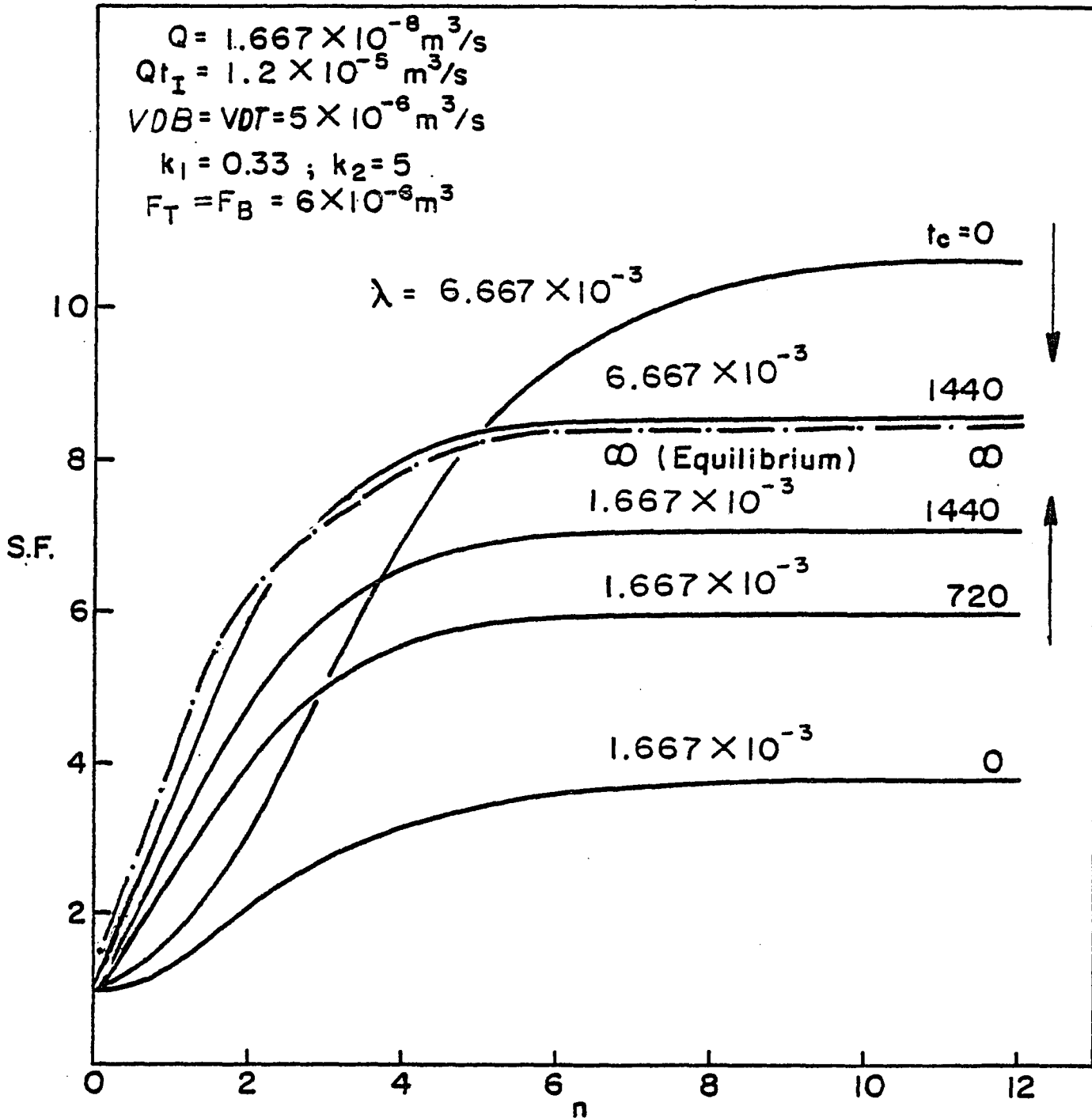


Figure 9.3 Effect of Circulation on Separation

Figure 9.4 and 9.5 show the typical experimental results respectively by Modes 8 and 9. As expected, hemoglobin does migrate downward and accumulate at the bottom end. In both top and bottom product streams, albumin concentration is essentially unaffected.

The experimental data shown in Figure 9.4 were obtained based on $t_c = 1440$ sec. Although not shown, the results for $t_c > 1440$ secs are essentially identical to those for $t_c = 1440$ secs. This is to say that the data shown in Figure 9.4 were obtained at equilibrium. These data were used to predict the equilibrium constants as follows: (1) assume values of K_1 and K_2 , (2) Let λ be infinity and calculate the transients using the STOP-GO method, and (3) If the calculated results fit the data K_1 and K_2 are the desired values. If not, assume new equilibrium constants and repeat steps 2 and 3. The estimated values of K_1 and K_2 for runs 2 and 3 (Figure 8-4) are respectively,

$$K_1 = 0.33 ; K_2 = 5.$$

Figure 9.5 shows the experimental results via Mode 8 for $Q = 1.667 \times 10^{-2}$ and 5×10^{-2} cm/Sec. The data were used to determine the velocity dependence of λ . The values of λ were obtained by matching calculated plots of separation factor vs. n with experimental data using the following procedures: (1) Assume the value of λ , (2) Using the K values obtained above, calculate the

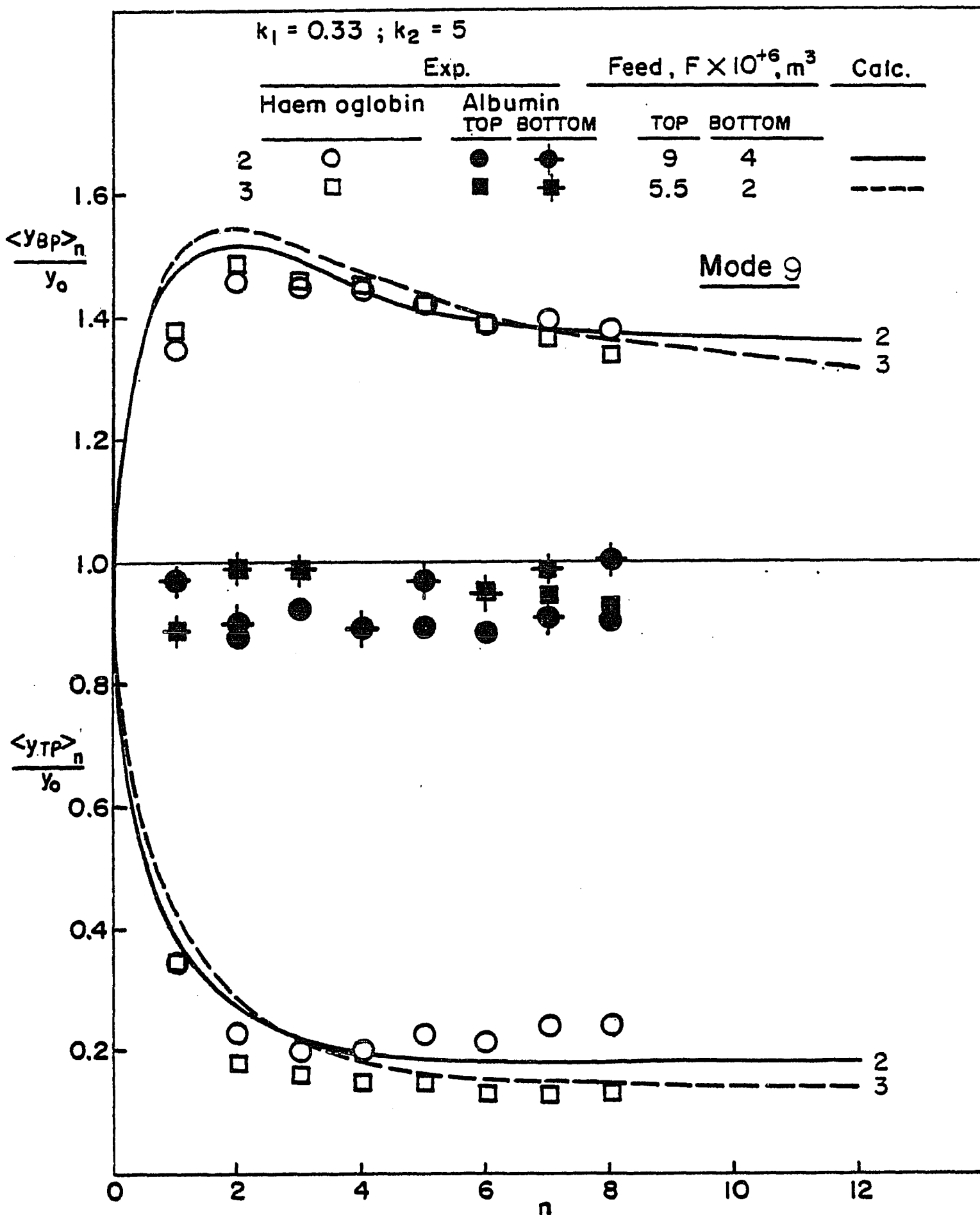


Figure 9.4 Experimental and Calculated Concentration Transient.

SF vs. n (by Stop and GO method), and (3) If the calculated results check with the data, the λ is the desired one. If not, assume a new λ and repeat steps 2 and 3. The estimated λ 's for Runs 4 and 8 are:

$$\begin{array}{ll} \text{Run 4: } \lambda_1 = 5 \times 10^{-3} & \text{for } Q_1 = 1.667 \times 10^{-2} \\ \text{Run 8: } \lambda_2 = 2.33 \times 10^{-3} & \text{for } Q_2 = 5 \times 10^{-2} \end{array}$$

By applying the following model (Sweed and Wilhelm^[31])

$$\frac{\lambda_2}{\lambda_1} = \left(\frac{Q_1}{Q_2} \right)^a \quad (9.1)$$

obtains $a=0.693$, thus, the correlation of rate constant with the flow velocity is:

$$\lambda = \lambda_1 \left(\frac{Q_1}{Q} \right)^a = 2.036 \times 10^{-2} Q^{-0.693} \quad (9.2)$$

From the equation 9.2, one can calculate λ for any given Q . Equation (9.2) and the estimated K values are based on Runs 4 and 8, and can only be applied to a parapump for which the buffer pH levels and ionic strengths are identical to those for Run 4 and 8.

In most mass transfer operations, the film mass transfer coefficient is increased with the increase of flow velocity. It is seen in this ionic exchanger gel, that the mass transfer rate constant (λ) is decreased with the increase of flow velocity.

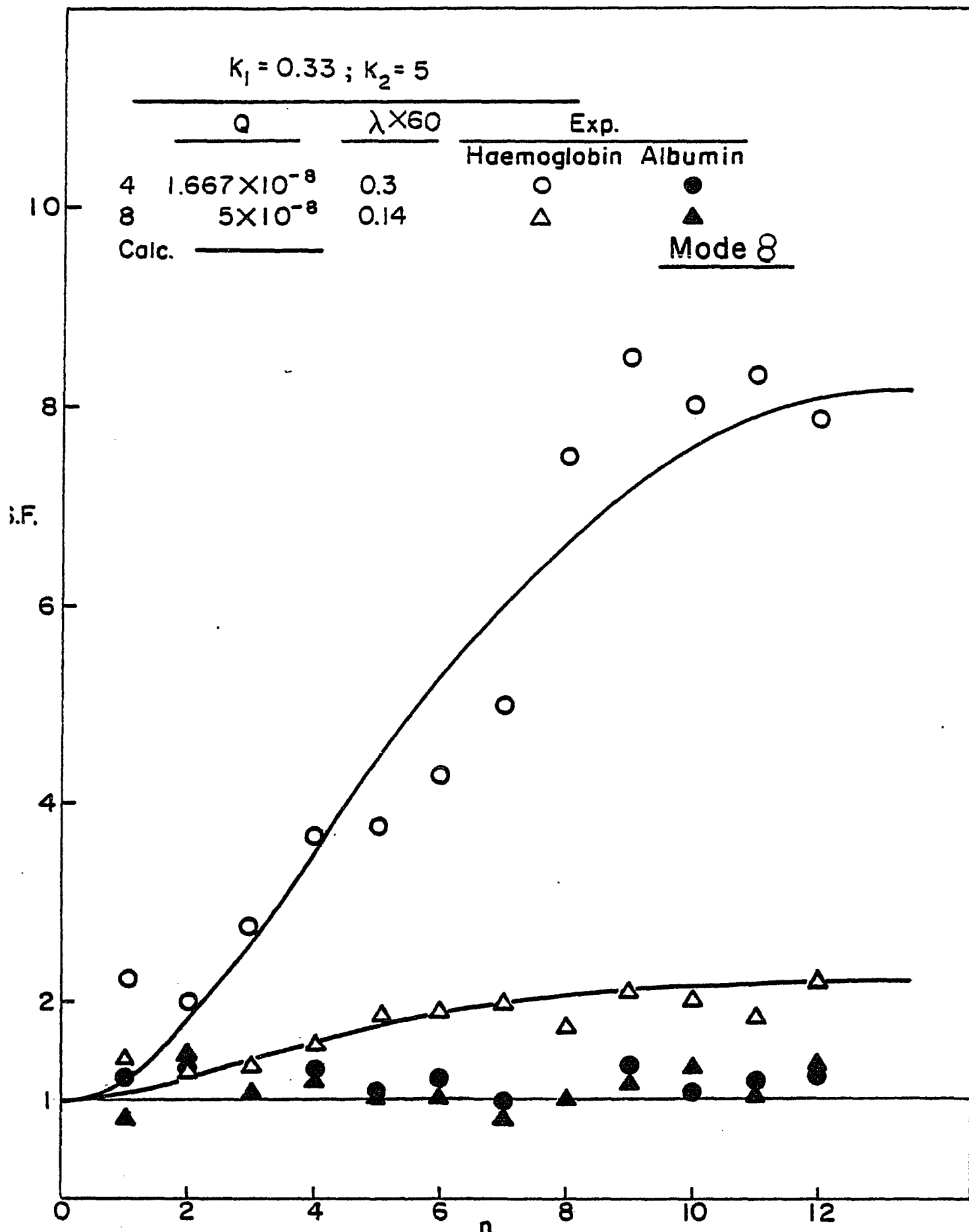


Figure 9.5 Experimental and Calculated Separation Factors

This observation may be explained by the smaller volume of exchanger gel in higher flow rate. Figure 9.6 plots the volume of exchanger gel versus the flow rate at the buffer ionic strength IS1 (0.1 M Tris + 0.1 N NaCl). Since λ is the product of mass transfer coefficient and specific surface. The reduction of exchanger volume will reduce the specific surface, and affect the mass transfer coefficient in a rather complicated way. The overall mass transfer coefficient consists of the external film coefficient, intra-particle coefficient, and the surface coefficient. The reduction of exchanger volume will increase the intra-particle (pores) resistance. Thus the reduction of exchanger volume in a higher flow rate leads to the following. (1) reduce the specific surface, (2) increase the intra-particle resistance, (3) increase the surface resistance. These three effects may overwhelm the effect of external film coefficient which is increased as flow velocity is increased; hence a smaller λ results. Further quantitative treatment of the intra-particle coefficient would be an interesting research, however, such work is not included in this thesis.

9.3 : Validity of Model and Result of Theoretical Exploration

The model equations and the correlated values of λ , K_1 , and K_2 were further tested with additional experimental results, and were applied to explore the behavior of the semi-continuous

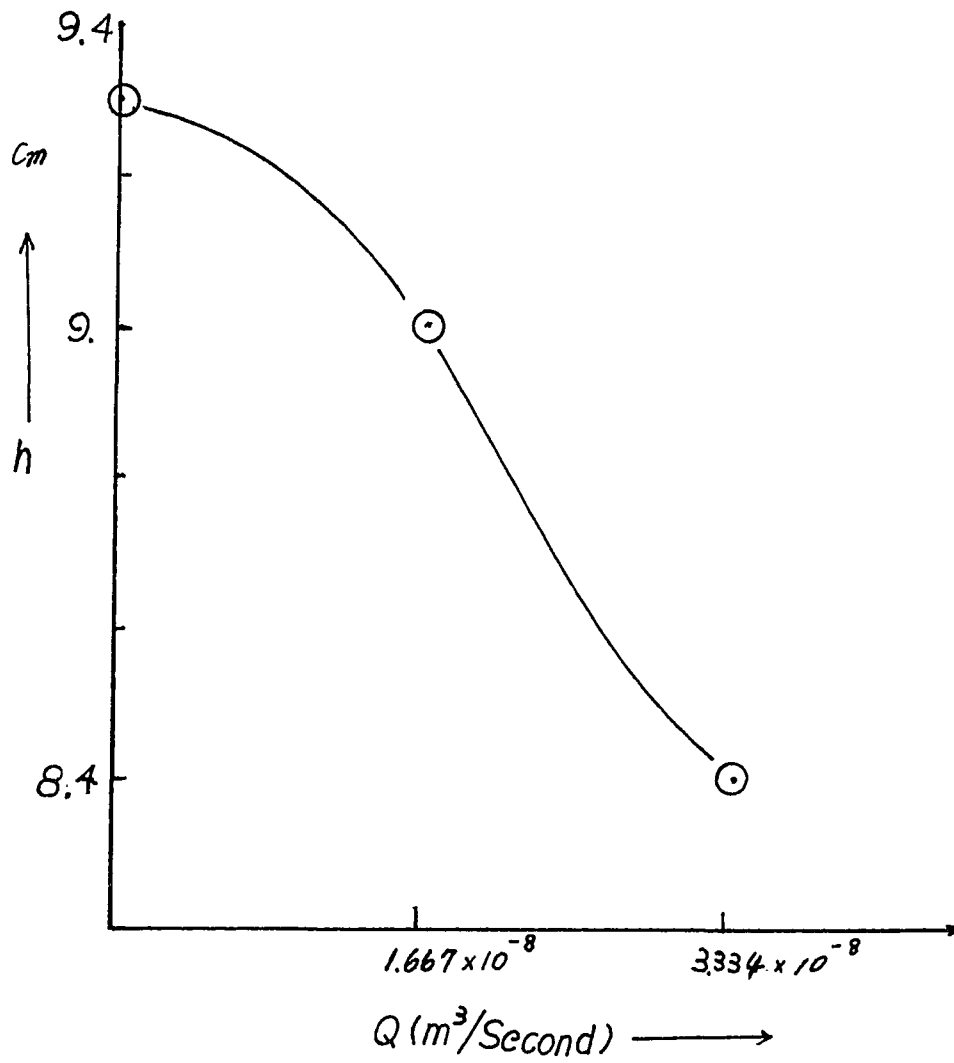


Figure 9.6 Effect of Flow Rate on the Height of Bed

one-column parapump. It should be pointed out that equation (9.2) is derived from the data of separation factor (SF) vs. number of cycles, n . It can also be applied to the prediction of concentration transients (Figure 9.7). The agreement between calculated results and the data is quite good. Figure 9.8 shows two additional experimental runs used in verifying the validity of the model. The experimental and model parameters are summarized in Table 7. The effect of Q on separation is also shown in Figures 9.7 and 9.8. A decrease in Q results in an increase in λ , and thus separation. However, if Q becomes too small, axial diffusion may become significant, and a poor separation may result.

Figure 8 illustrates the effect of feed on separation. This figure shows the calculated results (for $F_T = F_B$) with $tc=0$. F_B and F_T are respectively equal to Qt_{III} (bottom feed) and Qt_{VII} (top feed). For small λ (i.e., $\lambda = 0.005$) the separation factor at steady state (SF_{ss}) decreases as F_T (or F_B) increases. For large λ (or a parapump operated near equilibrium), separation factor (SF_{ss}) increases very rapidly reaching a maximum value as F_T (or F_B) increases. Further increase in feed size results in a drop of SF_{ss}, because the intermixing between the feed and product streams.

Wilhelm et al.^[31] studied thermal recuperative parapumps and showed that for large values of λ (heat transfer rate

$k_1 = 0.33 ; k_2 = 5 ; t_c = 0$

	Q	Exp.	$\lambda \times 60$
4	1.667×10^{-8}	\circ	0.30
8	5×10^{-8}	\triangle	0.14

Calc. —————

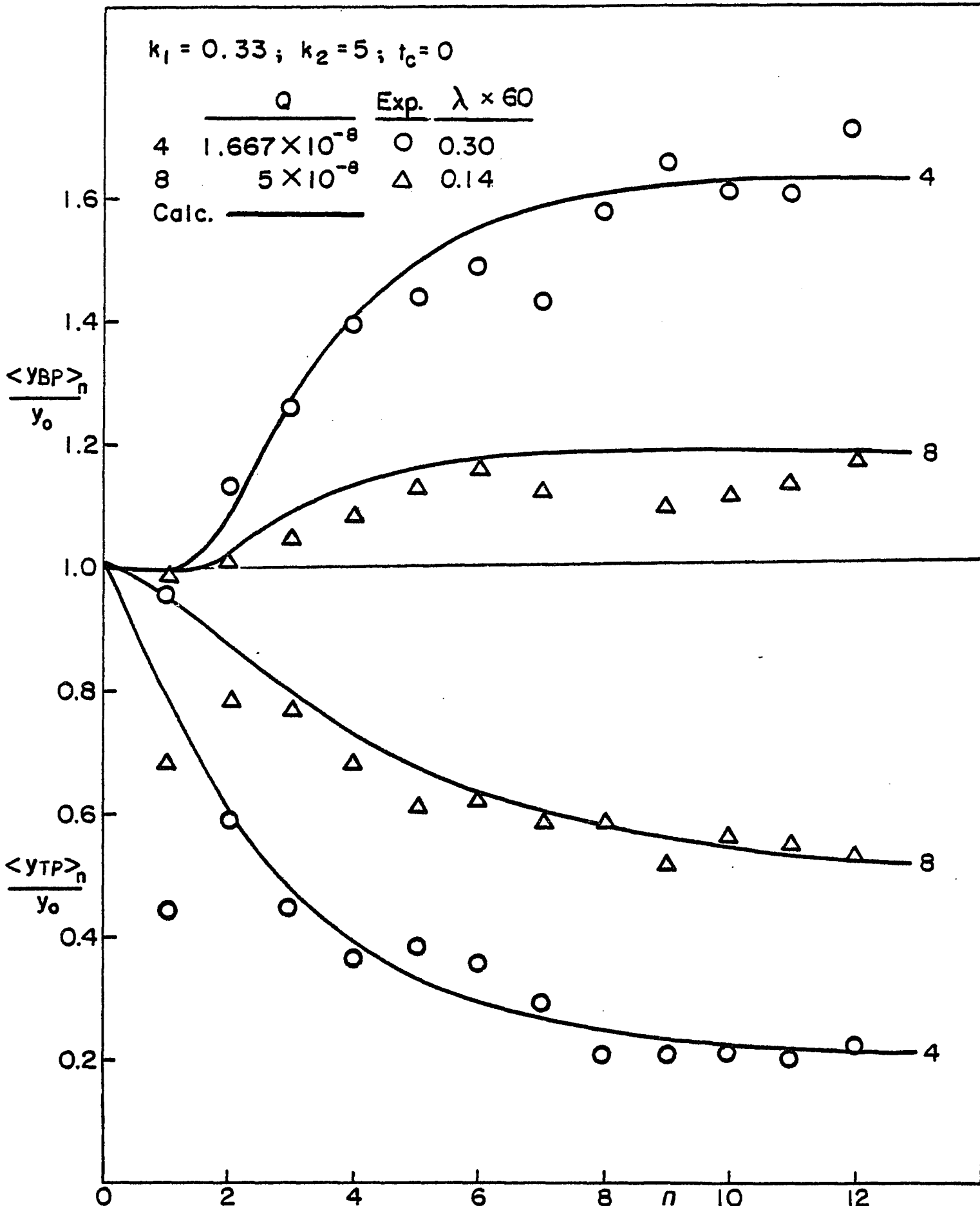


Figure 9.7 Comparison of Calculated Transients with Experimental Data for Runs 4 and 8.

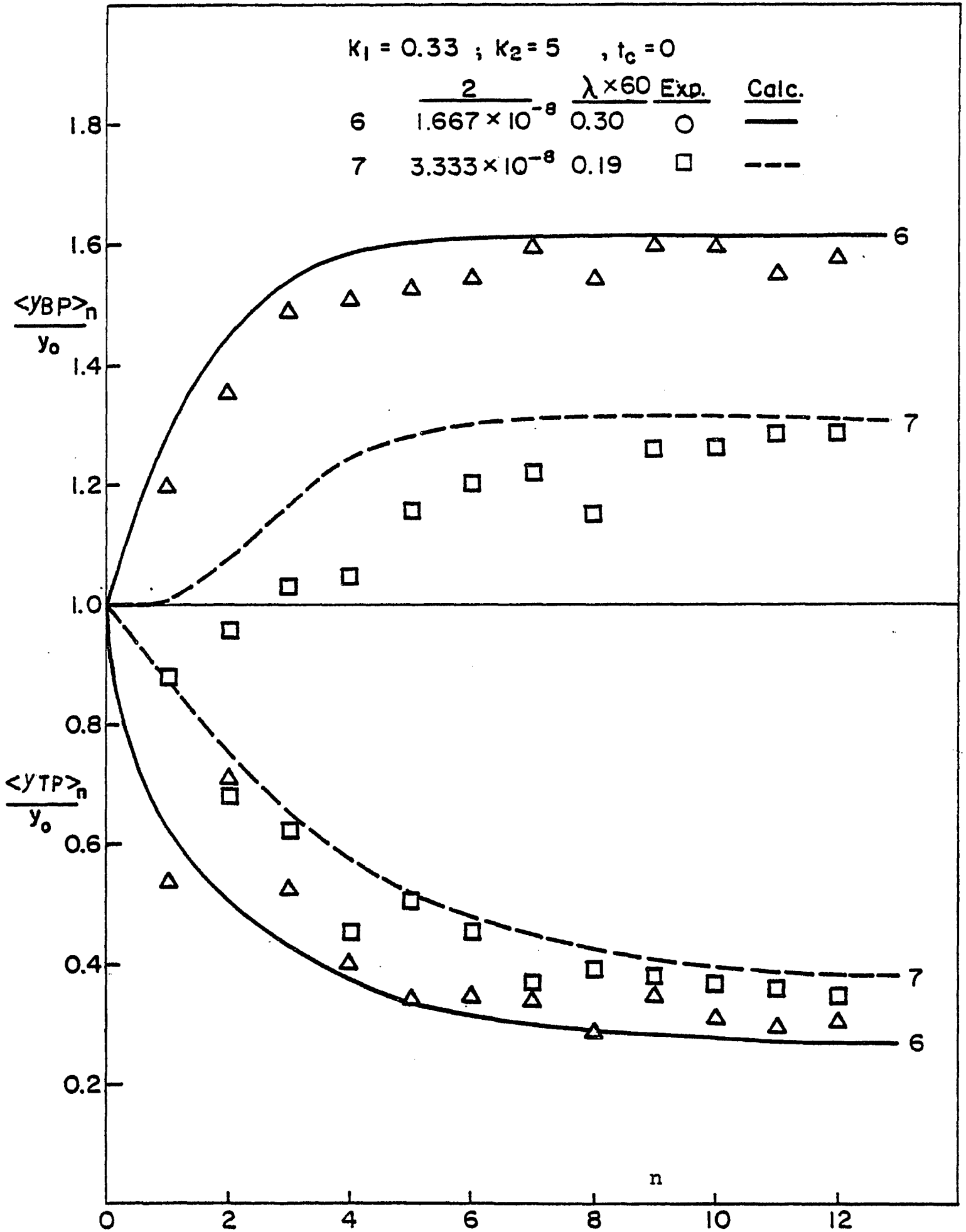


Figure 9.8 Comparison of Calculated Transients with Experimental Data for Run 6 and 7

Table 7. Experimental and Model Parameters

$k_1 = 0.33$ $P_1 = 8$; $IS_1 = 0.2M NaH_2PO_4 + 0.2M Na_2HPO_4 + 0.1M NaCl$

$k_2 = 5$ $P_2 = 6$; $IS_2 = 0.05M NaH_2PO_4 + 0.05M Na_2HPO_4$

$L = 0.08m$, $y_0 = 0.02$ weight % of haemoglobin + 0.02 weight % of Albumin

$Qt_I = 1.2 \times 10^{-5} m^3$

Run	Q m^3/s	t_c s	$\lambda \times 60$	F_B, m^3	F_T, m^3	$VDT = VDB, m^3$	y_{CO} / y_0	
							Haemoglobin	Albumin
2	1.667×10^{-8}	1,440	Equilibrium	4×10^{-6}	9×10^{-6}	5×10^{-6}	0.9	1.0
3	1.667×10^{-8}	1,440	Equilibrium	2×10^{-6}	5.5×10^{-6}	5×10^{-6}	0.9	1.0
4	1.667×10^{-8}	0	0.3	5×10^{-6}	6.5×10^{-6}	15×10^{-6}	0.5	1.0
6	1.667×10^{-8}	0	0.3	10×10^{-6}	12×10^{-6}	15×10^{-6}	0.5	1.0
7	3.333×10^{-8}	0	0.19	4×10^{-6}	9×10^{-6}	15×10^{-6}	0.5	1.0
8	$5. \times 10^{-8}$	0	0.14	3×10^{-6}	9×10^{-6}	15×10^{-6}	0.7	1.0

constant between the solid and fluid phases) the steady state separation factor for a batch pump is essentially a constant and does not change with λ . This is consistent with what we have shown in Figure 9.9. Note that this figure is based on the assumption that there is no lag between the fluid displacement and pH transfer flux(i.e., $B=1$ and $C=0$, in Equation (4.7)), corresponding to that of GUMA approaches infinity in Wilhelm's thermal parapump. At $F_T=F_B=0$ (batch parapump), the SF_{ss} is 15 and is independent of λ . This occurs because for a batch pump, regardless of λ , compositional equilibrium exists between phases at steady state(when n is infinity).

Figure 9.10 shows the effect of F_T and F_B on the bottom product concentration. The volumes of top and bottom feeds(F_T and F_B) are respectively equal to those for bottom and top products (PB and PT). As F_T decreases or F_B increases, ($\langle YBP \rangle_{ss}/Y_o$) increases. The effect becomes more profound at low values of F_T . If one desires, for example, to obtain a very high concentration of a desired protein from a mixture, one would operate a parapump at a low value of F_T and high value of F_B . Also, for a given ($\langle YBP \rangle_{ss}/Y_o$), an increase in the bottom feed (F_B) results in an increase in the bottom product(PB).

Figure 9.11 shows the effect of the column height on the separation. Two cases are considered; $h=0.08$ and $h=0.16$ m. The values of Qt_I , F_T and F_B for $h=0.16$ m are set to be twice

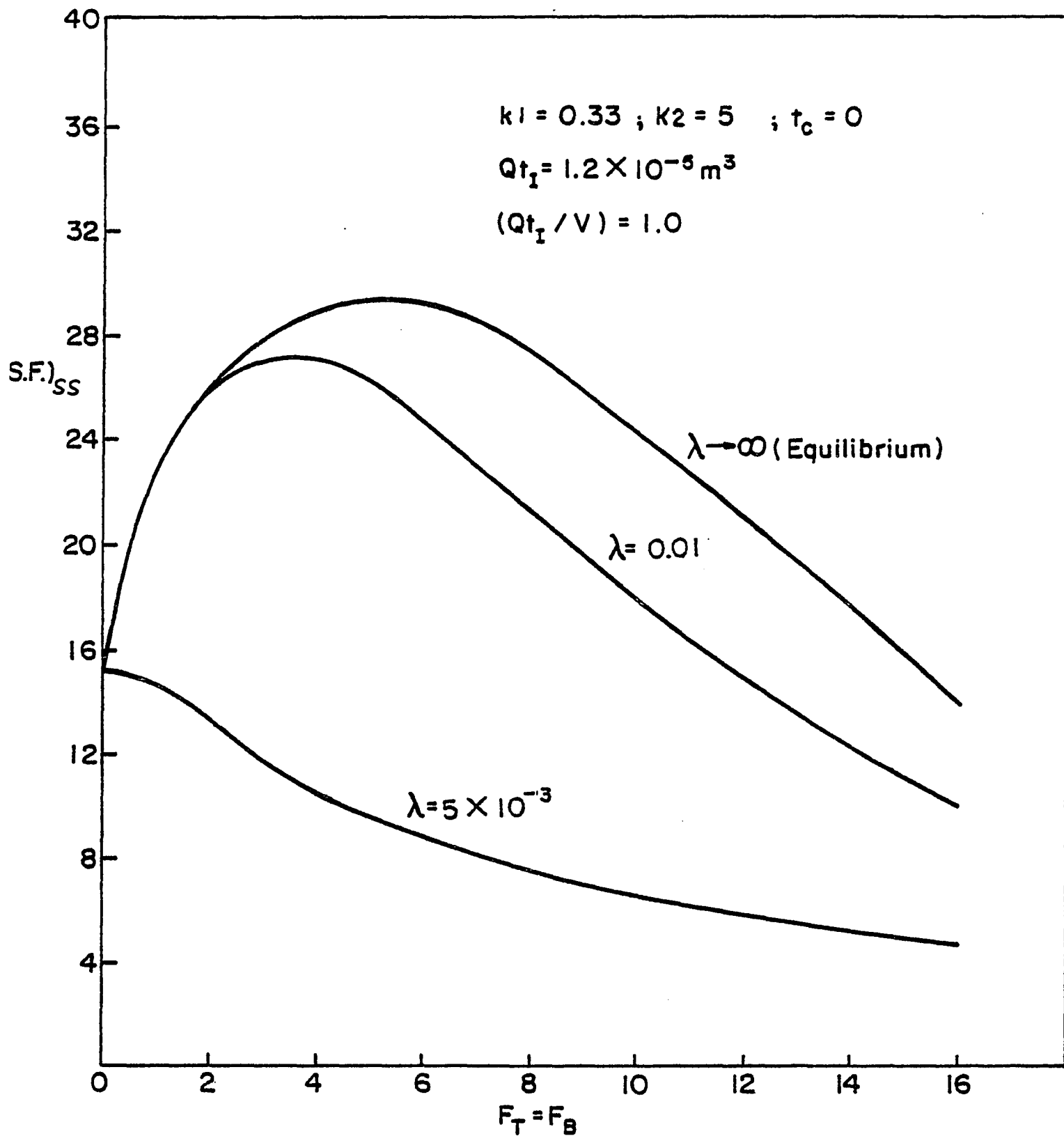


Figure 9.9 Effect of Feed Size on Separation

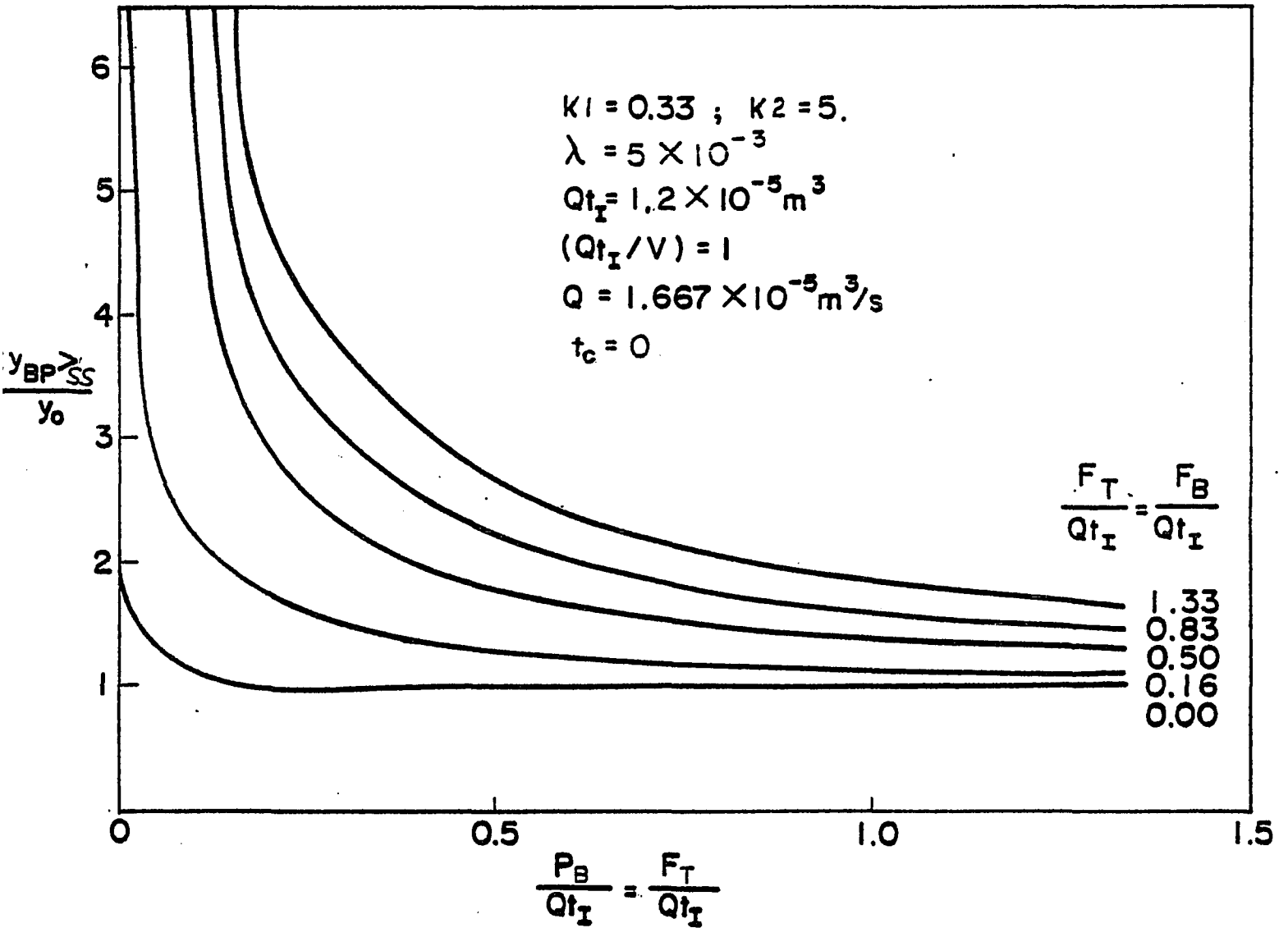


Figure 9.10 Effect of The Feed Size on the Bottom Concentration

of those for $h=0.08\text{m}$. For the equilibrium case (λ is infinity) h has essentially no effect on the separation. For the case of finite mass transfer, separation increases with h . The influence of the dead volume (VDT or VDB) in the reservoir is shown in Figure 9.12. Increasing the volume shows a slow down in the separation, but does not affect the ultimate separation.

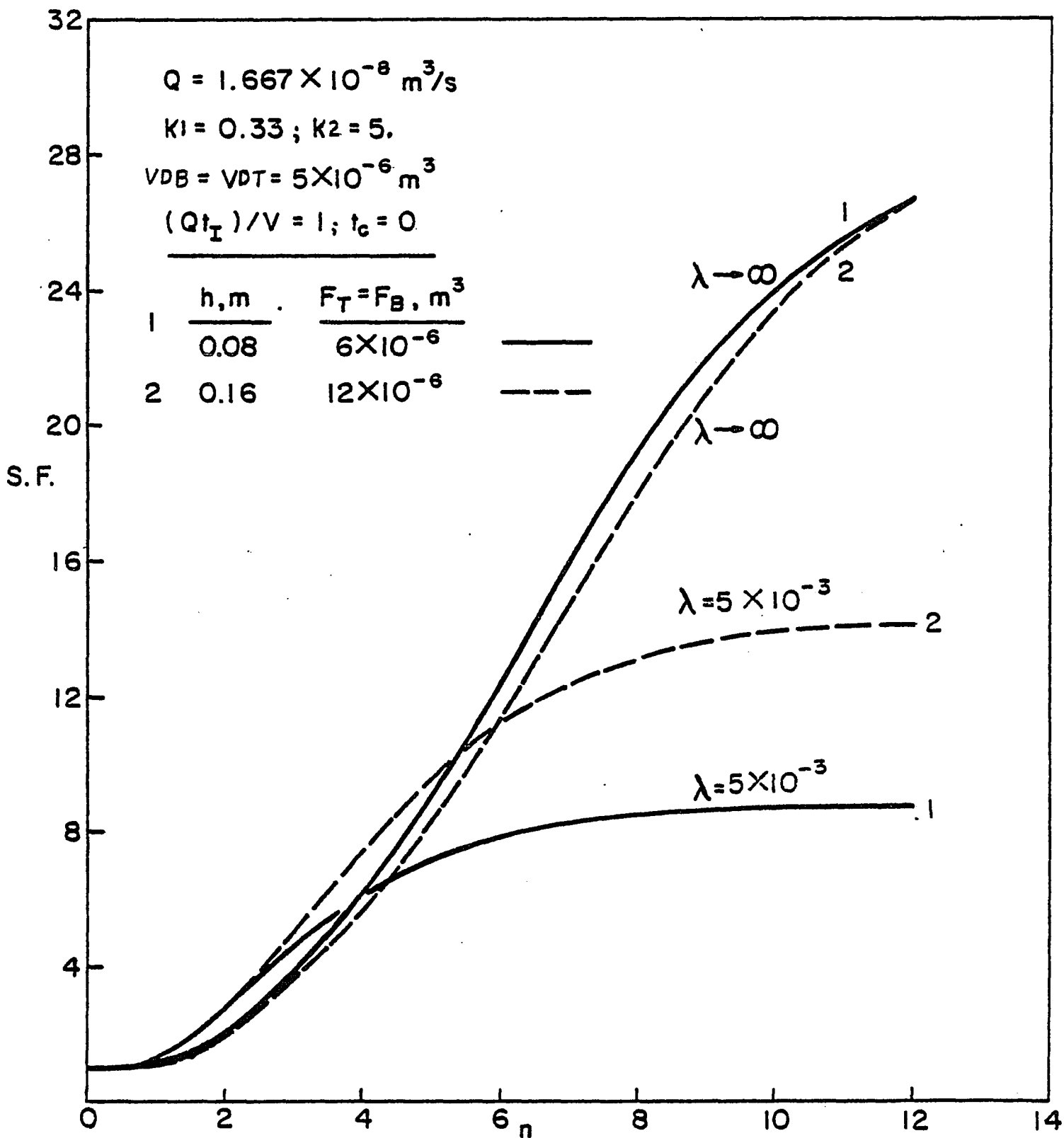


Figure 9.11 Effect of Column Height on Separation

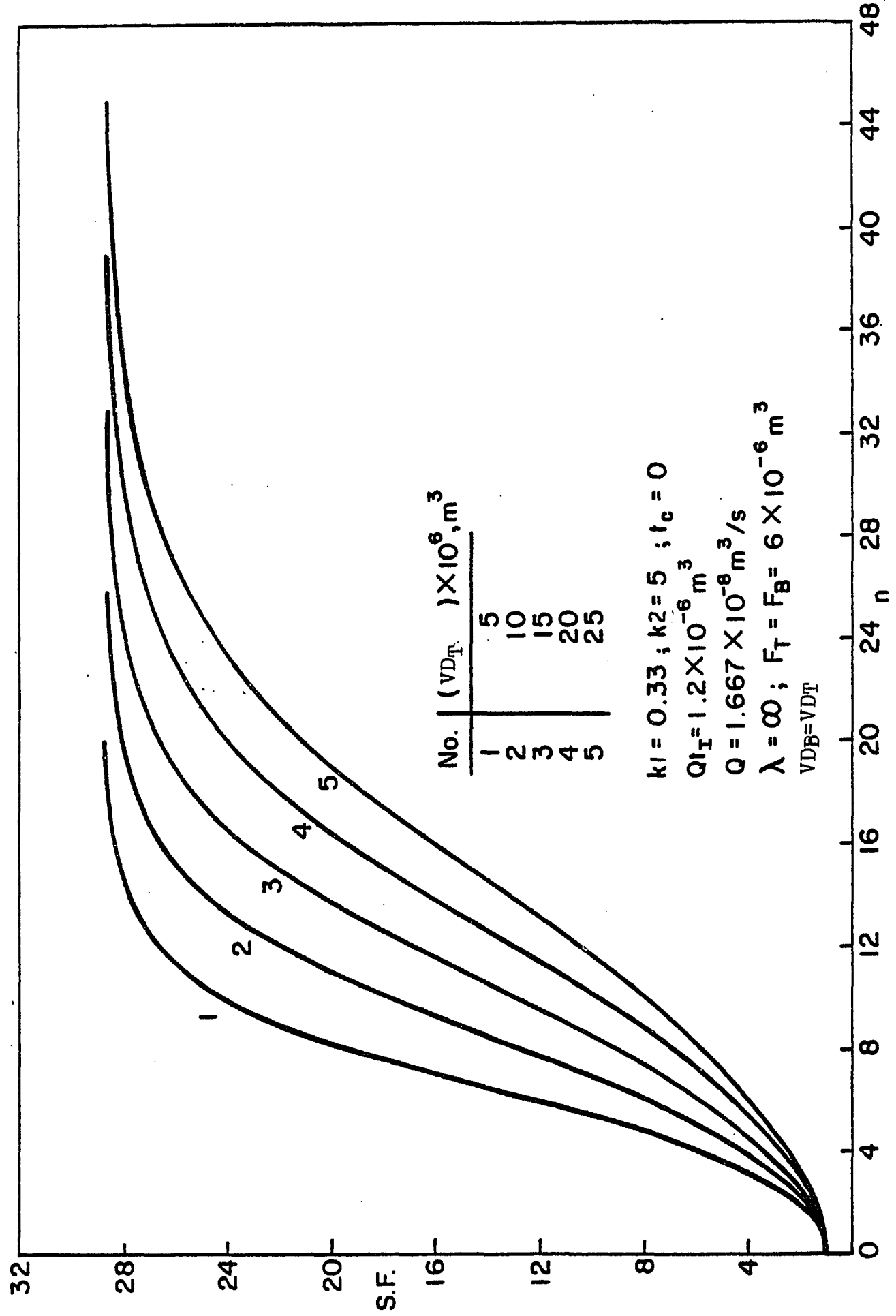


Figure 9.12 Effect of Dead Volume on Separation

Chapter 10: Comparison of Separation by Cycling Zone and Parametric Pumping, with Multi-Cell Model and pH Wave Equation

10.1 : Cycling Zone and Parametric Pumping

Parametric pumping and cycling zone are two separation techniques which separate a fluid mixture by applying a periodic change of control variable to a system. The common separation principle of these two techniques is:

- (1) periodic alternation of the control variable to induce interphase mass transfer in the column.
- (2) the interphase mass transfer flux is reversible.

The difference between parametric pumping and cycling zone is:

- (1) the fluid flow is reversible for parametric pumping and unidirectional for cycling zone.
- (2) parametric pumping has one more degree of freedom (displacement) than cycling zone.

10.2 : Model Equations

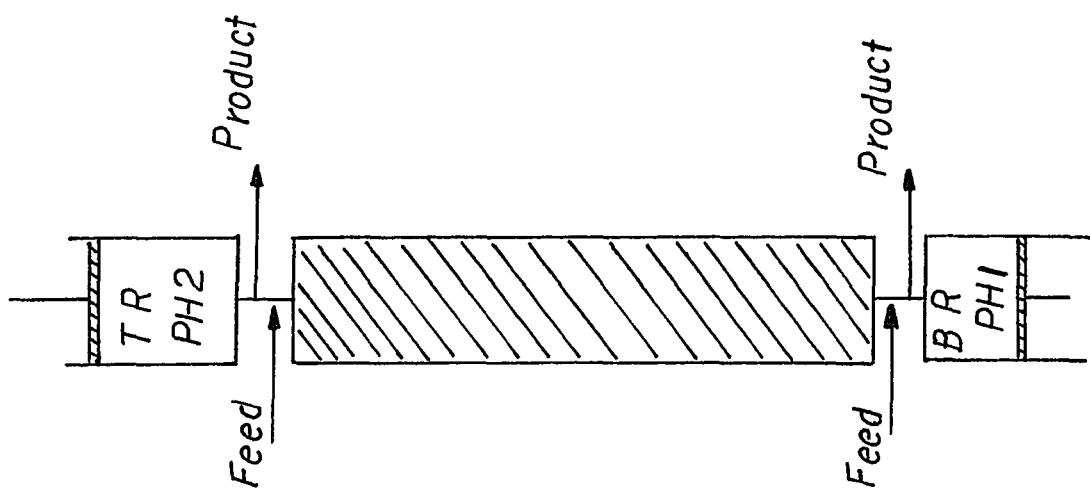
In the previous chapter, we assume that the velocity of the pH wave is equal to the velocity of fluid flow. Such assumption is not held in this chapter, and equation (4.7) is applied to correlate the pH wave velocity. Again, the STOP and GO method is applied to solve pH, X, and Y from equations (4.7), (4.3), and

3.2 (local equilibrium theory is applied) along with the equilibrium relations. Since the equilibrium relation is pH dependent, and the pH is a continuous function in (z,t) domain when B is not equal to unity and C not equal to zero, an expression for equilibrium relation to pH is required to compute the control variables of systems. In this chapter, we apply the linear iso-pH equilibrium relationship, $X=K(\text{pH}) Y$, and the iso-pH equilibrium constant, $K(\text{pH})$, is assumed to have a linear relation to pH in the range from P1 to P2, as stated in equation (10.1).

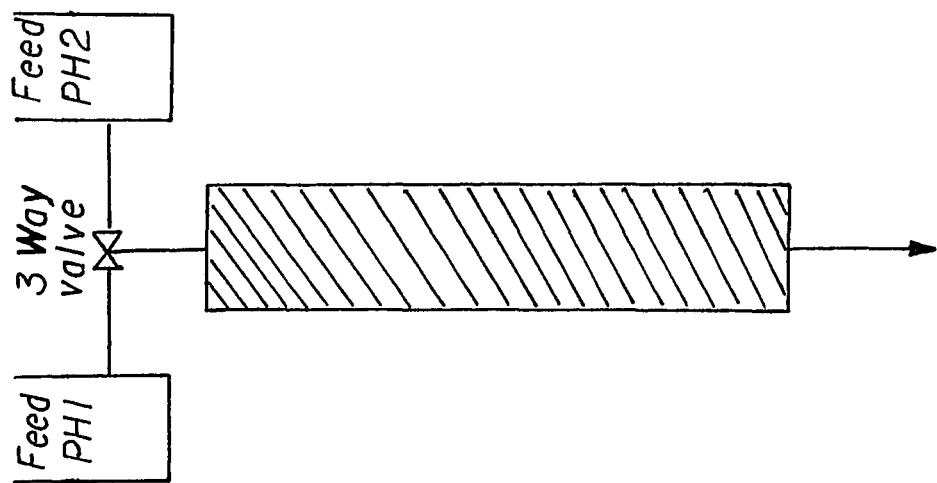
$$K(\text{pH}) = K(\text{P1}) + \{K(\text{P2})-K(\text{P1})\} (\text{pH}-\text{P1})/(\text{P2}-\text{P1}) \quad (10.1)$$

10.3 : Analytical solution of pH Breakthrough Curve

We first examine the pH breakthrough curve with pH wave equation (4.7) in the multi-cell model. For a column consisting of N cells in series, as shown in Figure 10.1(a), fluid is introduced to the 1st cell and exits at the Nth cell. In the multi-cell model, the fluid flow is considered as being transferred down discretely and sequentially from the top cell to the bottom cell, and each transfer displaces the void volume of a cell. For example, the fluid at the i-th cell and at time=(j-1) dt, is transferred to the (i+1)-th cell at time=j, and the i-th cell receives the fluid transferred from the (i-1)-th cell. The



(c) Parametric Pumping



(b) Cyclic Zone



(a) N Cells Column

Figure 10.1

equations for the pH model and the boundary conditions for a breakthrough operation is stated in equations (4.7), (10.2), and (10.3) .

$$pH(i,j) = pH(i-1,j-1) \cdot B + pH(i,j-1) \cdot C \quad (4.7)$$

$$IC: \quad pH(i,0) = pH_0 \quad \text{for } i=1,2,\dots,N \quad (10.2)$$

$$BC: \quad pH(0,j) = pH_N \quad \text{for } j=1,2,\dots \quad (10.3)$$

When B and C are constants, the equation 5 has a solution

$$pH(i,j) = pH_N B^i \sum_{k=1}^{j-i+1} \binom{k+i-2}{k-1} \cdot C^{k-1} + pH_0 C^{j-i+1} \sum_{k=1}^i \binom{k+j-i-1}{k-1} \cdot B^{k-1} \cdot (B+C)^{i-k} \quad (10.4)$$

$$\text{Where :} \quad \binom{j}{i} = \frac{j!}{i! (j-i)!}$$

$$j! = j \cdot (j-1) \cdot (j-2) \cdot \dots \cdot 2 \cdot 1$$

In the special case where $C=1-B$, the solution becomes:

$$pH(i,j) = pH_N B^i \sum_{k=1}^{j-i+1} \binom{k+i-2}{k-2} \cdot (1-B)^{k-1} + pH_0 (1-B)^{j-i+1} \sum_{k=1}^i \binom{k+j-i-1}{k-1} \cdot B^{k-1} \quad (10.5)$$

$pH(i,j)$ can be calculated for given i,j with the process constants pHN , pH_0 , B , and C . This analytical solution is derived from a column which is initially uniform, as stated in the initial condition (10.2). The calculated numerical results by the above analytical solution are shown in Figure 10.2, 10.3. Figure 10.2 shows the pH wave versus dimensionless volume flow through volume, j/N . It is also shown that pH transition with respect to dimensionless elution volume (j/N) is affected by the value of N . For example, in order to shift the pH from pH_0 to 7.5 it takes $j/N = 1.2$ for $N=2$, and takes $j/N=1.53$ for $N=4$. If we have two columns, say Column 1 and Column 2, we may denote the height of the columns as L_1 and L_2 , respectively, and $L_2=2 * L_1$. In order to achieve the same change of pH in the last cell, Column 2 needs an elution volume which is more than double of the elution volume required for Column 1.

It is shown that the steepness of the pH curve is increased as N increased. pH changes abruptly at $j/N = 1/B$ when N is very large. Figure 10.3 shows the pH versus j/N with $B=0.4, 0.5, 0.8$ respectively and $N=1000$. In real world the experimental pH elution curve is shown in Figure 10.4(a) and 10.4(b) for a column packed with CM-Sepharose ionic exchanger. The experimental data of pH breakthrough curve are matched with the theoretical results shown in Figures 10.2 and 10.3, and give an estimated value of $(1/B)$ roughly equal to 1.68 from Figure 10.4(a) and 2.4 from

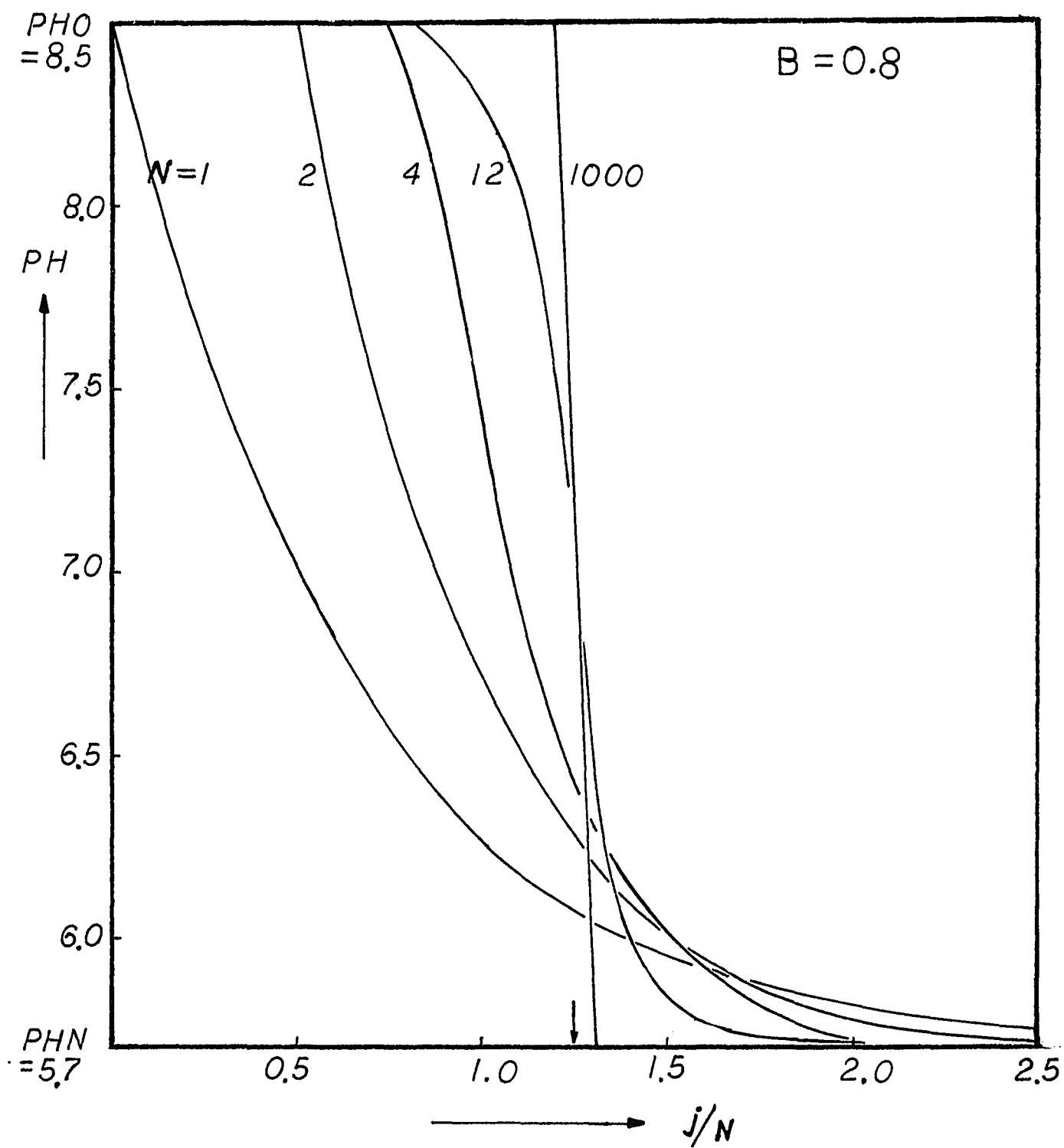


Figure 10.2 Calculated pH Breakthrough Curve

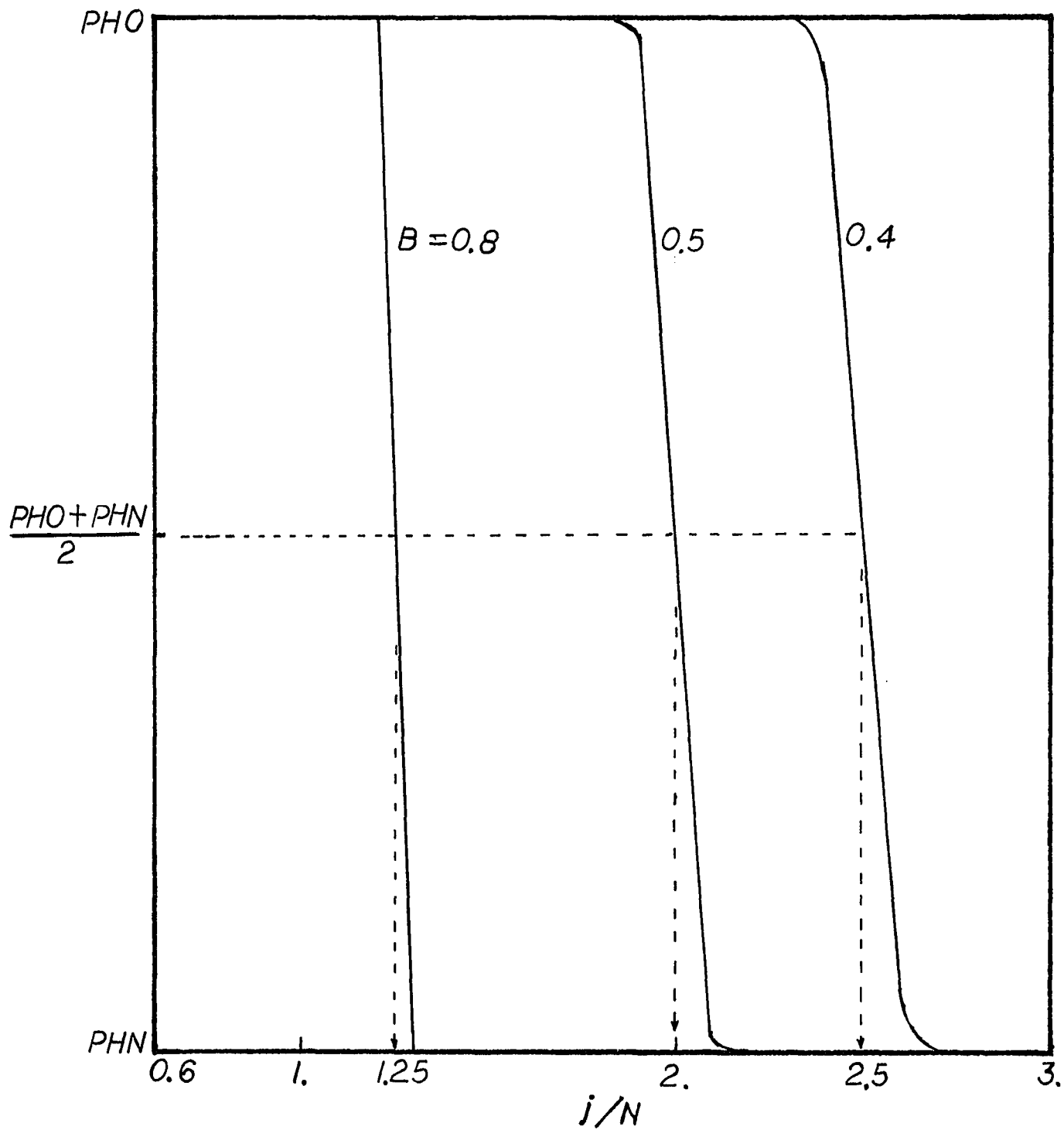


Figure 10.3 Calculated pH Breakthrough Curve for $N=1000$

Figure 10.4(b). Thus the corresponding estimated value of B ranges from 0.6 to 0.4. Since the pH data in Figures 10.4(a) and 10.4(b) is not steep enough, the B value obtained here is rather a rough estimation. In the following section, the B value is obtained from the data fitting of pH in cycling operation, which gives a B value ranging from 0.5 to 0.55, and confirms the previous estimation.

10.4 : Separation of Cycling Zone for Single Solute System

A cycling zone device is schematically shown in Figure 10.1(b). The apparatus includes an adsorptive column and two reservoirs in top of the column. The reservoirs contain feed fluid mixture, and the pH of the two reservoirs are kept at P_1 and P_2 respectively. The cycling zone is operated in such a way that the fluid mixture is introduced into the top of column alternatively from two reservoirs. Thus the the pH level of a particular location in this column is periodically changing and with the same frequency as the periodic alternation of the pH of fluid entered the column. The periodic change of control variable (pH) in the column, synchronizes the change of adsorptive equilibrium, and is coupled with the interphase transfer in the column. The fluid phase concentration is depleted in adsorption favor zones (with large equilibrium constant), and enriched in the adsorption unfavour zones (with small equilibrium constant).

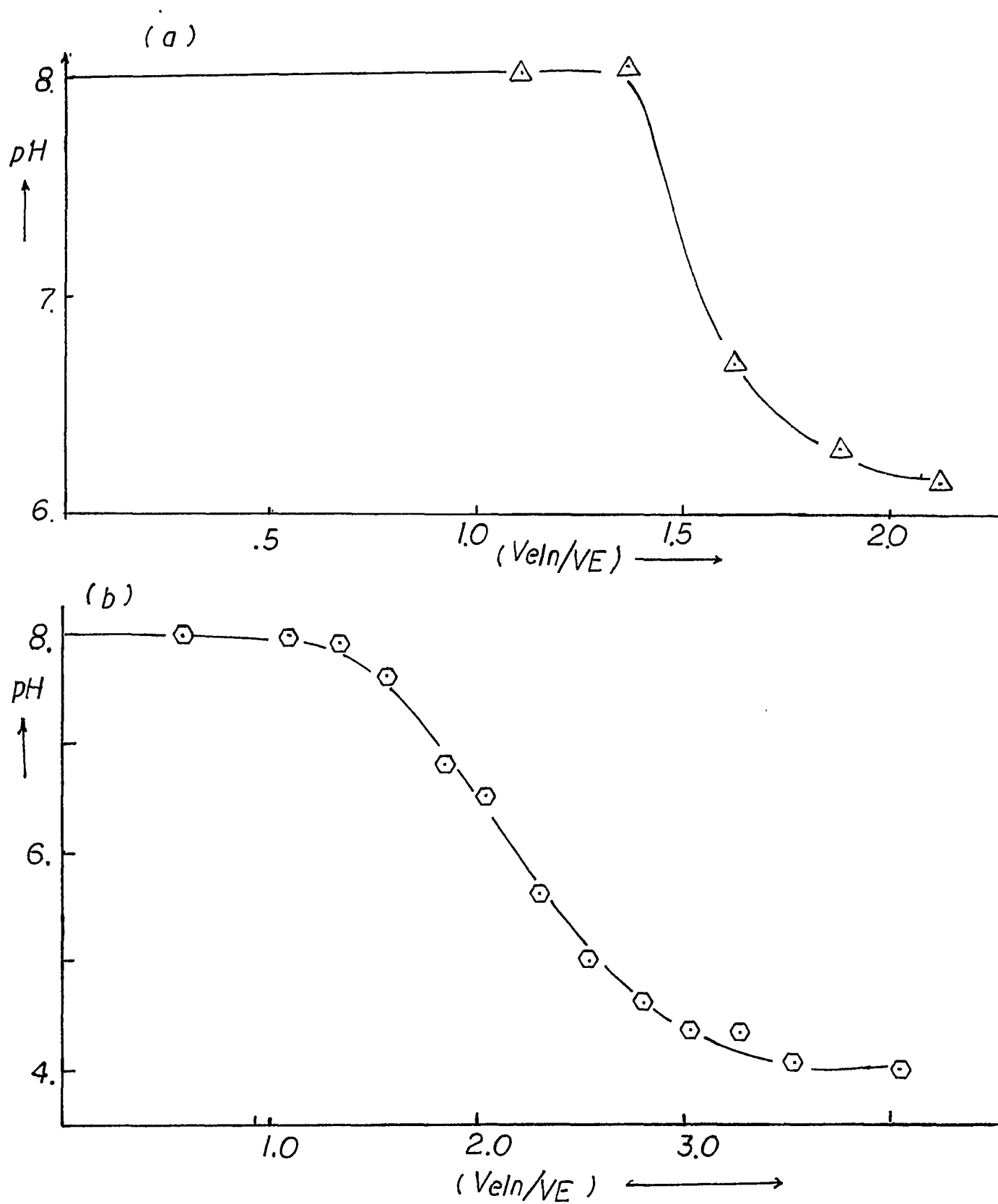


Figure 10.4 Experimental pH Breakthrough Curve

Figure 10.5 shows the experimental cycling waves of pH and concentration of albumin in anion exchanger column. It is seen that the peak of solute concentration occurred when the pH changed from adsorptive favor pH to adsorptive unfavor pH. This is simply explained as follows. The solute moves to solid phase when adsorptive favor pH dominates the cell, and solute moves back to the fluid phase when adsorptive unfavor pH dominates the cell. Thus the peak of solute concentration is enriched at the adsorptive unfavor pH front as seen in Figure 10.6 and 10.8.

The model equation of pH and concentration for cycling zone fluid flows down from top in multi-cells in series can be written in the following equations.

$$\text{pH}(i,j) = \text{pH}(i-1,j-1) \cdot B + \text{pH}(i,j-1) \cdot (1-B) \quad (10.6)$$

$$\text{pH}(0,j) = P1 \quad \text{for 1st half cycle} \quad (10.7)$$

$$\text{pH}(0,j) = P2 \quad \text{for 2nd half cycle} \quad (10.8)$$

$$\text{pH}(i,0) = \text{pH}0 \quad \text{for } i = 1, 2, 3, \dots, N \quad (10.9)$$

mass balance of solute:

$$\begin{aligned} V_f Y(i-1,j-1) + V_s K(\text{pH}(i,j-1)) Y(i,j-1) \\ = Y(i,j) [V_f + V_s K(\text{pH}(i,j))] \end{aligned} \quad (10.10)$$

$$Y(0,j) = YF \quad \text{for } j = 1, 2, 3, \dots \quad (10.11)$$

$$Y(i,0) = Y0 \quad \text{fo } i = 1, 2, 3, \dots, N \quad (10.12)$$

Equations (10.6)-(10.9) are applied to calculate the pH value, with the calculated pH and equations (10.10) - (10.12), and (10.1) are applied to calculate the solute concentration in each

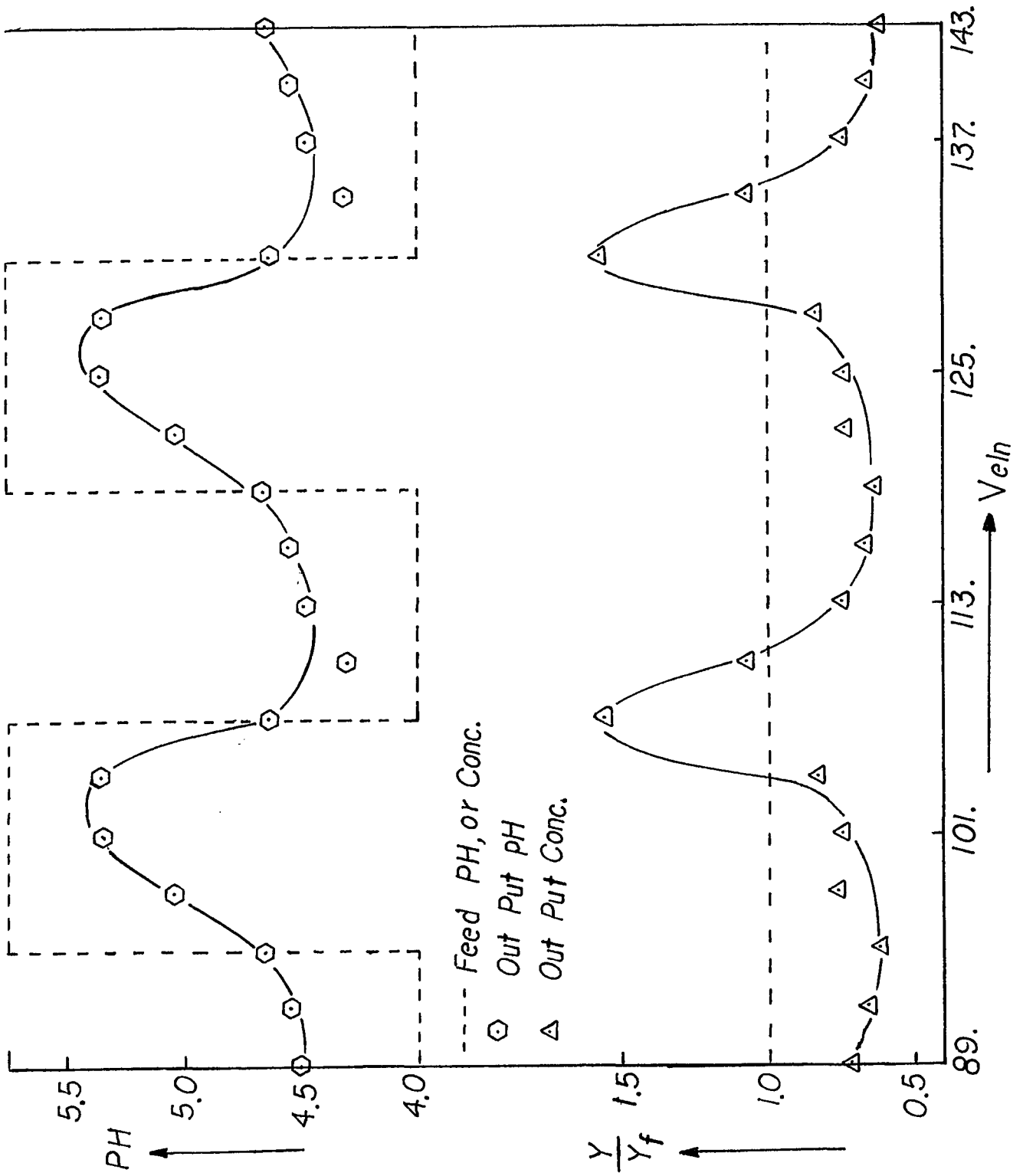


Figure 10.5 pH and Concentration Wave for Albumin in R⁺ Column

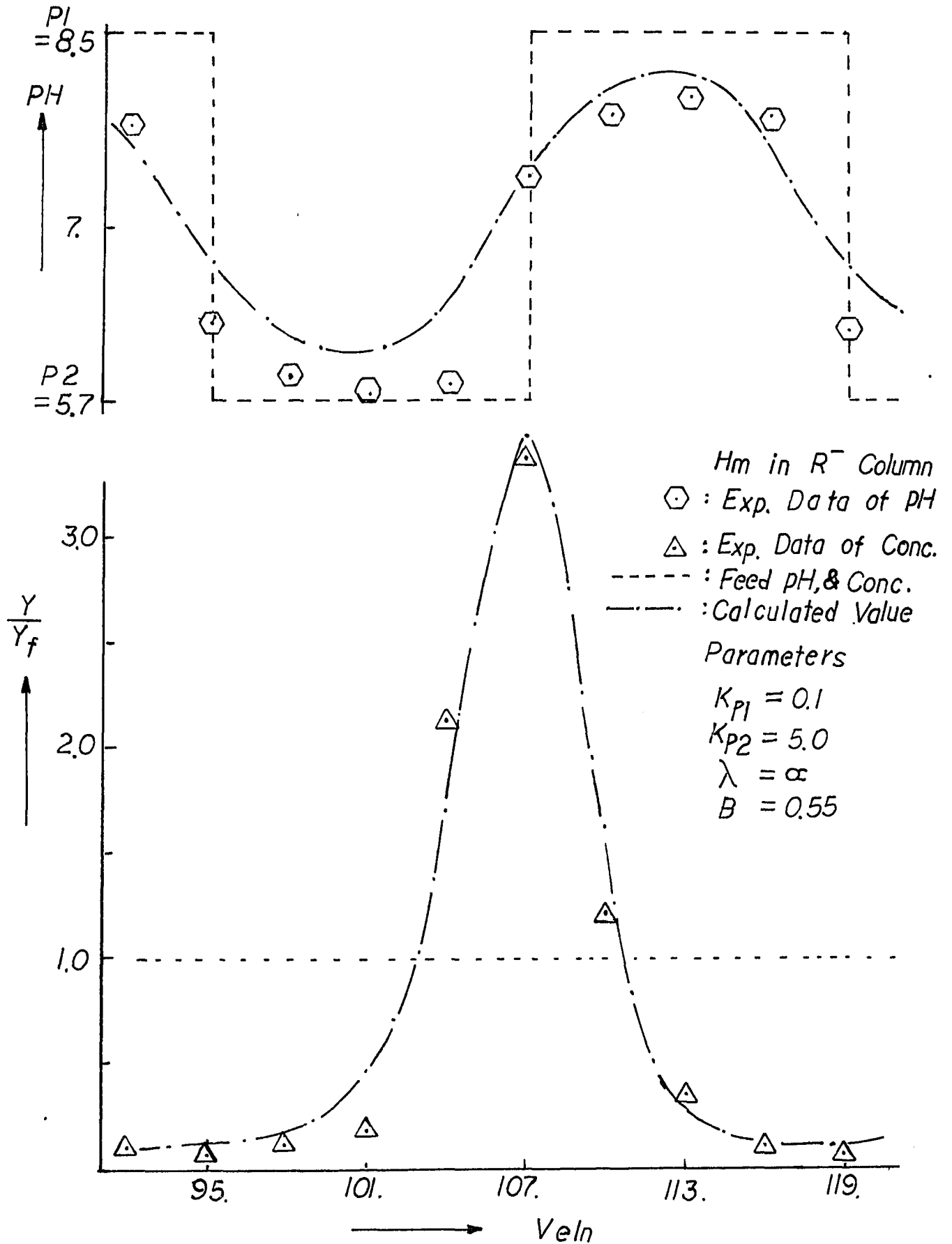
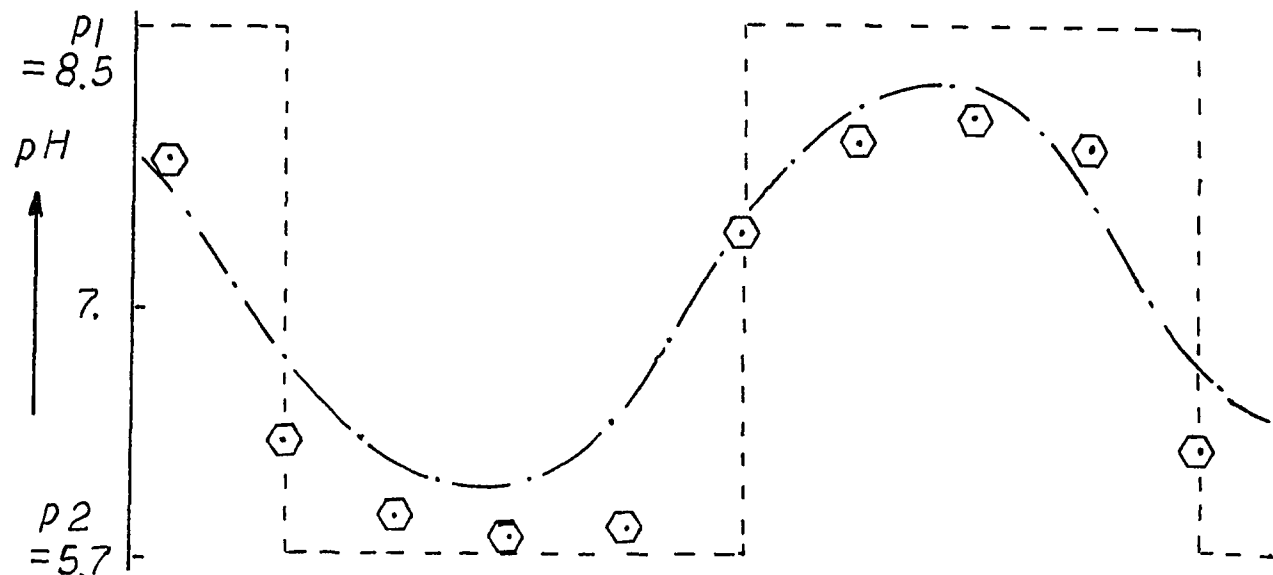


Figure 10.6 pH and Concentration Wave for Hemoglobin in R⁻ Column P1=8.5, P2=5.7

cell after a transfer step. Figure 10.6 and 10.8 show the correlation of pH wave and concentration wave for hemoglobin in cation exchanger column, and albumin in anion exchanger column. Separation of solute occurred, and the model gave a fair correlation in pH and concentration wave in these two cases. Figure 10.7 and 10.9 show no essential separation though the state variable, pH, is periodically changed in the column. This is because the rather insensitive adsorptive equilibrium for both pH level is far higher (or lower than) the isoelectric point of this protein. The value of K_{p1} , K_{p2} , N , and B , as shown in the figures, are obtained from best fitting of experimental data.

10.5 : Separation of Parametric Pumping for a Single Solute System

A parametric pumping device is again schematically shown in Figure 10.1(c) as a comparison to the cycling zone device. The apparatus of parametric pumping is described in Chapter 6. As stated before, the fluid in the two reservoirs is alternatively pumped up and down into the column, and the fluid originally existing in the column is collected in the reservoir at the other end of the column. Thus the flow direction and the pH level at a particular location in this column is periodically changed with the same frequency as the the flow direction and pH alternation. Notice that parametric pumping involves reverse fluid flow and



Ab in R⁻ Column
 ◊ : Exp. Data of pH
 △ : Exp. Data of Conc.
 - - - : Feed
 · - - - : Calculated Value
 $K_{p1} = 0.1$
 $K_{p2} = 0.1$
 $\lambda = \alpha$
 $B = 0.55$

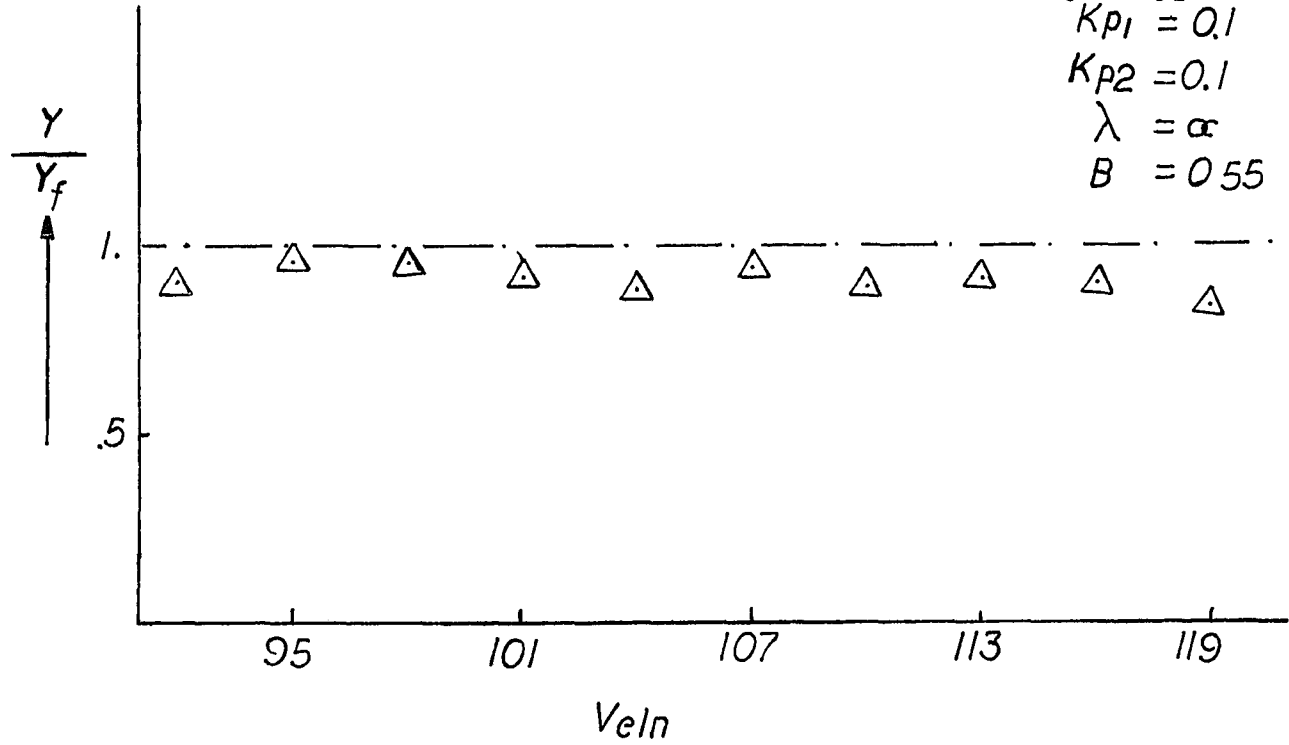


Figure 10.7 pH and Concentration Wave for Albumin in R⁻ Column P1=8.5; P2=5.7

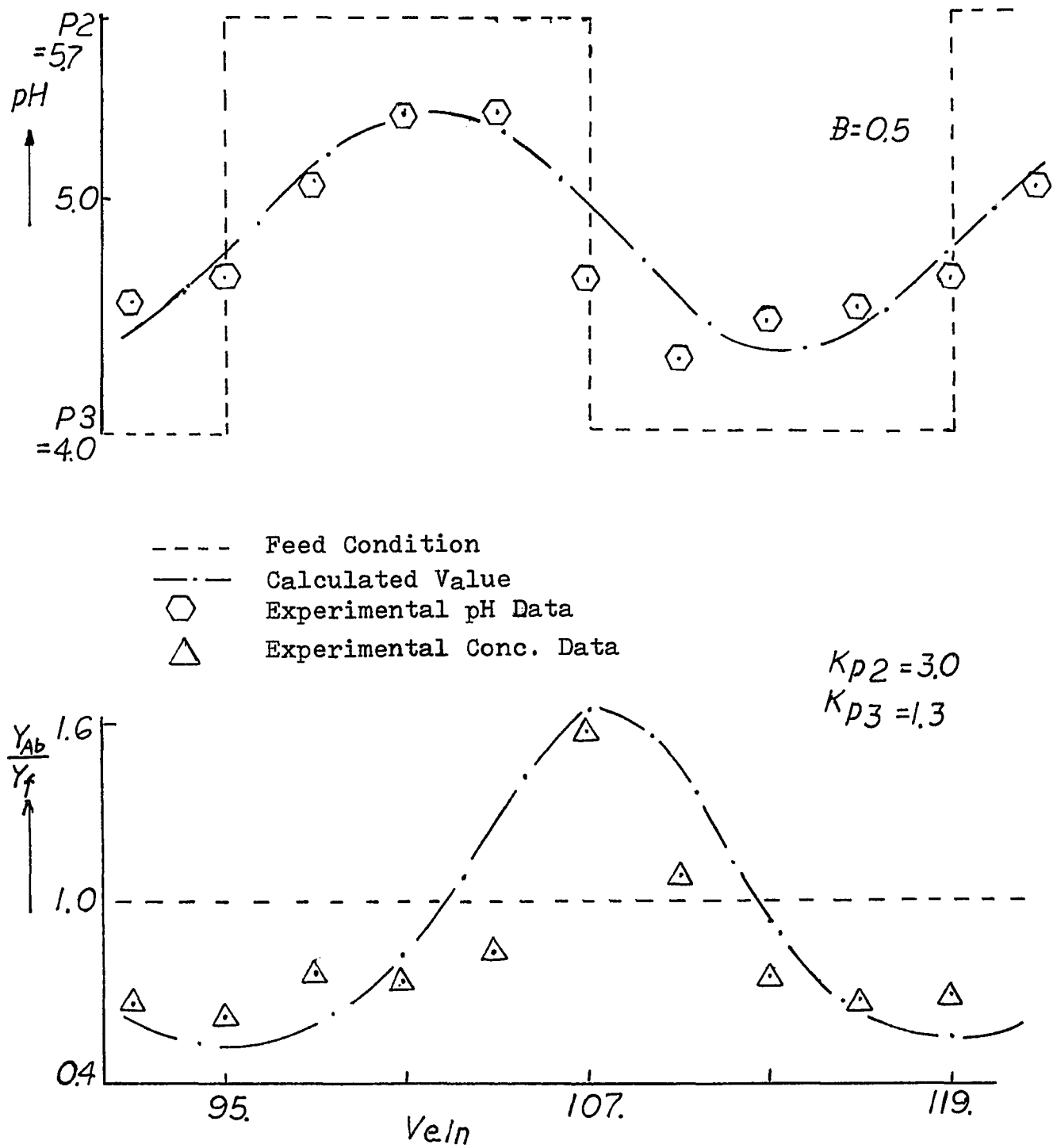


Figure 10.8 pH and Concentration Wave for Albumin in R^+ Column; $P2=5.7$; $P3=4.0$

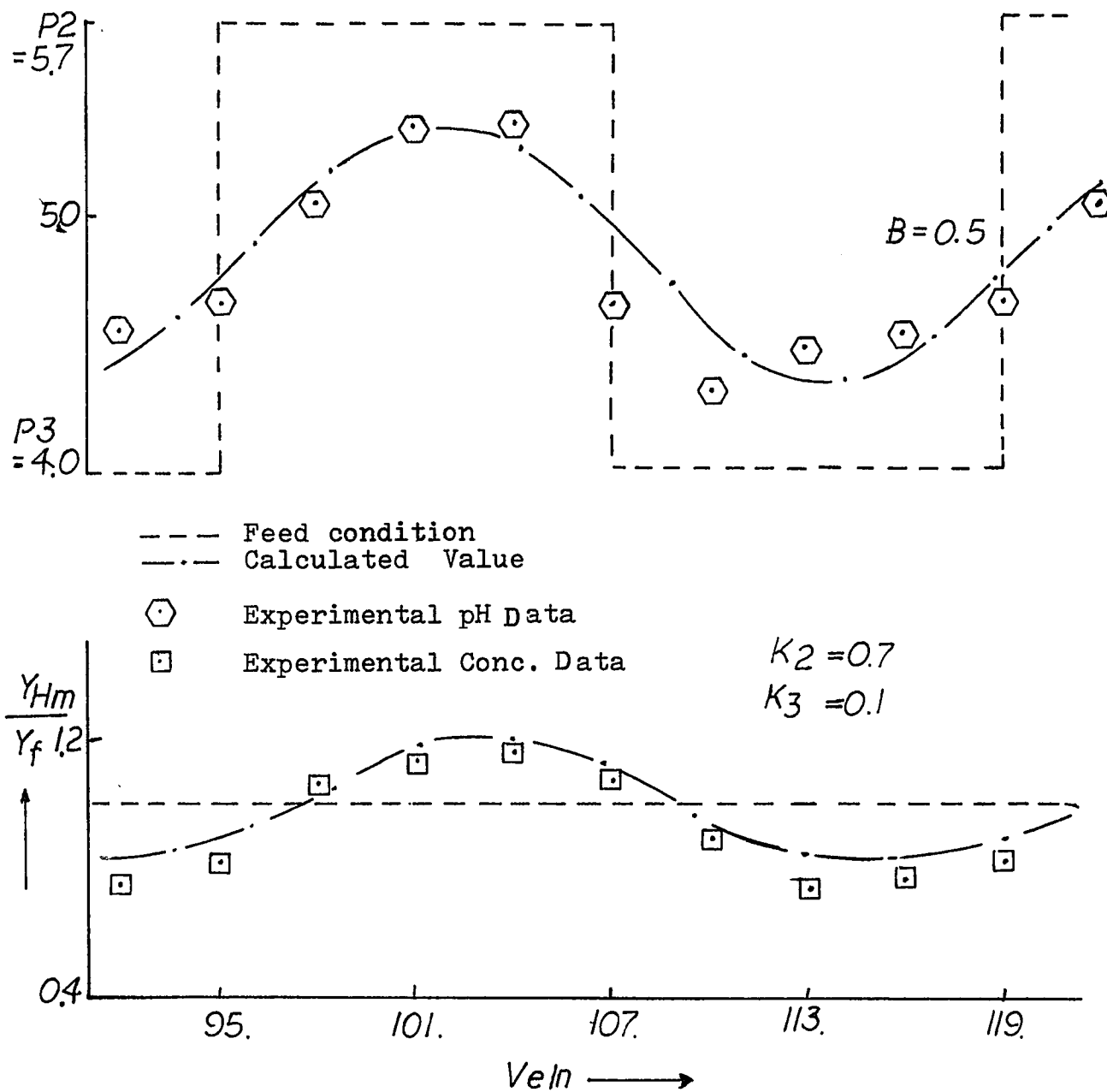


Fig 10.9 pH and Concentration Wave for Hemoglobin in R+ Column
 $P2 = 5.7, P3 = 4.0$

cycling zone only involves unidirectional fluid flow.

Equation (10.1) to (10.2) and local equilibrium are applied in parametric pumping separation. The displacement of parametric pumping is another parameter which affects separation. The optimal displacement for parapump operation versus the amount of feed with fixed B value is shown in Figure 10.10. It is seen that when $B=1.0$, the optimal displacement is always equal to the void volume of column. The optimal displacement increases as the B value decreases. Also, the optimal displacement decreases when feed increases. The control variable (pH) is closer to being completely changed when the feed or displacement is increased, and thus enhances separation.

10.6 : Comparison of Parametric Pumping and Cycling Zone in Single Solute System

The comparison of cyclic zone and single column parametric pumping in terms of separation factor and production rate is shown in Figure 10.11 and 10.12. It is clear that parametric pumping is favored for higher separation factor and the advantage is significant for small feed and small B value. The cycling zone is favored for production rate at any feed amount and B value. In Figure 10.13, the separation factor is plotted against the production throughput for cycling zone and parametric pumping. It is seen that the domain of parametric pumping

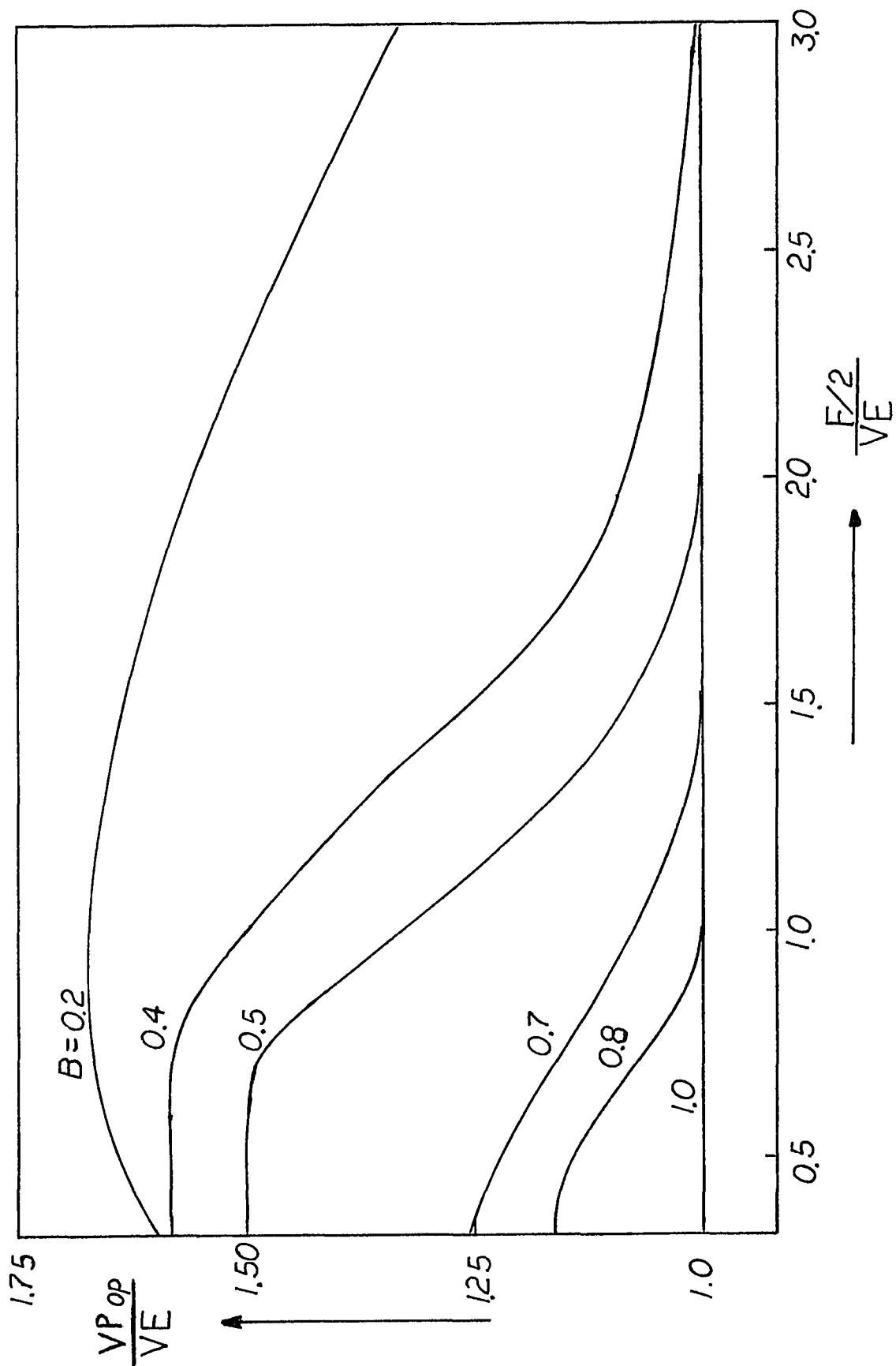


Figure 10.10 Optimal Displacement of One-Column Parapump

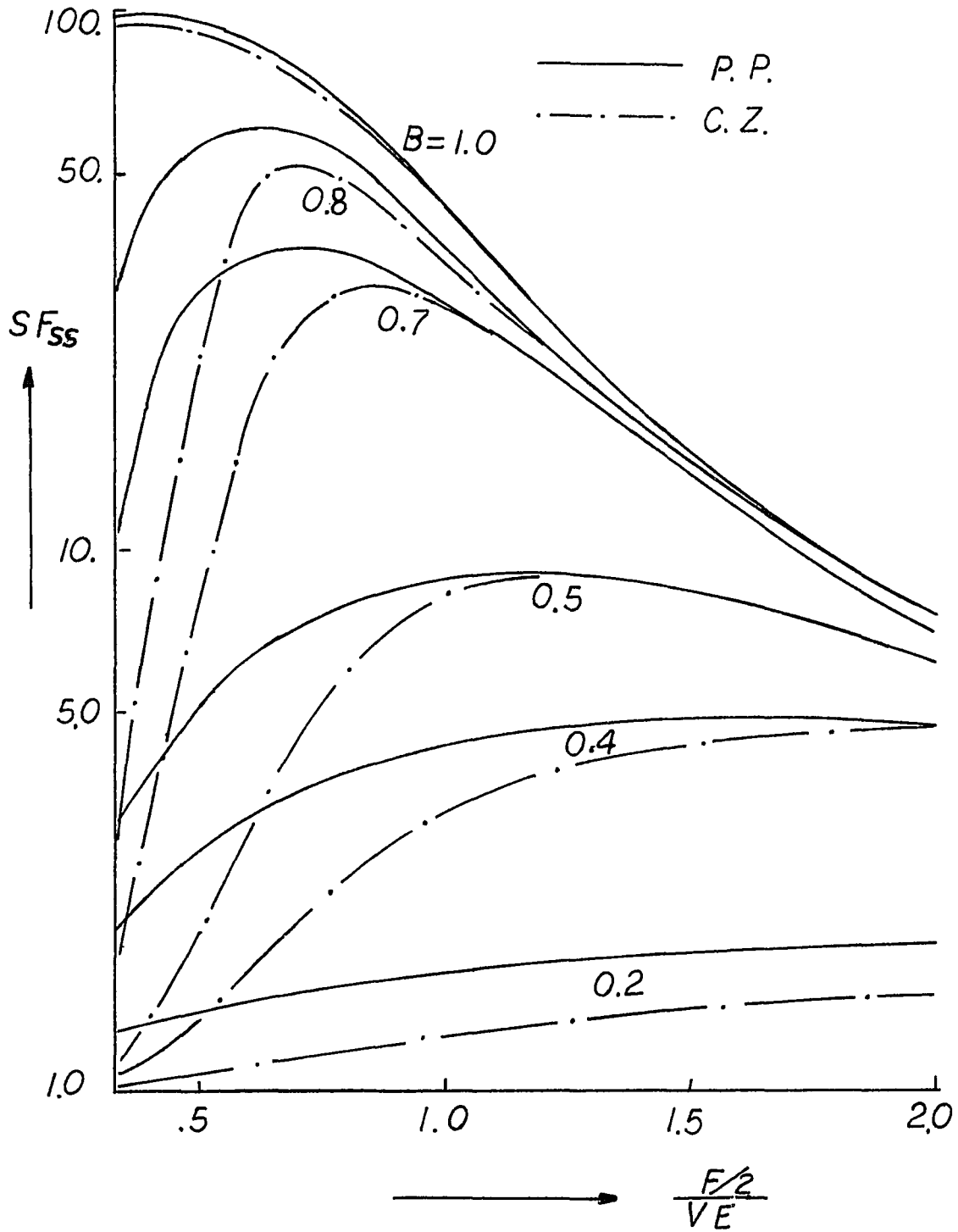


Figure 10.11 Separation Factor vs. Feed Size for One-Column Parapump and Cycling Zone

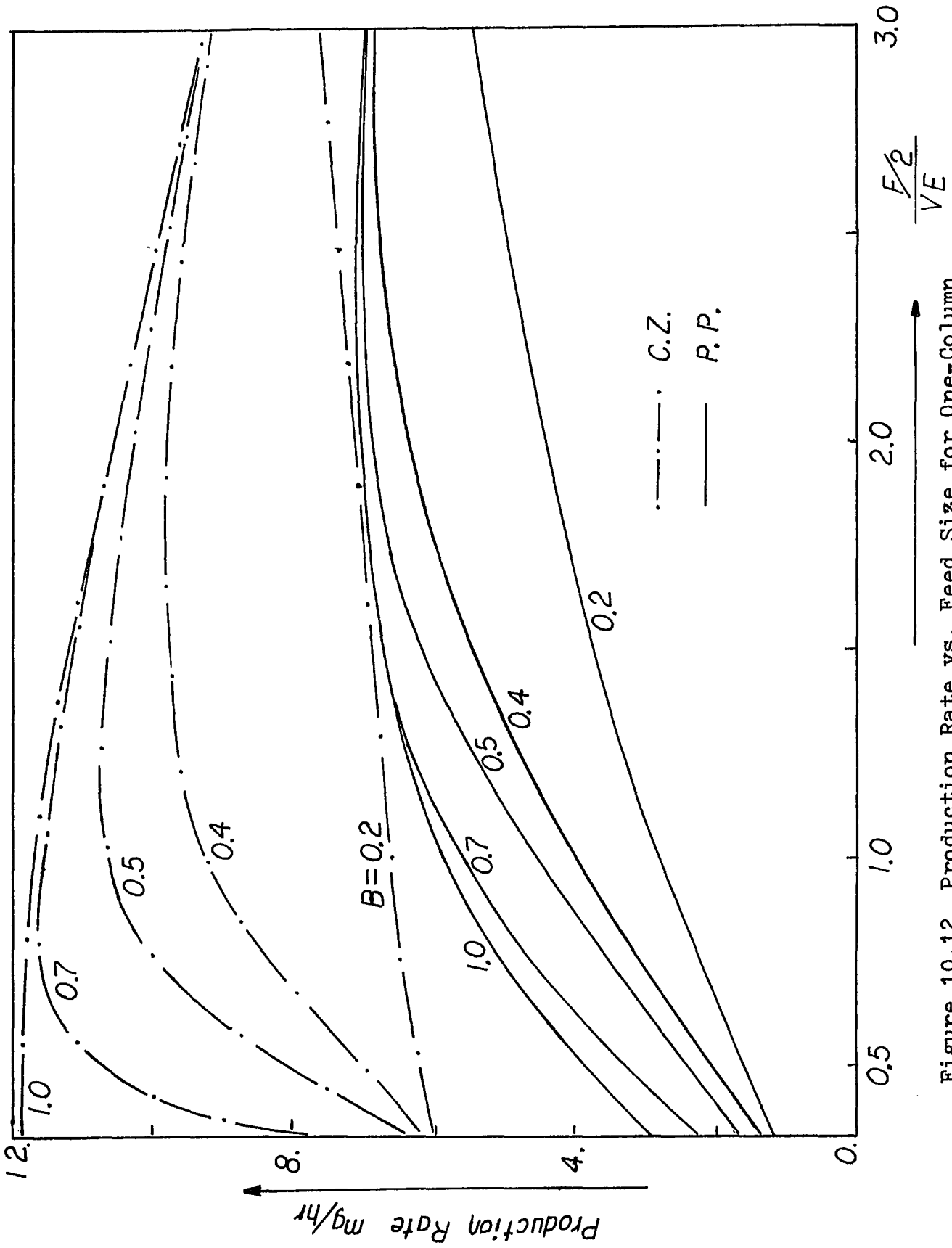


Figure 10.12 Production Rate vs. Feed Size for One-Column Parapump and Cycling Zone

occupies the area in up and left, and the domain of cycling zone is nearly a curve on the right of the figure. Figure 10.13 again shows that parametric pumping favors separation factor and the cycling zone favors throughput. Two experimental points are indicated on this figure as a reference to a real situation. The above comparison is based on the same size column in parapump and cycling zone with semi-continuous operation. It is possible to operate cycling zone continuously by using two parallel units, and parapump continuously by using 4 parallel units. The continuous parapump and cycling zone, as shown schematically in Figure 10.14, are studied in computer simulation. The results of these 2 continuous process are shown in Figures 10.15 and 10.16. It is seen that the domain of continuous parapump (4 parallel units) is shifted toward the right, and its right margin overlaps the domain curve of continuous cycling zone (2 parallel units). Thus the parapump can obtain the same throughput as the cycling zone does, and it is still possible to obtain a higher separation factor under certain operation conditions. The result for $B=0.7$ is shown more clearly in Figure 10.16. The parapump can obtain a higher separation factor under some operating conditions and can also operate for a large throughput.

10.7 : 3 pH Level Cycling Zone

Hemoglobin can be separated by cycling zone operation with

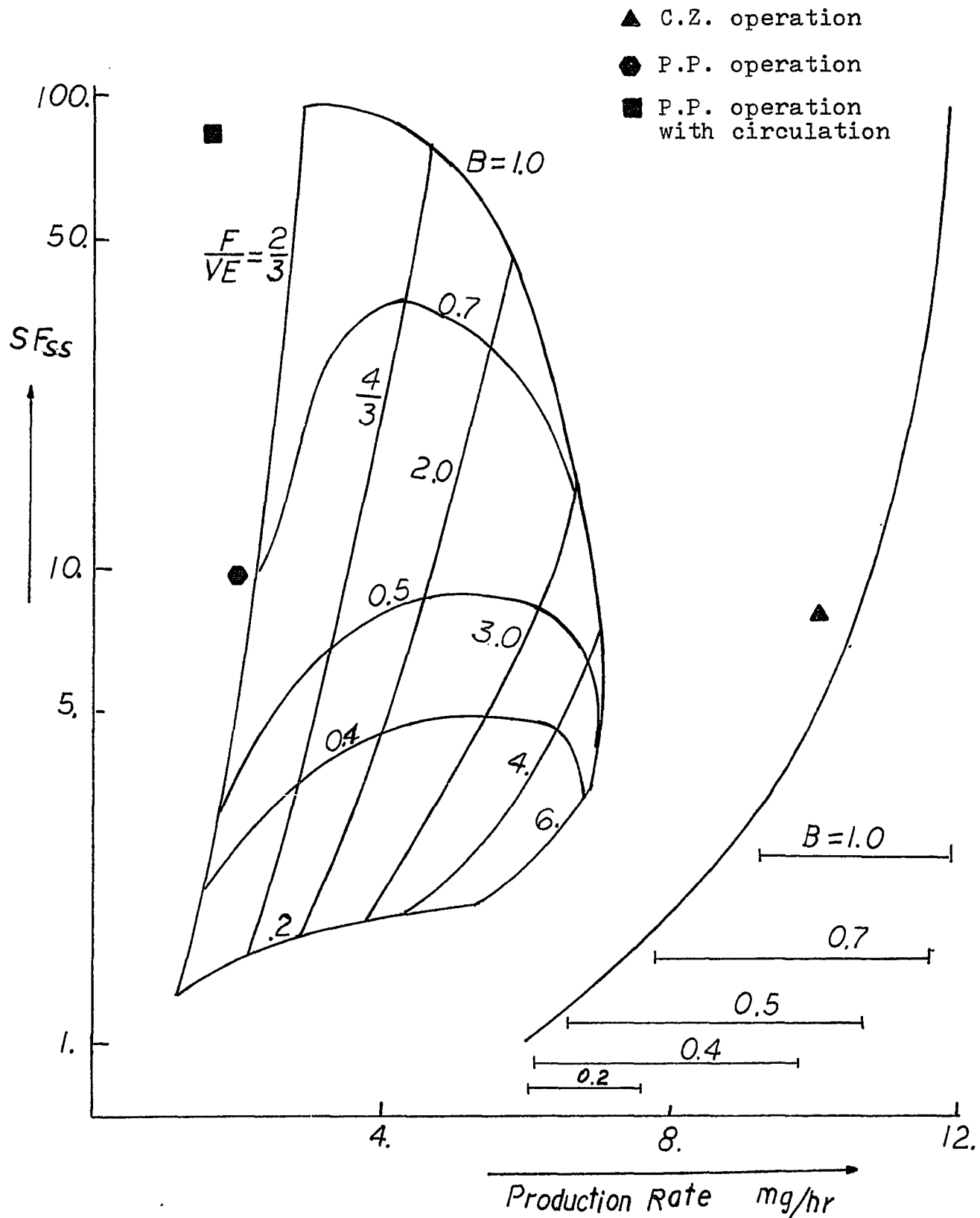


Figure 10.13 Comparison of Cycling Zone and Parapump in Separation for B ranges from 0.0 to 1.0

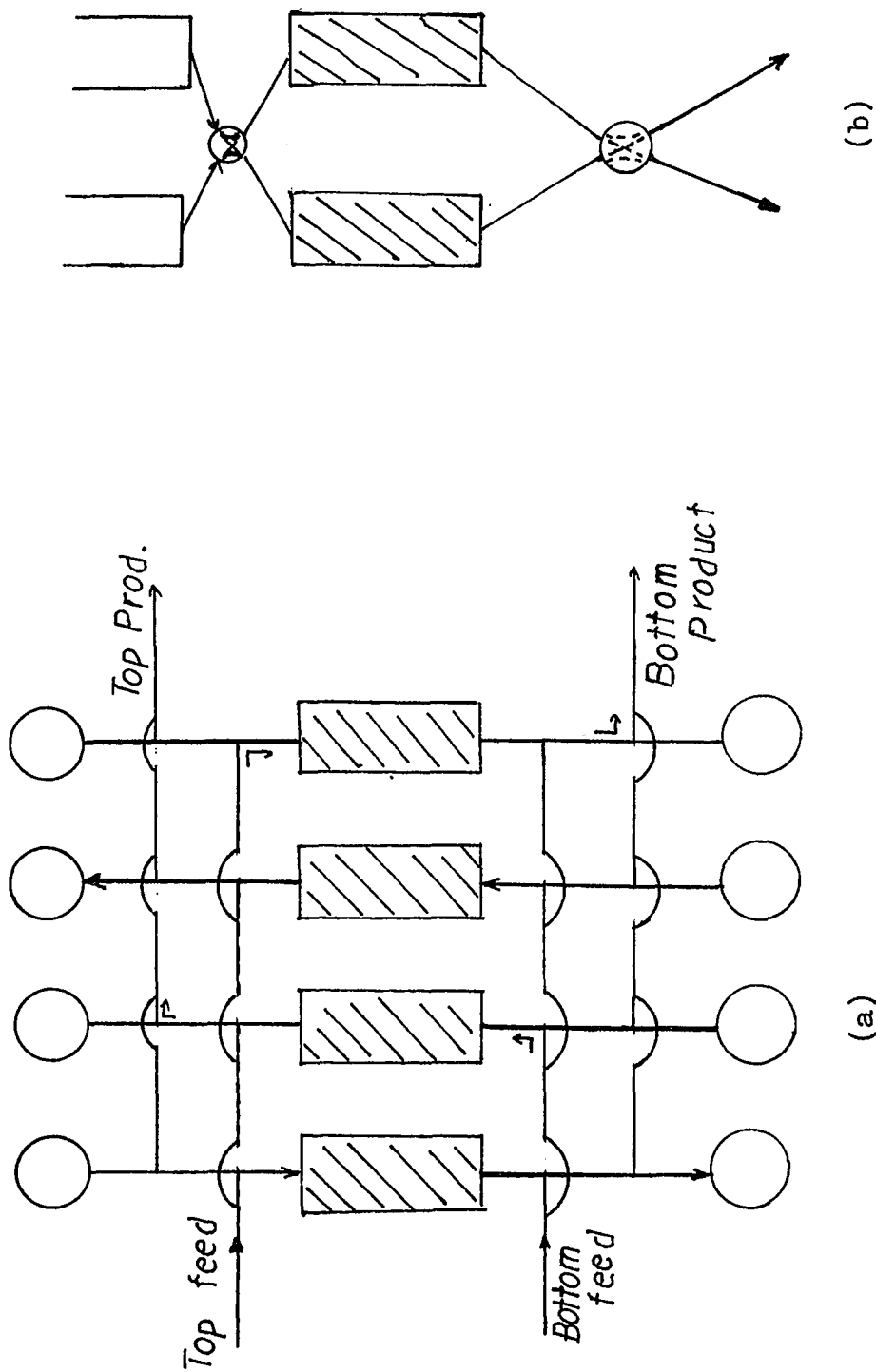


Figure 10.14 Continuous Operation of (a) Parametric Pumping, (b) Cycling Zone

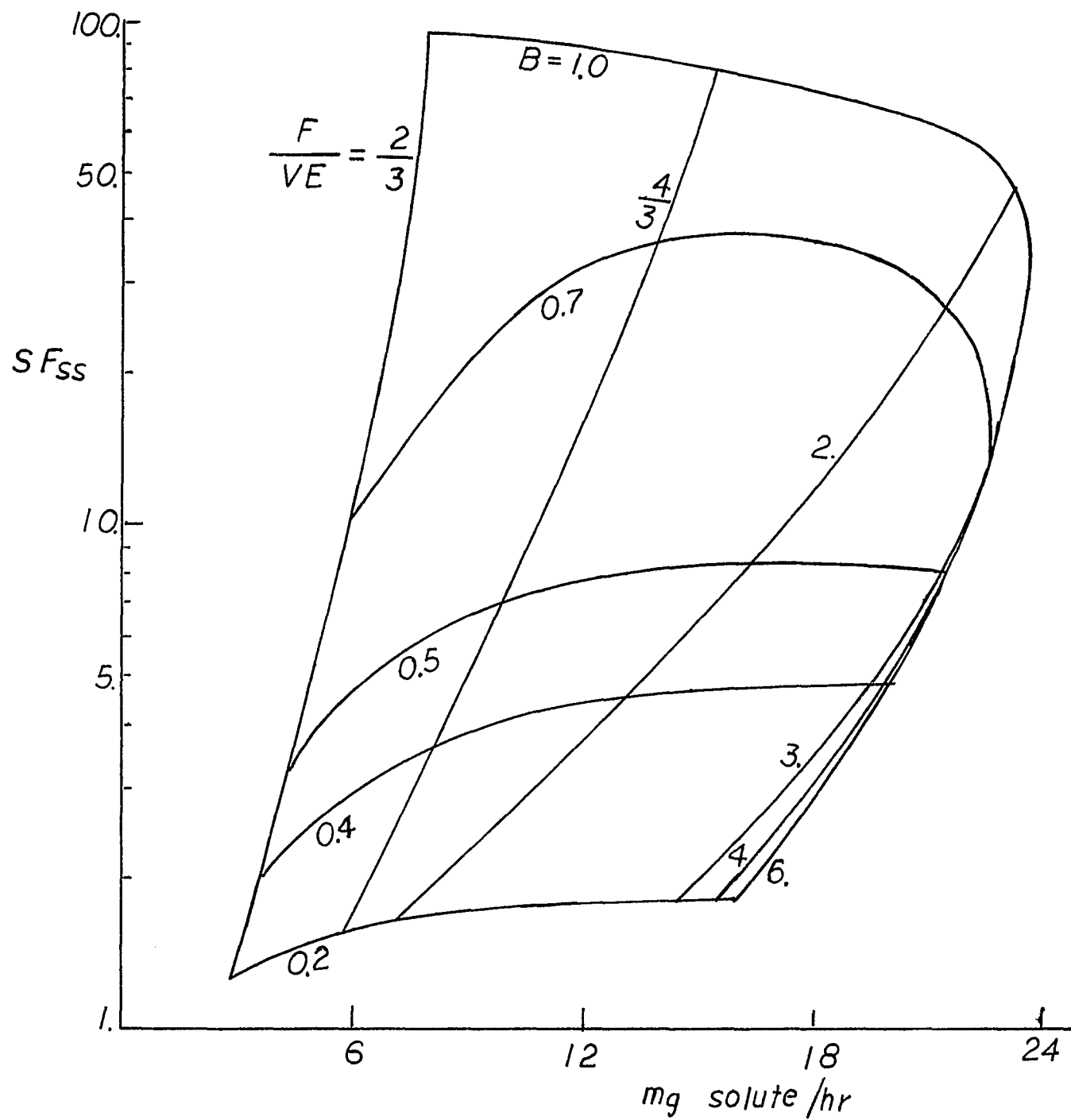


Figure 10.15 Comparison of Continuous Parapump and Cycling Zone for B ranges from 0.0 to 1.0

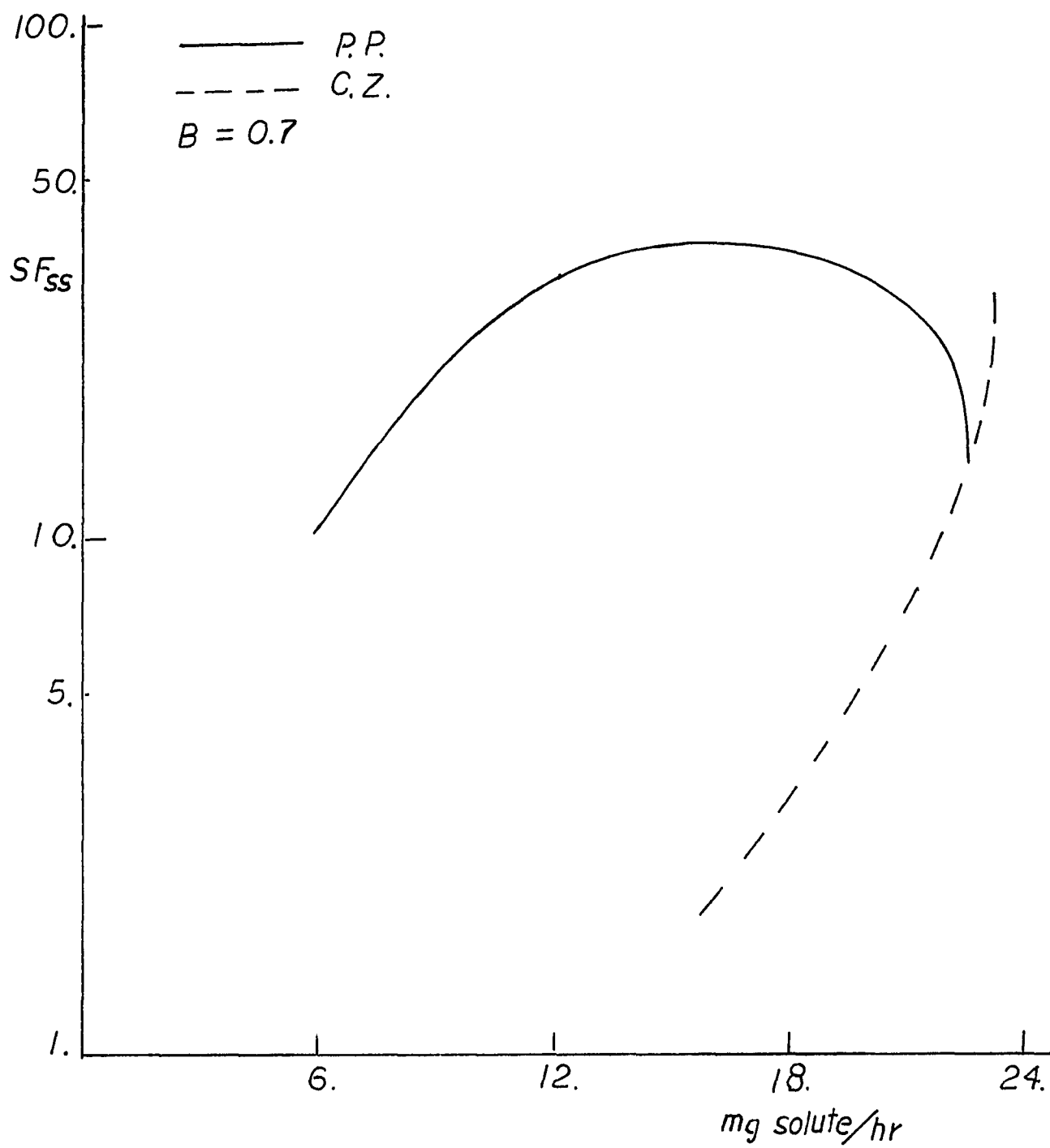


Figure 10.16 Comparison of Continuous Parapump with Cycling Zone at $B=0.7$

periodic alternation of pH from 6 to 8, and albumin can be separated by cycling zone operation with periodic alternation of pH from 4 to 6. A three pH level cycling zone operation is theoretically investigated by computer simulation. It is assumed that the adsorptive equilibrium of individual species is uninterfered by the other in the multiple solutes mixture. A 3 pH cycling zone device is schematically shown in Figure 10.17. The apparatus of the 3 pH level cycling zone includes an adsorptive column and three reservoirs in top of the column. Reservoirs contains feed fluid mixture, and the pH of the three reservoirs are kept at P1 ,P2, and P3 respectively. The cycling zone is operated in such a way that the fluid mixture is introduced into the top of column alternatively from three reservoirs. Thus the pH level of a particular location in this column is periodically changing from P1 to P3 and with certain time duration in which pH close to P2 synchronizes the alternation of the pH of the fluid mixture entered the column. Figure 10.18 shows the output pH wave and concentration wave of 2 components. It is shown that there are 3 pH plateaus, say high, middle, and low, in the output pH wave. It is also shown that there are two distinct peaks of output concentration wave for the two components, A and B. The separation factor for two solutes mixture is defined by equation (10.13).

$$SF = \left[\frac{Y1}{Y2} \right]_{PD1} \left[\frac{Y2}{Y1} \right]_{PD2} \frac{PD1}{(F/2)} \frac{PD2}{(F/2)} \quad (10.13)$$

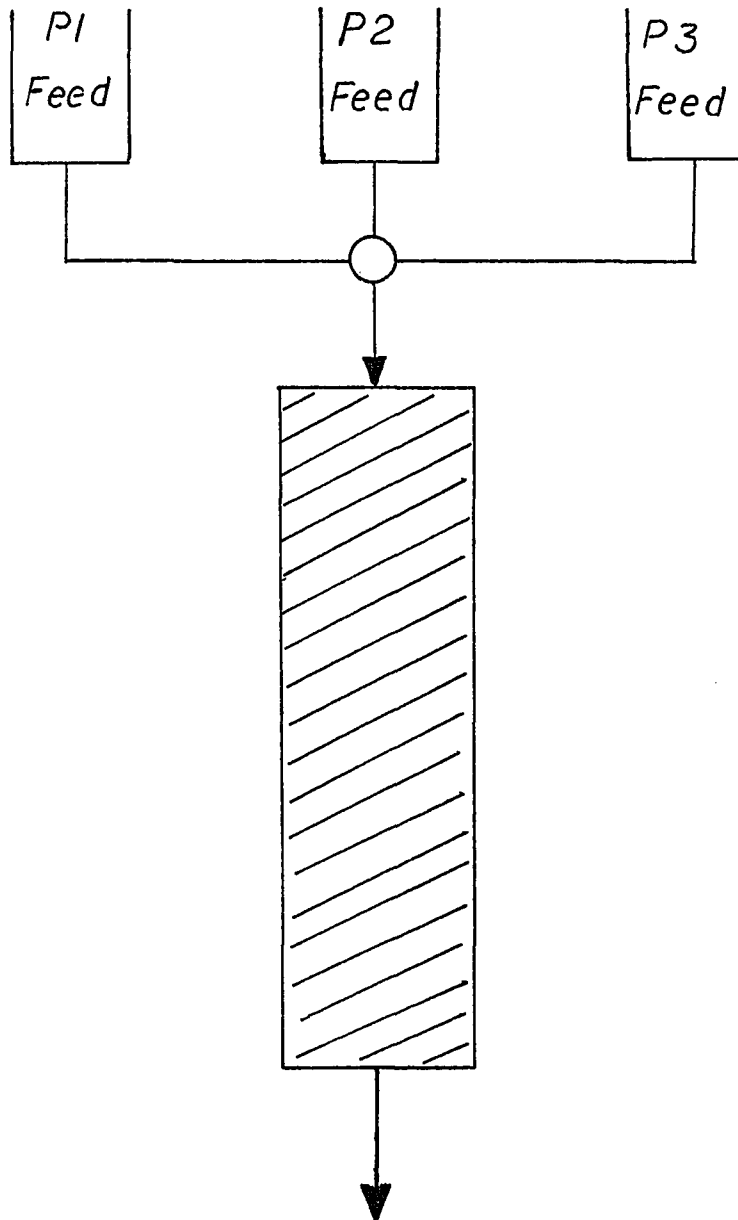


Figure 10.17 Schematic Diagram of 3-pH Cycling Zone

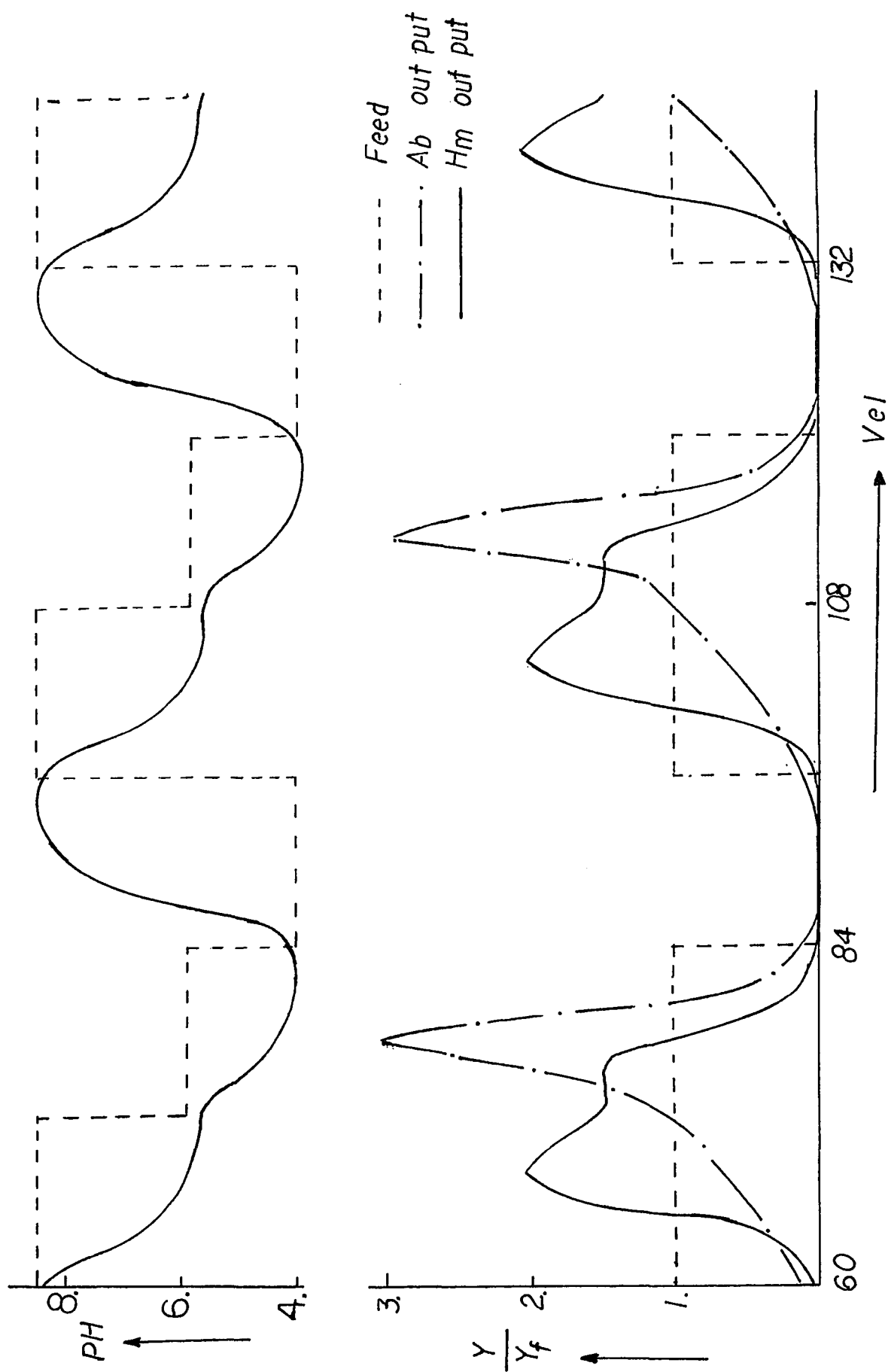
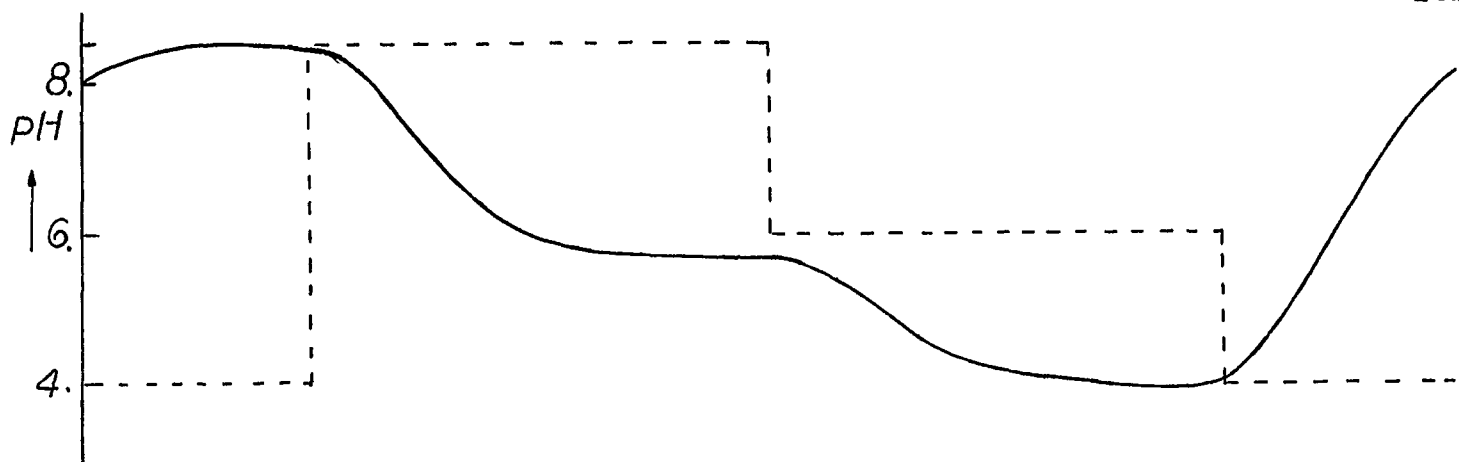


Figure 10.18 pH and Concentration Wave in 3 pH Cycling Zone



3 PH C. Z.

PH	8.5	6.	4.
K_A	6.	2.	1.
K_B	5.	4.	1.
Y_f	1.	1.	0.
F	12.	12.	12.

$B = 0.8$
 $HT = 8.$
 $NITV = 12$

--- Feed Conc.
 -.-.- Ab out put
 — Hm out put

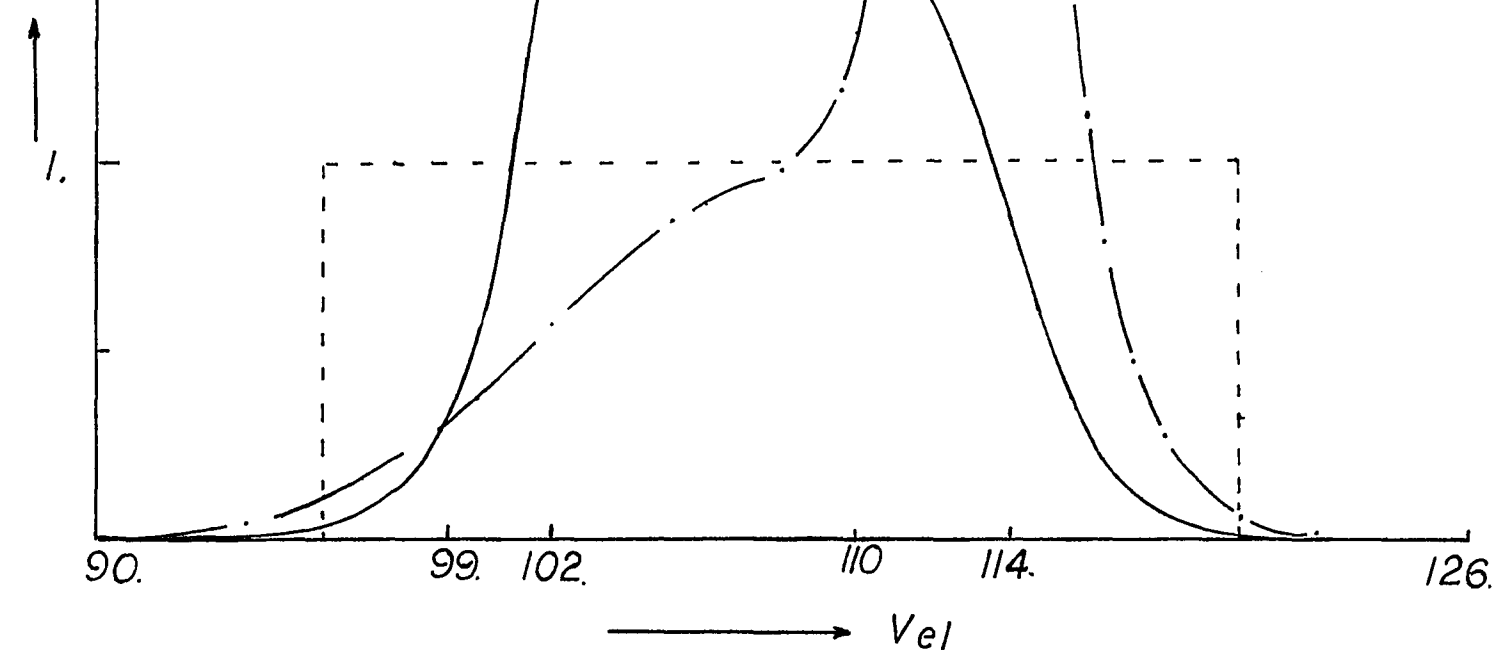


Figure 10.19 pH and Concentration Wave in 3 pH Cycling Zone
 (Enlargement of Figure 10.18)

where Y_i : concentration of component i ; ($i=1,2$)

PD_i : volume of throughput in which the concentration
the i -th component is higher.

$F = PD_1 + PD_2$: total volume of feed

For a system contains protein A and B, PD_1 is the product which favors A concentration fraction, while PD_2 is the product which favors B concentration fraction. As shown in Figure 10.19, PD_2 consists of the elution volume from 90 - 99 and 110 - 126, and PD_1 consists of the rest of the elution volume in this particular cycle. Figure 10.22 shows the effect of B value on the separation of 2 solutes by cycling zone operation. As it is seen, an optimal B value exists for a particular height of column. It is understood that, for small B value, the change of control variable is flat so that mass transfer is slower in the column. Mass transfer increased as B value increased, which gives sharper control variable change in the columns, and hence increases the separation factor. Separation drops when B reaches unity, which can be explained by the fact that the relative travelling speed of 2 concentration wave is decreased. It is also seen from Figure 10.24 that a higher separation is given by $B=0.5$, and a lower separation is given by $B=1.0$ in the long column region. This is because the difference in equilibrium constant for these two components is largest at pH near P2. When $B=1$, the pH shifts sharply to one of the 3 pH levels (P1, P2 and P3); when $B=0.5$, the pH range is narrowed down and the pH stays

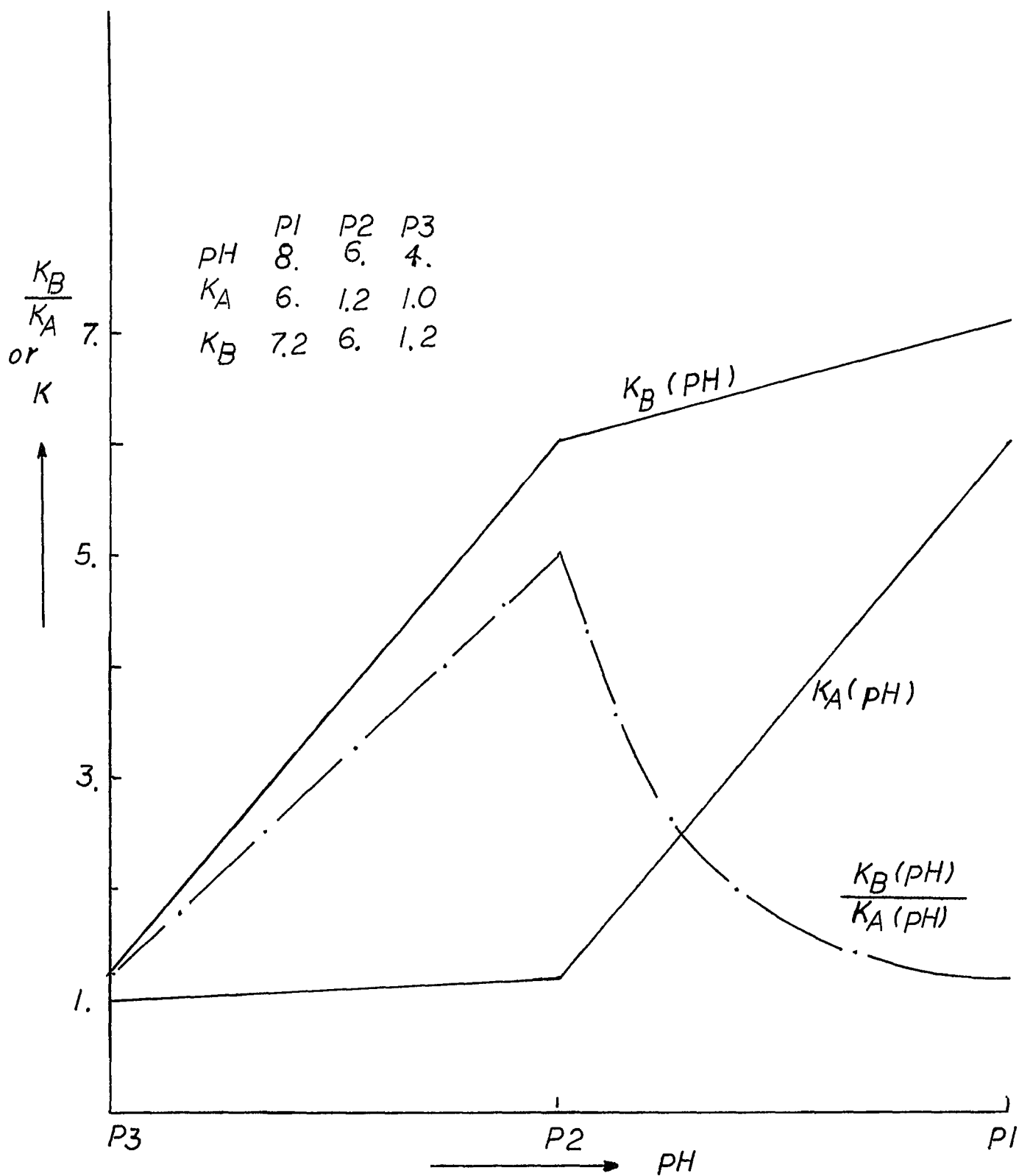
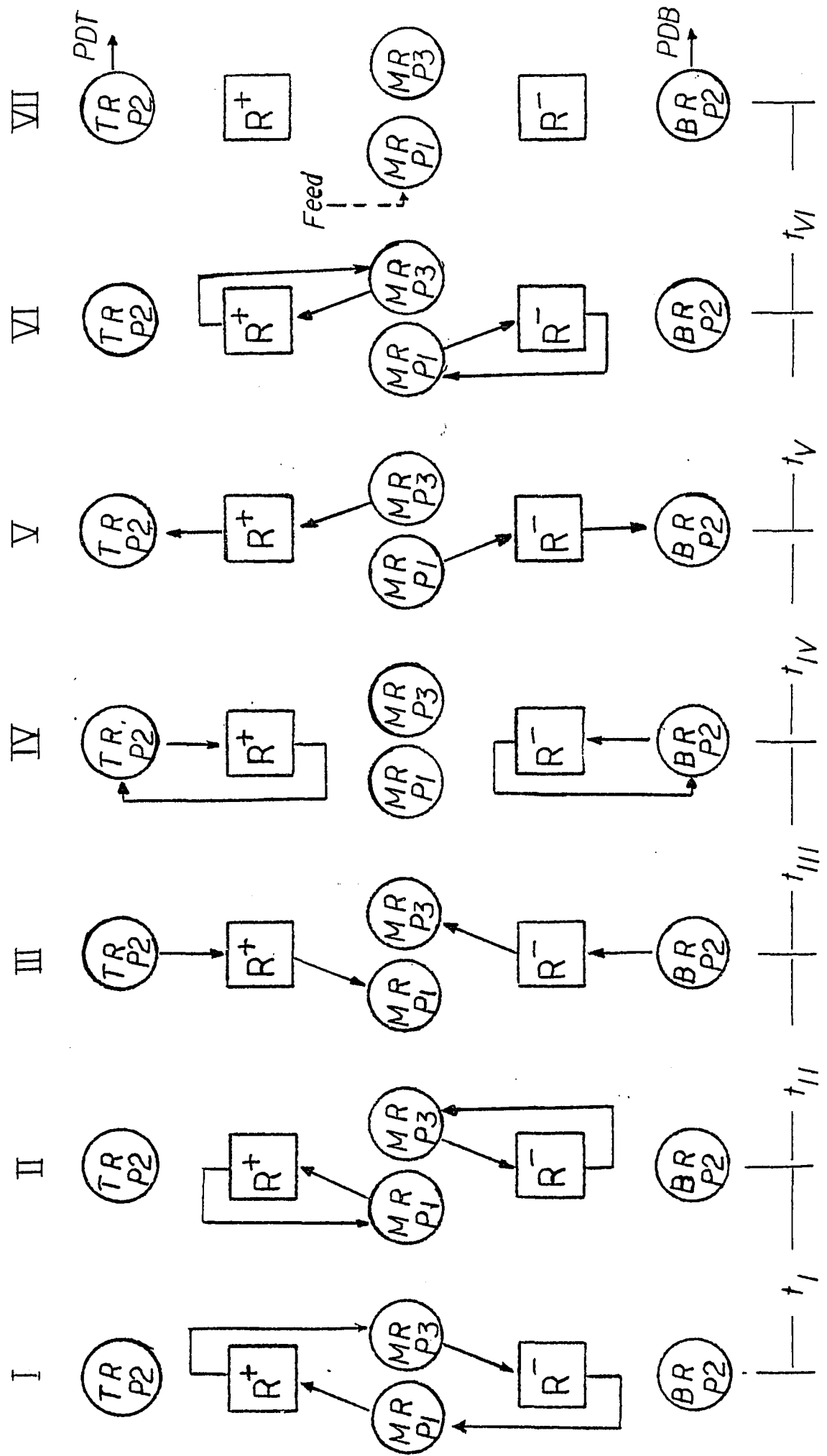


Figure 10.20 Effect of pH on Relative Equilibrium Constant (KB/KA)



Mode 3B — Open Operation : $P1 > I_A > P2 > I_B > P3$

Figure 10.21 System of 3 pH open Parapump

around P2 more often. As shown in Figure 10.20, the relative equilibrium constant, $K(A,pH)/K(B,pH)$, is largest at the region of $pH=P2$, and the smallest at the region of $pH=P1$ and $P3$. Although the increase of B value enhances the mass transfer of both components, the relative mass transfer at the area near $P1$ and $P3$ is small, thus the average of relative mass transfer is smaller for the case of $B=1.0$. Thus separation given by $B=0.5$ will be better than that for $B=1$ as long as the column is long enough. Figure 10.24 also shows that there is an optimal height of column at a given B value and feed size. Poor separation occurs when the column is too long for the same reasons as stated above.

10.8 : Comparison of 2-Column Parapump and Cycling Zone in Splitting 2-Solutes System

The idea of 3 pH levels cycling zone can be applied to parametric pumping. In chapter 8, we have discussed the 3 pH parapump under the single cell model; here the parapump is studied in multi-cell model. Figure 10.21 shows a 3-pH 2-column parapump which is essentially the same as the parapump described in chapter 8. The apparatus includes two adsorptive columns and four reservoirs. One of the columns is packed with cation exchanger and the other with anion exchanger. As shown in Figure 10.21, one operation cycle includes 7 steps, fluid from one

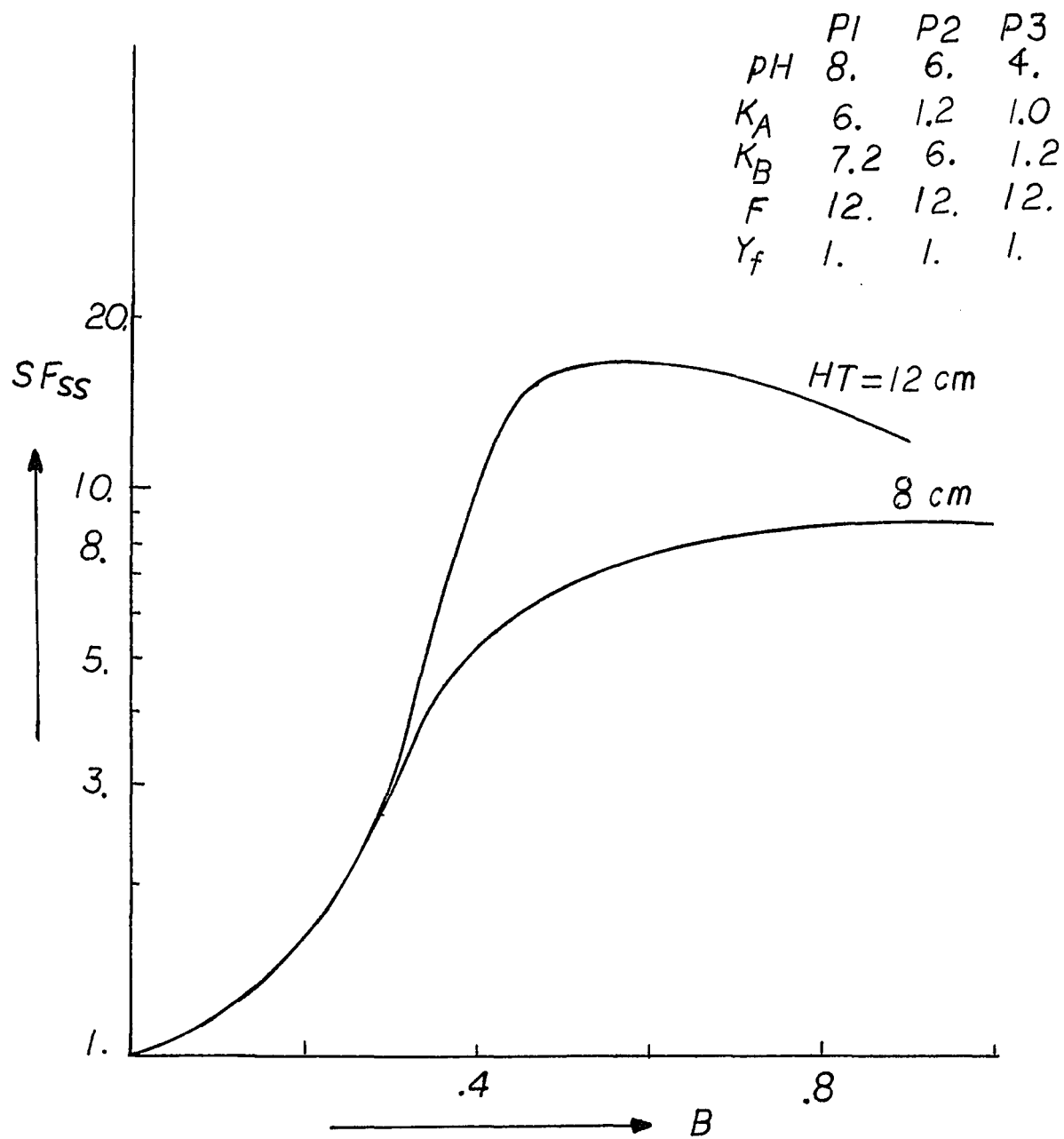


Figure 10.22 Effect of B on Separation in 3-pH Parapump

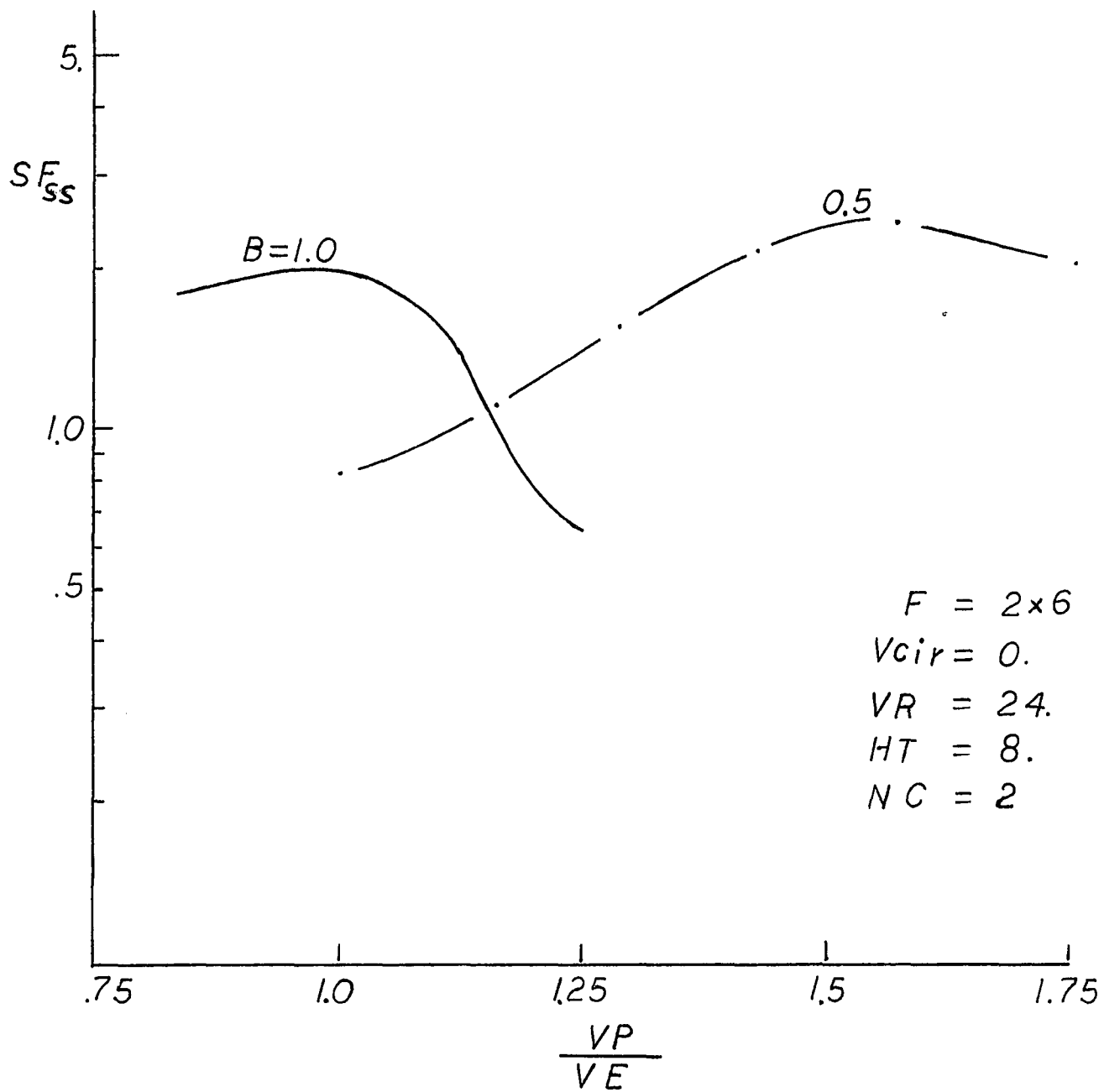


Figure 10.23 Effect of Displacement on SF_{ss} for -pH parapump

reservoir is pumped into the column ; the fluid emerged from the other end of the column is received by another reservoir. In Figure 10.21, the displacement flow (as shown in step I, III, and V,) is followed by circulation flow (as shown in the step II, IV, and VI). In Step VII, products are withdrawn and then feeds are introduced to reservoirs. The fluid is pumped into the column in the sequential order of P1, P2, and P3 for the anion exchanger column, and in the order of P3, P2, and P1 for cation exchanger column.

The model equations, used in single column, are again applied to examine the separation of this process. As shown in Figure 10.23 and Figure 10.25 , there exists an optimal displacement and optimal secondary displacement for a particular value of B. The optimal primary displacement and secondary displacement are used in operating the 2 column parametric pumping. The calculated separation is shown in Figures 10.26. The figure also shows the comparison of separation by cycling zone(solid curve) and parametric pumping(broken curve). It is seen that parametric pumping gives a higher separation factor in smaller size of feed, while cycling zone does better for large size of feed. It is also an advantage of cycling zone that it is operated without reverse flow. However, cycling zone is physically difficult to operate with a small size feed.

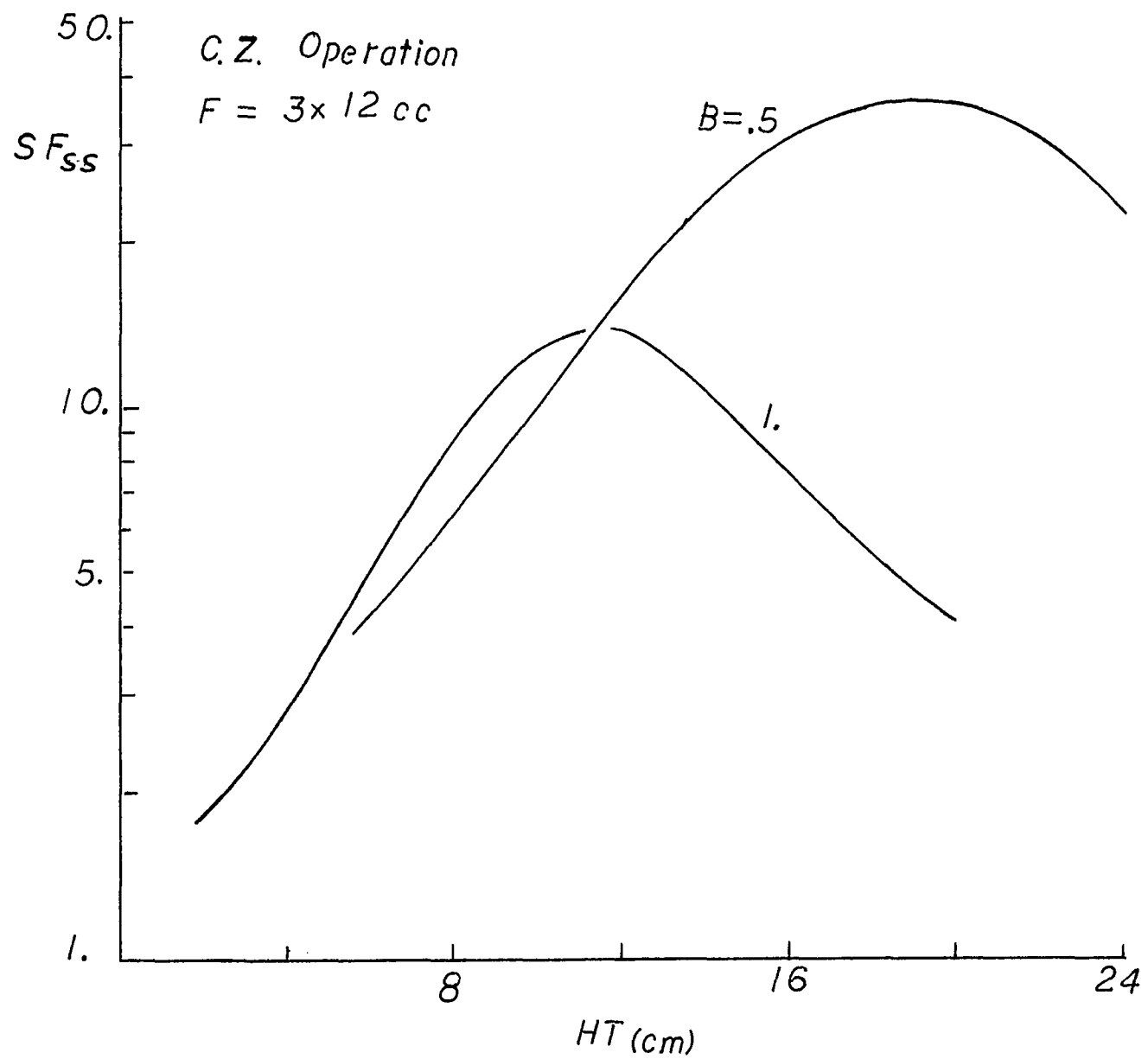


Figure 10.24 Effect of Column Height on SF_{ss} in 3-pH Parapump

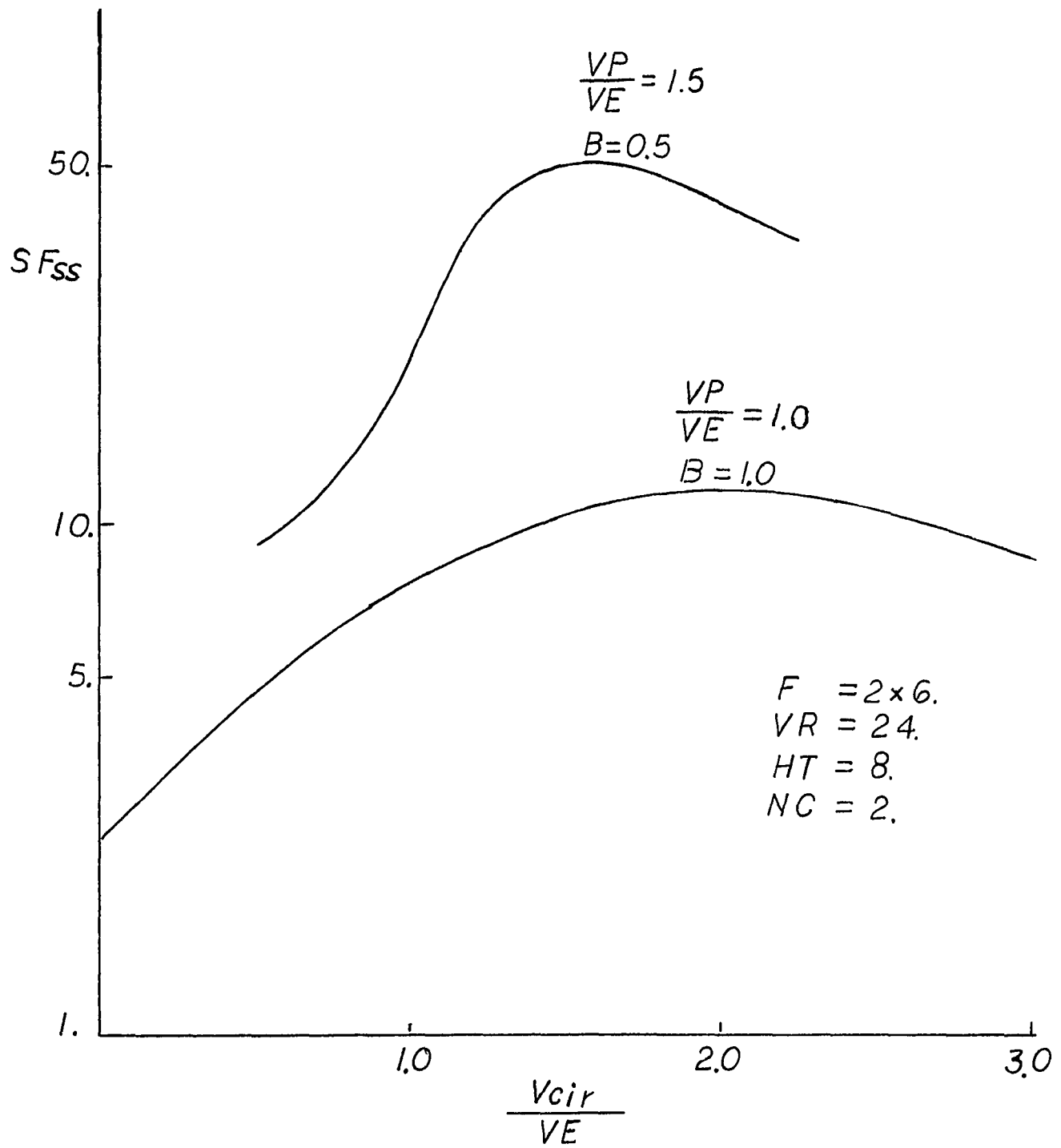


Figure 10.25 Effect of Circulation on SF_{ss} for 3 pH Parapump

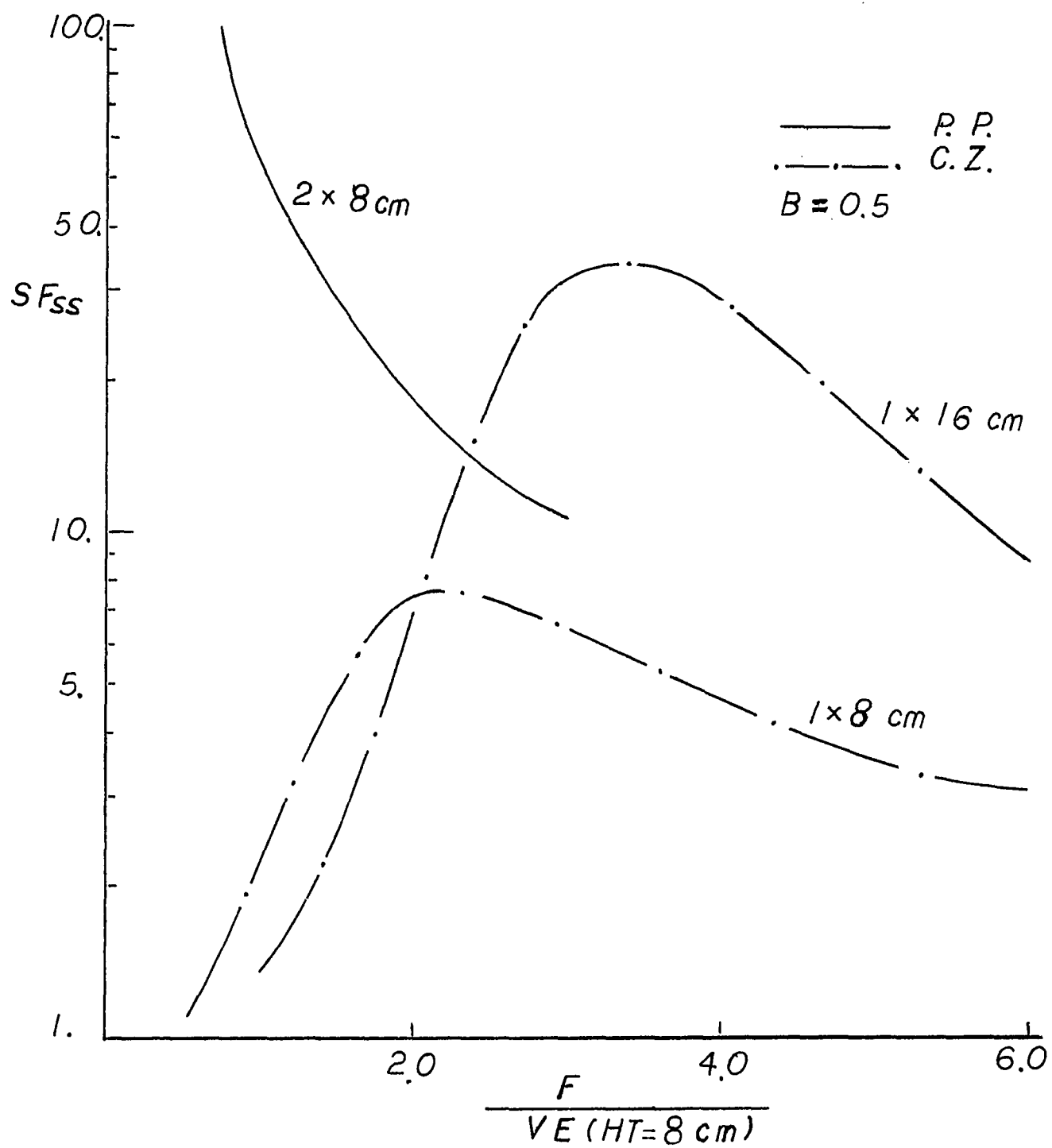


Figure 10.26 Effect of Feed on SF_{ss} for Parapump and Cycling Zone at $B=0.5$

Chapter 11 : Conclusions

In concluding this thesis, the most significant results are listed as follows:

- (1) pH parametric pumping is very functional for separating liquid mixture. The separation principle is based on the periodic alternation of the control variable (i.e., pH in this case), and on the coupling of the transport actions (i.e., the interfacial mass transfer and bulk fluid flow).
- (2) The separation capability of multi-column parapump is superior to that of one-column parapump. An increase in the number of columns gives a corresponding increase in the capability (quality and quantity) of separation.
- (3) At steady state, the state variables are periodic functions of time, thus the parapump operation has the following two major advantages over the conventional separation processes. i: As shown in chapter 9, a better separation can be obtained by open parapump than that by batch parapump. ii: the operation parameters, such as the products withdrawn time, can be optimized according to the objective function of the operation.
- (4) The 2-pH parapump is capable of enriching the product stream with proteins; 3-pH parapump is capable of splitting proteins into two product streams.

- (5) To split two components is a rather complicated process, and the separation is dependent on the relative mass transfer rate of the two components in the columns.
- (6) Parametric pumping gives a higher separation factor (purer products) as compared to cycling zone operation, but cycling zone operation gives a larger throughput.
- (7) The experimental model system, hemoglobin and albumin, has demonstrated the separation capability of multi-column pH parametric pumping. The theoretical model has been verified by the experimental results. The Single Cell Model and the Multi-Cell Model with Stop and Go method give a good prediction and correlation for pH parametric pumping operation.

NOMENCLATURE

A_c	= column cross sectional area cm^2
B	= buffer capacity of fluid phase
C	= buffer capacity of solid phase
e	= voidage of packed bed, dimensionless
F_B	= PDT = bottom feed, cc/cycle
F_T	= PDB = top feed, cc/cycle
h	= column height, cm
I_i	= isoelectric point of i
I.E.	= Isoelectric point
IS	= ionic strength of solution
K	= equilibrium constant, dimensionless
n	= number of cycles of parapump operation
M	= number of columns
P_i	= i-th pH level
PDi	= Product Stream cc/cycle ; $i=1, 2, T, \text{or } B.$
Q	= fluid flow rate in the column, cc/sec
SF	= separation factor, dimensionless
t_i	= time duration of i-th step, sec
t_c	= circulation time sec
VP	= displacement volume, cc/step of cycle
VD_i	= dead volume of reservoir i ($i = T, M, B$)
V_e	= volume of fluid phase per stages, cc
VE	= total void volume of column, cc
VR	= total volume of reservoir (dead volume + Displacement), cc

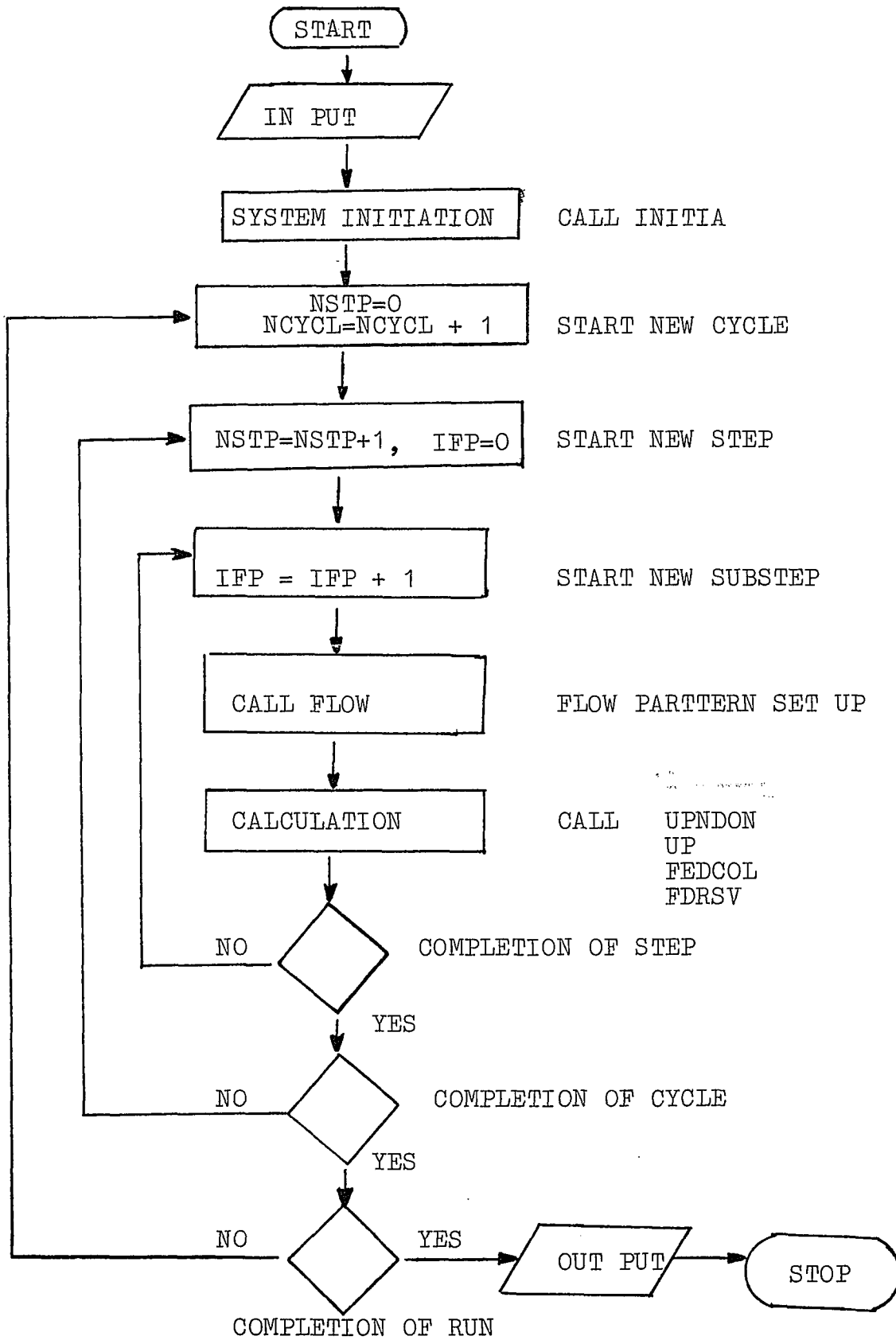
V_s	=	volume of solid phase per cell, cc
u	=	linear velocity, cm/sec
X	=	Concentration of solute in solid phase, g moles/cc
Y	=	concentration of solute in fluid phase, gmoles/cc
Y_{co}	=	initial concentration of solute in the column, g moles/cc
Y_o	=	Y_f = concentration of solute in the feed, g moles/cc
z	=	vertical dimension , cm
λ	=	Mass transfer rate constant , 1/sec

Superscripts

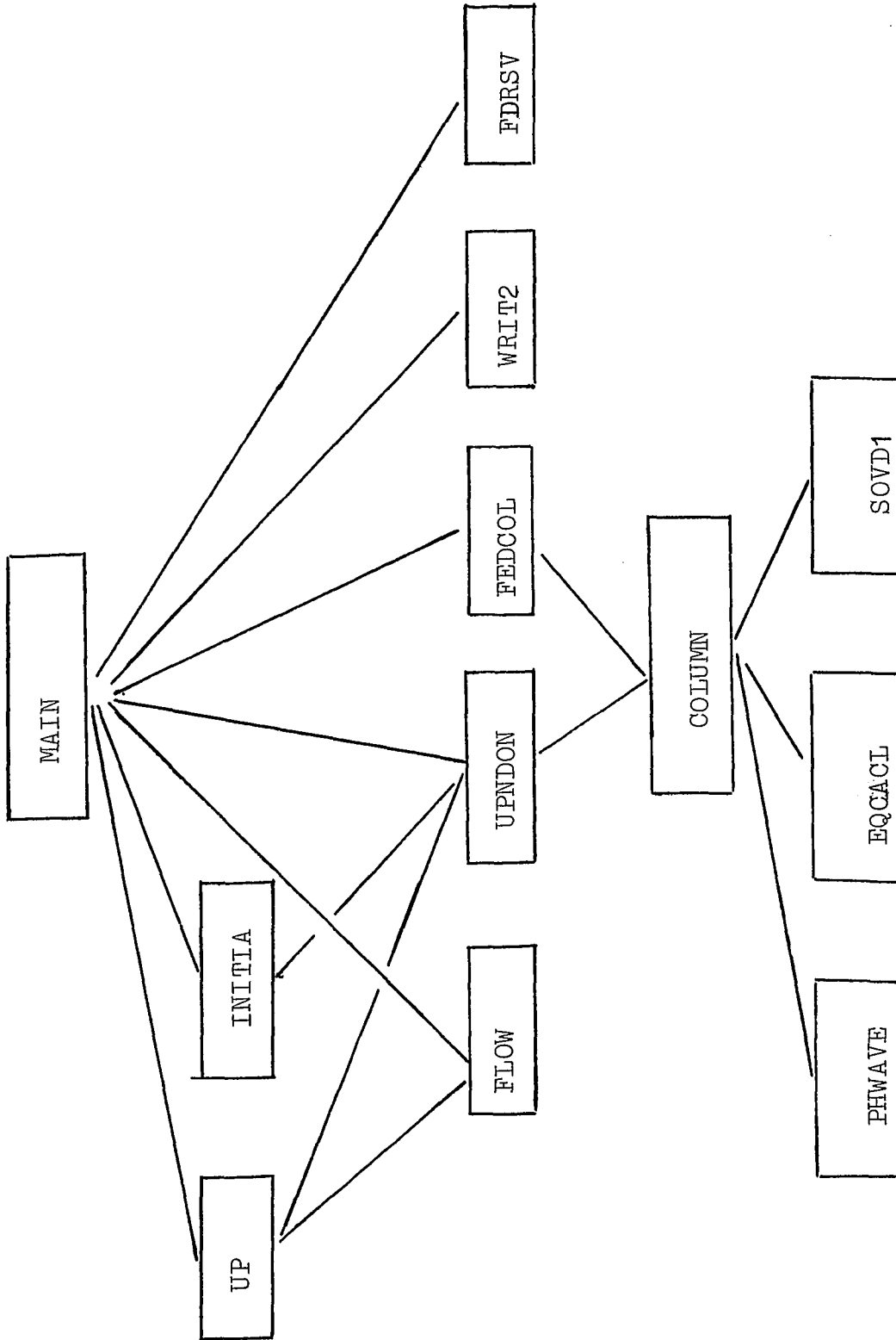
*	=	equilibrium condition
+	=	anion exchanger
-	=	cation exchanger

Subscripts

B	=	bottom reservoir
T	=	top reservoir
MR	=	middle reservoir
SR	=	side reservoir
op	=	optimal value
ss	=	steady state
n	=	n-th cycle
1,2,3	=	index for pH levels or ionic strength



YUP FLOWCHART: PARAMETRIC PUMPING



YUP : MAIN & SUB-PROGRAM INTERACTION

Appendix-A Fortran Program YUP

```

C   YUP:OVER ALL P-P;FEED TO COLUMN & TO RESERVOIR; PHWAVE
C   STP=1
C       IFP=11   DOWN FLOW;    L2=F;    L3=F
C       IFP=12   DOWN CIRC;    L2=F;    L3=T
C       IFP=13   FEED UP ;    L2=T;    L3=F
C       IFP=14   UP   CIRC;    L2=T;    L3=T
C   STP=2
C       IFP=21   UP   FLOW;    L2=T;    L3=F
C       IFP=22   UP   CIRC;    L2=T;    L3=T
C       IFP=23   FEED DOWN;    L2=F;    L3=F
C       IFP=24   DOWN CIRC;    L2=F;    L3=T
C   STP=3
C       IFP=31   DOWN FLOW;    L2=F;    L3=F
C       IFP=32   DOWN CIRC;    L2=F;    L3=T
C       IFP=33   FEED UP ;    L2=T;    L3=F
C       IFP=34   UP   CIRC;    L2=T;    L3=T
COMMON B,MA,NPHL,JD,JCIR,I,IFP,J,K,L,NCP,NRS,NRL,NSTP,NTS,
/NCYCL,NCYCLP,NITV,M,TCEL,E,R,RANDA,VP,AK,PHL,PHC0,PHOLD,
/PH,PHR,YOLD,XOLD,Y,X,YF,YR,YC0,YRP,YCP,YCPX,JDSP,JFC,JDXA,VDP,VFR,
/VRS,VPRZ,VDXTRA,VFC,NZ,IEX,L2,L3,L4,L7,L9,LWR1,LWR2
DIMENSION AK(3,2,2),PHL(3),PHC0(5),PHOLD(5,30),PH(5,30),PHR(8),
/YOLD(4,16,2),XOLD(4,16,2),Y(4,16,2),X(4,16,2),YF(8,2),YR(8,2),
/YC0(5,2),YRP(4,2,177),YCP(4,2,177),YCPX(4,2,177),JFC(8),JDXA(8),
/JDSP(8),VDP(8),VFR(8),VRS(8),VPRZ(8),VDXTRA(8),VFC(8),NZ(8),IEX(8)
DIMENSION KXS(4),KXN(4),KFD(4),KPD(4),YRP1(4,2,177),YRP2(4,2,177),
&YRP3(4,2,177),NSFR(8)
LOGICAL L2,L3,L4,L7,L9,LWR1,LWR2
NEVE(I)=I-(I/2)*2
NQDP(I)=I-I/2*4
50  CONTINUE
READ(5,36) L4,L7,L9,LWR1,LWR2,KS,KN,NFCYCL
IF( KS.EQ. 0 )GO TO 1000
KNX=KN+1
NRS=KS+(KS-1)/2
NRL=KNX+KNX/2
36  FORMAT(5L10,5I10)
READ(5,61) NITV,NCP,NPHL,NTS
61  FORMAT(8I10)
READ(5,60) HTS,AC,E,UVOLM,RANDA,B
READ(5,60) (VDP(I),I=1,NTS),VCIR
READ(5,60) (VDXTRA(II),II=1,NTS)
READ(5,61) (KXS(I),KXN(I),I=1,NTS)
READ(5,60) (VFC(II),II=1,NTS)
READ(5,61) (KFD(I),KPD(I),I=1,NTS)
READ(5,60) (VPRZ(I),I=NRS,NRL)
READ(5,60) (VFR(I),I=NRS,NRL)
READ(5,61) (NSFR(I),I=NRS,NRL)
READ(5,60) (VRS(I),I=NRS,NRL)
READ(5,59) ((AK(I,K,L),I=1,NPHL),K=1,2),L=1,NCP)

```

```

      READ(5,59) ((YF(I,L),I=NRS,NRL),(YCO(J,L),J=KS,KN),(YR(K,L),
/ K=NRS,NRL),L=1,NCP)
      READ(5,59) (PHR(I),I=NRS,NRL),(PHCO(J),J=KS,KN),(PHL(K),K=1,NPHL)
59  FORMAT(14F5.2)
60  FORMAT(8F10.4)
      WRITE(6,30)
30  FORMAT('1')
      WRITE(6,36) L4,L7,L9,LWR1,LWR2,KS,KN,NFCYCL
      WRITE(6,61) NITV,NCP,NPHL,NTS
      WRITE(6,60) HTS,AC,E,UVOLM,RANDA,B
      WRITE(6,60) (VDP(I),I=1,NTS),VCIR
      WRITE(6,60) (VDXTRA(II),II=1,NTS)
      WRITE(6,61) (KXS(I),KXN(I),I=1,NTS)
      WRITE(6,60) (VFC(II),II=1,NTS)
      WRITE(6,61) (KFD(I),KPD(I),I=1,NTS)
      WRITE(6,60) (VPRZ(I),I=NRS,NRL)
      WRITE(6,60) (VFR(I),I=NRS,NRL)
      WRITE(6,61) (NSFR(I),I=NRS,NRL)
      WRITE(6,60) (VRS(I),I=NRS,NRL)
      WRITE(6,59) ((AK(I,K,L),I=1,NPHL),K=1,2),L=1,NCP)
      WRITE(6,59) ((YF(I,L),I=NRS,NRL),(YCO(J,L),J=KS,KN),(YR(K,L),
/ K=NRS,NRL),L=1,NCP)
      WRITE(6,59) (PHR(I),I=NRS,NRL),(PHCO(J),J=KS,KN),(PHL(K),K=1,NPHL)
      VBED=HTS*AC
      WRITE(6,6601)
6601 FORMAT(/,2X,'IPH',4X,'K',4X,'L','      AK(I,K,L)')
      WRITE(6,6600) ((I,K,L,AK(I,K,L),I=1,NPHL),K=1,2),L=1,NCP)
6600 FORMAT(3I5,F10.3)
      IF(L9) WRITE(6,52)
      IF(.NOT.L9) WRITE(6,53)
52  FORMAT('0      THEORY : FINITE MASS TRANSFER, NON-EQUILIBRIUM,
/ INTEGRAL METHODE ')
53  FORMAT('0      THEORY : EQUILIBRIUM')
      ULIN = UVOLM/(AC*E)
      HTCEL=HTS/NITV
      TCEL=HTCEL/ULIN
      VP=VBED*E/NITV
      R=(1-E)/E
      M=NITV+2
      MA=M-1
      MB=M-2
      KN1=KN+1
      DO 70 I=1,NTS
      JDSP(I)=VDP(I)/VP
70  JDXA(I)=VDXTRA(I)/VP
      JCIR=VCIR/VP
      DO 72 I=1,NTS
72  JFC(I)=VFC(I)/VP
      JCIR=VCIR/VP
      WRITE(6,82)
82  FORMAT('0',5X,'VP',8X,'R',9X,'HTCEL',5X,'TCEL',6X,'VBED')
      WRITE(6,60) VP,R,HTCEL,TCEL,VBED

```

```

      WRITE(6,84) (I,I=1,NTS)
84   FORMAT(3X,'M',4X,'MA',10X,8('  NSTP=',I2))
      WRITE(6,80) M,MA,(JDSP(I),I=1,NTS)
      WRITE(6,81) (JDXA(I),I=1,NTS)
      WRITE(6,85) (JFC(I),I=1,NTS)
      WRITE(6,83) JCIR
80   FORMAT(2I5,5X,'JDSP=',10I10)
81   FORMAT(15X,'JDXA=',10I10)
85   FORMAT(15X,' JFC=',10I10)
83   FORMAT(15X,'JCIR=',10I10)
99   CONTINUE

```

```

C
C
C  INITIALIZATION OF SYSTEM
C
C

```

```

      NCYCL=-1
      NSTP=-1
      IFP=-1
      DO 101 I=NRS,NRL
      DO 101 L=1,NCP
      YRP1(I,L,1)=1.
      YRP2(I,L,1)=1.
      YRP3(I,L,1)=1.
      YRP(I,L,1)=1.
      YCP(I,L,1)=1.
101   CONTINUE
      DO 112 K=1,KN
      IF(L7.AND.(NEVE(K).EQ.0)) IEX(K)=2
      IF(L7.AND.(NEVE(K).NE.0)) IEX(K)=1
      IF(.NOT.L7.AND.(NEVE(K).EQ.0)) IEX(K)=1
      IF(.NOT.L7.AND.(NEVE(K).NE.0)) IEX(K)=2
      DO 103 J=1,NPHL
103   IF(PHC0(K).EQ.PHL(J)) IPH=J
      DO 111 I=2,MA
      DO 105 L=1,NCP
      YOLD(K,I,L)=YC0(K,L)
      XOLD(K,I,L)=YC0(K,L)*AK(IPH,IEX(K),L)
      Y(K,I,L)=YC0(K,L)
105   X(K,I,L)=YC0(K,L)*AK(IPH,IEX(K),L)
      PHOLD(K,I)=PHC0(K)
111   PH(K,I)=PHC0(K)
112   CONTINUE
      IF(LWR2) CALL WRIT2(KS,KN)

```

```

C
      IF(.NOT.L7) VRS(3)=VRS(3)-JDSP(1)*VP
      IF(.NOT.L7) VRS(5)=VRS(5)-JDSP(1)*VP
      IF(.NOT.L7) GO TO 116
      DO 114 I=2,NRL,3
114   VRS(I)=VRS(I)-JDSP(1)*VP
      DO 115 I=3,NRL,3
115   VRS(I)=VRS(I)-JDSP(1)*VP

```

```

116  NCYCL=0
      NSTP=0
      IFP=0
      IF(LWR2)CALL WRIT2(KS,KN)
C
      IF(.NOT.LWR2)WRITE(6,602) ((IR,L,IR=NRS,NRL),L=1,NCP)
602  FORMAT(//' CYCLE',3X,14('R(',I1,',',I1,')',2X))
C*****
C  START OF CYCLE
C
C
120  CONTINUE
      NCYCL=NCYCL+1
      DO 151 IR=NRS,NRL
      DO 151 L=1,NCP
      YRP(IR,L,NCYCL)=0.000
      YCPX(IR,L,NCYCL)=0.000
151  YCP(IR,L,NCYCL)=0.000
C
C
      NSTP=1
      IFP=11
      CALL FLOW(KS,KN,NZ,NSTP,IFP)
      L2=.FALSE.
      L3=.TRUE.
      JD=JDSP(NSTP)
      IF(JD.EQ.0)GO TO 200
      CALL UPNDON(KS,KN)
      IF(LWR2)CALL WRIT2(KS,KN)
C
200  IFP=12
      L2=.FALSE.
      L3=.TRUE.
      JD=JCIR
      IF(JD.EQ.0)GO TO 210
      CALL UPNDON(KS,KN)
      IF(LWR2)CALL WRIT2(KS,KN)
C
C
210  IFP=13
      L2=.TRUE.
      L3=.FALSE.
      JD=JFC(NSTP)
      IF(JD.EQ.0)GO TO 268
      IF(KFD(NSTP).NE.99)GO TO 230
      DO 220 KFP=KS,KN
220  CALL FEDCOL(KFP,KFP)
230  IF(KFD(NSTP).NE.99)CALL FEDCOL(KFD(NSTP),KPD(NSTP))
      IF(LWR2)CALL WRIT2(KS,KN)
C
C
260  IF((JCIR.EQ.0).OR..NOT.L4) GO TO 268

```



```

IFP=14
CALL FLOW(KS,KN,NZ,NSTP,IFP)
L2=.TRUE.
L3=.TRUE.
JD=JCIR
CALL UPNDON(KS,KN)
IF(LWR2)CALL WRIT2(KS,KN)
C
268 DO 270 L=1,NCP
DO 270 IR=NRS,NRL
270 YRP1(IR,L,NCYCL)=YR(IR,L)
DO 280 I=NRS,NRL
280 IF(NSFR(I).EQ.NSTP) CALL FDRSV(I)
C
C
300 NSTP=2
IFP=21
L2=.TRUE.
L3=.FALSE.
JD=JDSP(NSTP)
IF(JD.EQ.0)GO TO 360
DO 350 KK=KS,KN
CALL FLOW(KK,KN,NZ,NSTP,IFP)
350 CALL UPNDON(KK,KN)
IF(LWR2)CALL WRIT2(KS,KN)
360 JD=JDXA(NSTP)
IF(JD.EQ.0)GO TO 400
DO 370 KK=KS,KN
CALL FLOW(KK,KN,NZ,NSTP,IFP)
370 CALL UPNDON(KK,KN)
IF(LWR2)CALL WRIT2(KS,KN)
C
C
400 IFP=22
L2=.TRUE.
L3=.TRUE.
JD=JCIR
IF(JD.EQ.0)GO TO 410
DO 450 KK=KS,KN
CALL FLOW(KK,KN,NZ,NSTP,IFP)
450 CALL UPNDON(KK,KN)
IF(LWR2)CALL WRIT2(KS,KN)
C
C
410 IFP=23
L2=.FALSE.
L3=.FALSE.
JD=JFC(NSTP)
IF(JD.EQ.0)GO TO 468
IF(KFD(NSTP).NE.99)GO TO 430
DO 420 KFP=KS,KN
420 CALL FEDCOL(KFP,KFP)

```

```
430  IF(KFD(NSTP).NE.99)CALL FEDCOL(KFD(NSTP),KPD(NSTP))
      IF(LWR2)CALL WRIT2(KS,KN)
C
C
460  IF((JCIR.EQ.0).OR..NOT.L4) GO TO 468
      IFP=24
      L2=.FALSE.
      L3=.TRUE.
      JD=JCIR
      DO 466 KK=KS,KN
      CALL FLOW(KK,KN,NZ,NSTP,IFP)
466  CALL UPNDON(KK,KN)
      IF(LWR2)CALL WRIT2(KS,KN)
C
468  DO 470 L=1,NCP
      DO 470 IR=NRS,NRL
470  YRP2(IR,L,NCYCL)=YR(IR,L)
      DO 480 I=NRS,NRL
480  IF(NSFR(I).EQ.NSTP) CALL FDRSV(I)
C
C
500  NSTP=3
      IFP=31
      L2=.FALSE.
      L3=.FALSE.
      JD=JDSP(NSTP)
      IF(JD.EQ.0)GO TO 600
      DO 540 KK=KS,KN
      CALL FLOW(KK,KN,NZ,NSTP,IFP)
540  CALL UPNDON(KK,KN)
      IF(LWR2)CALL WRIT2(KS,KN)
C
C
600  IFP=32
      L2=.FALSE.
      L3=.TRUE.
      JD=JCIR
      IF(JD.EQ.0)GO TO 610
      DO 605 KK=KS,KN
      CALL FLOW(KK,KN,NZ,NSTP,IFP)
605  CALL UPNDON(KK,KN)
      IF(LWR2)CALL WRIT2(KS,KN)
C
C
610  IFP=33
      L2=.TRUE.
      L3=.FALSE.
      JD=JFC(NSTP)
      IF(JD.EQ.0)GO TO 668
      IF(KFD(NSTP).NE.99)GO TO 630
      DO 620 KFP=KS,KN
620  CALL FEDCOL(KFP,KFP)
```

```

630  IF(KFD(NSTP).NE.99)CALL FEDCOL(KFD(NSTP),KPD(NSTP))
      IF(LWR2)CALL WRIT2(KS,KN)
C
C
660  IF((JCIR.EQ.0).OR..NOT.L4) GO TO 668
      IFP=34
      L2=.TRUE.
      L3=.TRUE.
      JD=JCIR
      DO 665 KK=KS,KN
      CALL FLOW(KK,KN,NZ,NSTP,IFP)
665  CALL UPNDON(KK,KN)
      IF(LWR2)CALL WRIT2(KS,KN)
C
668  DO 670 L=1,NCP
      DO 670 IR=NRS,NRL
670  YRP3(IR,L,NCYCL)=YR(IR,L)
      DO 680 I=NRS,NRL
680  IF(NSFR(I).EQ.NSTP) CALL FDRSV(I)
C
C
      IF(LWR2)GO TO 915
      WRITE(6,601)NCYCL,((YRP1(IR,L,NCYCL),IR=NRS,NRL),L=1,NCP)
      WRITE(6,601)NCYCL,((YRP2(IR,L,NCYCL),IR=NRS,NRL),L=1,NCP)
      WRITE(6,601)NCYCL,((YRP3(IR,L,NCYCL),IR=NRS,NRL),L=1,NCP)
915  CONTINUE
C
C *** COMPLETION OF A CYCLE
C
      IF(NCYCL.LT.11)GO TO 120
      DYRP3=YRP3(NRS,1,NCYCL)-YRP3(NRS,1,NCYCL-1)
      IF(ABS(DYRP3).LT.0.00010)GO TO 918
      IF(NCYCL.LT.NFCYCL)GO TO 120
C
C *** COMPLETION OF A RUN
C
C
918  DO 921 I=1,NTS
921  IF(JFC(I).NE.0)GO TO 926
      WRITE(6,672)((IR,L,IR=NRS,NRL),L=1,NCP)
672  FORMAT(//' CYCLE',3X,14('PR(',I1,',',I1,')',1X))
      DO 922 N=1,NCYCL
922  WRITE(6,601)N,((YRP(IR,L,N),IR=NRS,NRL),L=1,NCP)
      GO TO 940
926  WRITE(6,604)((IR,L,IR=NRS,NRL),L=1,NCP)
604  FORMAT(//' CYCLE',3X,14('YP(',I1,',',I1,')',2X))
      DO 930 N=1,NCYCL
      WRITE(6,601)N,((YCPX(IR,L,N),IR=NRS,NRL),L=1,NCP)
930  WRITE(6,601)N,((YCP(IR,L,N),IR=NRS,NRL),L=1,NCP)
C
940  WRITE(6,603)
603  FORMAT(//)

```

```

WRITE(6,36) L4,L7,L9,LWR1,LWR2,KS,KN,NFCYCL
WRITE(6,61) NITV,NCP,NPHL,NTS
WRITE(6,60) HTS,AC,E,UVOLM,RANDA,B
WRITE(6,60) (VDP(I),I=1,NTS),VCIR
WRITE(6,60) (VDXTRA(II),II=1,NTS)
WRITE(6,61) (KXS(I),KXN(I),I=1,NTS)
WRITE(6,60) (VFC(II),II=1,NTS)
WRITE(6,61) (KFD(I),KPD(I),I=1,NTS)
WRITE(6,60) (VPRZ(I),I=NRS,NRL)
WRITE(6,60) (VFR(I),I=NRS,NRL)
WRITE(6,61) (NSFR(I),I=NRS,NRL)
WRITE(6,60) (VRS(I),I=NRS,NRL)
WRITE(6,59) ((AK(I,K,L),I=1,NPHL),K=1,2),L=1,NCP)
WRITE(6,59) ((YF(I,L),I=NRS,NRL),(YCO(J,L),J=KS,KN),(YR(K,L),
/K=NRS,NRL),L=1,NCP)
WRITE(6,59) (PHR(I),I=NRS,NRL),(PHCO(J),J=KS,KN),(PHL(K),K=1,NPHI
IF(L9) WRITE(6,52)
IF(.NOT.L9) WRITE(6,53)
601  FORMAT(I4,4X,14(F8.4))
GO TO 50
1000  STOP
END
C
C
C
SUBROUTINE FLOW(KF1,KF2,NZ,NSTP,IFP)
DIMENSION NZ(8)
KF3=KF2+1
IF(NSTP.NE.1)GO TO 100
IF(IFP.EQ.14)GO TO 50
NZ(1)=2
NZ(2)=3
  NZ(3)=4
RETURN
50  DO 60 K=KF1,KF3
60  NZ(K)=K+(K-2)/2
RETURN
100 IF(KF1.NE.KF2)GO TO 888
IF(NSTP.NE.2)GO TO 300
IF(IFP.EQ.24)GO TO 200
KEVE=(KF1/2)*2
IF(KF1.EQ.KEVE)GO TO 110
NZ(KF1)=KF1+1
NZ(KF1+1)=KF1
RETURN
110 NZ(KF1)=KF1+1
NZ(KF1+1)=KF1+2
RETURN
200 IF(KF1.NE.1)GO TO 230
NZ(1)=1
NZ(2)=4
RETURN

```

```

230  IF(KF1.NE.2)GO TO 888
      NZ(2)=4
      NZ(3)=4
      RETURN
300  IF(NSTP.NE.3) GO TO 888
      IF(IFP.EQ.34)GO TO 400
      KEVEN=(KF1/2)*2
      IF(KF1.EQ.KEVE)GO TO 320
      NZ(KF1)=KF1+2
      NZ(KF1+1)=KF1
      RETURN
320  NZ(KF1)=KF1
      NZ(KF1+1)=KF1+2
      RETURN
400  IF(KF1.NE.1) GO TO 430
      NZ(1)=1
      NZ(2)=3
      RETURN
430  IF(KF1.NE.2)GO TO 888
      NZ(2)=4
      NZ(3)=2
      RETURN
888  WRITE(6,6)KF1,KF2,NSTP
6    FORMAT( '/ ERROR : KF1=',I3,'      KF2=',I3,'      NSTP=',I3)
      STOP
      END

```

C
C
C

```

SUBROUTINE UPNDON(K1ST,KLST)
COMMON B,MA,NPHL,JD,JCIR,I,IFP,J,K,L,NCP,NRS,NRL,NSTP,NTS,
/NCYCL,NCYCLP,NITV,M,TCEL,E,R,RANDA,VP,AK,PHL,PHC0,PHOLD,
/PH,PHR,YOLD,XOLD,Y,X,YF,YR,YC0,YRP,YCP,YCPX,JDSP,JFC,JDXA,VDP,VFR,
/VRS,VPRZ,VDXTRA,VFC,NZ,IEX,L2,L3,L4,L7,L9,LWR1,LWR2
DIMENSION AK(3,2,2),PHL(3),PHC0(5),PHOLD(5,30),PHR(8),
/YOLD(4,16,2),XOLD(4,16,2),Y(4,16,2),X(4,16,2),YF(8,2),YR(8,2),
/YC0(5,2),YRP(4,2,177),YCP(4,2,177),YCPX(4,2,177),JFC(8),JDXA(8),
/JDSP(8),VDP(8),VFR(8),VRS(8),VPRZ(8),VDXTRA(8),VFC(8),NZ(8),IEX(8)
LOGICAL L2,L3,L4,L7,L9,LWR1,LWR2
DIMENSION VRZSB(8)
KLSTP1=KLST+1
DO 50 K=K1ST,KLST
PHOLD(K,1)=PHR(NZ(K))
IF(K.NE.K1ST)PHOLD(K-1,M)=PHOLD(K,1)
VRZSB(K)=VRS(NZ(K))
DO 50 L=1,NCP
YOLD(K,1,L)=YR(NZ(K),L)
50  IF(K.NE.K1ST)YOLD(K-1,M,L)=YOLD(K,1,L)
PHOLD(KLST,M)=PHR(NZ(KLSTP1))
DO 55 L=1,NCP
55  YOLD(KLST,M,L)=YR(NZ(KLSTP1),L)
VRZSB(KLSTP1)=VRS(NZ(KLSTP1))

```

```

CALL COLUMN(K1ST,KLST,VRZSB)
DO 850 K=K1ST,KLSTP1
VRS(NZ(K))=VRZSB(K)
IF(LWR1)WRITE(6,1)K,NZ(K),VRZSB(K),VRS(NZ(K))
1  FORMAT('  K=',I3,'      NZ(K)=',I3,5X,'  VOLRZ=',5F10.3)
DO 850 L=1,NCP
IF(K.EQ.KLSTP1)YR(NZ(KLSTP1),L)=Y(KLST,M,L)
850 IF(K.NE.KLSTP1)YR(NZ(K),L)=Y(K,1,L)
RETURN
END

```

C
C
C

```

SUBROUTINE COLUMN(K1ST,KLST,VRZSB)
COMMON B,MA,NPHL,JD,JCIR,I,IFP,J,K,L,NCP,NRS,NRL,NSTP,NTS,
/NCYCL,NCYCLP,NITV,M,TCEL,E,R,RANDA,VP,AK,PHL,PHC0,PHOLD,
/PH,PHR,YOLD,XOLD,Y,X,YF,YR,YC0,YRP,YCP,YCPX,JDSP,JFC,JDXA,VDP,VFR,
/VRZ,VPRZ,VDXTRA,VFC,NZ,IEX,L2,L3,L4,L7,L9,LWR1,LWR2
DIMENSION AK(3,2,2),PHL(3),PHC0(5),PHOLD(5,30),PH(5,30),PHR(8),
/YOLD(4,16,2),XOLD(4,16,2),Y(4,16,2),X(4,16,2),YF(8,2),YR(8,2),
/YC0(5,2),YRP(4,2,177),YCP(4,2,177),YCPX(4,2,177),JFC(8),JDXA(8),
/JDSP(8),VDP(8),VFR(8),VRS(8),VPRZ(8),VDXTRA(8),VFC(8),NZ(8),IEX(8)
LOGICAL L2,L3,L4,L7,L9,LWR1,LWR2
DIMENSION VRZSB(8)
YRCLT(VRES,VPUSH,YR,YEND)=(VRES*YR+VPUSH*YEND)/(VRES+VPUSH)
YRTNC(VRES,VPUSH,YR,YC)=(1.-VPUSH/VRES)*YR+(VPUSH/VRES)*YC
YPCLT(JFP,VPUSH,YOLD,YOUT)=((JFP-2)*VPUSH*YOLD+
9VPUSH*YOUT)/((JFP-1)*VPUSH)
PHWAVE(PHF,PHS,BB)=B*PHF+(1-B)*PHS
KLSTP1=KLST+1
DO 800 J=1,JD
DO 500 K=K1ST,KLST
DO 400 I=1,M
IF(I.NE.1)GO TO 135
DO 100 L=1,NCP
IF(L2)GO TO 95
IF(IFP.NE.11)GO TO 80
IF(K.EQ.K1ST)Y(K1ST,1,L)=YRTNC(VRZSB(K1ST),VP,YOLD(K1ST,1,L),
&YOLD(KLST,MA,L))
IF(K.NE.K1ST)Y(K,1,L)=YRTNC(VRZSB(K),VP,YOLD(K,1,L),
&YOLD(K-1,MA,L))
GO TO 100
80 IF(L3)Y(K,1,L)=YRTNC(VRZSB(K),VP,YOLD(K,1,L),
&YOLD(K,MA,L))
IF(.NOT.L3.AND.(K.EQ.K1ST))Y(K,I,L)=YOLD(K,I,L)
IF((.NOT.L3).AND.(K.NE.K1ST))Y(K,1,L)=YRTNC(VRZSB(K),VP,
&YOLD(K,1,L),YOLD(K-1,MA,L))
GO TO 100
95 IF(L3.AND.(K.NE.K1ST))Y(K,1,L)=YRTNC(VRZSB(K),VP,YOLD(K,1,L),
&YOLD(K-1,2,L))
IF(L3.AND.(K.EQ.K1ST))Y(K,1,L)=YOLD(K,1,L)
IF(.NOT.L3.AND.(K.EQ.K1ST))Y(K,1,L)=YRCLT(VRZSB(K),VP,

```

```

/YOLD(K,1,L),YOLD(K,2,L))
  IF(.NOT.L3.AND.(K.NE.K1ST))Y(K,1,L)=YRTNC(VRZSB(K),VP,
&YOLD(K,1,L),YOLD(K,2,L))
100  CONTINUE
    PH(K,1)=PHOLD(K,1)
    GO TO 400
135  IF(I.EQ.M)GO TO 220
    IF(.NOT.L2)PH(K,I)=PHWAVE(PHOLD(K,I-1),PHOLD(K,I),B)
    IF(L2)PH(K,I)=PHWAVE(PHOLD(K,I+1),PHOLD(K,I),B)
    DO 200 L=1,NCP
    IF(.NOT.L9)CALL EQCALC
200  IF(L9) CALL SOVOD1
    GO TO 400
220  CONTINUE
    IF(K.EQ.K1ST) GO TO 400
    DO 300 L=1,NCP
300  Y(K-1,M,L)=Y(K,1,L)
    PH(K-1,M)=PH(K,1)
400  CONTINUE
500  CONTINUE
    DO 550 L=1,NCP
    IF(.NOT.L2.AND.(.NOT.L3))Y(KLST,M,L)=YRCLT(VRZSB(KLSTP1),VP,
&YOLD(KLST,M,L),YOLD(KLST,MA,L))
    IF(.NOT.L2.AND.L3)Y(KLST,M,L)=YOLD(KLST,M,L)
    IF(L2.AND..NOT.L3)Y(KLST,M,L)=YOLD(KLST,M,L)
550  IF(L2.AND.L3)Y(KLST,M,L)=YRTNC(VRZSB(KLSTP1),VP,YOLD(KLST,M,L),
&YOLD(KLST,2,L))
    PH(KLST,M)=PHOLD(KLST,M)
    DO 700 K=K1ST,KLST
    DO 700 I=1,M
    DO 600 L=1,NCP
    YOLD(K,I,L)=Y(K,I,L)
600  IF((I.NE.1).AND.(I.NE.M))XOLD(K,I,L)=X(K,I,L)
    PHOLD(K,I)=PH(K,I)
700  CONTINUE
    IF((.NOT.L3).AND.(.NOT.L2))VRZSB(K1ST)=VRZSB(K1ST)-VP
    IF((.NOT.L3).AND.(.NOT.L2))VRZSB(KLSTP1)=VRZSB(KLSTP1)+VP
    IF((.NOT.L3).AND.L2)VRZSB(K1ST)=VRZSB(K1ST)+VP
    IF((.NOT.L3).AND.L2)VRZSB(KLSTP1)=VRZSB(KLSTP1)-VP
    IF(LWR1)WRITE(6,6615)(I,I=1,M)
    DO 730 K=K1ST,KLST
730  IF(LWR1)WRITE(6,6620)J,K,(PH(K,I),I=1,M)
    DO 760 L=1,NCP
    DO 760 K=K1ST,KLST
    IF(LWR1)WRITE(6,6621)J,K,L,(Y(K,I,L),I=1,M)
760  IF(LWR1)WRITE(6,6622)J,K,L,(X(K,I,L),I=1,M)
800  CONTINUE
6615  FORMAT(/,' J K L ',14(4X,'I=',I2))
6620  FORMAT(' ',2I2,' PH',14F8.4)
6621  FORMAT(' ',3I2,' Y',14F8.4)
6622  FORMAT(' ',3I2,' X',14F8.4)
RETURN

```

END

C
C
C

```

SUBROUTINE FEDCOL(KF,KP)
COMMON B,MA,NPHL,JD,JCIR,I,IFP,J,K,L,NCP,NRS,NRL,NSTP,NTS,
/NCYCL,NCYCLP,NITV,M,TCEL,E,R,RANDA,VP,AK,PHL,PHC0,PHOLD,
/PH,PHR,YOLD,XOLD,Y,X,YF,YR,YC0,YRP,YCP,YCPX,JDSP,JFC,JDXA,VDP,VFR,
/VRS,VPRZ,VDXTRA,VFC,NZ,IEX,L2,L3,L4,L7,L9,LWR1,LWR2
DIMENSION AK(3,2,2),PHL(3),PHC0(5),PHOLD(5,30),PH(5,30),PHR(8),
/YOLD(4,16,2),XOLD(4,16,2),Y(4,16,2),X(4,16,2),YF(8,2),YR(8,2),
/YC0(5,2),YRP(4,2,177),YCP(4,2,177),YCPX(4,2,177),JFC(8),JDXA(8),
/JDSP(8),VDP(8),VFR(8),VRS(8),VPRZ(8),VDXTRA(8),VFC(8),NZ(8),IEX(8)
LOGICAL L2,L3,L4,L7,L9,LWR1,LWR2
DIMENSION VRZSB(8)
KFP1=KF+1
KPP1=KP+1
IF(.NOT.L2)GO TO 600
DO 60 L=1,NCP
YOLD(KP,1,L)=0.
60 YOLD(KF,M,L)=YF(NZ(KP),L)
VRZSB(KP)=0.
VRZSB(KFP1)=999
PHOLD(KP,1)=PHR(NZ(KP))
PHOLD(KF,M)=PHR(NZ(KF))
IF(KPP1.GT.KF)GO TO 205
DO 200 K=KPP1,KF
PHOLD(K,1)=PHR(NZ(K))
PHOLD(K-1,M)=PHOLD(K,1)
VRZSB(K)=VRS(NZ(K))
DO 200 L=1,NCP
200 YOLD(K,1,L)=YR(NZ(K),L)
205 YOLD(K-1,M,L)=YR(NZ(K),L)
CONTINUE
CALL COLUMN(KP,KF,VRZSB)
DO 240 L=1,NCP
IF(NSTP.LE.2)YCPX(NZ(KP),L,NCYCL)=Y(KP,1,L)
240 IF(NSTP.GE.3)YCP(NZ(KP),L,NCYCL)=Y(KP,1,L)
IF(KPP1.GT.KF)GO TO 465
DO 460 K=KPP1,KF
VRS(NZ(K))=VRZSB(K)
DO 460 L=1,NCP
460 YR(NZ(K),L)=Y(K,1,L)
465 CONTINUE
RETURN
600 DO 660 L=1,NCP
YOLD(KP,M,L)=0.
660 YOLD(KF,1,L)=YF(NZ(KP),L)
VRZSB(KPP1)=0.
VRZSB(KF)=999
PHOLD(KP,M)=PHR(NZ(KP+1))
PHOLD(KF,1)=PHR(NZ(KFP1))

```



```

IF(KFPL.GT.KP)GO TO 705
DO 700 K=KFPL,KP
PHOLD(K,1)=PHR(NZ(K))
PHOLD(K-1,M)=PHOLD(K,1)
VRZSB(K)=VRS(NZ(K))
DO 700 L=1,NCP
YOLD(K,1,L)=YR(NZ(K),L)
700 YOLD(K-1,M,L)=YR(NZ(K),L)
705 CONTINUE
CALL COLUMN(KF,KP,VRZSB)
DO 740 L=1,NCP
IF(NSTP.LE.2)YCPX(NZ(KPPL),L,NCYCL)=Y(KP,M,L)
740 IF(NSTP.GE.3)YCP(NZ(KPPL),L,NCYCL)=Y(KP,M,L)
IF(KFPL.GT.KP)GO TO 800
DO 760 K=KFPL,KP
VRS(NZ(K))=VRZSB(K)
DO 760 L=1,NCP
760 YR(NZ(K),L)=Y(K,1,L)
800 CONTINUE
RETURN
END

```

C
CC
C
C
C

```

SUBROUTINE SOVOD1
COMMON B,MA,NPHL,JD,JCIR,I,IFP,J,K,L,NCP,NRS,NRL,NSTP,NTS,
/NCYCL,NCYCLP,NITV,M,TCEL,E,R,RANDA,VP,AK,PHL,PHCO,PHOLD,
/PH,PHR,YOLD,XOLD,Y,X,YF,YR,YC0,YRP,YCP,YCPX,JDSP,JFC,JDXA,VDP,VFR,
/VRS,VPRZ,VDXTRA,VFC,NZ,IEX,L2,L3,L4,L7,L9,LWR1,LWR2
DIMENSION AK(3,2,2),PHL(3),PHCO(5),PHOLD(5,30),PH(5,30),PHR(8),
/YOLD(4,16,2),XOLD(4,16,2),Y(4,16,2),X(4,16,2),YF(8,2),YR(8,2),
/YC0(5,2),YRP(4,2,177),YCP(4,2,177),YCPX(4,2,177),JFC(8),JDXA(8),
/JDSP(8),VDP(8),VFR(8),VRS(8),VPRZ(8),VDXTRA(8),VFC(8),NZ(8),IEX(8)
LOGICAL L2,L3,L4,L7,L9,LWR1,LWR2
FMSBS(YPF,XPF,XF,EF)=YPF-((1.-EF)/EF)* (XF-XPF)
IF(PH(K,I)-PHL(2))30,40,40
30 AAK=AK(3,IEX(K),L)+(AK(2,IEX(K),L)-AK(3,IEX(K),L))*
&(PH(K,I)-PHL(3))/(PHL(2)-PHL(3))
GO TO 45
40 AAK=AK(2,IEX(K),L)+(AK(1,IEX(K),L)-AK(2,IEX(K),L))*
&(PH(K,I)-PHL(2))/(PHL(1)-PHL(2))
45 IF(.NOT.L2)YPSV=YOLD(K,I-1,L)
IF(L2) YPSV=YOLD(K,I+1,L)
XPSV=XOLD(K,I,L)
AA=RANDA*(YPSV+(1-E)/E)*XPSV)
BB=RANDA*((1-E)/E+1/AA)
BTNEG=(-1)*BB*TCEL
X(K,I,L)=(AA/BB)-(AA/BB-XPSV)*EXP(BTNEG)
Y(K,I,L)=FMSBS(YPSV,XPSV,X(K,I,L),E)
RETURN

```

END

C
C
C

SUBROUTINE EQCALC

```

COMMON B,MA,NPHL,JD,JCIR,I,IFP,J,K,L,NCP,NRS,NRL,NSTP,NTS,
/NCYCL,NCYCLP,NITV,M,TCEL,E,R,RANDA,VP,AK,PHL,PHC0,PHOLD,
/PH,PHR,YOLD,XOLD,Y,X,YF,YR,YC0,YRP,YCP,YCPX,JDSP,JFC,JDXA,VDP,VFR,
/VRS,VPRZ,VDXTRA,VFC,NZ,IEX,L2,L3,L4,L7,L9,LWR1,LWR2
DIMENSION AK(3,2,2),PHL(3),PHC0(5),PHOLD(5,30),PH(5,30),PHR(8),
/YOLD(4,16,2),XOLD(4,16,2),Y(4,16,2),X(4,16,2),YF(8,2),YR(8,2),
/YC0(5,2),YRP(4,2,177),YCP(4,2,177),YCPX(4,2,177),JFC(8),JDXA(8),
/JDSP(8),VDP(8),VFR(8),VRS(8),VPRZ(8),VDXTRA(8),VFC(8),NZ(8),IEX(8)
LOGICAL L2,L3,L4,L7,L9,LWR1,LWR2
IF(PH(K,I)-PHL(2))30,40,40
30 AKD=AK(3,IEX(K),L)+(AK(2,IEX(K),L)-AK(3,IEX(K),L))*
&(PH(K,I)-PHL(3))/(PHL(2)-PHL(3))
GO TO 45
40 AKD=AK(2,IEX(K),L)+(AK(1,IEX(K),L)-AK(2,IEX(K),L))*
&(PH(K,I)-PHL(2))/(PHL(1)-PHL(2))
45 IF(PHOLD(K,I)-PHL(2))50,60,60
50 AKN=AK(3,IEX(K),L)+(AK(2,IEX(K),L)-AK(3,IEX(K),L))*
&(PHOLD(K,I)-PHL(3))/(PHL(2)-PHL(3))
GO TO 65
60 AKN=AK(2,IEX(K),L)+(AK(1,IEX(K),L)-AK(2,IEX(K),L))*
&(PHOLD(K,I)-PHL(2))/(PHL(1)-PHL(2))
65 IF(L2)YIJO=YOLD(K,I+1,L)
IF(.NOT.L2)YIJO=YOLD(K,I-1,L)
Y(K,I,L)=(YIJO+R*AKN*YOLD(K,I,L))/(1+R*AKD)
X(K,I,L)=Y(K,I,L)*AKD
RETURN
END
```

C
C
C

SUBROUTINE WRIT2(KS,KN)

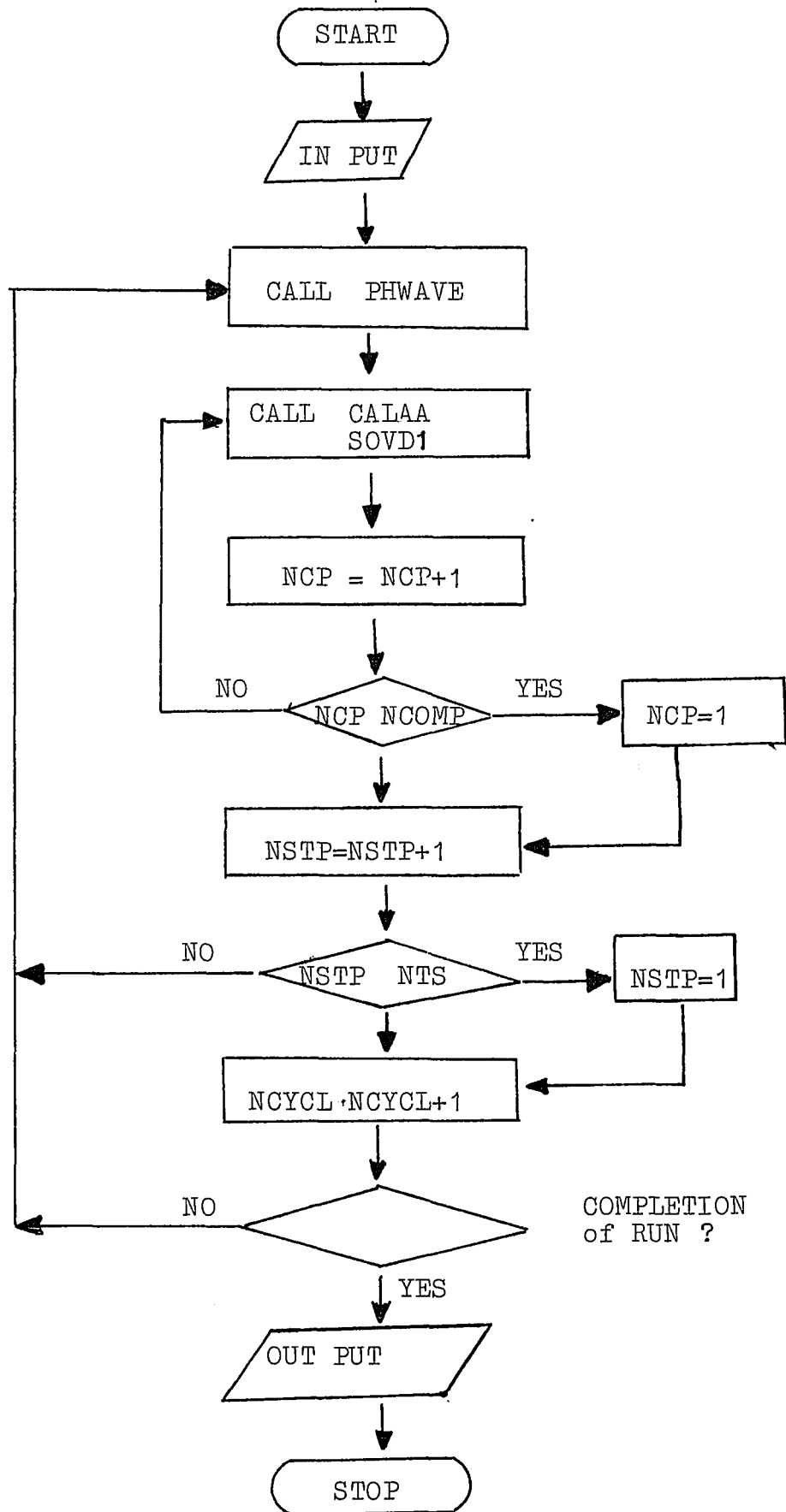
```

COMMON B,MA,NPHL,JD,JCIR,I,IFP,J,K,L,NCP,NRS,NRL,NSTP,NTS,
/NCYCL,NCYCLP,NITV,M,TCEL,E,R,RANDA,VP,AK,PHL,PHC0,PHOLD,
/PH,PHR,YOLD,XOLD,Y,X,YF,YR,YC0,YRP,YCP,YCPX,JDSP,JFC,JDXA,VDP,VFR,
/VRS,VPRZ,VDXTRA,VFC,NZ,IEX,L2,L3,L4,L7,L9,LWR1,LWR2
DIMENSION AK(3,2,2),PHL(3),PHC0(5),PHOLD(5,30),PH(5,30),PHR(8),
/YOLD(4,16,2),XOLD(4,16,2),Y(4,16,2),X(4,16,2),YF(8,2),YR(8,2),
/YC0(5,2),YRP(4,2,177),YCP(4,2,177),YCPX(4,2,177),JFC(8),JDXA(8),
/JDSP(8),VDP(8),VFR(8),VRS(8),VPRZ(8),VDXTRA(8),VFC(8),NZ(8),IEX(8)
LOGICAL L2,L3,L4,L7,L9,LWR1,LWR2
KNP1=KN+1
WRITE(6,610)NCYCL,NSTP,IFP,(KW,NZ(KW),KW=KS,KNP1)
WRITE(6,620)(I,I=NRS,NRL)
WRITE(6,630)(VRS(I),I=NRS,NRL)
DO 11 L=1,NCP
11 WRITE(6,640)L,(YR(K,L),K=NRS,NRL)
WRITE(6,630)(PHR(I),I=NRS,NRL)
```

```

WRITE(6,650)(I,I=1,M)
DO 730 K=KS,KN
730 WRITE(6,660)J,K,(PH(K,I),I=1,M)
DO 760 L=1,NCP
DO 760 K=KS,KN
WRITE(6,670)J,K,L,(Y(K,I,L),I=1,M)
760 WRITE(6,680)J,K,L,(X(K,I,L),I=1,M)
650 FORMAT(/,' J K L ',14(4X,'I=',I2))
660 FORMAT(' ',2I2,' PH',14F8.4)
670 FORMAT(' ',3I2,' Y',14F8.4)
680 FORMAT(' ',3I2,' X',14F8.4)
C
610 FORMAT(/10X,' NCYCL=',I3,5X,'NSTP=',I3,5X,'IFP=',I3,5X,'NZ(',
&5(I1,')=',I2,5X,'NZ('))
620 FORMAT(10X,10(' RSV(',I1,')'))
630 FORMAT(10X,11F10.4)
640 FORMAT(' COMP=',I2,2X,10F10.4)
C
C
RETURN
END
SUBROUTINE FDRSV(IR)
COMMON B,MA,NPHL,JD,JCIR,I,IFP,J,K,L,NCP,NRS,NRL,NSTP,NTS,
/NCYCL,NCYCLP,NITV,M,TCEL,E,R,RANDA,VP,AK,PHL,PHC0,PHOLD,
/PH,PHR,YOLD,XOLD,Y,X,YF,YR,YC0,YRP,YCP,YCPX,JDSP,JFC,JDXA,VDP,VFR,
/VRS,VPRZ,VDXTRA,VFC,NZ,IEX,L2,L3,L4,L7,L9,LWR1,LWR2
DIMENSION AK(3,2,2),PHL(3),PHC0(5),PHOLD(5,30),PH(5,30),PHR(8),
/YOLD(4,16,2),XOLD(4,16,2),Y(4,16,2),X(4,16,2),YF(8,2),YR(8,2),
/YC0(5,2),YRP(4,2,177),YCP(4,2,177),YCPX(4,2,177),JFC(8),JDXA(8),
/JDSP(8),VDP(8),VFR(8),VRS(8),VPRZ(8),VDXTRA(8),VFC(8),NZ(8),IEX(8)
C
DO 20 L=1,NCP
20 YRP(IR,L,NCYCL)=YR(IR,L)
VRS(IR)=VRS(IR)-VPRZ(IR)
IF(VFR(IR).EQ.0.)GO TO 50
DO 30 L=1,NCP
30 YR(IR,L)=(YR(IR,L)*VRS(IR)+VFR(IR)*YF(IR,L))/(VRS(IR)+VFR(IR))
VRS(IR)=VRS(IR)+VFR(IR)
50 CONTINUE
RETURN
END

```



APPENDIX-B FORTRAN PROGRAM Z2C

```

C   Z2C : CYCLIC ZON USE PHWAVE MODEL
C   LAST REVISION : OCT.7/80
C
C   L1=F:  FIRST HALF CYCLE
C   L2=T:  SECOND HALF CYCLE
C
COMMON B,MA,AK,PHL,PH,Y,VP, YT,YB, NITV ,L,
/FIT,FIB,JF1,JF2, NTF,NBF,I,J ,RANDA,NCYCL,NCYCLP,HTS,AC,
/JD,M,TCEL,YF1,YF2,X, E ,L1, L2, L3 ,L7,L9
DIMENSION Y(2,37,66),PH(37,66),AK(2,3),PHL(3),
/X(2,37,66),YEXT(2,588),YPD(2,133),YP(2),VPD(133),
/PHEXT(588),SPNO(277),YSMP(2,277),XODPT(588),PHEPT(588),
&YE1PT(588),YE2PT(588),VEXT(588)
LOGICAL L1, L2, L3, L5 ,L7,L9 ,L10
EQUIVALENCE (YE1PT(1),YE2PT(1),PHEPT(1)),(XODPT(1),VEXT(1))
PHWAVE(PHF,PHS,B,C,D)=PHF*B*(1.-ABS(PHF-D)*C)+
&PHS*(1.-B*(1.-ABS(PHF-D)*C))
22  READ (5,36) L7,L9,NITV,NFINAL,NCPLLOT,NCOMP,IH0
IF( NITV .EQ. 0) GO TO 997
READ(5,60)VF1,VF2,VF3,VSMP,YF1,YF2,YF3,YCLMO
READ(5,60)((AK(L,IH),IH=1,3),L=1,NCOMP)
READ(5,60)(PHL(IH),IH=1,3)
50  CONTINUE
READ(5,60)E,HTS,AC,UVOLM,RANDA,B,CBF,DPH
IF( E .EQ.0.) GO TO 22
VBED=HTS*AC
WRITE(6,30)
30  FORMAT ('1')
36  FORMAT( 2L10,6I10 )
60  FORMAT(8F10.4)
IF(L9) WRITE(6,52)
IF(.NOT.L9) WRITE(6,53)
52  FORMAT ('0      THEORY : FINITE MASS TRANSFER, NON-EQUILIBRIUM,
/ INTEGRAL METHODE ')
53  FORMAT ('0      THEORY : EQUILIBRIUM')
WRITE(6,59)
59  FORMAT('0',7X,'L7',8X,'L9',6X,'NITV',4X,'NFINAL',4X,'NCPLLOT',5X,
&'NCOMP',5X,'IH0')
WRITE(6,36) L7,L9,NITV,NFINAL,NCPLLOT,NCOMP,IH0
WRITE(6,62)
62  FORMAT('0',5X,'VF1',7X,'VF2',7X,'VF3',6X,'VSMP',7X,'YF1',7X,
&'YF2',7X,'YF3',6X,'YCLMO')
WRITE(6,60)VF1,VF2,VF3,VSMP,YF1,YF2,YF3,YCLMO
WRITE(6,66)
65  FORMAT('0',5X,'PH1',7X,'PH2',7X,'PH3')
66  FORMAT('0',5X,'KHM1',6X,'KHM2',6X,'KHM3',6X,'KAB1',6X,'KAB2',
&6X,'KAB3')
WRITE(6,60)((AK(L,IH),IH=1,3),L=1,NCOMP)
WRITE(6,65)

```

```

WRITE(6,60) (PHL(IH), IH=1,3)
WRITE(6,64)
64  FORMAT('0',7X,'E',7X,'HTS',7X,'AC',8X,'UVOLM',5X,'RANDA',5X,
&'B',9X,'CBF',7X,'DPH')
WRITE(6,60) E,HTS,AC,UVOLM,RANDA,B,CBF,DPH
ULIN = UVOLM/(AC*E)
HTCEL=HTS/NITV
TCEL=HTCEL/ULIN
VP=VBED*E/NITV
R=(1-E)/E
M=NITV+2
MA=M-1
MB=M-2
JF2 = VF2/VP + 1
JF1 =VF1/VP + 1
JF3=VF3/VP +1
IF(L7)WRITE(6,82)
82  FORMAT ('0',5X,'VP',8X,'R',9X,'HTCEL',5X,'TCEL', 6X,'VBED')
IF(L7)WRITE(6,60) VP,R,HTCEL,TCEL,VBED
IF(L7)WRITE(6,84)
84  FORMAT('0',8X,'M',9X,'MA',8X,'JF1',7X,'JF2',7X,'JF3')
IF(L7)WRITE(6,80) M,MA,JF1,JF2,JF3
IF(L7) WRITE (6,88)
88  FORMAT ('0',5X, 'DETAIL PRINT : YES ' )
IF ( .NOT. L7 ) WRITE( 6,89 )
89  FORMAT ('0',5X, 'DETAIL PRINT : NO ' )
33  CONTINUE
DO 111 I=2,M
PH(I,1)=PHL(IH0)
DO 106 L=1,NCOMP
Y(L,I,1)=YCLMO
106  X(L,I,1)=YCLMO*AK(L,IH0)
111  CONTINUE
JMAX=JF3
IF(JF2.GT.JMAX)JMAX=JF2
IF(JF3.GT.JMAX)JMAX=JF3
DO 115 L=1,NCOMP
DO 115 J=1,JMAX
X(L,1, J) =0.
X(L,M, J) =0.
115  CONTINUE
IF(L7)WRITE(6,686)
IF((NITV.GT.12).AND.L7) WRITE(6,187)
IF(L7)WRITE(6,661) (PH(I,1),I=1,M)
DO 116 L=1,NCOMP
IF(L7)WRITE(6,663)L,(Y(L,I,1),I=1,M)
116  IF(L9.AND.L7)WRITE(6,189) (X(L,I,1),I=1,M)
JD=JF1
NSTP=1
NPD=0
NSAMPL=0
DO 118 L=1,NCOMP

```

```

118  YP(L)=1.
      YEXT(L,1)=1.
      PHEXT(1)=PHL(3)
      VEXT(1)=0.
      NCYCL=0
120  NCYCL=NCYCL+1
      IF(NCYCL.GT.NFINAL) GO TO 300
      IF(L7)WRITE(6,645)NCYCL
      IF(L7)WRITE(6,686)
      IF((NITV.GT.12).AND.L7) WRITE(6,187)
125  CONTINUE
      DO 183 J=1, JD
      IF(NSTP.EQ.1)PH(1,J)=PHL(1)
      IF(NSTP.EQ.2)PH(1,J)=PHL(2)
      IF(NSTP.EQ.3)PH(1,J)=PHL(3)
      DO 128 L=1, NCOMP
      IF(NSTP.EQ.1)Y(L,1,J)=YF1
      IF(NSTP.EQ.2)Y(L,1,J)=YF2
128  IF(NSTP.EQ.3)Y(L,1,J)=YF3
      IF(J.EQ.1) GO TO 183
      DO 131 I=2, MA
      PHO=PH(I,J-1)
      PH(I,J)=PHWAVE(PH(I-1,J-1),PH(I,J-1),B,CBF,DPH)
      DO 130 L=1, NCOMP
      IF(.NOT.L9)Y(L,I,J)=CALAA(R,AK(L,1),AK(L,2),AK(L,3),Y(L,I-1,J-1),
&Y(L,I,J-1),PHO,PH(I,J),PHL(1),PHL(2),PHL(3))
      IF(L9) CALL SOVOD1
130  CONTINUE
131  CONTINUE
      PH(M,J)=PH(MA,J-1)
      DO 133 L=1, NCOMP
133  Y(L,M,J)=Y(L,MA,J-1)
      L10=(Y(1,M,J-1).GE.Y(2,M,J-1).AND.Y(1,M,J).LT.Y(2,M,J)).OR.
&(Y(1,M,J-1).LT.Y(2,M,J-1).AND.Y(1,M,J).GE.Y(2,M,J))
      IF(.NOT.L10) GO TO 150
      NPD=NPD+1
      VPD(NPD)=NSAMPL*VP
      DO 140 L=1, NCOMP
      YPD(L,NPD)=YP(L)
140  YP(L)=0.
      NSAMPL=0
150  NSAMPL=NSAMPL+1
      DO 152 L=1, NCOMP
152  YP(L)=(Y(L,M,J)+(NSAMPL-1)*YP(L))/NSAMPL
      IF(NSTP.EQ.1)NTE=(NCYCL-1)*(JF1+JF2+JF3-3)+J
      IF(NSTP.EQ.2)NTE=(NCYCL-1)*(JF1+JF2+JF3-3)+JF1-1+J
      IF(NSTP.EQ.3)NTE=(NCYCL-1)*(JF1+JF2+JF3-3)+JF2+JF1-2+J
      DO 160 L=1, NCOMP
160  YEXT(L,NTE)=Y(L,M,J)
      PHEXT(NTE)=PH(M,J)
      VEXT(NTE)=(NTE-1)*VP
      IF(L7)WRITE(6,661)(PH(I,J),I=1,M)

```

```

DO 167 L=1, NCOMP
IF(L7)WRITE(6,663)L,(Y(L,I,J),I=1,M)
167 IF(L9.AND.L7)WRITE(6,189)(X(L,I,J),I=1,M)
183 CONTINUE
DO 186 I=2,M
DO 184 L=1, NCOMP
IF(L9) X(L,I,1)=X(L,I,JD)
184 Y(L,I,1)=Y(L,I,JD)
186 PH(I,1)=PH(I,JD)
NSTP=NSTP+1
IF(NSTP.GE.4)NSTP=NSTP-3
IF(NSTP.EQ.2) JD=JF2
IF(NSTP.EQ.3) JD=JF3
IF(NSTP.NE.1)GO TO 125
JD=JF1
GO TO 120
300 LINE1=NTE/3
IF(NTE.GT.(3*LINE1)) LINE1=LINE1+1
WRITE(6,355)
355 FORMAT(///,1X,3(' VOL. ELT',3X,'PHEXT',5X,'YEX(1)',4X,'YEX(2)'))
DO 360 I=1,LINE1
360 WRITE(6,470) (VEXT(II),PHEXT(II),(YEXT(L,II),L=1,NCOMP),
&II=I,NTE,LINE1)
470 FORMAT(' ',3(F10.2,3F10.4))
WRITE(6,475)
475 FORMAT(///,3(8X,'I',6X,'YPD1',6X,'YPD2',7X,'VPD ') )
LINE2=NPD/3
IF(NPD.GT.(3*LINE2)) LINE2=LINE2+1
IF(LINE2.LT.1) GO TO 492
DO 480 I=1,LINE2
480 WRITE(6,490) (II,(YPD(L,II),L=1,NCOMP),VPD(II),II=I,NPD,LINE2)
490 FORMAT(' ',3(I8,2X,3F10.4))
492 JSMP=VSMP/VP
NSMP=NTE/JSMP
DO 550 I=JSMP,NTE,JSMP
K=I/JSMP
SPNO(K)=I*VP
DO 550 L=1, NCOMP
SUMYS=0.
DO 540 II=1,JSMP
540 SUMYS=SUMYS+YEXT(L,I-II+1)
550 YSMP(L,K)=SUMYS/JSMP
WRITE(6,555)
555 FORMAT(///,1X,4(' NO. SAMPL',3X,'YSMP 1',4X,'YSMP 2'))
LINE3=NSMP/4
IF(NSMP.GT.(LINE3*4))LINE3=LINE3+1
DO 560 I=1,LINE3
560 WRITE(6,570) (SPNO(II),(YSMP(L,II),L=1,NCOMP),II=I,NSMP,LINE3)
570 FORMAT(' ',12(F10.4))
IF(L9) WRITE(6,52)
IF(.NOT.L9) WRITE(6,53)
WRITE(6,59)

```



```

WRITE(6,36) L7,L9,NITV,NFINAL,NCPLT,NCOMP,IH0
WRITE(6,62)
WRITE(6,60)VF1,VF2,VF3,VSMP,YF1,YF2,YF3,YCLMO
WRITE(6,66)
WRITE(6,60)((AK(L,IH),IH=1,3),L=1,NCOMP)
WRITE(6,65)
WRITE(6,60)(PHL(IH),IH=1,3)
WRITE(6,64)
WRITE(6,60)E,HTS,AC,UVOLM,RANDA,B,CBF,DPH
600 CONTINUE
80 FORMAT('0',12I10)
686 FORMAT(' I= ',1',7X,'2',7X,'3',7X,'4',7X,'5',7X,'6',7X,'7',7X,
/'8',7X,'9',6X,'10',6X,'11',6X,'12',6X,'13',6X,'14' )
187 FORMAT(' I= ',15',6X,'16',6X,'17',6X,'18',6X,'19',6X,'20',6X,
/'21',6X,'22',6X,'23',6X,'24',6X,'25',6X,'26',6X,'27',6X,'28' )
663 FORMAT (' Y',I1,'=',14F8.3)
661 FORMAT (/,' PH=',14F8.3)
189 FORMAT (' X=',14F8.4)
IF(NCPLT.LE.0)GO TO 50
NCOMT=NFINAL-NCPLT
NPTOMT=NCOMT*(JF1+JF2-2)
NPTACT=NTE-NPTOMT
DO 710 I=1,NPTACT
XODPT(I)=VEXT(I+NPTOMT)
710 PHEPT(I)=PHEXT(I+NPTOMT)
WRITE(6,632)
CALL XYPLOT(NPTACT,XODPT,PHEPT)
WRITE(6,631)
DO 720 I=1,NPTACT
YE1PT(I)=YEXT(1,I+NPTOMT)
720 CALL XYPLOT(NPTACT,XODPT,YE1PT)
WRITE(6,634)
DO 730 I=1,NPTACT
YE2PT(I)=YEXT(2,I+NPTOMT)
730 CALL XYPLOT(NPTACT,XODPT,YE2PT)
WRITE(6,633)
CALL XYPLOT(NSMP,SPNO,YSMP)
GO TO 50
631 FORMAT('1 *** COMP 1 CONCENTRATION WAVE')
634 FORMAT('1 *** COMP 2 CONCENTRATION WAVE')
632 FORMAT('1 *** PH WAVE')
633 FORMAT('1 *** WAVE OF SAMPLE CONC.')
645 FORMAT('0 NCYCL=',I3)
997 STOP
END

```

C
C

```

FUNCTION CALAA(R,AK1,AK2,AK3,YIJO,YJO,PHO,PH,PH1,PH2,PH3)
IF(PH1.LT.PH2)GO TO 50
IF(PH.GT.PH2)AKD=AK1+(PH-PH1)*(AK2-AK1)/(PH2-PH1)
IF(PHO.GT.PH2)AKN=AK1+(PHO-PH1)*(AK2-AK1)/(PH2-PH1)
IF(PH.LE.PH2)AKD=AK3+(PH-PH3)*(AK2-AK3)/(PH2-PH3)

```

```

IF (PHO.LE.PH2)AKN=AK3+(PHO-PH3)*(AK2-AK3)/(PH2-PH3)
CALAA=(YIJO+R*AKN*YJO)/(1+R*AKD)
RETURN
50 IF (PH.LT.PH2)AKD=AK1+(PH-PH1)*(AK2-AK1)/(PH2-PH1)
IF (PHO.LT.PH2)AKN=AK1+(PHO-PH1)*(AK2-AK1)/(PH2-PH1)
IF (PH.GE.PH2)AKD=AK3+(PH-PH3)*(AK2-AK3)/(PH2-PH3)
IF (PHO.GE.PH2)AKN=AK3+(PHO-PH3)*(AK2-AK3)/(PH2-PH3)
CALAA=(YIJO+R*AKN*YJO)/(1+R*AKD)
RETURN
END

```

C
C

```

SUBROUTINE SOVOD1
COMMON B,MA,AK,PHL,PH,Y,VP, YT,YB, NITV ,L,
/FIT,FIB,JF1,JF2, NTF,NBF,I,J ,RANDA,NCYCL,NCYCLP,HTS,AC,
/JD,M,TCEL,YF1,YF2,X, E ,L1, L2, L3 ,L7,L9
LOGICAL L1, L2, L3, L7
DIMENSION Y(2,37,66),PH(37,66),AK(2,3),PHL(3),
/X(2,37,66)
FMSBS(YPF, XPF,XF,EF )= YPF-((1.-EF)/EF) * (XF-XPF)
PHSV=PH(I,J)
IF (PHSV.GE.PHL(2))AAK=AK(L,2)+(PHSV-PHL(2))*(AK(L,1)-AK(L,2))/
&(PHL(1)-PHL(2))
IF (PHSV.LT.PHL(2))AAK=AK(L,2)+(PHSV-PHL(2))*(AK(L,3)-AK(L,2))/
&(PHL(3)-PHL(2))
YPSV=Y(L,I-1,J-1)
XPSV=X(L,I,J-1)
AA=RANDA*( YPSV + ((1-E)/E) * XPSV )
BB=RANDA*((1-E)/E + 1/AAK )
BTNEG=(-1)*BB*TCEL
X(L,I,J)=(AA/BB) - (AA/BB - XPSV) * EXP(BTNEG)
Y(L,I,J) =FMSBS(YPSV,XPSV,X(L,I,J) ,E )
RETURN
END

```

C
C

```

C SUBROUTINE XYPLOT
C:0664 TEMP.PUNCH CC05348 07/13/79 CCDP010

```

```

SUBROUTINE XYPLOT(N,X,Y)
INTEGER*4 PA,PB
LOGICAL*1 STAR,BLANK,PLUS,BAR,HYPHEN,GRAPH(111,51),L(5)
REAL*4 X(N),Y(N),XSCALE(12),YSCALE(6)
EQUIVALENCE (STAR,L(1)),(BLANK,L(2)),(PLUS,L(3))
EQUIVALENCE (BAR,L(4)),(HYPHEN,L(5)),(PA,L(1)),(PB,L(5))
DATA PA/'* +|'/,PB/'-???'/
IF(N.LT.2) RETURN

```

C
C
C

```

INITIALIZE GRID TO BLANKS

DO 1010 J=1,51
DO 1000 I=1,111
GRAPH(I,J)=BLANK

```

```

1000 CONTINUE
1010 CONTINUE
C
C   SETUP HORIZ GRID
C
      DO 1030 J=1,51,10
        DO 1020 I=1,111
          GRAPH(I,J)=HYPHEN
1020 CONTINUE
1030 CONTINUE
C
C   SETUP VERT GRID
C
      DO 1050 I=1,111,10
        DO 1040 J=1,51
          GRAPH(I,J)=BAR
1040 CONTINUE
1050 CONTINUE
C
C   SETUP GRID CROSSINGS
C
      DO 1070 I=1,111,10
        DO 1060 J=1,51,10
          GRAPH(I,J)=PLUS
1060 CONTINUE
1070 CONTINUE
C
C   CALC SCALE FACTORS
C
      XMAX=X(1)
      XMIN=X(1)
      YMAX=Y(1)
      YMIN=Y(1)
      DO 1080 I=2,N
        XMAX=AMAX1(XMAX,X(I))
        XMIN=AMIN1(XMIN,X(I))
        YMAX=AMAX1(YMAX,Y(I))
        YMIN=AMIN1(YMIN,Y(I))
1080 CONTINUE
      DELX=(XMAX-XMIN)/11.
      DELY=(YMAX-YMIN)/5.
      IF(DELX.LT.0.1E-55) DELX=0.1E-55
      IF(DELY.LT.0.1E-55) DELY=0.1E-55
      DO 1090 I=1,6
        YSCALE(I)=YMAX-DELY*(I-1)
1090 CONTINUE
      DO 1100 I=1,12
        XSCALE(I)=XMIN+DELX*(I-1)
1100 CONTINUE
C
C   SET AXIS (IF NEEDED)
C

```

```

IF( (ABS(YMAX)+ABS(YMIN)-ABS(YMAX+YMIN)).EQ.0.0) GOTO 1120
  J=51-INT((-YMIN)/(YMAX-YMIN)*50.)
  DO 1110 I=1,111
    GRAPH(I,J)=PLUS
1110  CONTINUE
1120 CONTINUE
IF( (ABS(XMAX)+ABS(XMIN)-ABS(XMAX+XMIN)).EQ.0.0) GOTO 1140
  I=INT((-XMIN)/(XMAX-XMIN)*110.)+1
  DO 1130 J=1,51
    GRAPH(I,J)=PLUS
1130  CONTINUE
1140 CONTINUE
C
C  PLOT CURVE IN GRID
C
DELX=(XMAX-XMIN)/110.
DELY=(YMAX-YMIN)/50.
IF(DELX.LT.0.1E-55) DELX=0.1E-55
IF(DELY.LT.0.1E-55) DELY=0.1E-55
DO 1150 K=1,N
  I=INT((X(K)-XMIN)/DELX)+1
  J=51-INT((Y(K)-YMIN)/DELY)
  GRAPH(I,J)=STAR
1150 CONTINUE
C
C  PRINT GRAPH AND SCALE LABELS
C
DO 1170 K=1,5
  J=(K-1)*10+1
  WRITE(6,1180) YSCALE(K), (GRAPH(I,J),I=1,111)
  JJJ=J+1
  NN=J+9
  DO 1160 JJ=JJJ,NN
    WRITE(6,1190) (GRAPH(I,JJ),I=1,111)
1160  CONTINUE
1170 CONTINUE
  WRITE(6,1200) YSCALE(6), (GRAPH(I,51),I=1,111),
  % (XSCALE(I),I=1,11,2), (XSCALE(I),I=2,12,2)
  RETURN
1180 FORMAT(4X,G11.4,1X,'-',111A1)
1190 FORMAT(17X,111A1)
1200 FORMAT(4X,G11.4,1X,'-',111A1,/,11X,6(G11.4,9X),
  % /,12X,6(9X,G11.4))
  END

```

BIBLIOGRAPHY

1. Baker, B., and R. L. Pigford, "Cycling Zone Adsorption: Quantitative Theory and Experimental Results," *Ind. Eng. Chem. Fundam.*, 10, 288 (1971).
2. Blum, D.E., "Cycling Zone Adsorption, Separation of Gas Mixture" PhD Thesis, Univ. California-Berkeley (1971).
3. Breck, "Zeolite Molecular Sieves, Structure, Chemistry & Use," N.Y.: Wiley (1974).
4. Busbice, M.E., and P.C. Wankat, "pH Cyclic Zone Separation of Sugars," *J. Chromatog.*, 114, 369 (1975).
5. Chen, H.T., J.L. Rak, J.D. Stoke, and F.B. Hill "Separation via Continuous Parametric Pumping," *AIChE J.*, 18, 356 (1972).
6. Chen, H.T., E.H. Reiss, J.D. Stokes, and F.B. Hill, "Separation Via Semi-Continuous Parametric Pumping," *AIChE J.*, 19, 589 (1973).
7. Chen, H.T., J.A. Park, and J.L. Rak, "Equilibrium Parametric Pumps" *Separation Sci. & Tech.*, 9, 35 (1974).
8. Chen, H.T. and V.J. D'Emidio, "Separation of Isomers Via Thermal Parametric Pumping," *AIChE J.*, 21, 813 (1975).
9. Chen, H.T., T.K. Hsieh, H.C. Lee, and F.B. Hill, "Separation of Proteins via Semicontinuous pH-Parametric Pumping," *AIChE J.* 23, 695 (1977).
10. Chen, H.T., Y.W. Wong, and S. Wu, "Continuous Fractionation of Protein Mixtures by pH Parametric Pumping:

- Experiment," *AIChE J.*, 25, 320 (1979).
11. Chen, H.T., U. Pancharoen, W.T. Yang, C.O. Kerobo, and R.J. Parisi, "Separation of Proteins Via pH Parametric Pumping," *Separation sci. & Tech.*, 15 (6), 1377 (1980).
 12. Chen, H.T., W.T. Yang, U. Pancharoen, and R.J. Parisi, "Separation of Proteins Via Multi-Column pH Parametric Pumping," *AIChE J.*, 26, 839 (1980b).
 13. Chen, H.T., W.T. Yang, C.M. Wu, C.O. Kerobo, and V. Jajalla, "Semi-Continuous pH Parametric Pumping: Process Characteristics and Protein Separations," *Separation Sci. & Tech.*, 16(1) (1981).
 14. Dore, J.C., and P.C. Wankat, "Multicomponent Cycling Zone Adsorption," *Chem. Eng. Sci.*, 32, 921 (1976).
 15. Gregory, R.A., and N.H. Sweed, "Parametric Pumping: Behavior of Open Systems Part II: Experiment and Computation," *Chem. Eng. J.*, 4, 139 (1972).
 16. Gupta, R., and N.H. Sweed, "Equilibrium Theory of Cycling Zone Adsorption," *Ind. Eng. Chem. Fundam.*, 10, 280 (1971).
 17. Latty, J.A., "The Use of Thermally Sensitive Ion Exchange Resins or Electrically Sensitive Liquid Crystals as Adsorbent", PhD thesis, Univ. California, Berkeley (1974).
 18. Linde Division-Union Carbide, "IsoSiv", *Hydrocarbon Processing*, 51(9), 210 (1972).
 19. Pigford, R.L., B. Baker and D.E. Blum, "A Equilibrium Theory

of the Parametric Pump," Ind. Eng. Chem.Fundam., 8, 144 (1969a).

20. Pigford, R.L., B. Baker and D.E. Blum, "Cycling Zone Adsorption, A New Separation Process," Ind. Eng. Chem.Fundam., 8, 848 (1969b).
21. Rice, R.G., "Progress in Parametric Pumping" Sep. & Pur. Methods, 5 (1), 139 Marcel Dekker (1976).
22. Rieke, R.D., "Large Separation Via Cycling Zone Adsorption", PhD Thesis, Univ. California, Berkeley(1972).
23. Sabadell, J.E, and N.H. Sweed, "Parametric Pumping with pH, " Separation Sci. & Tech., 5, 171 (1970).
24. Skarstrom, C.W., "Recent Developments in Separation Science, " Vol. II, pp95-106, Cleveland, CRC Press (1972).
25. Van Der Vlist, E., "Oxygen & Nitrogen Enrichment in Air By Cycling Zone Adsorption", Separation Sci. & Tech., 6, 727 (1971).
26. Wakao, H, H. Mastsumoto, K. Suzuki, and A. Kawahara, Kagaku Koaku, 32, 169 (1968), (in Japanese).
27. Wankat, P.C., "Thermal Wave Cycling Zone Adsorption, " J. Chromatography, 88, 211 (1974).
28. Wankat, P.C., "Cyclic Separation Techniques", Nato Portugee Meeting (1978).
29. Weaver, K., and C.E. Harmrin, "Aeparation of Hydrogen Isotopes by Heatless Adsorption," Chem. Eng. Sci., 29, 1873 (1974).
30. Wilhelm, R.H., A.W. Rice, and A.R. Bendelius, "Parametric

Pumping: A Dynamic Principle for Separating Fluid Mixtures," Ind. Eng. Chem. Fundam., 5, 141 (1966).

31. Wilhelm, R.H., A.W. Rice, R.W. Rolke, and N.H. Sweed, "Parametric Pumping," Ind. Eng. Chem. Fundam., 7, 337 (1968).

32. Wilhelm, R.H., and N.H. Sweed, "Parametric Pumping: Separation of Mixture of Toulene and n-Heptane," Science, 159, 522 (1968).